TECHNICAL REPORT

73-24-GP

STRESS-STRAIN RESPONSE OF FABRICS UNDER TWO-DIMENSIONAL LOADING

PART I: RACETRACK YARN CROSS-SECTION

by

W. D. Freeston, Jr.

M. M. Schoppee

FABRIC RESEARCH LABORATORIES, INC.

and

M. A. Wall

U. S. ARMY NATICK LABORATORIES

Contract No. DAAG 17-70-C-0030

March 1971

UNITED STATES ARMY
NATICK LABORATORIES
Natick, Massachusetts 01760

General Equipment & Packaging Laboratory

STRESS-STRAIN RESPONSE OF FABRICS UNDER TWO-DIMENSIONAL LOADING. PART I: RACE-TRACK YARN CROSS-SECTION

W. Denney Freeston, Jr., et al

Fabric Research Laboratories, Incorporated

Prepared for:

Army Natick Laboratories

March 1971

DISCLAIMER NOTICE

THIS DOCUMENT IS BEST QUALITY PRACTICABLE. THE COPY FURNISHED TO DTIC CONTAINED A SIGNIFICANT NUMBER OF PAGES WHICH DO NOT REPRODUCE LEGIBLY.

UNCLASSIFIED

Security Classification

DOCUMENT CONTROL DATA - R & D

(Security classification of title, body of abstract and indexing annotation must be entered when the overall report is classified)

1. ORIGINATING ACTIVITY *(Corporate author)*

Fabric Research Laboratories, Inc.
Dedham, Massachusetts 02026

2a. REPORT SECURITY CLASSIFICATION

UNCLASSIFIED

2b. GROUP

3. REPORT TITLE

Stress-strain response of fabrics under two-dimensional loading, Part I: Racetrack yarn cross-section

4. DESCRIPTIVE NOTES *(Type of report and inclusive dates)*

Technical Report March 1971

5. AUTHOR(S) *(First name, middle initial, last name)*

W. Denney Freeston, Jr. and Meredith M. Schoppee, Fabric Research Laboratories, Inc.
Mary Ann Wall, U. S. Army Natick Laboratories

6. REPORT DATE	7a. TOTAL NO. OF PAGES	7b. NO. OF REFS
March 1971	176/192	7 7

8a. CONTRACT OR GRANT NO.	9a. ORIGINATOR'S REPORT NUMBER(S)
DAAG 17-70-C-0030	
b. PROJECT NO. 1J662708D503)	73-24-GP
c. 1J662708DJ40)--36 1J662713DJ40)	9b. OTHER REPORT NO(S) *(Any other numbers that may be assigned this report)*
d.	

10. DISTRIBUTION STATEMENT

Approved for public release; distribution unlimited.

11. SUPPLEMENTARY NOTES	12. SPONSORING MILITARY ACTIVITY
Details of illustrations in this document may be better studied on microfiche.	U. S. Army Natick Laboratories Natick, Massachusetts 01760

13. ABSTRACT

A theoretical analysis of the load-elongation behavior of idealized plain-weave fabrics comprised of yarns having a racetrack cross-section and subjected to biaxial stresses is presented. Fabric strains resulting from both crimp interchange and yarn extension are considered.

The analytical expressions derived have been solved with a digital computer for both extensible and linearly elastic materials. Generalized plots of the results are presented for two extremes of initial fabric structure: (1) equal crimp distribution in both sets of yarns; (2) one set of yarns noncrimped -- straight.

DD FORM 1 NOV 68 1473 REPLACES DD FORM 1473, 1 JAN 64, WHICH IS OBSOLETE FOR ARMY USE.

I-a

UNCLASSIFIED

Security Classification

14. KEY WORDS	LINK A		LINK B		LINK C	
	ROLE	WT	ROLE	WT	ROLE	WT
Evaluation	8					
Tensile Testers	8,9		10		10	
Biaxial	0		0		0	
Measurement	4		8		8	
Strains	4					
Fabrics	4		9		9	
Racetrack yarns	4		9		9	
Tensile Properties			9		7	
Tensile Strength			9		7	
Armed Forces Equipment			4			
Elasticity					7	
Crimped Yarns					6	
Yarns					0	
Straight					0	

FOREWORD

This report was prepared by Fabric Research Laboratories, Inc. under U.S. Army Contract No. DAAG 17-70-C-0030. The work was carried out under the direction of the U.S. Army Natick Laboratories, with Messrs. Constantin J. Monego and Robert W. Lauder acting as project engineers.

TABLE OF CONTENTS

LIST OF TABLES

LIST OF ILLUSTRATIONS

LIST OF ILLUSTRATIONS (Cont.)

LIST OF ILLUSTRATIONS (Cont.)

LIST OF ILLUSTRATIONS (Cont.)

LIST OF ILLUSTRATIONS (Cont.)

LIST OF ILLUSTRATIONS (Cont.)

LIST OF ILLUSTRATIONS (Cont.)

LIST OF ILLUSTRATIONS (Cont.)

STRESS-STRAIN RESPONSE OF FABRICS UNDER TWO-DIMENSIONAL LOADING

Part I: RACETRACK YARN CROSS-SECTION

INTRODUCTION

In a previous publication [1] a theoretical analysis of the load-extension behavior of idealized, plain-weave fabrics woven from round yarns and subjected to biaxial stresses was presented. Fabric strains resulting from both crimp interchange and yarn extension were determined. The round-yarn geometry is a good approximation to reality for fabrics woven from monofilaments or high-twist yarns [5]. However, it is not applicable to fabrics comprised of low-twist yarns which flatten during weaving. Since most fabrics for industrial/military applications are woven from moderate to low-twist yarns, a fabric model is needed which incorporates a flattened yarn cross-sectional shape and is amenable to a geometrical analysis similar to that for the round-yarn fabric model.

The analysis developed herein is an initial attempt to overcome this shortcoming of the previous work. It is particularly applicable to calendered fabrics. Analytical expressions are developed describing the initial geometry and the geometry after biaxial loading of plain-weave fabrics woven from yarns of racetrack cross-sectional shape. Fabric strains resulting from both crimp interchange and yarn extension are included. The analytical expressions are solved for infinitely flexible, inextensible yarn and infinitely flexible, extensible, linearly elastic yarn. The inclusion of the effects of fiber and yarn bending rigidity is left to a future publication.

Generalized plots of the results are presented for two extremes of initial fabric structure: (1) equal crimp distribution in both sets of yarns; (2) one set of yarns straight (noncrimped). An equal number of warp and filling yarns per unit width before loading is assumed for both extremes. The fabric extension in both the warp and filling directions is given as a function of the loads applied along the warp and filling axes, a parameter comprised of the yarn cross-sectional area and the number of yarns per unit width in the unloaded fabric, the ratio of the yarn width-to-thickness, the yarn packing factor, and the filament tensile properties. The results for various loading ratios, fabric constructions and degrees of yarn flattening are compared.

A procedure for predicting the strength and rupture elongation of plain-weave fabrics comprised of flattened yarns with a racetrack cross-section and subjected to biaxial loading is also developed.

The extension of the analysis to other than plain weaves is discussed.

Assumptions

The analysis developed assumes the following:

1. The fabric is a plain weave.

2. The cross-sectional shape and area of the yarn does not vary along its length nor does it vary with increasing applied loads; the yarns have a racetrack cross-sectional shape.

3. The cross-sectional area of a fiber in the yarn is negligibly small compared to the yarn cross-sectional area.

4. The fibers are homogeneous and either inextensible or linearly elastic.

5. The influences of strain rate, creep and stress relaxation on the response of the fibers are negligible.

6. The yarn twist is sufficiently low that it has a negligible effect on the yarn load-extension response.

7. The axes of the yarns are combinations of circular arcs and straight lines prior to loading [3,4]. At yarn crossovers each crossing yarn conforms to the cross-sectional contour of the other; between crossovers the axes of the yarns are straight.

8. The warp yarns are initially perpendicular to the filling yarns and remain so during loading.

9. Orthogonal yarns remain in contact during the loading cycle; there is no yarn slippage at yarn crossovers.

10. The intrinsic tensile response of the bent yarn is the same as that of the yarn when straight.

11. The yarns are initially relaxed and contain no residual stresses prior to loading.

12. The fabric is loaded in its mid-plane. The loads are uniformly distributed along the fabric edges. The load on the edges parallel to the filling yarns is parallel to the warp yarns, and the load on the edges parallel to the warp yarns is parallel to the filling yarns.

LIST OF SYMBOLS

The following symbols are used in the analysis:

subscript w - warp yarn or warp direction in fabric
subscript f - filling yarn or filling direction in fabric
subscript 1 - value of parameter before application of loads
subscript 2 - value of parameter after application of loads

No numerical subscript means the parameter has the same value after application of loads as before. No alphabetic subscript means the parameter is the same for both the warp and filling yarns or in both the warp and filling directions.

A = yarn cross-sectional area

a = one half the thickness of the yarn as it lies in the fabric

b = one half the width of the yarn as it lies in the fabric

E = efficiency by which yarn strength is translated into fabric strength

E_f = fiber modulus of elasticity

E_y = yarn modulus of elasticity

h = distance perpendicular to the fabric plane between yarn cross-section centers at two successive yarn crossovers

L = length along yarn between centers of adjacent crossing yarns

N = number of yarns per unit width of fabric

n_f = number of fibers in yarn

p = yarn packing factor: ratio of the sum of the filament cross-sectional areas to the yarn cross-sectional area

P_y = total axial tensile load on a yarn

r_f = fiber radius

R = yarn radius

S = tensile stress (force per unit area) acting on a fiber

ε = tensile strain in a fiber; fractional fabric extension

ε_y = yarn tensile strain

θ = angle between the yarns and the fabric plane at the mid-point between yarn crossovers; the angle subtended by one-half the length of the circular arc over which contact is made between yarns at yarn crossovers

μ = "effective" fabric Poisson's ratio

ν = yarn Poisson's ratio

σ = external load on the fabric per unit width of fabric

Fabric Model

The geometry of the fabric model corresponding to the above assumptions is illustrated in Figure 1. As shown, a racetrack yarn cross-section is a rectangle capped with semicircles. Eight geometric parameters are required to describe this model: warp and filling yarn cross-sectional area; ratio of yarn cross-section width-to-thickness; number of warp and filling yarns per unit length of fabric; angle between warp and filling yarns and the fabric plane at the mid-point between yarn crossovers.

The cross-sectional areas of the warp and filling yarns are given by:

$$A_w = a_{lw}^2(\pi-4)+4a_{lw}b_{lw} \tag{1}$$

$$A_f = a_{lf}^2(\pi-4)+4a_{lf}b_{lf} \tag{2}$$

The equations describing the geometry before loading of plain-weave fabrics woven from racetrack yarns using the symbols illustrated in Figure 1 and defined in the list of symbols are:

$$\frac{1}{N_{lw}} = [L_{lf}-2(b_{lw}-a_{lw})-2(a_{lw}+a_{lf})\theta_{lf}]\cos\theta_{lf} + 2(a_{lw}+a_{lf})\sin\theta_{lf}+2(b_{lw}-a_{lw}) \tag{3}$$

$$\frac{1}{N_{lf}} = [L_{lw}-2(b_{lf}-a_{lf})-2(a_{lw}+a_{lf})\theta_{lw}]\cos\theta_{lw} + 2(a_{lw}+a_{lf})\sin\theta_{lw}+2(b_{lf}-a_{lf}) \tag{4}$$

$$h_{lf} = [L_{lf}-2(b_{lw}-a_{lw})-2(a_{lw}+a_{lf})\theta_{lf}]\sin\theta_{lf} + 2(a_{lw}+a_{lf})(1-\cos\theta_{lf}) \tag{5}$$

$$h_{lw} = [L_{lw}-2(b_{lf}-a_{lf})-2(a_{lw}+a_{lf})\theta_{lw}]\sin\theta_{lw} + 2(a_{lw}+a_{lf})(1-\cos\theta_{lw}) \tag{6}$$

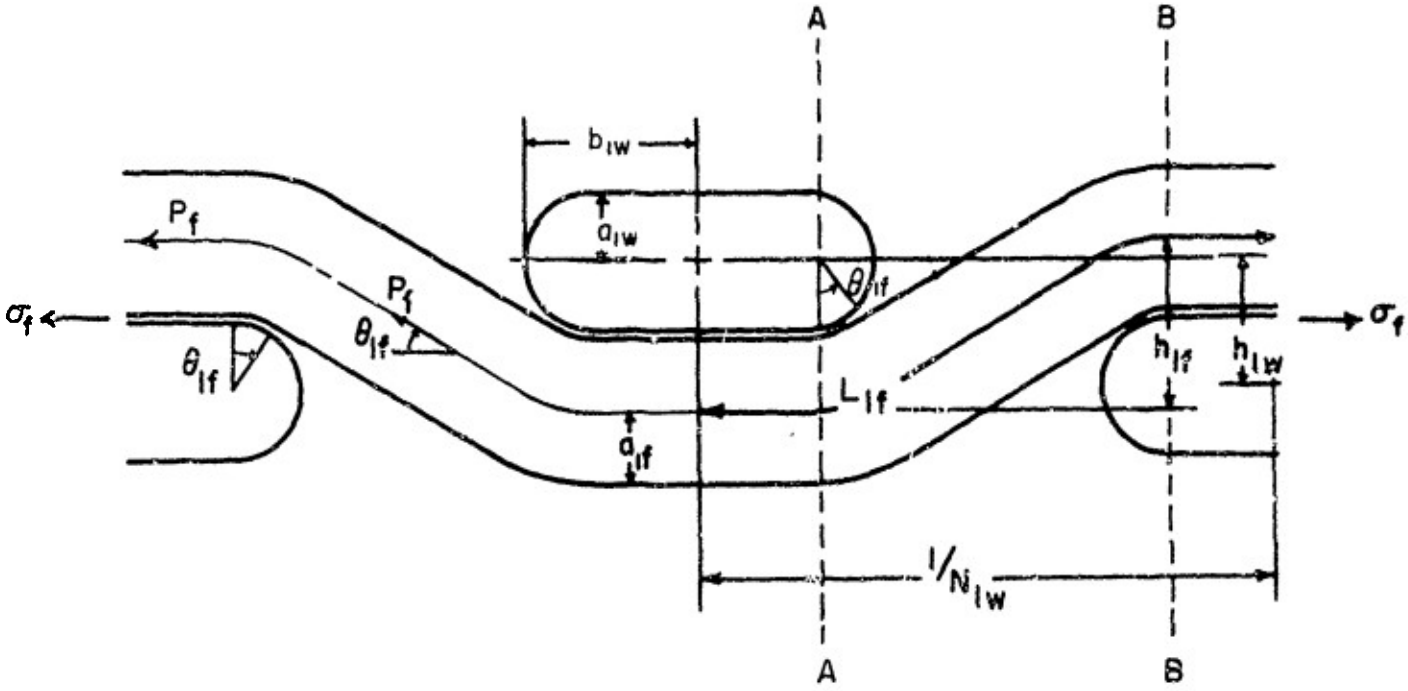

Figure 1. Fabric Model with Racetrack Yarns

$$h_{1w}+h_{1f} = 2(a_{1w}+a_{1f}) \tag{7}$$

Assuming infinitely flexible yarns, these equations also describe the geometry of the fabric after loading with the subscript "1" replaced by the subscript "2". Except for the inclusion of the additional terms, 2(b-a), representing the length of the rectangular portion of the yarn cross-section, the equations are identical to those describing the round-yarn fabric [1]. If the yarn aspect ratio, b/a, becomes unity, the equations reduce to those describing a round-yarn fabric of yarn radius, a. It is thus apparent that the analysis of racetrack yarn fabric differs from the analysis of the round-yarn fabric only by the inclusion of terms expressing the degree and character of yarn flattening (b/a > 1).

Specification of Initial Parameters

Those geometric quantities describing a fabric structure in the unloaded state that are most easily measured or specified are the number of warp and filling yarns per unit width, N_{1w} and N_{1f}, the yarn cross-sectional areas, A_w and A_f, and the yarn aspect ratios, b_{1w}/a_{1w} and b_{1f}/a_{1f}.

The cross-sectional area of a low-twist yarn can be calculated from the number of filaments in the yarn n_f and the filament radius r_f (assuming an approximately round filament cross-sectional contour) as follows:

$$A = \frac{n_f \pi r_f^2}{p} = \frac{\text{yarn denier}}{\text{fiber denier}} \left(\frac{\pi r_f^2}{p}\right) \tag{8}$$

For a low-twist yarn containing a relatively large number of round filaments packed in cross-section into concentric circular rings the theoretical packing factor p is on the order of 0.750 [2]. In an extreme case of yarn flattening where the filaments are arranged in a rectangular cross-sectional array of dimensions $2r_f \times 2r_f n_f$ the packing factor is the same as that of a circle in a square, namely, 0.785. Since the difference between the packing factors for these two extreme degrees of yarn flattening is not great (<5%) the cross-sectional area of the yarn flattened to any degree can be assumed the same as that of a yarn with a round cross-sectional configuration, i.e., p = 0.750.

The yarn aspect ratio b/a is uniquely determined by the yarn cross-sectional area and yarn width b. The average yarn width b can be calculated from the fabric light transmission and expressions for cover factor and yarn cross-sectional area can be determined from the yarn denier (using an appropriate packing factor). With these two parameters known, the yarn thickness a and aspect ratio b/a can then be calculated. Thus with specification of N_{1w} and N_{1f}, A_w and A_f, and b_{1w}/a_{1w} and b_{1f}/a_{1f} the length of yarn between cross-overs, L_{1w} and L_{1f}, and the initial warp and filling yarn angles, θ_{1w} and θ_{1f}, can be determined from Equations 1-7 for the two extremes of initial fabric geometry: (1) equal crimp distribution in both sets of yarns; (2) one set of yarns straight (noncrimped). While the geometry of most real fabrics lies between these two extremes, their response will be bracketed by the response of these two cases. For initial fabric geometries between these two extremes, one additional parameter must be specified, e.g., either the distance between successive filling yarn cross-section centers perpendicular to the plane of the fabric, h_{1f}, the similar distance between yarn cross-section centers, h_{1w}, the filling yarn crimp, or the warp yarn crimp as the yarn lies in the fabric. However, these parameters are not easily determined. One method is to imbed the fabric, section it and examine the section under a microscope.

Fabric Deformation

Referring to Figure 1 and the List of Symbols the equations of static equilibrium become

$$\sigma_f = P_f \cos\theta_{2f} N_{2f} \tag{9}$$

from summing the forces in the filling direction, and

$$\sigma_w = P_w \cos\theta_{2w} N_{2w} \tag{10}$$

from summing the forces in the warp direction Summing the components of the forces perpendicular to the fabric plane gives

$$P_w \sin\theta_{2w} - P_f \sin\theta_{2f} = 0 \tag{11}$$

Combining Equations 9, 10, and 11

$$\frac{\sigma_w}{\sigma_f} = \frac{\tan\theta_{2f}(N_{2w})}{\tan\theta_{2w}(N_{2f})} \tag{12}$$

which relates the final fabric geometry to the imposed loading ratio.

If it is assumed that there is no axial yarn extension ($L_{2w} = L_{1w} = L_w$, $L_{2f} = L_{1f} = L_f$), that the yarn cross-sectional dimensions do not change during loading ($a_{2w} = a_{1w} = a_w$, $b_{2w} = b_{1w} = b_w$), and that the yarns are infinitely flexible; the fabric load-extension behavior consists entirely of an interchange of crimp between the warp and filling yarns. The magnitude of this crimp interchange is governed only by the value of the loading ratio, σ_w/σ_f, and not by the magnitudes of the individual loads σ_w and σ_f. Therefore, in addition to the initial parameters already discussed, only the loading ratio need be specified in this case to characterize the final geometry of the fabric after loading and hence its load-extension response.

If it is desired to include the effects of axial yarn extension in characterizing the response of a fabric to loading, Equations 9 and 10 must be used separately and the functional relationship between the tensile loads P_f and P_w acting on the yarns in the fabric and yarn construction, filament properties and change in yarn length between crossovers considered.

It is assumed that the load-elongation response of the fabric yarns can be represented by

$$P_y = SpA = c+d\varepsilon \tag{13}$$

where ε = fiber tensile strain, σ = tensile stress (force per unit area) acting on a fiber, and c and d are constants. Since the fabrics are assumed to be comprised of flattened yarns, the twist would be low. Therefore, it is assumed that the effect of twist on the tensile response of the fabric yarns is negligibly small and hence the fiber tensile strain is equivalent to the yarn tensile strain, $\varepsilon = \varepsilon_y$. If it is further assumed that the yarn cross-sectional area remains constant during yarn extension ($\nu = 0$) and that the yarn material is linearly elastic, $c = 0$ and

$$P_y = pE_f A\varepsilon_y \tag{14}$$

where E_f is the fiber modulus of elasticity for fabrics woven from continuous filament yarns. (The effects of twist, elastoplastic stress-strain response, and constant volume extension ($\nu = 1/2$) on the load-extension response of the yarn, are discussed in reference 1..

The extension of the filling yarns in the fabric is given by $\varepsilon_y = (L_{2f}-L_{1f})/L_{1f}$, and similarly for the warp yarns by $\varepsilon_y = (L_{2w}-L_{1w}/L_{1w}$. Utilizing these expressions for the strain in the fabric yarns and Equation 16, Equations 9 and 10 can be rewritten in the following form

$$\sigma_w = N_{2w}pE_f A_{2w}\left(\frac{L_{2w}}{L_{1w}} - 1\right)\cos\theta_{2w} \tag{15}$$

$$\sigma_f = N_{2f}pE_f A_{2f}\left(\frac{L_{2f}}{L_{1f}} - 1\right)\cos\theta_{2f} \tag{16}$$

From Equation 12 and Equations 3-7, with the subscript "1" replaced by the subscript "2", the final warp and filling yarn spacing, N_{2w} and N_{2f}, and the warp and filling yarn angles, θ_{2w} and θ_{2f} can be determined for fabrics woven from infinitely flexible, inextensible ($E = \infty$) or extensible yarn. The resulting fabric fractional extension in the warp and filling directions is given by

$$\varepsilon_w = \frac{N_{1f}}{N_{2f}} - 1, \tag{17}$$

$$\varepsilon_f = \frac{N_{1w}}{N_{2w}} - 1. \tag{18}$$

Limiting Fabric Geometries

The foregoing discussion of fabric deformation under biaxial loading does not take into account the possibility of geometric limitations on the final fabric configuration imposed by a combination of the initial fabric geometry and the loading ratio. Analysis of the idealized fabric model being considered suggests that there are three

possible limiting geometries. (It is assumed that the load applied to the fabric in the warp direction is greater than the load applied in the filling direction, $\sigma_w > \sigma_f$).

(1) Warp yarns pulled straight - If the length of the filling yarns between crossovers is great enough to permit it, the warp yarns can be pulled straight. When this occurs, $1/N_{2f} = L_{2w}$. This limiting geometry, if attained, defines the maximum fabric extension possible from crimp interchange; any further fabric extension requires yarn extension.

(2) Maximum filling contraction - The fabric extension in the warp direction can be limited by the inability of the fabric to contract further in the filling direction. The maximum attainable crimp has been developed in the filling yarns when there are no straight sections between adjacent warp yarn crossovers.

(3) Contact between adjacent warp yarns - Fabric extension in the warp direction can also be limited by adjacent warp yarns coming into contact with each other at the fabric mid-plane between crossovers [6]. When this occurs $1/N_{2w} = 2b_w$. Detailed discussion of these limiting geometries is presented in later sections.

ANALYTICAL RESULTS

The analytical expressions derived above for the load-extension behavior of idealized plain-weave fabrics subjected to biaxial stresses have been solved for various combinations of initial fabric geometries and filament properites. The Newton-Raphson iterative method for the solution of simultaneous non-linear algebraic equations and a digital computer were used to obtain the solutions (see Appendix, Ref. 7). Descriptions of the cases solved and the results obtained are given below.

Solutions are given first for the case of no axial yarn extension ($E = \infty$) during fabric loading. Only the contribution of crimp interchange to the load-extension response of the biaxially stressed fabrics is considered. Results are given for the two extremes of initial fabric structure: (1) equal crimp distribution in both sets of yarns; (2) one set of yarns straight (noncrimped). For both extreme cases, an equal number of warp and filling yarns per unit width before loading is assumed. As noted previously, the results are a function only of the loading ratio σ_w/σ_f and not of the magnitudes of the imposed loads.

I. Square Fabric, Inextensible, Infinitely Flexible Yarn

For an initially square, plain-weave fabric with the same infinitely flexible and inextensible yarn in both directions

$$N_{1w} = N_{1f} = N_1,$$

$$\theta_{1w} = \theta_{1f} = \theta_1,$$

$$L_{1w} = L_{1f} = L_{2f} = L_{2w} = L,$$

and assuming the yarn cross-sectional dimensions do not change during loading

$$b_{1w} = b_{1f} = b_{2w} = b_{2f} = b,$$

$$a_{1w} = a_{1f} = a_{2w} = a_{2f} = a,$$

$$b_w/a_w = b_f/a_f = b/a.$$

These assumptions allow considerable simplification of the equations describing the initial and final fabric geometry. Equations 1-7 reduce to the following three expressions

$$A = a^2(\pi-4)+4ab \tag{19}$$

$$\frac{1}{N_1 a} = \frac{2(2\cos\theta_1-1)\cos\theta_1}{\sin\theta_1} + 4\sin\theta_1 + 2(b/a-1) \tag{20}$$

$$\frac{L}{a} = \frac{2(2\cos\theta_1-1)}{\sin\theta_1} + 4\theta_1 + 2(b/a-1) \tag{21}$$

The dimensionless parameters $N_1 a$ and L/a are plotted versus θ_1 for various values of the aspect ratio, b/a, in Figures 2 and 3 respectively; Figure 4 shows L/a as a function of $N_1 a$ for various aspect ratios. (The value of L/a for $b/a = 10$ is so large for all values of $N_1 a$ that it was excluded from Figures 3 and 4.) Since both

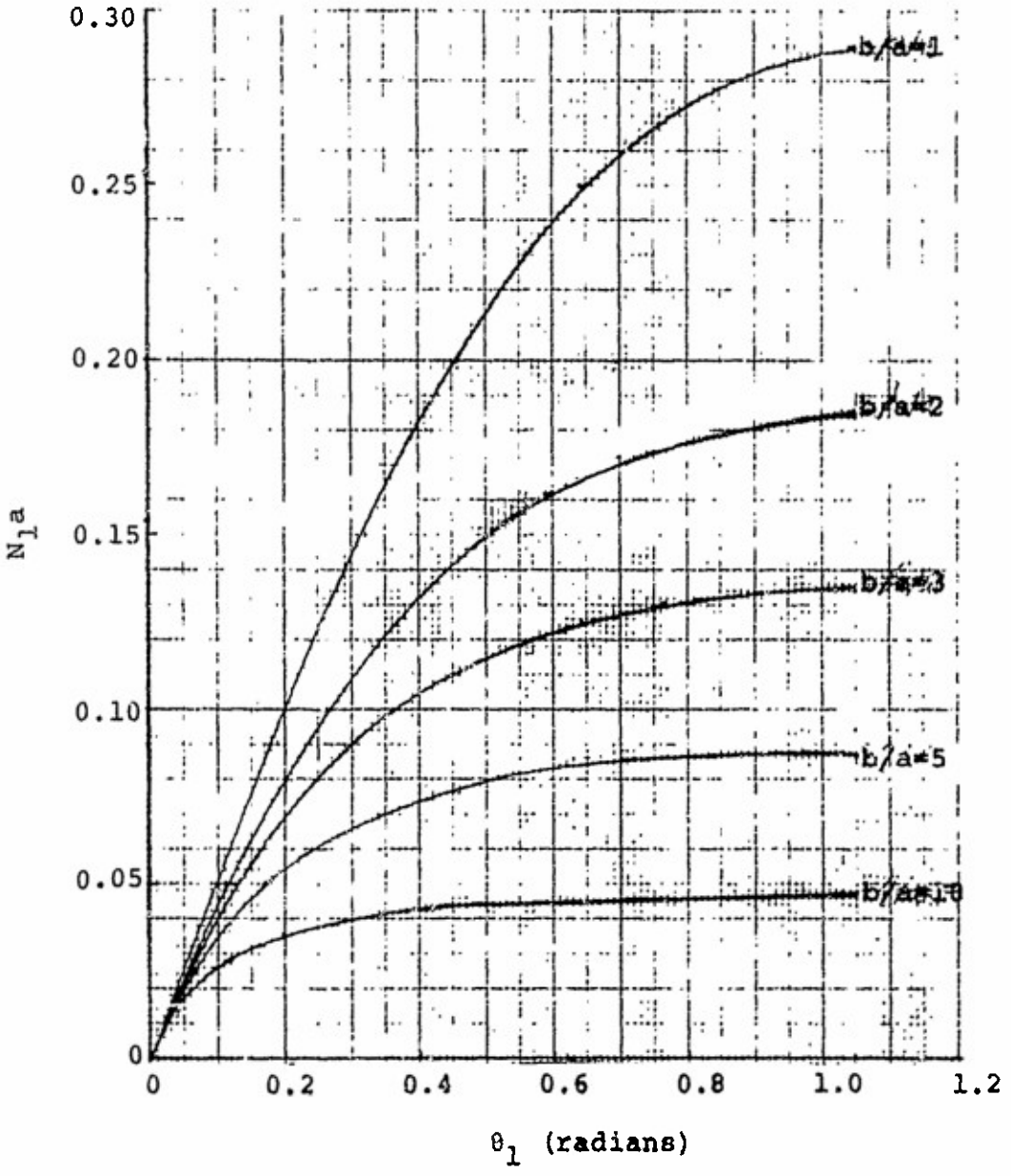

Figure 2. N_1a vs θ_1 for Square Fabric

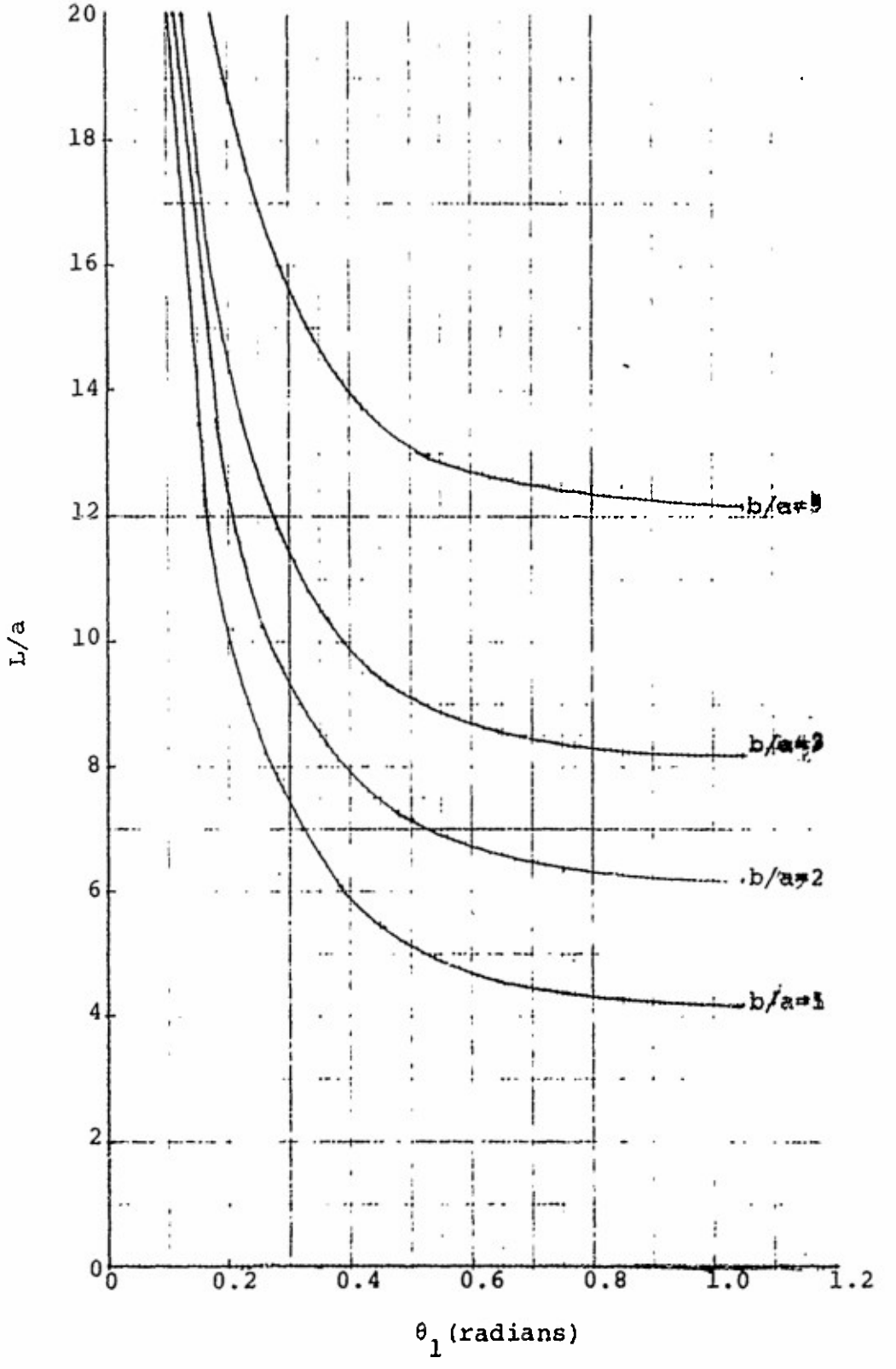

Figure 3. L/a vs θ_1 for Square Fabric

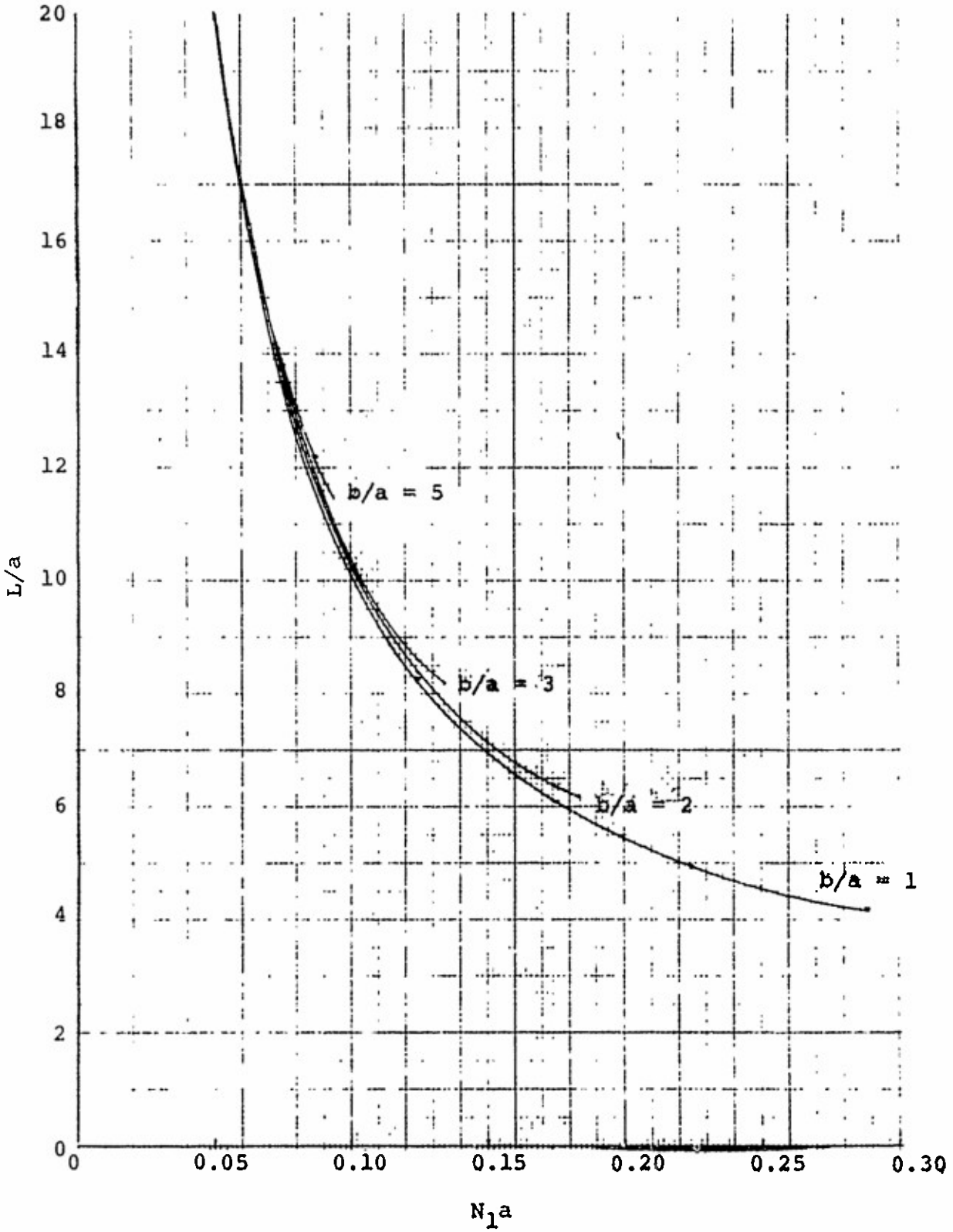

Figure 4. L/a vs N_1a for Square Fabric

"a" and the radius of a round yarn are measures of one-half the yarn thickness, the parameters $N_1 a$ and L/a are analogous to the quantities $N_1 R$ and L/R used in the analysis of the round-yarn fabric [1]. The curves in Figures 2 through 4 are terminated at $\theta_1 = 1.047$, i.e., 60°. This is the angle of the yarns in an initially jammed fabric as discussed in a subsequent section below.

Although Figures 2, 3 and 4 effectively and simply illustrate the behavior of Equations 20 and 21, they are not satisfactory means for investigating the interrelationships between the number of yarns per unit width, the yarn cross-sectional area and the degree of yarn flattening, as well as the effect of varying these parameters separately, upon the initial fabric crimp and crimp angles. It would be desirable, for instance, to see graphically the effects on fabric structure of varying only the yarn aspect ratio while maintaining a constant yarn cross-sectional area. Since the area does remain constant for various degrees of yarn flattening, as the aspect ratio changes, both "a" and "b" obviously must change also. Thus, in Figure 2 a line of constant $N_1 a$ cannot imply either a constant value of N_1 or of "a" as it intersects b/a curves. Furthermore, maximum values of $N_1 a$ indicated in Figure 2 for different aspect ratios cannot be readily related to the maximum achievable number of yarns per unit width for any particular value of cross-sectional area. Similar problems arise in the interpretation of Figures 3 and 4.

In an effort to be able to compare the results of the present analysis to those for the round-yarn analysis and at the same time permit a more versatile representation of the information given by Equations 20 and 21 in terms of initially specified quantities, the dimensionless parameters $N_1\sqrt{A/\pi}$ and $L/\sqrt{A/\pi}$ are utilized. The basis of this choice is Equation 19 which can be rearranged to give:

$$\sqrt{A/\pi} = a[4(b/a-1)/\pi+1]^{1/2}. \qquad (22)$$

Values relating the two parameters, $N_1 a$ and $N_1\sqrt{A/\pi}$, for various aspect ratios, are given in Table 1.

TABLE 1

AREA NORMALIZING FACTORS FOR RACETRACK YARNS

b/a	$[4(b/a-1)/\pi+1]^{1/2}$
1	1.000
2	1.508
3	1.883
5	2.468
10	3.529

Figure 5 shows $N_1\sqrt{A/\pi}$ plotted against the crimp angle θ_1; Figure 6 gives $L/\sqrt{A/\pi}$ as a function of $N_1\sqrt{A/\pi}$. The curves in Figure 5 may be interpreted as showing for a range of aspect ratios the way in which the crimp angle θ_1 increases with: (1) increasing number of yarns per unit length N_1 for any specified yarn cross-sectional area A or; (2) increasing cross-sectional area A for any specified number of yarns per unit length. Maximum achievable values of N_1 for any A or of A for any N_1 are readily apparent for various yarn aspect ratios; alternately the maximum amount of yarn flattening which can occur for any combination of values of N_1 and A can be determined. As would be expected, the more open fabrics (low values of $N_1\sqrt{A/\pi}$) can accommodate a greater degree of yarn flattening. One interesting fact shown in Figure 5 which is not apparent in Figure 2 is that in more open fabrics the crimp angle is greatest when the aspect ratio is lowest; while above a critical value of tightness, which differs for each aspect ratio, the converse is true. The lower the aspect ratio the thicker the yarn and thus the greater the angle the yarns make with the plane of the fabric at their mid-point between yarn crossovers in an open fabric. However, in a more tightly woven fabric the higher the yarn aspect ratio the closer to a jammed construction the fabric is and thus the greater the angle the yarns must make with the plane of the fabric at their mid-point between yarn crossovers in order to pass over one yarn and then under the next in the plain-weave construction (see Figure 1).

It can be seen from Figure 6 that the length L of yarn between crossovers is not strongly dependent on the degree of yarn flattening - particularly for the more open fabrics. This length is governed almost exclusively by the number of ends per unit length in the fabric

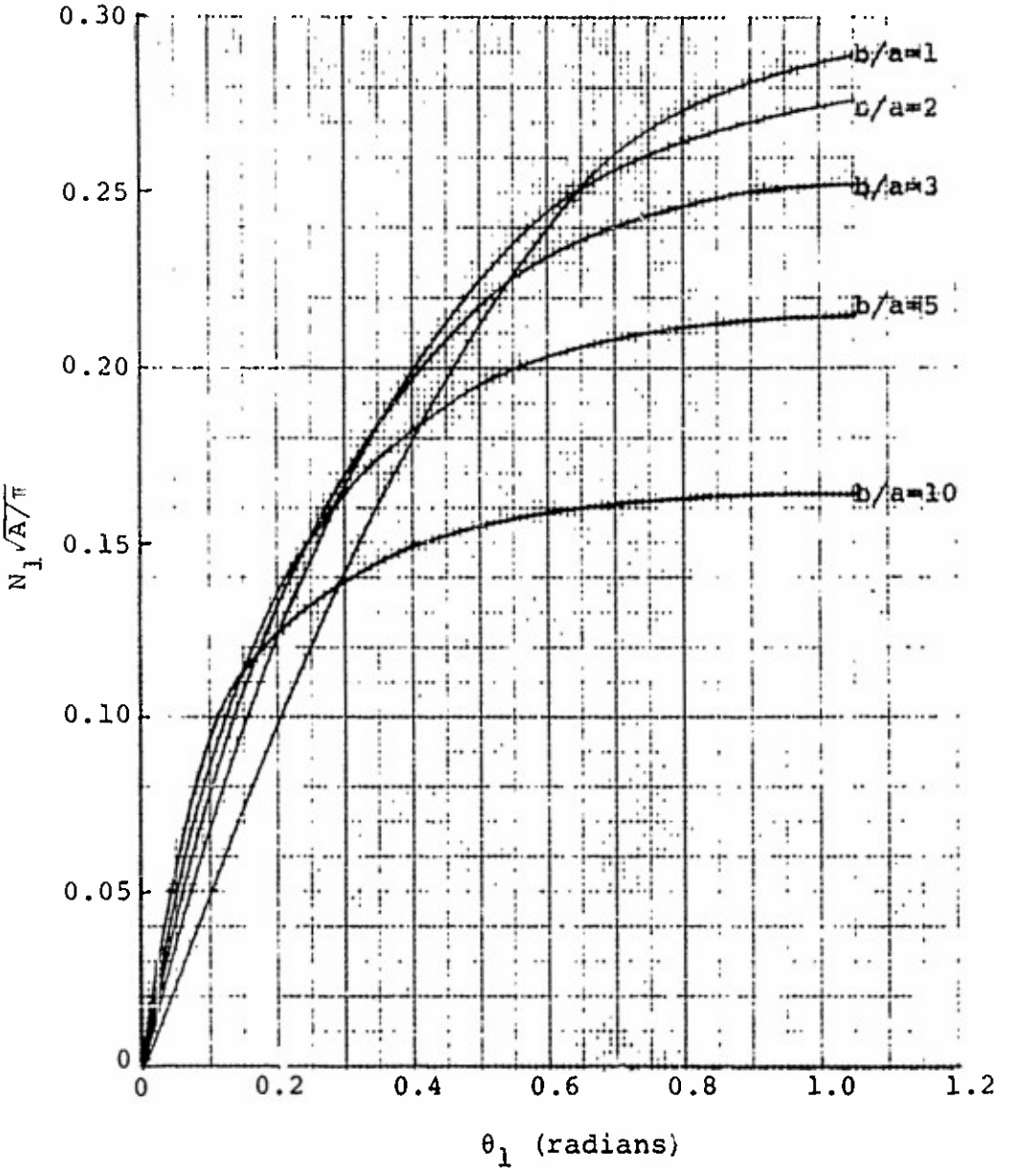

Figure 5. $N_1\sqrt{A/\pi}$ vs θ_1 for Square Fabric

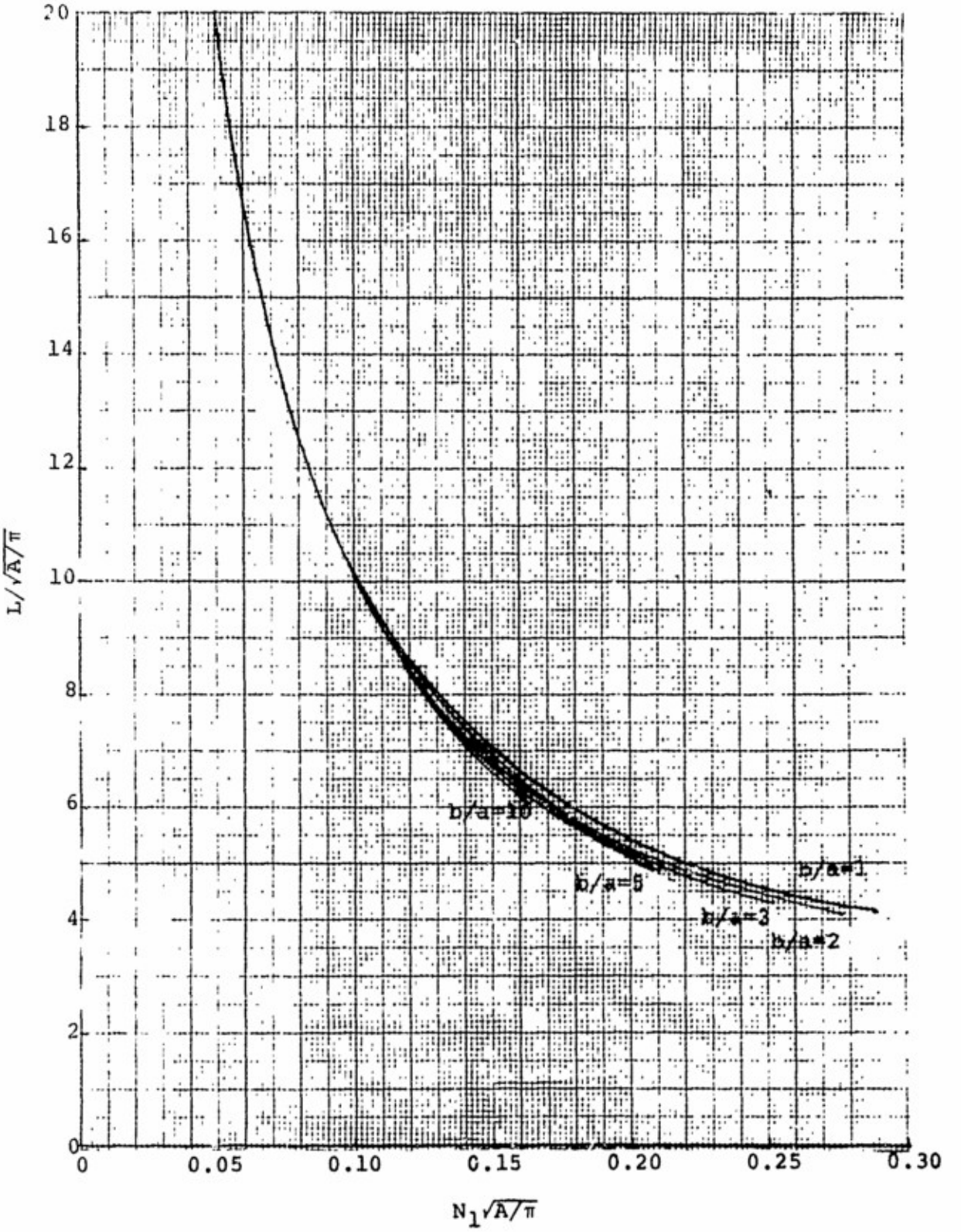

Figure 6. $L/\sqrt{A/\pi}$ vs $N_1\sqrt{A/\pi}$ for Square Fabric

in relation to the yarn cross-sectional area, i.e., by the tightness of the fabric construction.

It is interesting to examine graphically the various components of the length L between crossovers for different degrees of yarn flattening. These components, normalized for yarn cross-sectional area, are illustrated in Figures 7 through 9 and defined as follows:

(1) The straight length between contact points at adjacent yarn crossovers inclined at an angle θ_1 to the plane of the fabric,

$$L_I = L-4a\theta_1-2(b-a) = L-L_{II}-L_{III},$$

$$\frac{L_I}{\sqrt{A/\pi}} = \frac{1}{\sqrt{A/\pi}}(L-L_{II}-L_{III}). \tag{23}$$

(2) The curved length which wraps around the crossing yarn defined by the wrap angle θ_1,

$$L_{II} = 4a\theta_1,$$

$$\frac{L_{II}}{\sqrt{A/\pi}} = \frac{4\theta_1}{[4(b/a-1)/\pi+1]^{1/2}}. \tag{24}$$

(3) The length parallel to the plane of the fabric defined by the rectangular section of the racetrack contour,

$$L_{III} = 2(b-a),$$

$$\frac{L_{III}}{\sqrt{A/\pi}} = \frac{2(b/a-1)}{[4(b/a-1)/\pi+1]^{1/2}}. \tag{25}$$

As would be anticipated L_{III} increases with increasing aspect ratio. As previously noted L, the total yarn length between yarn crossovers does not vary greatly with the aspect ratio, therefore, as shown in the figures, the length of crimped yarn between crossovers, $L-L_{III}$, decreases as the yarn aspect ratio increases. Also, as the aspect ratio decreases the component L_{II} becomes an increasingly greater portion of the total length.

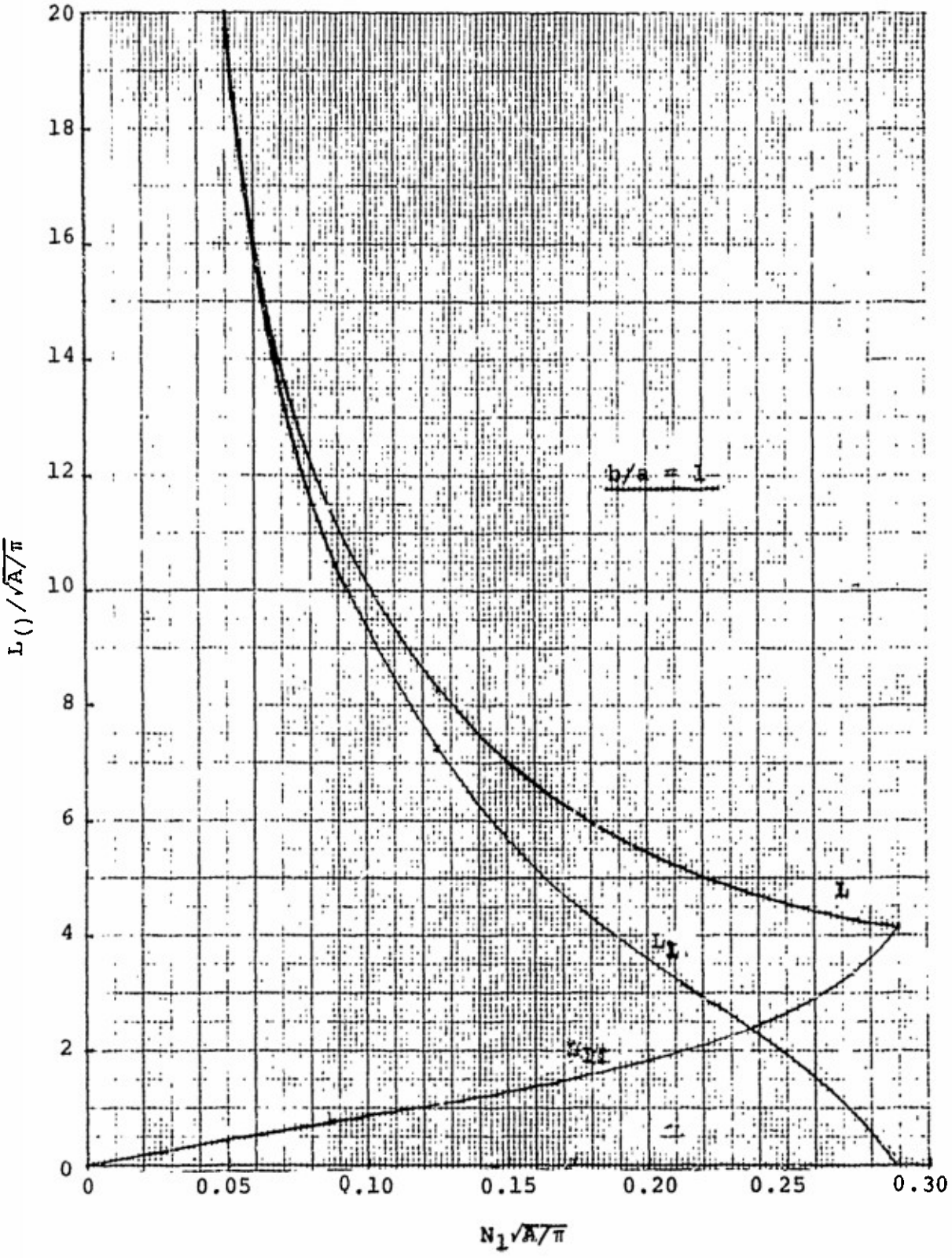

Figure 7. Components of Yarn Length Between Crossovers Before Loading as Function of $N_1\sqrt{A/\pi}$ for Square Fabric (Aspect Ratio = 1)

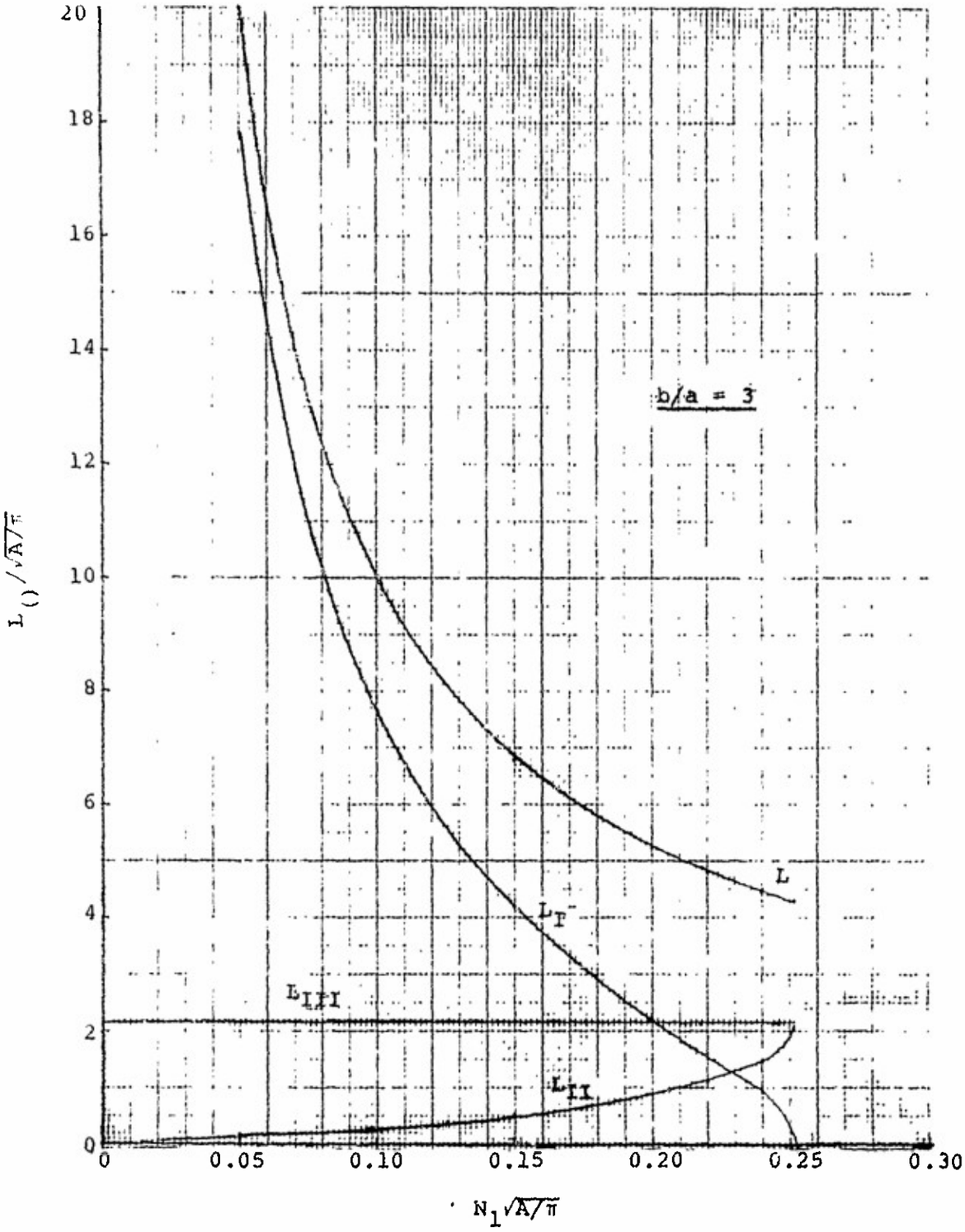

Figure 8. Components of Yarn Length Between Crossovers Before Loading as a Function of $N_1\sqrt{A/\pi}$ for Square Fabric (Aspect Ratio = 3)

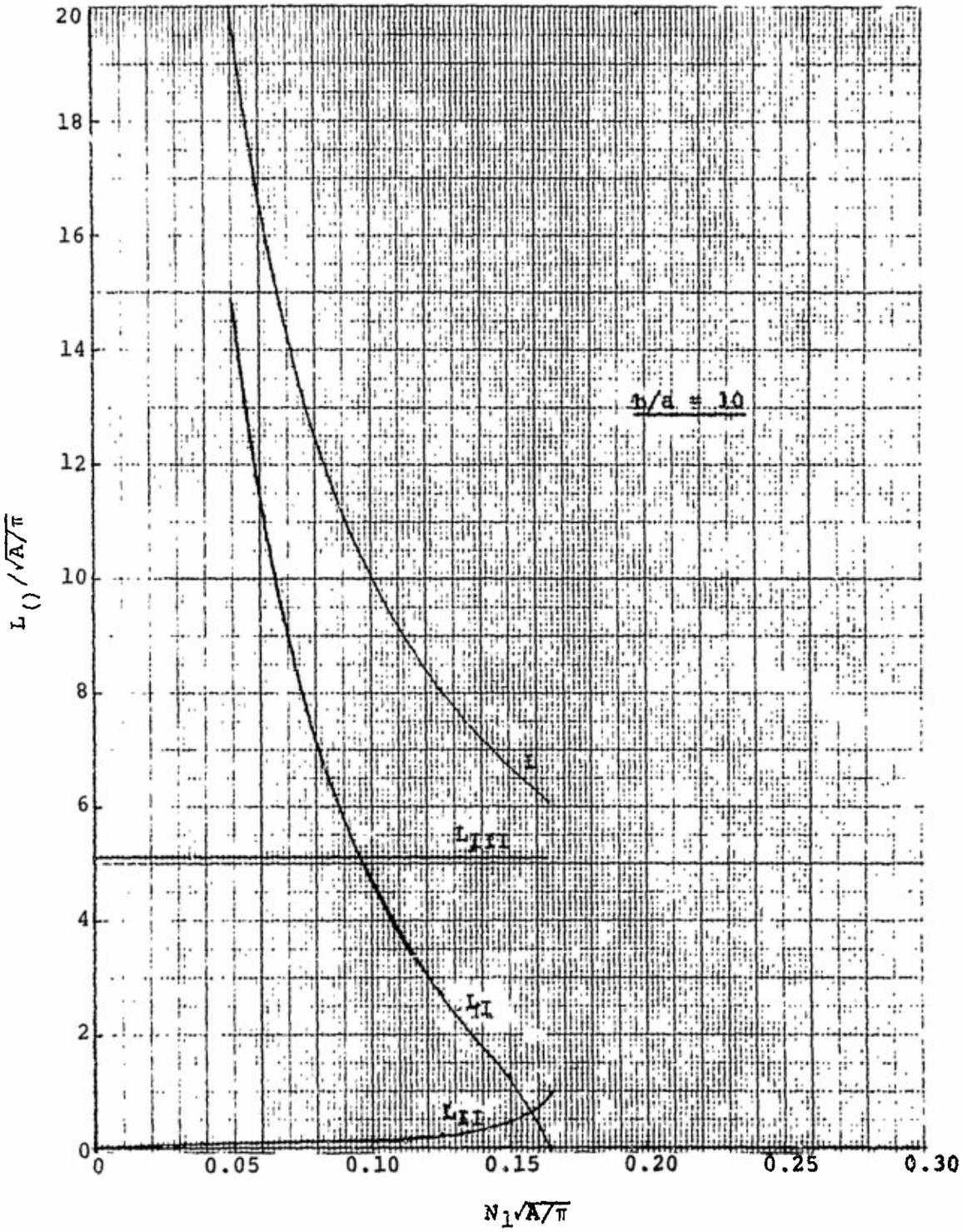

Figure 9. Components of Yarn Length Between Crossovers Before Loading as a Function of $N_1\sqrt{A/\pi}$ for Square Fabric (Aspect Ratio = 10)

After loading, assuming infinitely flexible, inextensible yarn, i.e., only taking into account crimp interchange ($L_1 = L_2 = L$), the yarn geometry of the deformed fabric can be found from the following four equations derived from Equations 3-7 and 12 after simplification and replacement of subscripts "1" by subscripts "2":

$$\frac{\sigma_w}{\sigma_f} = \frac{\cot\theta_{2w}\{[L/a-2(b/a-1)-4\theta_{2w}]\cos\theta_{2w}+4\sin\theta_{2w}+2(b/a-1)\}}{\cot\theta_{2f}\{[L/a-2(b/a-1)-4\theta_{2f}]\cos\theta_{2f}+4\sin\theta_{2f}+2(b/a-1)\}} \tag{26}$$

$$[L/a-2(b/a-1)-4\theta_{2w}]\sin\theta_{2w}-4\cos\theta_{2w} = 4(\cos\theta_{2f}-1)-[L/a-2(b/a-1)-4\theta_{2f}]\sin\theta_{2f} \tag{27}$$

$$\frac{1}{N_{2w}a} = [L/a-2(b/a-1)-4\theta_{2f}]\cos\theta_{2f}+4\sin\theta_{2f}+2(b/a-1) \tag{28}$$

$$\frac{1}{N_{2f}a} = [L/a-2(b/a-1)-4\theta_{2w}]\cos\theta_{2w}+4\sin\theta_{2w}+2(b/a-1) \tag{29}$$

By solving Equations 26 and 27 simultaneously for a specified loading ratio σ_w/σ_f, the final crimp angles θ_{2w} and θ_{2f} can be determined. These values can then be inserted into Equations 28 and 29 to give the appropriate values of $N_{2w}a$ and $N_{2f}a$. The resulting fabric strains are computed from Equations 17 and 18.

With the aid of a digital computer, the above equations were solved for various pairs of values of N_1a and b/a, for a series of loading ratios, $\sigma_w/\sigma_f \geq 1$. (The results are also valid for $\sigma_w/\sigma_f < 1$ if the subscripts "w" and "f" are everywhere reversed.) The values of N_1a used in the solutions at each value of aspect ratio are equivalent to the same set of $N_1\sqrt{A/\pi}$ values that were used in the previous round-yarn analysis ($b/a = 1$)[1].

The results of the computations are presented graphically in Figures 10 through 27. Fabric extensions in the warp direction and contractions in the filling direction are plotted versus the loading ratio, σ_w/σ_f, for various degrees of initial fabric tightness, $N_1\sqrt{A/\pi}$, and various amounts of yarn flattening, b/a. The fabric extensions in both the warp and filling directions are also given as a function of $N_1\sqrt{A/\pi}$ for various loading ratios and yarn aspect ratios.

Fabric extensions are also given for $\sigma_w/\sigma_f = \infty$, i.e., for uniaxial loading. These extension values represent the maximum fabric extensions possible from crimp interchange. Their derivation is discussed below. Figures 10 and 11 which show the response of the initially square round-yarn fabric (b/a = 1) are reprinted from reference 1.

Examination of Figures 10 through 19 shows that the amount of extension or contraction achieved in the fabric as the result of crimp interchange increases with both increasing loading ratio and in general with increasing $N_1\sqrt{A/\pi}$. This latter result is not surprising because although the length L of yarn between crossovers decreases with increasing number of ends per unit width N_1, the ratio of L to the yarn spacing $1/N_1$ increases. However a limiting geometry is reached at lower levels of the loading ratio for those fabrics characterized by higher values of $N_1\sqrt{A/\pi}$, as indicated by the curves which are terminated at loading ratios lower than 10. (These termination points represent the largest requested value of σ_w/σ_f for which solutions were possible and do not necessarily represent true maximum values.)

No fabric extension occurs for a loading ratio of one. Since the fabric is initially square containing an equal number of ends and equal crimp in both the warp and filling directions, no crimp interchange can take place under conditions of equal loading in both directions. For loading ratios greater than one, the fabric elongates in the warp direction and contracts in the filling direction. The magnitudes of these extensions increase with increasing values of the loading ratio, approaching the $\sigma_w/\sigma_f = \infty$ extension asymptotically. Additionally, the fabric contracts more in the filling direction than it extends in the warp direction.

Comparison of Figures 10, 12, 14, 16 and 18 and also Figures 11, 13, 15, 17 and 19 indicate that, generally, as the yarn aspect ratio increases, the fabric becomes stiffer in tension, i.e., the amount of extension or contraction resulting from the application of a particular loading ratio decreases as the degree of yarn flattening increases. This decrease in crimp interchange is primarily attributable to the small, but nonetheless significant, decrease in total yarn length between crossovers and decreasing level of initial crimp with increasing aspect ratio for particular values of $N_1\sqrt{A/\pi}$.

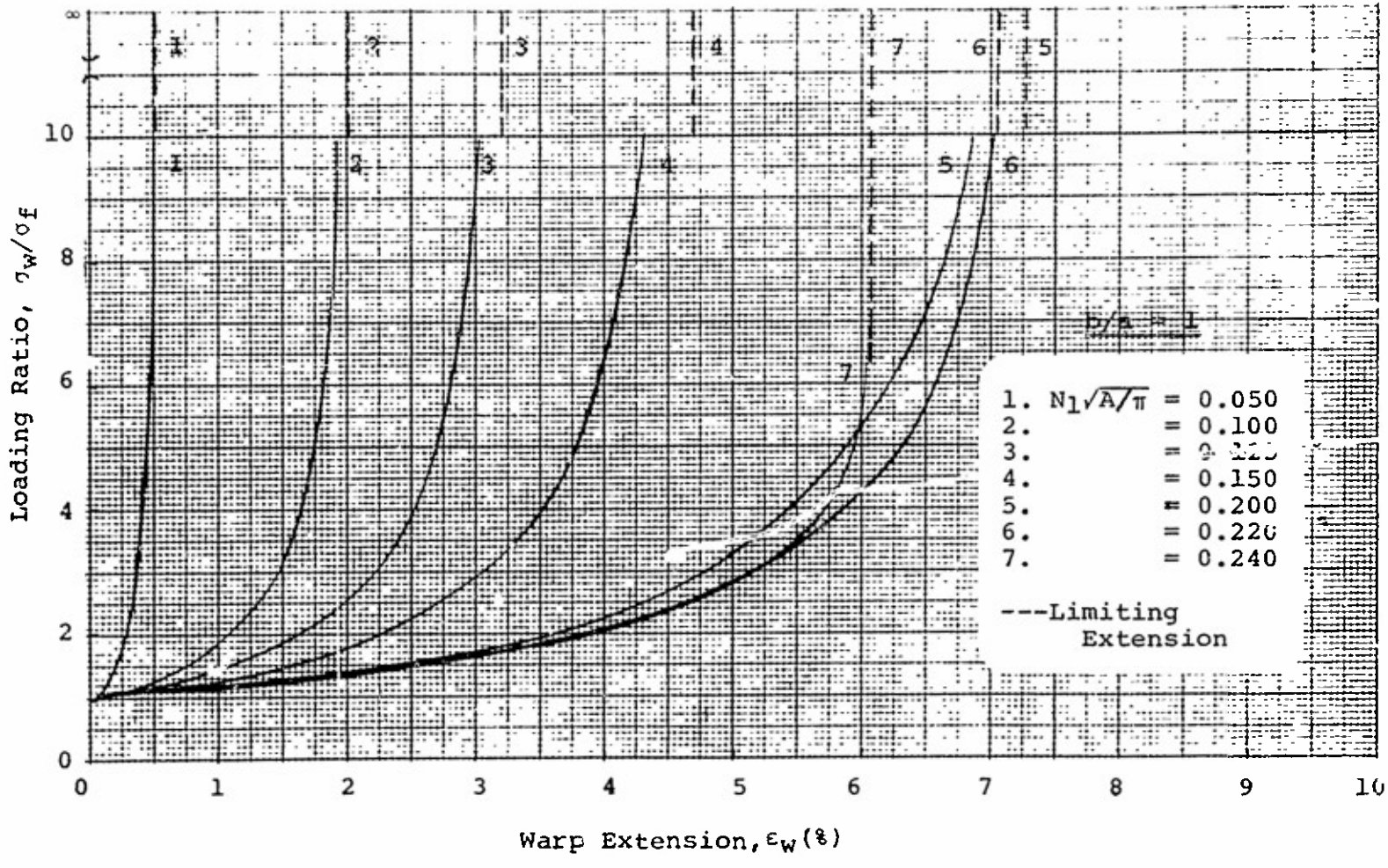

Figure 10(a). Fabric Extension in the Warp Direction: (Aspect Ratio = 1) Inextensible Yarn Initially Square Fabric

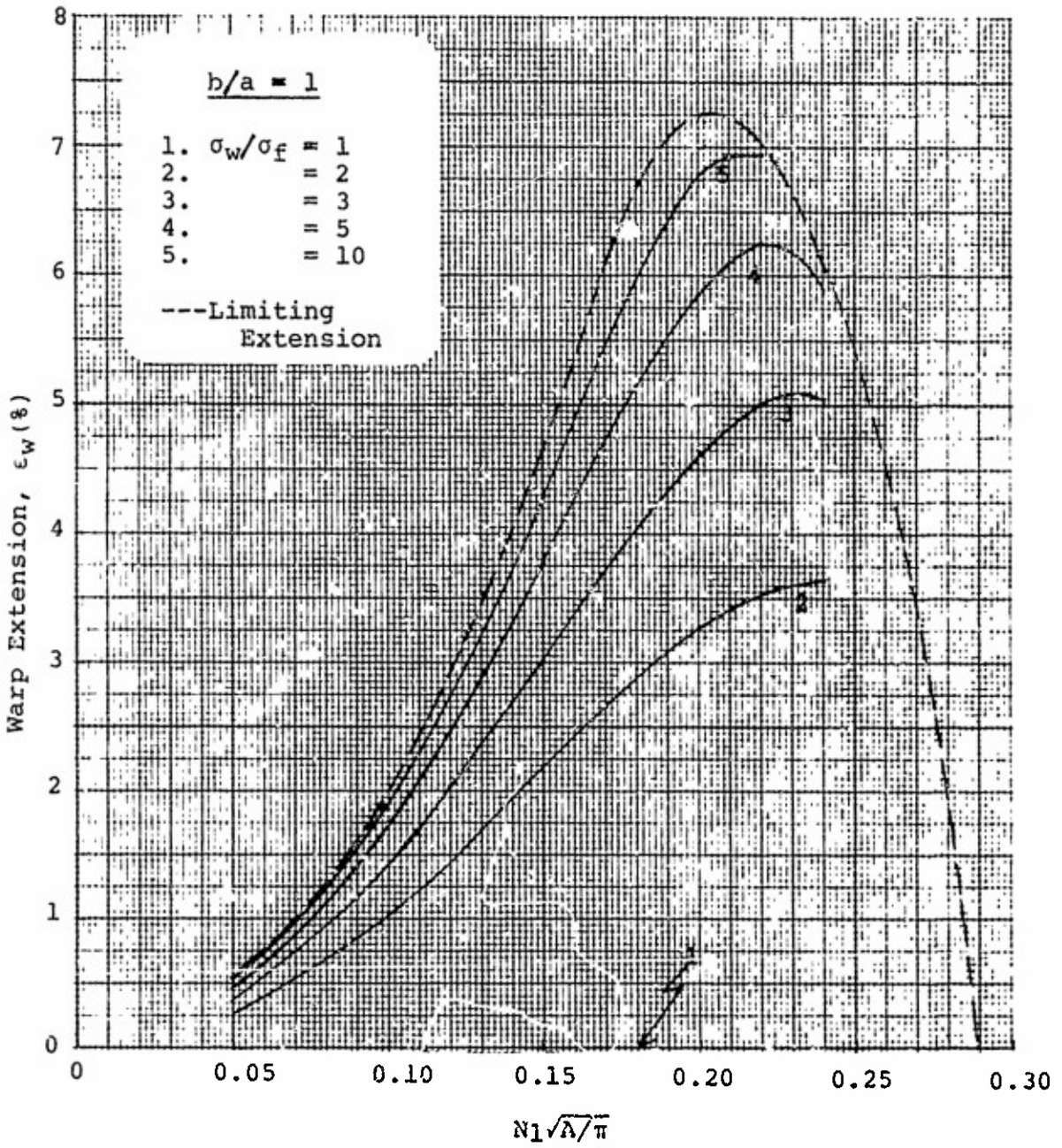

Figure 10 (b). Fabric Extension in the Warp Direction: (Aspect Ratio = 1) Inextensible Yarn Initially Square Fabric

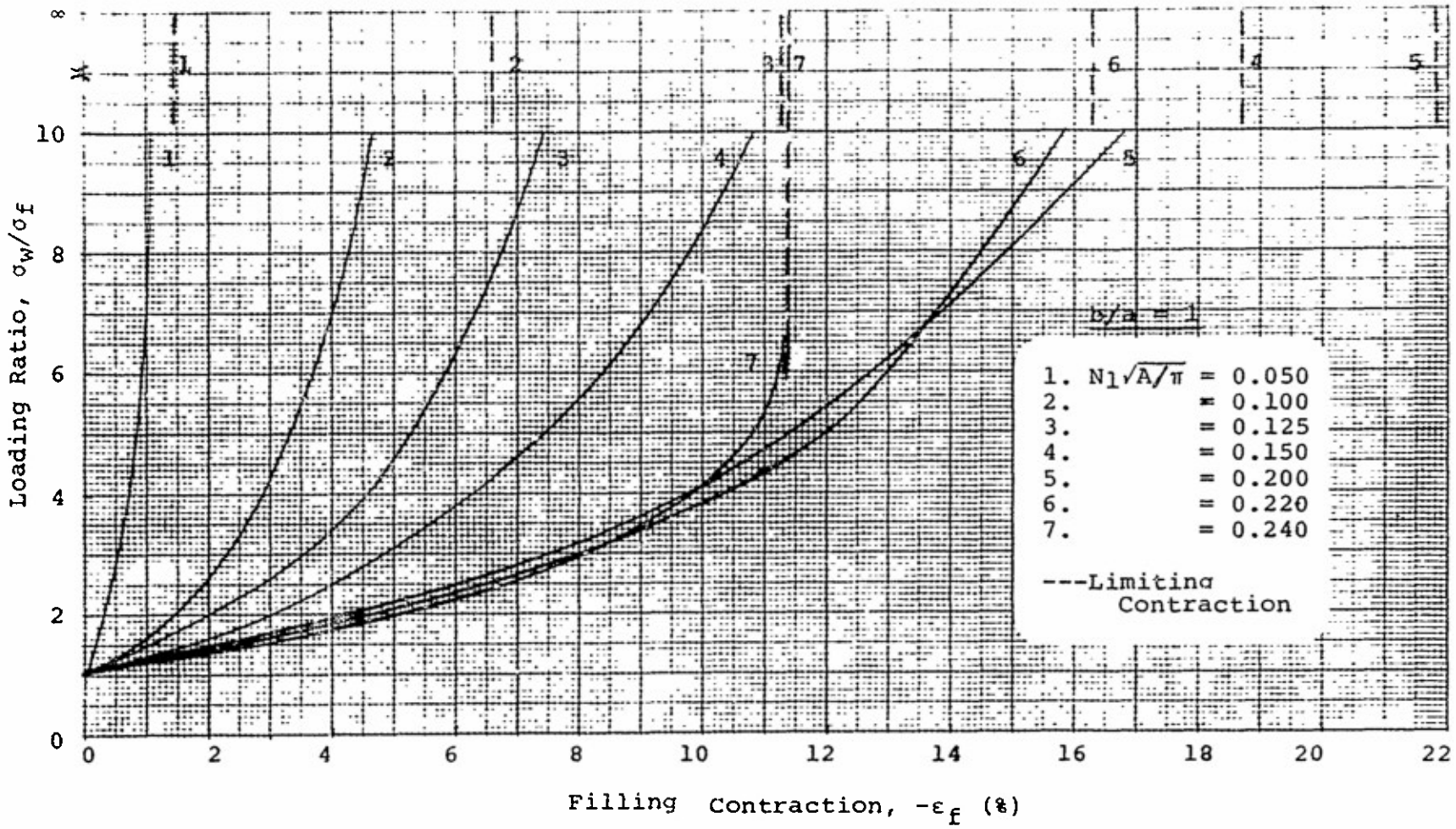

Figure 11 (a). Fabric Contraction in the Filling Direction: (Aspect Ratio = 1) Inextensible Yarn

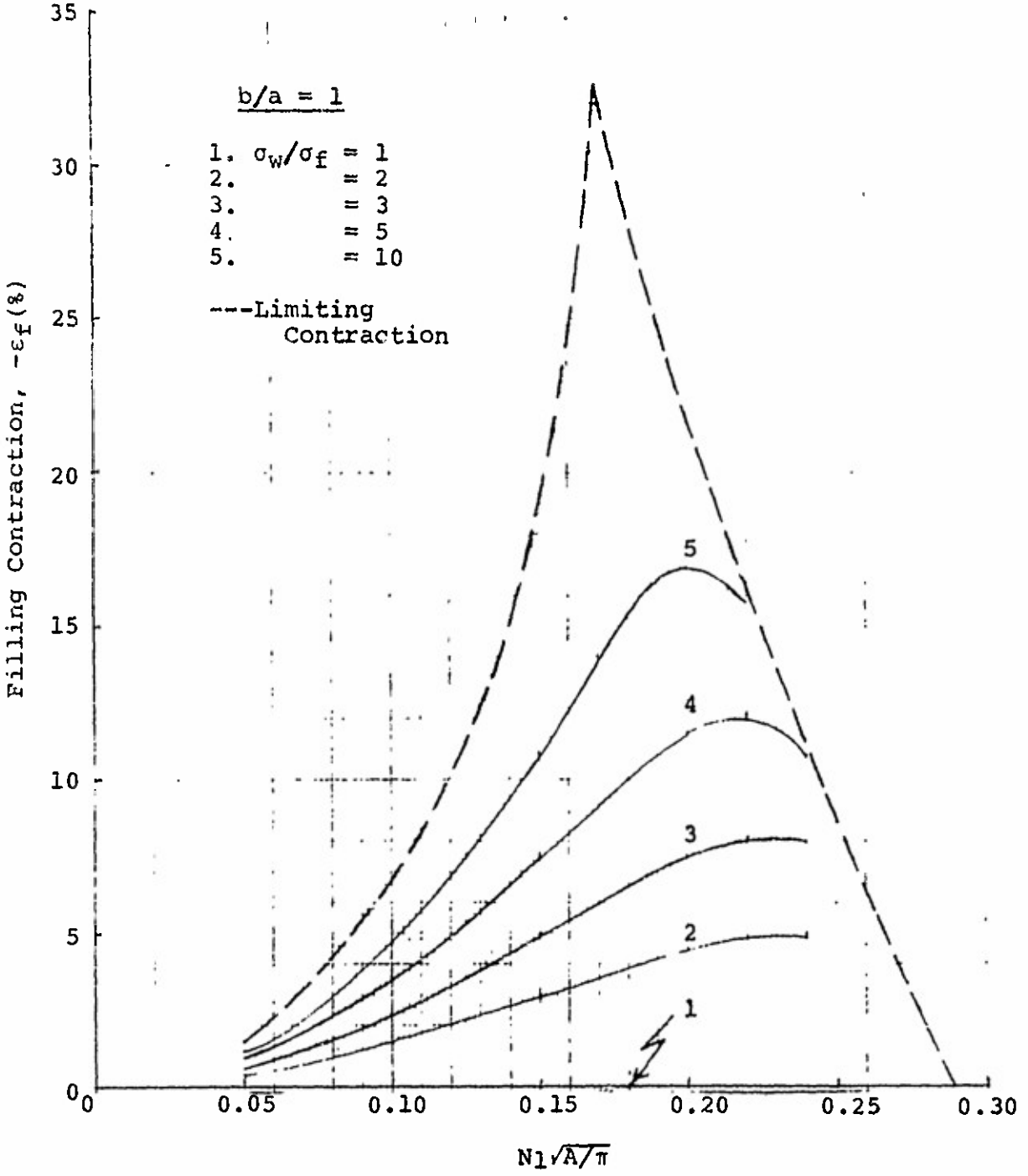

Figure 11(b). Fabric Contraction in the Filling Direction: (Aspect Ratio = 2) Inextensible Yarn

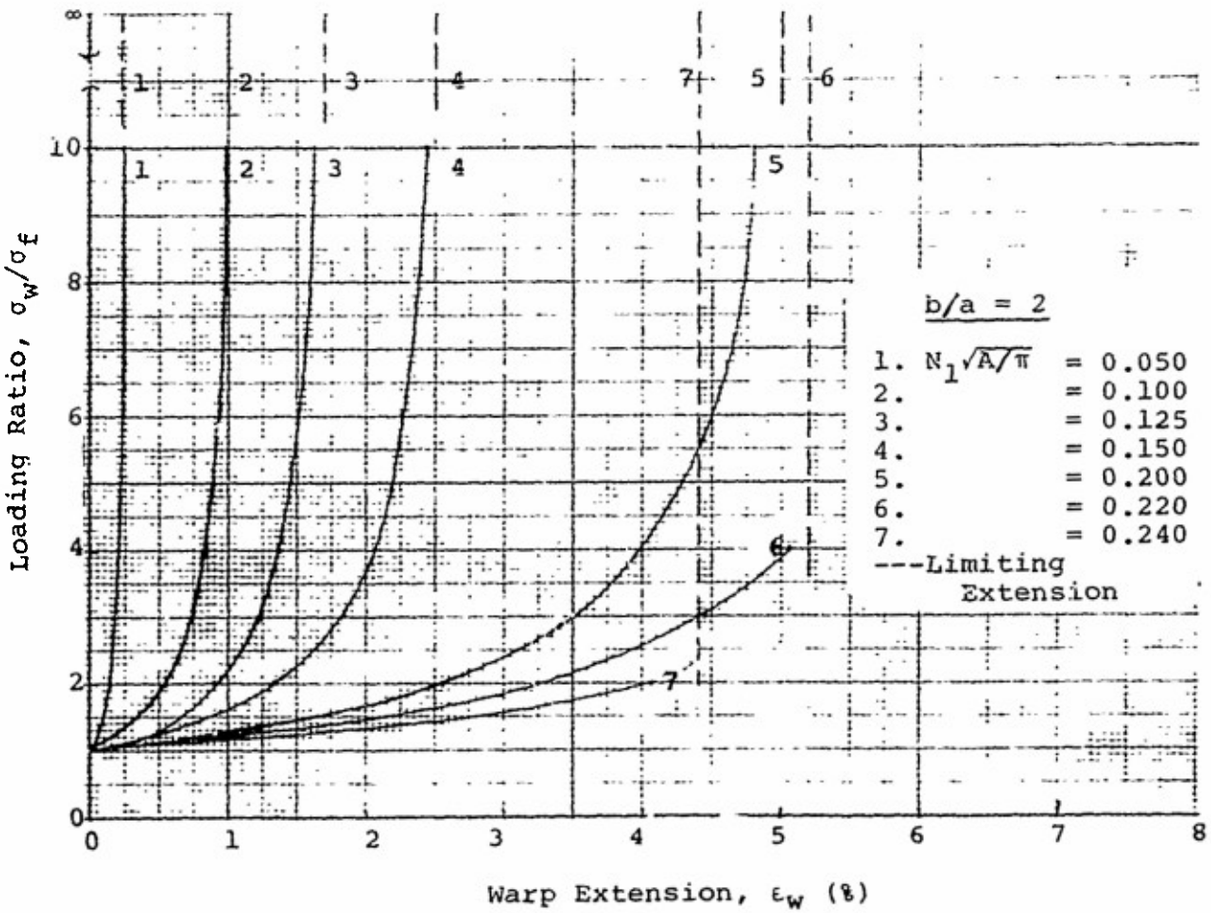

Figure 12(a). Fabric Extension in the Warp Direction: (Aspect Ratio = 2), Inextensible Yarn, Initially Square Fabric

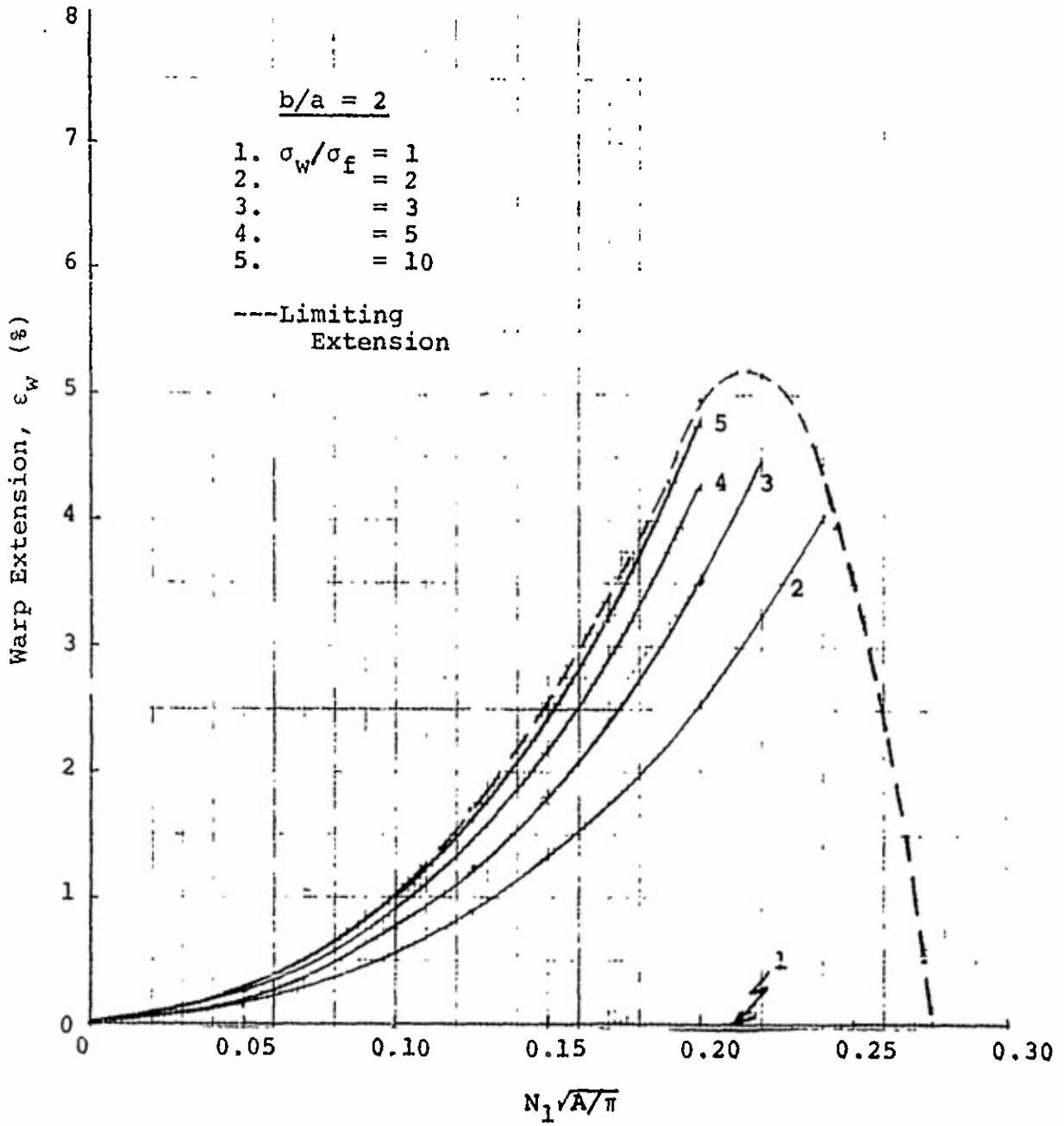

Figure 12(b). Fabric Extension in the Warp Direction: Aspect Ratio = 2), Inextensible Yarn, Initially Square Fabric

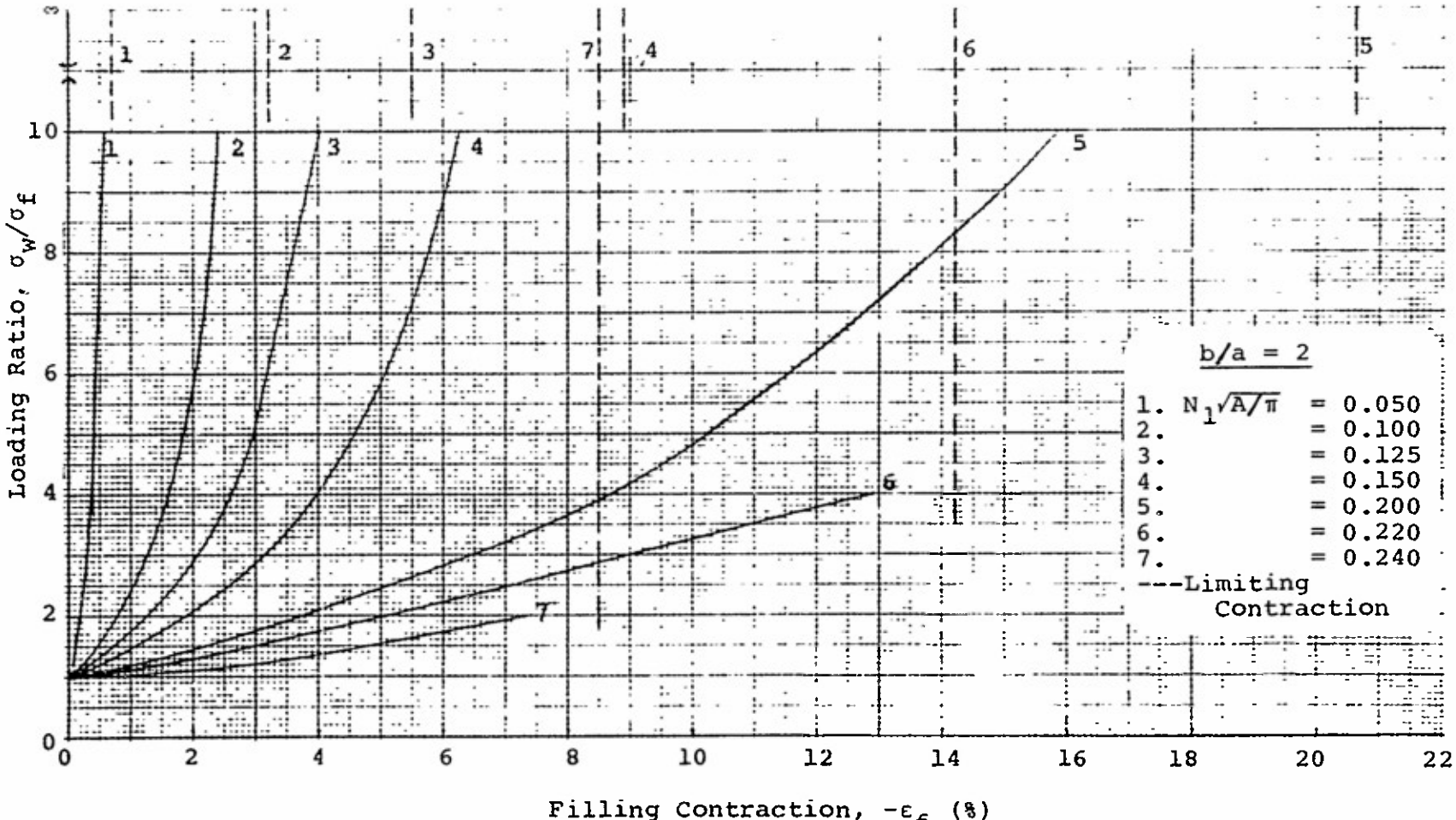

Figure 13(a). Fabric Contraction in the Filling Direction: (Aspect Ratio = 2), Inextensible Yarn, Initially Square Fabric

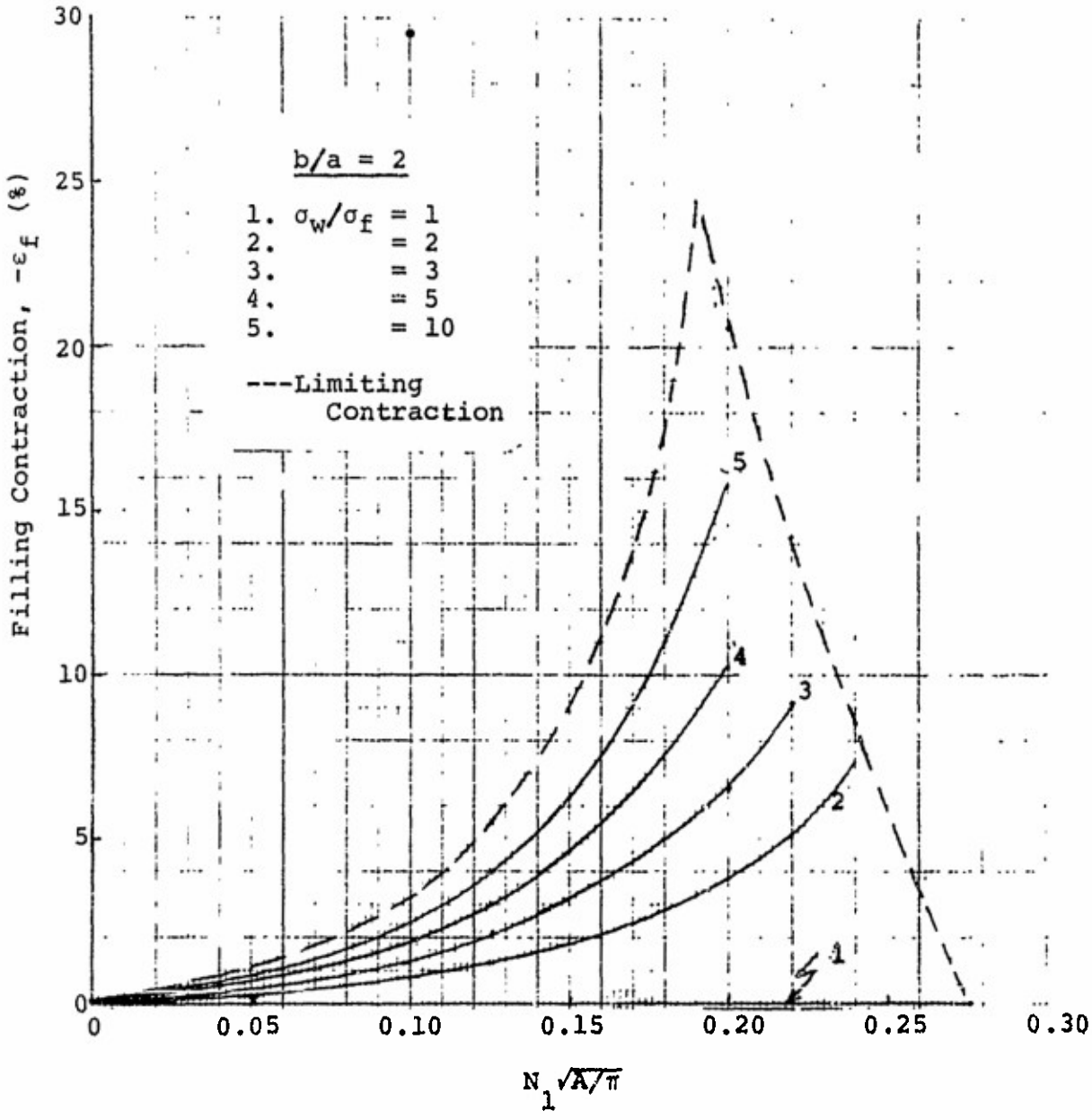

Fabric 13(b). Fabric Contraction in the Filling Direction: (Aspect Ratio = 2), Inextensible Yarn, Initially Square Fabric

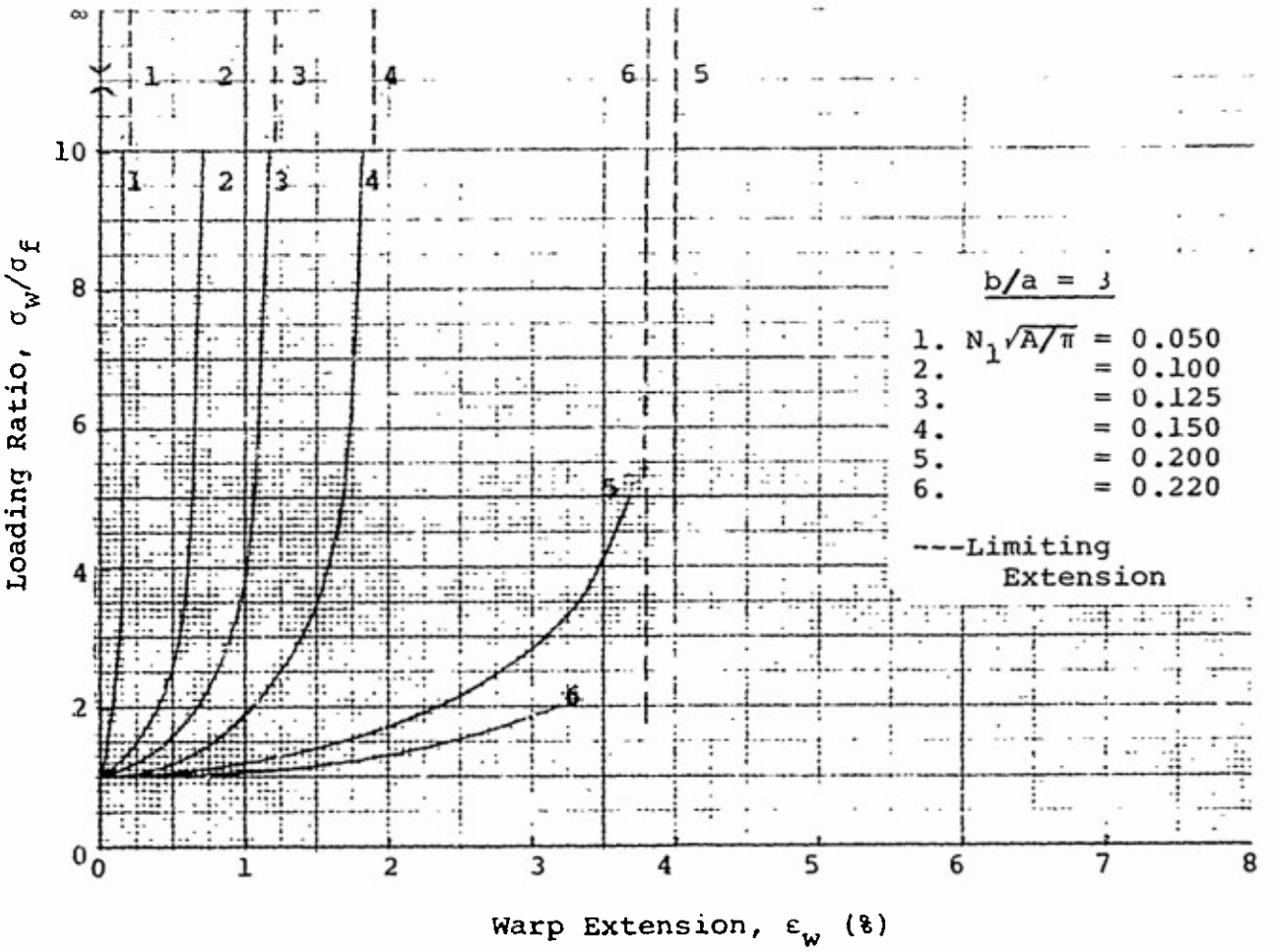

Figure 14(a). Fabric Extension in the Warp Direction: (Aspect Ratio = 3), Inextensible Yarn, Initially Square Fabric

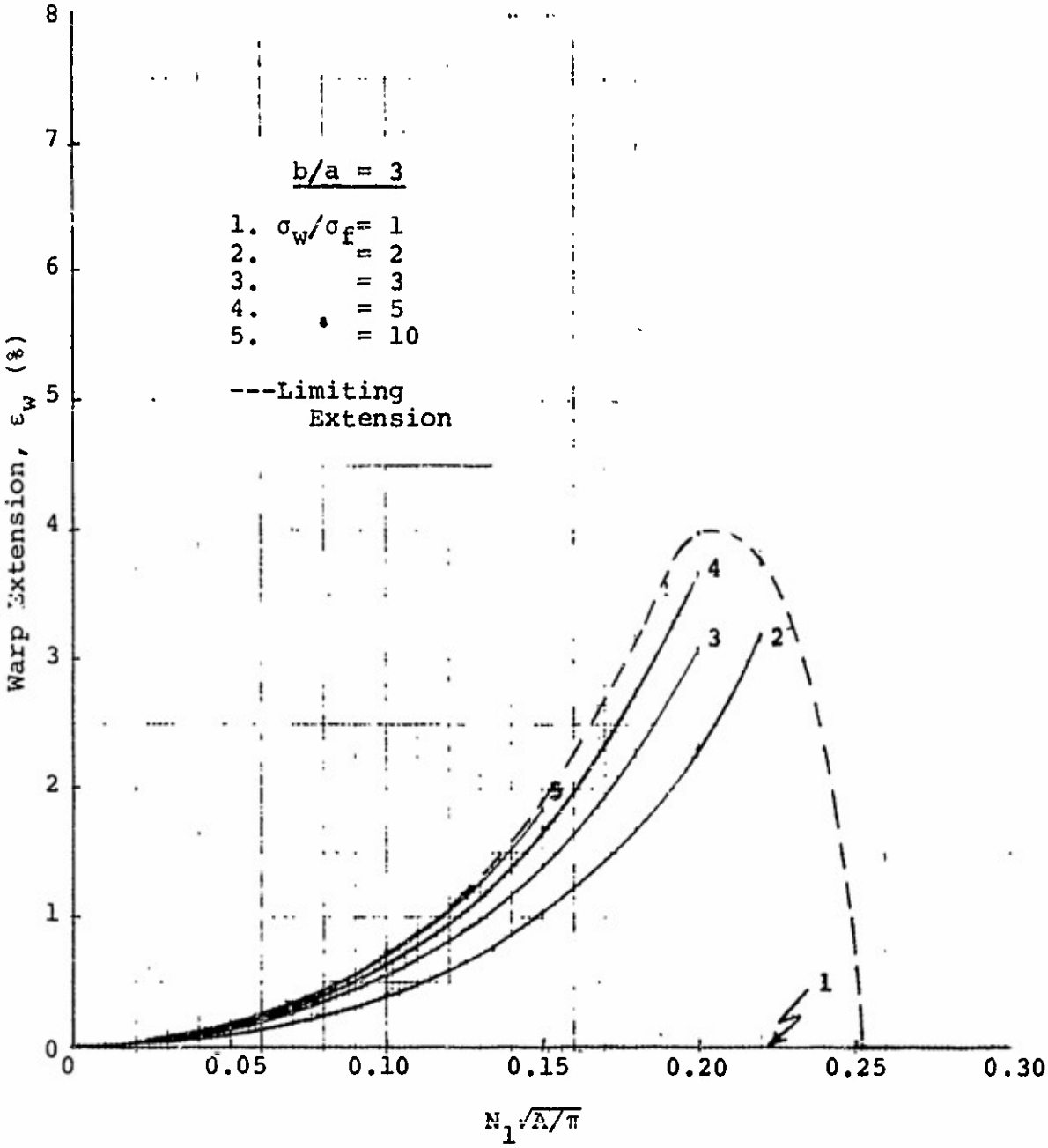

Figure 14(b). Fabric Extension in the Warp Direction: (Aspect Ratio = 3), Inextensible Yarn, Initially Square Fabric

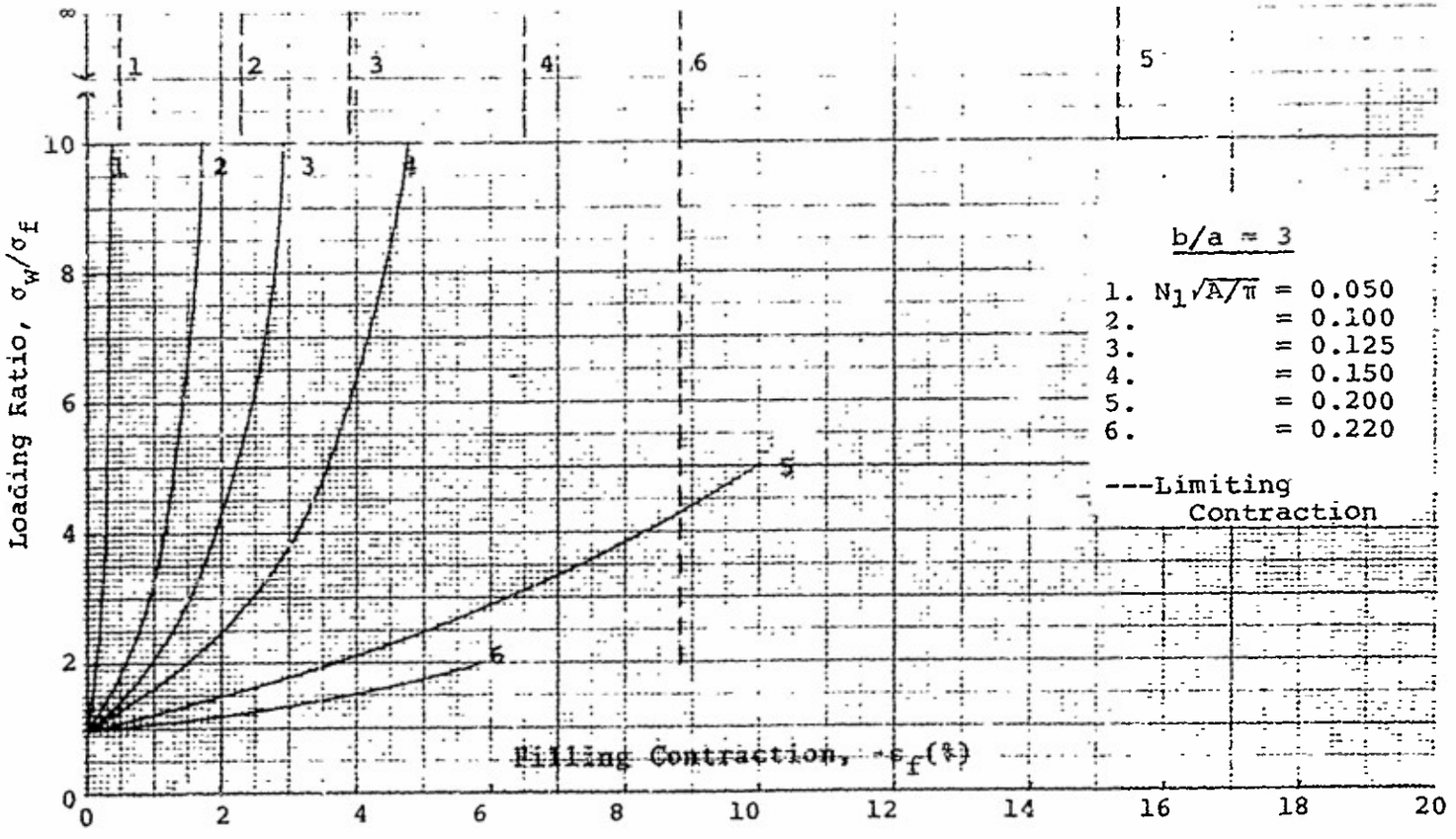

Figure 15(a). Fabric Contraction in the Filling Direction: (Aspect Ratio = 3), Inextensible Yarn, Initially Square Fabric

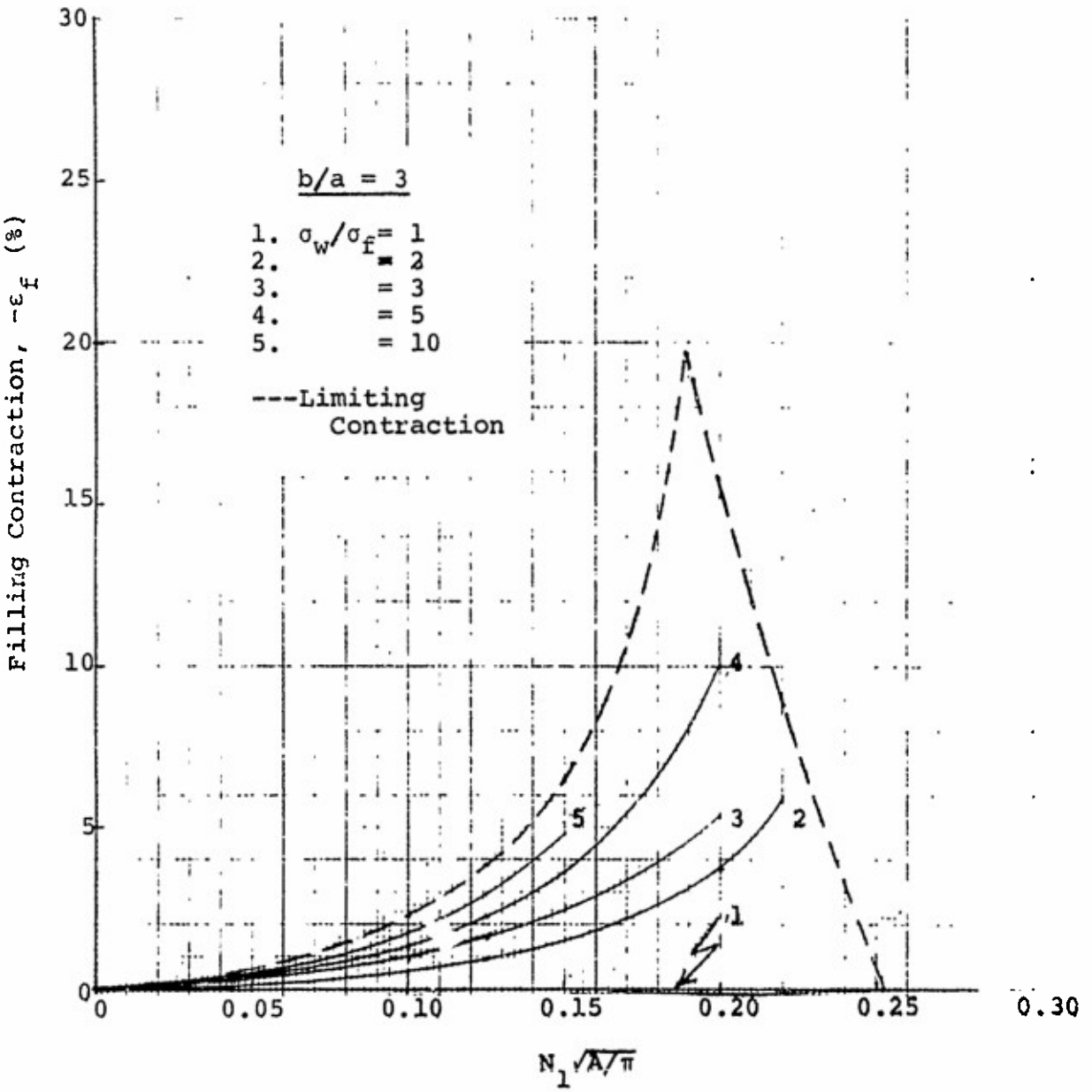

Figure 15(b). Fabric Contraction in the Filling Direction: (Aspect Ratio = 3), Inextensible Yarn, Initially Square Fabric

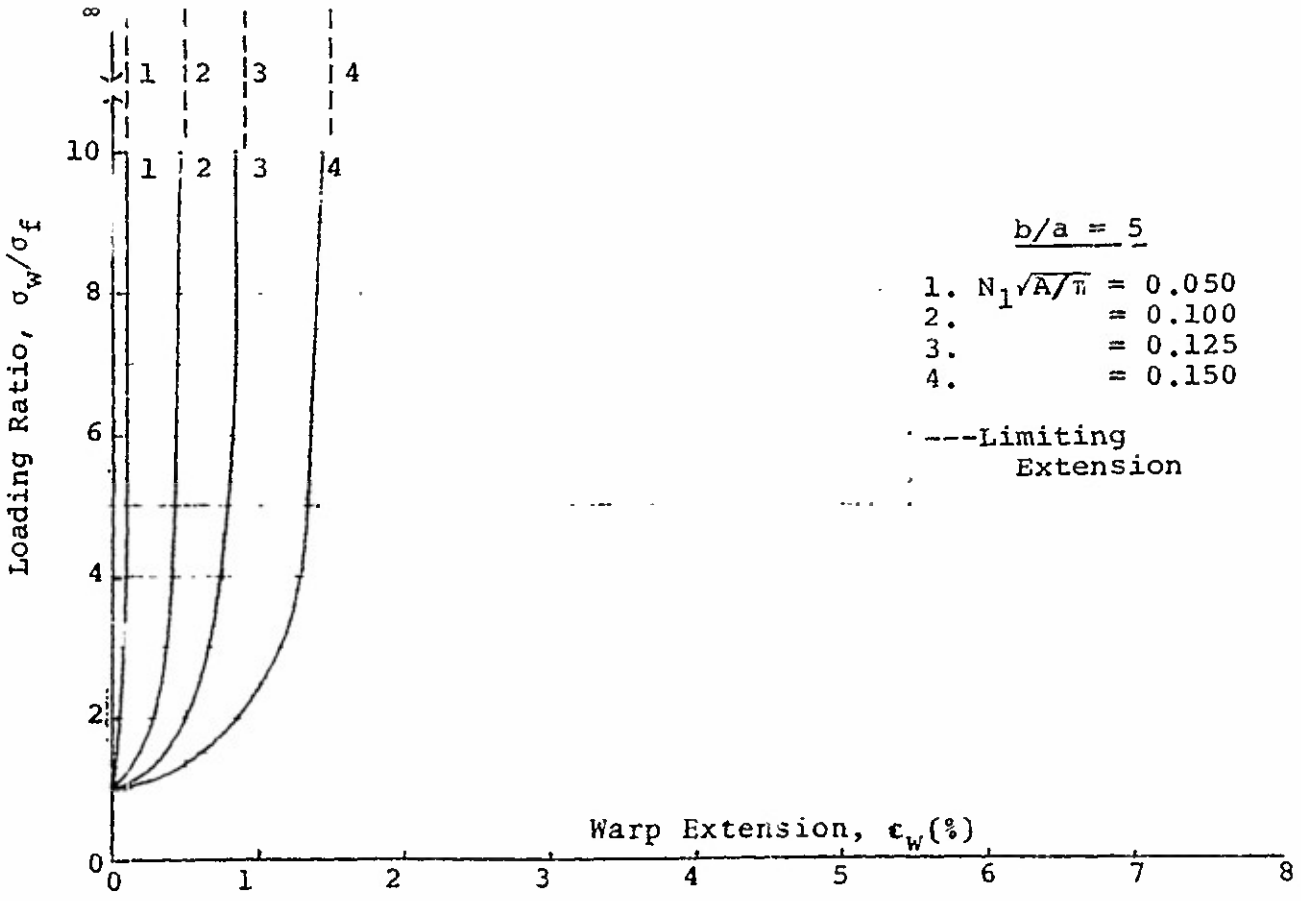

Figure 16(a). Fabric Extension in the Warp Direction: (Aspect Ratio = 5), Inextensible Yarn, Initially Square Fabric

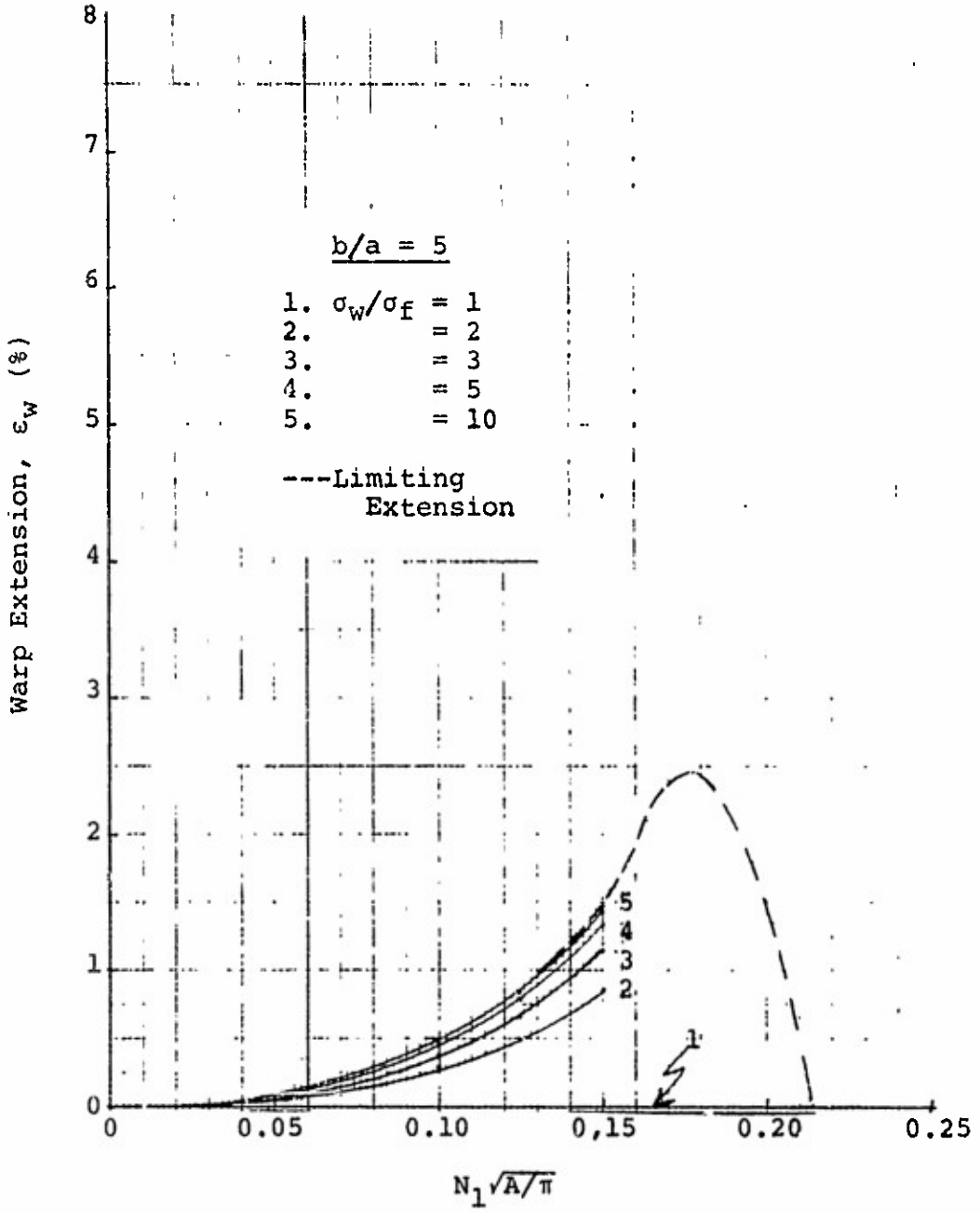

Figure 16(b). Fabric Extension in the Warp Direction: (Aspect Ratio = 5), Inextensible Yarn, Initially Square Fabric

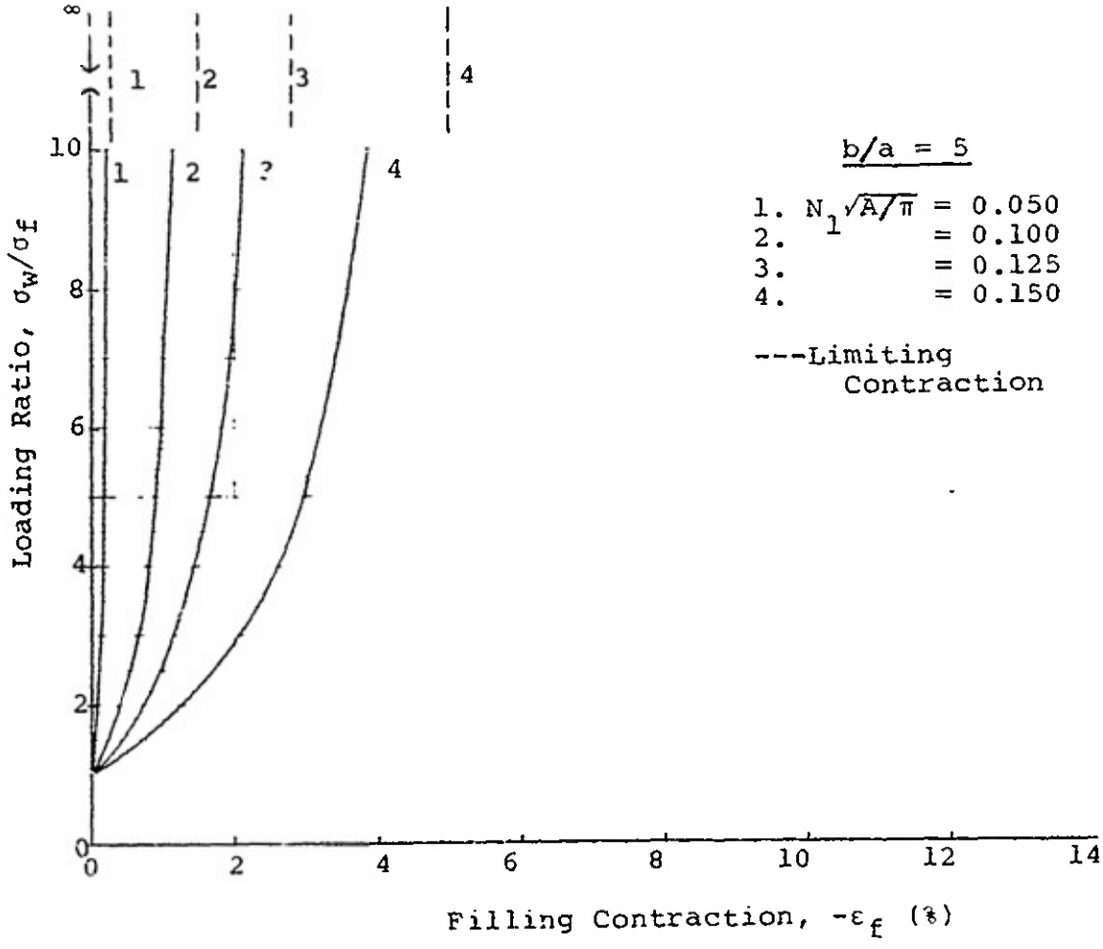

Figure 17(a). Fabric Contraction in the Filling Direction: (Aspect Ratio = 5), Inextensible Yarn, Initially Square Fabric

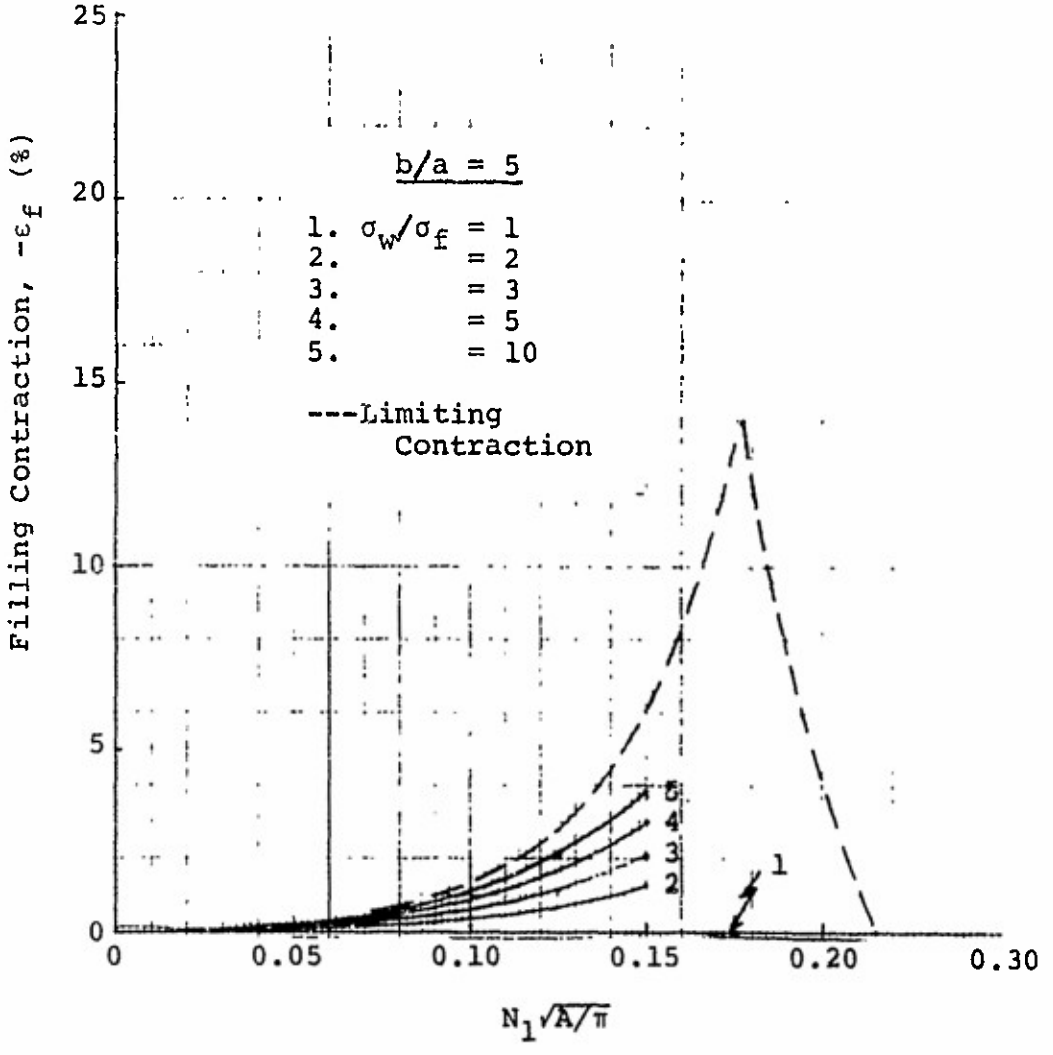

Figure 17(b). Fabric Contraction in the Filling Direction: (Aspect Ratio = 5), Inextensible Yarn, Initially Square Fabric

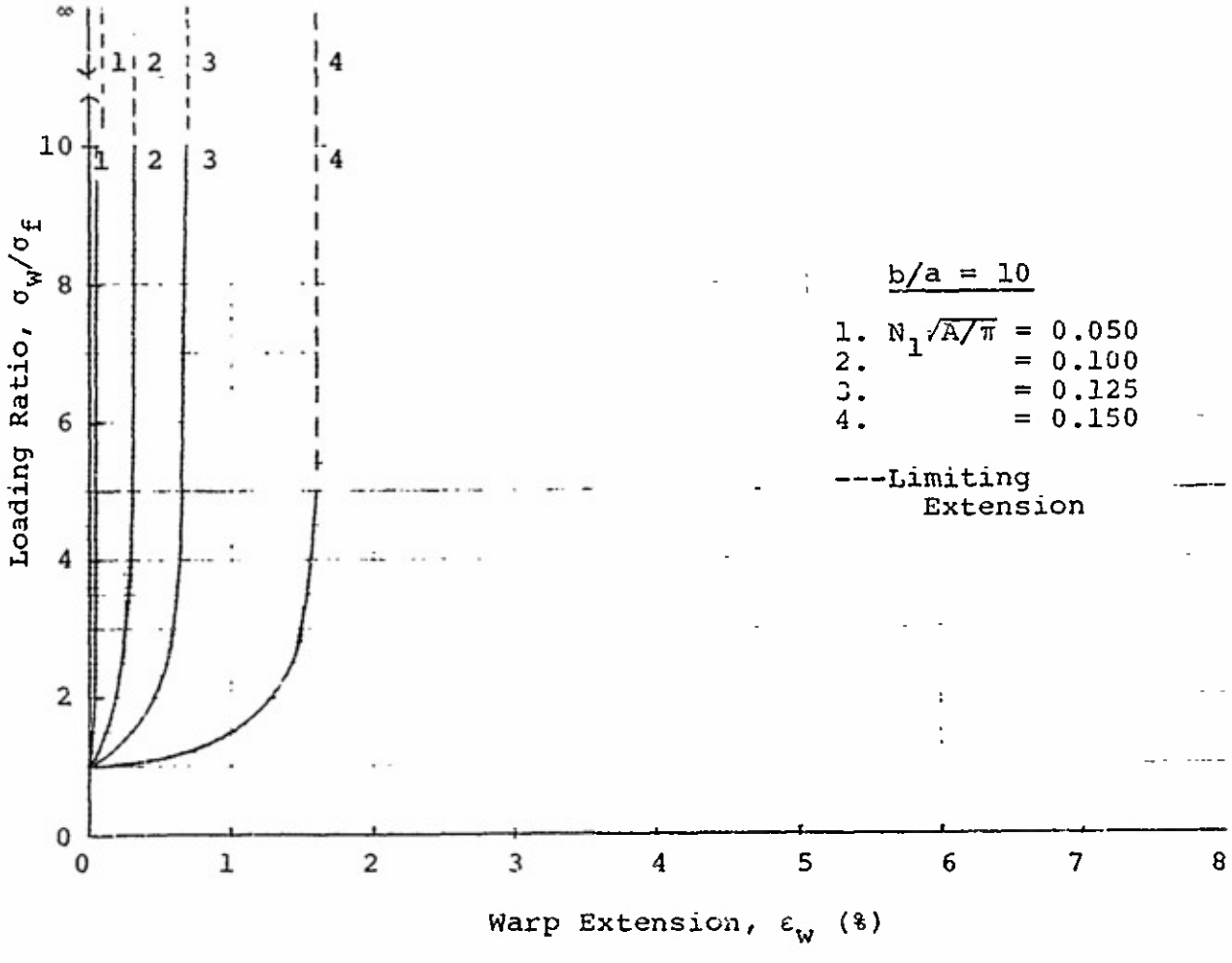

Figure 18(a). Fabric Extension in the Warp Direction: (Aspect Ratio = 10), Inextensible Yarn, Initially Square Fabric

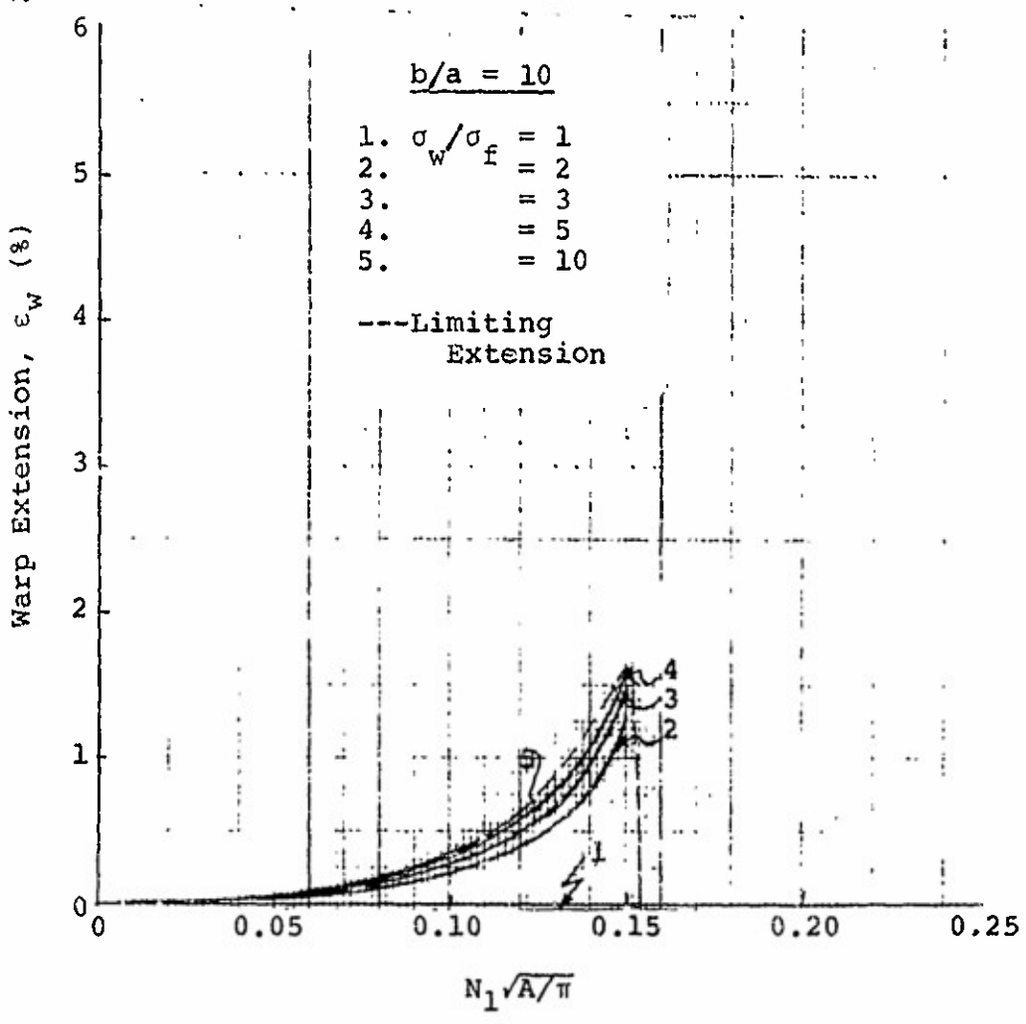

Figure 18(b). Fabric Extension in the Warp Direction: (Aspect Ratio = 10), Inextensible Yarn, Initially Square Fabric

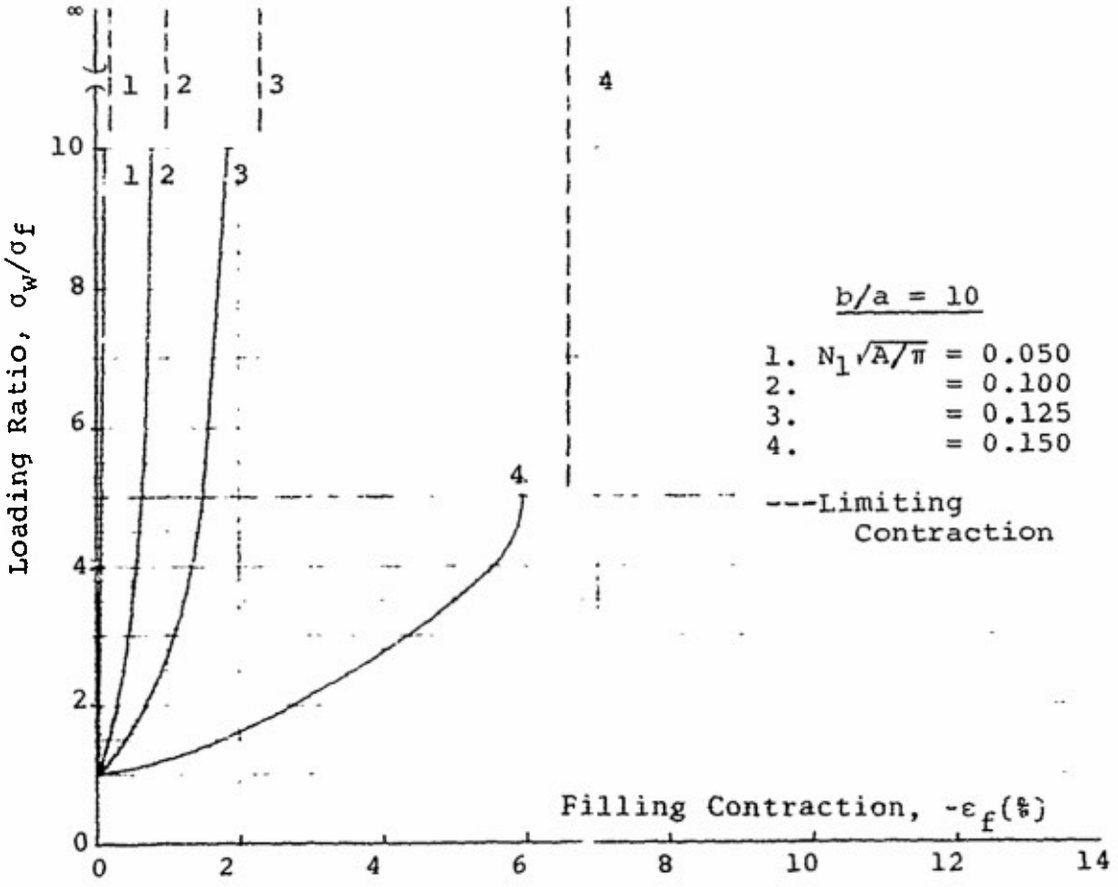

Figure 19(a). Fabric Contraction in the Filling Direction: (Aspect Ratio = 10), Inextensible Yarn, Initially Square Fabric

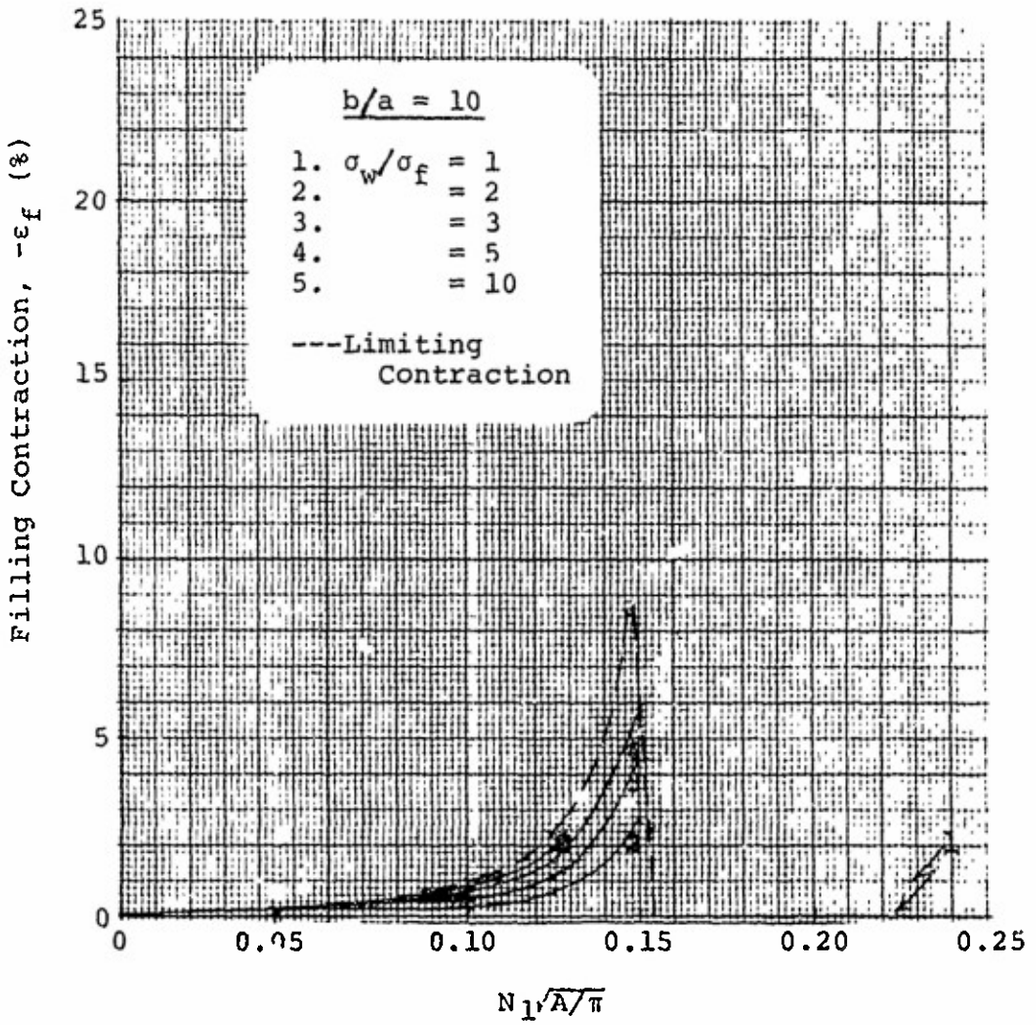

Figure 19(b). Fabri Contraction in the Filling Direc n: (Aspect Ratio = 10), Inex sible Yarn, Initially Square Fab ic

However, some exceptions to the trend of increasing stiffness with increasing aspect ratio occur for those fabric constructions initially near a limiting, or jammed, configuration. For instance, for $N_1\sqrt{A/\pi} = 0.150$ a higher level of both extension and contraction is achieved, over the range of loading ratios shown, by those fabrics having a yarn aspect ratio of 10 than by those whose yarn aspect ratio is 5.

Limiting Geometries

(1) Warp yarns pulled straight - If the length L of yarn between crossovers is long enough to accommodate this configuration, as the loading ratio σ_w/σ_f increases eventually all of the crimp will be pulled out of the warp yarns with an appropriate increase in the filling yarn crimp. Figure 20 illustrates this limiting configuration for the case in which the filling yarn length L (note $L_{1f} = L_{1w} = L$) is at a minimum value for which this geometry can be achieved (implying also a minimum yarn spacing $1/N_{2w}$). In this case the wrap angle θ_{2f} is at the maximum achievable value for racetrack yarns, namely 90°, $\pi/2$ radians. (The achievement of a wrap angle greater than 90° would be incompatible with the equations for static equilibrium.)

Thus, in order for it to be possible to achieve straight warp yarns, the length L of filling yarn between crossovers must be equal to or greater than a minimum value given by

$$L = 2(b-a)+4a(\pi/2),$$

i.e.,

$$L/a \geq 2(b/a-1)+2\pi.$$

A list of minimum values of $L/\sqrt{A/\pi}$ and the associated maximum values of $N_1\sqrt{A/\pi}$ for which this type of limiting geometry can be achieved are given in Table 2 for various yarn aspect ratios.

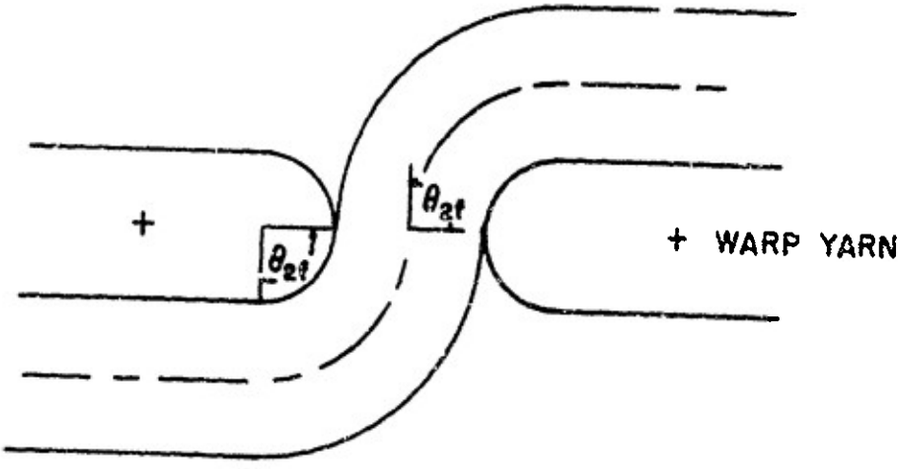

Figure 20. Warp Yarn Pulled Straight in Racetrack Yarn Fabrics (Minimum L/a)

TABLE 2

MAXIMUM VALUES OF $N_1\sqrt{A/\pi}$ FOR WHICH WARP YARNS CAN BE PULLED STRAIGHT - INITIALLY SQUARE FABRIC

b/a	Minimum $L/\sqrt{A/\pi}$	Maximum $N_1\sqrt{A/\pi}$
1	6.28	0.169
2	5.49	0.190
3	5.46	0.189
5	5.79	0.177
10	6.88	0.147

If the warp yarns are pulled straight

$$\frac{1}{N_{2f}} = L \text{ and}$$

the maximum fractional warp extension possible from crimp interchange based on the original yarn spacing is given by

$$\varepsilon_w = (N_1 L - 1)$$

or, more conveniently by

$$\varepsilon_w = [(N_1\sqrt{A/\pi})(L/\sqrt{A/\pi}) - 1].$$

Values of this maximum warp extension are tabulated in Table 3 for various degrees of initial weave tightness, various aspect ratios, and values of $N_1\sqrt{A/\pi}$ less than those listed in Table 2. The corresponding filling contraction and fabric effective Poisson's ratio are also given.

(2) Maximum filling yarn contraction - For those initial fabric constructions which cannot accommodate a complete uncrimping of the warp yarns, a jammed configuration is reached upon loading such that the fabric cannot contract further in the filling direction. As a result, the fabric cannot extend further in the warp direction unless axial yarn extension is considered. Figure 21 shows the jammed configuration for racetrack yarns. Table 2 can also be interpreted as giving the minimum values of $N_1\sqrt{A/\pi}$ for which this type of jamming can occur.

TABLE 3

MAXIMUM WARP EXTENSION POSSIBLE FROM CRIMP INTERCHANGE FOR INITIALLY SQUARE FABRICS

b/a	$N_1\sqrt{A/\pi}$	Maximum Warp Extension, ε_w (%)	Associated Filling Contraction, $-\varepsilon_f$ (%)	Effective Poisson's Ratio, μ
1	0.050	0.5	1.5	3.0
	0.100	2.0	6.7	3.3
	0.125	3.2	11.3	3.5
	0.150	4.7	19.7	4.0
	0.169	6.0	32.5	5.4
2	0.050	0.2	0.7	3.0
	0.100	1.0	3.2	3.2
	0.125	1.7	5.5	3.3
	0.150	2.5	8.9	3.5
	0.190	4.3	24.4	5.7
3	0.050	0.2	0.5	3.0
	0.100	0.7	2.3	3.1
	0.125	1.2	3.9	3.2
	0.150	1.9	6.5	3.4
	0.189	3.6	19.7	5.5
5	0.050	0.1	0.3	3.0
	0.100	0.5	1.5	3.1
	0.125	0.9	2.8	3.2
	0.150	1.5	5.0	3.4
	0.177	2.6	14.0	5.5
10	0.050	0.1	0.2	3.0
	0.100	0.3	1.0	3.1
	0.125	0.7	2.3	3.3
	0.147	1.5	8.5	5.7

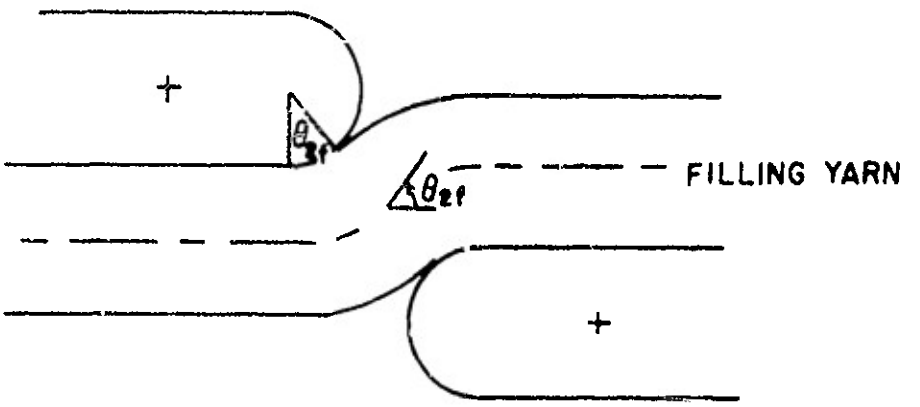

Figure 21. Maximum Filling Yarn Crimp in Racetrack-Yarn Fabrics

The distinguishing geometrical feature of this jammed state is that there is no component L_I of the length of yarn between crossovers. Therefore

$$L = 2(b-a)+4a\theta_{2f}$$

or

$$\theta_{2f} = [L/a-2(b/a-1)]/4.$$

Since equation 28 after loading becomes

$$\frac{1}{N_{2w}a} = 4\sin\theta_{2f}+2(b/a-1),$$

the maximum fractional filling yarn contraction is given by

$$\varepsilon_f = \frac{(N_1\sqrt{A/\pi})[4\sin\theta_{2f}+2(N/a-1)]-1}{[4(b/a-1)/\pi+1]^{1/2}}.$$

Values of this maximum filling contraction are tabulated in Table 4 for various aspect ratios and values of weave tightness $N_1\sqrt{A/\pi}$ greater than those listed in Table 2. The corresponding warp extension and fabric effective Poisson's ratios are also given.

The data given in Tables 3 and 4 are the maximum fabric extensions possible without yarn extension, and are plotted in Figures 10-19 as the fabric extension reached at an infinite loading ratio, i.e., $\sigma_w/\sigma_f = \infty$. For values of $N_1\sqrt{A/\pi}$ less than those given in Table 2 for each of the values of yarn aspect ratio, b/a, the yarns are pulled straight as $\sigma_w/\sigma_f \to \infty$; for $N_1\sqrt{A/\pi}$ values greater than those given in the table, the fabric extension in the warp direction is limited by the inability of the fabric to contract further in the filling direction as $\sigma_w/\sigma_f \to \infty$ because of the development of the maximum possible crimp in the filling yarns. When $N_1\sqrt{A/\pi}$ is equal to the values given in Table 2, the warp yarns are pulled straight and the maximum crimp is developed in the filling yarn. The values of filling contraction given in Table 4 could also be used to extrapolate somewhat approximately those curves in Figures 11-19 which are terminated at loading ratios less than 10 to the loading ratio at which the fabric actually reaches a jammed state.

TABLE 4

MAXIMUM FILLING CONTRACTION POSSIBLE FROM CRIMP INTERCHANGE FOR INITIALLY SQUARE FABRICS

b/a	$N_1\sqrt{A/\pi}$	Maximum θ_{2f} (radians)	$N_{2w}\sqrt{A/\pi}$	Maximum Filling Contraction $-\varepsilon_f$ (%)	Associated Warp Extension, ε_w (%)	Effective Poisson's Ratio μ
1	0.169	1.5708	0.250	32.5	6.0	5.4
	0.200	1.3581	0.256	21.8	7.3	3.0
	0.220	1.2577	0.263	16.3	7.0	2.3
	0.240	1.1774	0.271	11.3	6.0	1.9
2	0.190	1.5708	0.251	24.4	4.3	5.7
	0.200	1.4813	0.252	20.6	5.0	4.2
	0.220	1.3255	0.256	14.2	5.2	2.8
	0.240	1.2013	0.263	8.5	4.4	1.9
3	0.190	1.5708	0.235	19.7	3.6	5.5
	0.200	1.4525	0.236	15.3	4.0	3.9
	0.220	1.2612	0.241	8.8	3.8	2.3
10	0.147	1.5708	0.160	8.5	1.5	5.7
	0.150	1.4790	0.160	6.6	1.6	4.2

For a specified yarn aspect ratio and yarn cross-sectional area, the maximum number of ends which can be accommodated in an initially square fabric can be found by a similar procedure. When the fabric is initially "jammed",

$$L = 2(b-a)+4a\theta_1.$$

Combining this expression with Equation 21

$$\theta_1 = 1.047 \text{ radians or } 60°$$

independent of the yarn aspect ratio. This value of θ_1 in combination with Equations 20 and 21 determines the end points of the curves in Figures 2 to 9. The values of $N_1\sqrt{A/\pi}$ in Figure 5 corresponding to $\theta_1 = 60°$ for the various yarn aspect ratios determine the point where the $\sigma_w/\sigma_f = \infty$ curves in Figures 10(b) - 19(b) intersect the abscissa. The maximum $N_1\sqrt{A/\pi}$'s possible in an initially square fabric are shown in Figure 22 as a function of yarn aspect ratio.

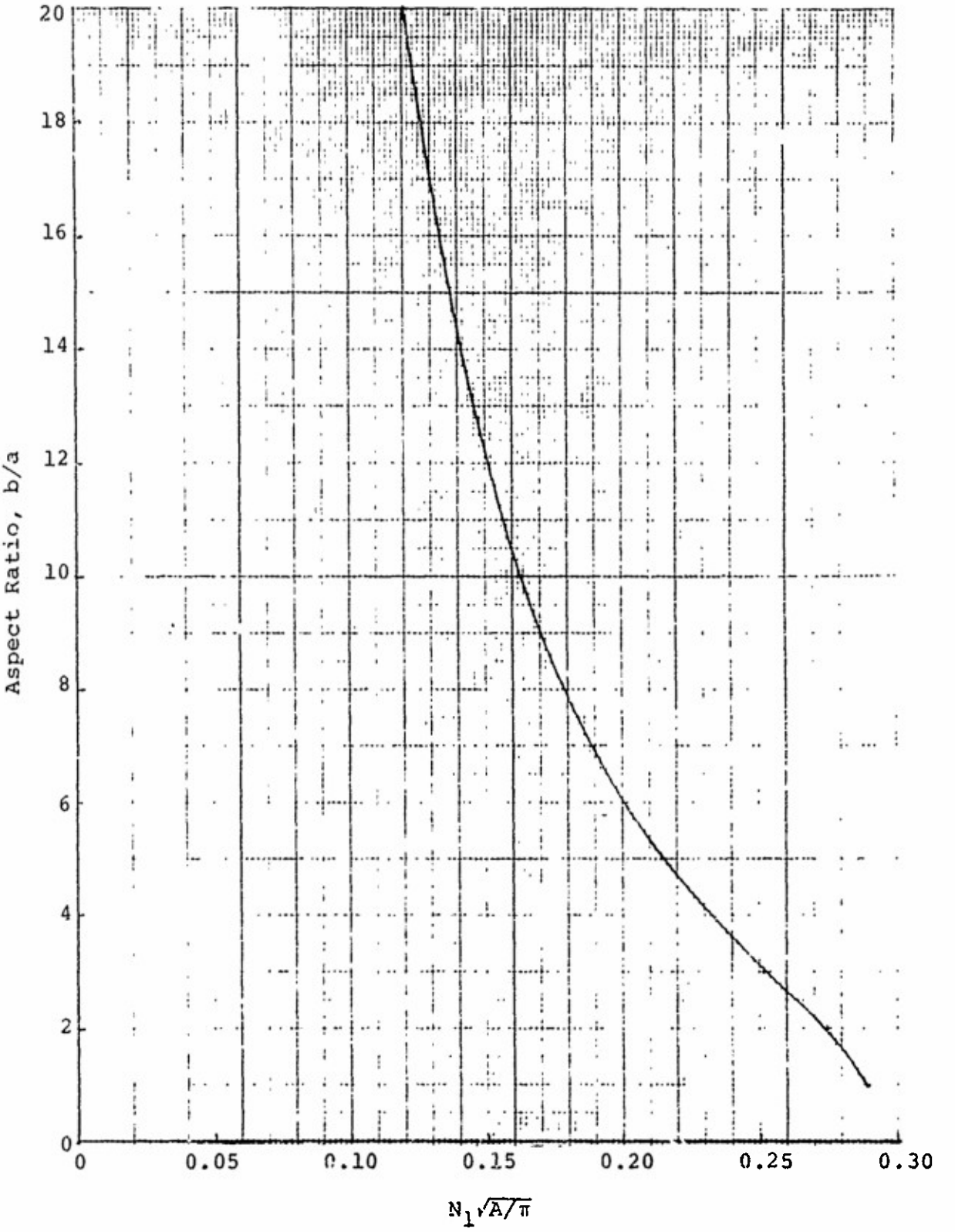

Figure 22. Maximum Number of Yarns Acccmmodatable In Initially Square Fabrics as a Function of Yarn Aspect Ratio

In Figures 14-19, curves are not plotted for the highest values of $N_1\sqrt{A/\pi}$ that appear possible from Figure 22. This is because for the seemingly missing values of $N_1\sqrt{A/\pi}$, the fabric extensions attain the limiting values at loading ratios σ_w/σ_f less than 2, the lowest value for which results were computed.

As also shown in Figures 10 and 11, the fabric extension in the warp direction and contraction in the filling direction increase with increasing $N_1\sqrt{A/\pi}$ up to an $N_1\sqrt{A/\pi}$ between 0.200 - 0.240 and 0.169 - 0.240, respectively for fabrics with a yarn aspect ratio b/a = 1, depending on the loading ratio. For greater $N_1\sqrt{A/\pi}$ values, the fabrics exhibit decreasing extension in the warp direction and decreasing contraction in the filling direction with increasing $N_1\sqrt{A/\pi}$. The value $N_1\sqrt{A/\pi}$ for which the greatest fabric extensions are obtained decreases with increasing loading ratio (see Figures 10(b) and 11(b)).

A similar trend with increasing $N_1\sqrt{A/\pi}$ is not evident for values of the yarn aspect ratio greater than b/a = 1 and loading ratios of 10 or less. This may be because such a trend does not exist or because results were not obtained for sufficiently high values of $N_1\sqrt{A/\pi}$ to make it evident. For $\sigma_w/\sigma_f = \infty$ the fabric extension in the warp direction and contraction in the filling direction for all values of yarn aspect ratio investigated increases with increasing $N_1\sqrt{A/\pi}$ up to a certain value of the parameter and then decreases for higher values. The $N_1\sqrt{A/\pi}$ for which the greatest fabric extensions are obtained increases with increasing yarn aspect ratio up to a b/a = 3 and then decreases for higher values of b/a.

As would be anticipated the $N_1\sqrt{A/\pi}$ values for which the fabric exhibits the greatest contraction in the filling direction coincide with the values given in Table 2. Fabrics with greater $N_1\sqrt{A/\pi}$ are closer to the jammed state initially and therefore reach this limiting geometry sooner upon loading. For b/a = 1, 2 and 3, the maximum warp extension occurs at $N_1\sqrt{A/\pi}$ values greater than those given in Table 2. However, for b/a = 5 and 10, the maximum warp extension occurs at values close to those given in Table 2.

(3) Contact between adjacent warp yarns at the fabric mid-plane -This type of limiting configuration cannot initially arise in a square fabric composed of racetrack yarns since it would require an impossible solution to Equation 20. Upon loading the first and second types of limiting

geometry are reached of values for the filling contraction lower than would be required for the third type of limitation given by $\varepsilon_f = 100[2N_1 a(b/a) - 1]$.

Effective Fabric Poisson's Ratio

The ratio of the fabric contraction in the filling direction to the corresponding extension in the warp direction, i.e., the effective Poisson's ratio, μ, of the fabric ($\mu = -\varepsilon_f/\varepsilon_w$), is plotted in Figures 23 - 27. It is recognized that this is a non-standard definition of Poisson's ratio [1] and should be distinguished from the classical Poisson's ratio.

The Poisson's ratios are given in Figures 23(a), 24(a), 25(a), 26(a), and 27(a) as a function of $N_1\sqrt{A/\pi}$ for various values of σ_w/σ_f and b/a. Similarly, they are given in Figures 23(b), 24(b), 25(b), 25(b), 26(b), 27(b) as a function of σ_w/σ_f for the various values of $N_1\sqrt{A/\pi}$ and b/a. The Poisson's ratios at an infinite loading ratio are also noted.

The slopes of the curves giving the fabric extension in the warp direction and contraction in the filling direction for $\sigma_w/\sigma_f = \infty$ appear to be equal as $N_1\sqrt{A/\pi}$ approaches the values for an initially jammed construction (see Figures 10(b), 11(b), 12(b), and 13(b), etc.). This indicates (via L'Hôpital's rule) that the Poisson's ratio for $\sigma_w/\sigma_f = \infty$ at the $N_1\sqrt{A/\pi}$ for which the fabric is initially jammed is 1. Consequently, the $\sigma_w/\sigma_f = \infty$ curves in Figure 23(b), 24(b) --- 27(b) have been extrapolated to this point.

As shown in Figures 23 through 27, the Poisson's ratio increases with increasing loading ratio. It also increases continuously with increasing $N_1\sqrt{A/\pi}$ for $b/a > 1$ and $\sigma_w/\sigma_f < \infty$. For $b/a = 1$, μ initially increases with increasing $N_1\sqrt{A/\pi}$, but shows evidence of a decrease at high values of $N_1\sqrt{A/\pi}$. For $\sigma_w/\sigma_f = \infty$ and all values of b/a, the Poisson's ratio increases with increasing $N_1\sqrt{A/\pi}$ up to the values of $N_1\sqrt{A/\pi}$ given in Table 2. At larger $N_1\sqrt{A/\pi}$, μ decreases with increasing $N_1\sqrt{A/\pi}$. The max. .m Poisson's ratio is roughly the same for all yarn aspect ratios. Additionally, at the lower values of $N_1\sqrt{A/\pi}$, μ is approximately the same for all b/a's. At higher $N_1\sqrt{A/\pi}$'s differences are evident.

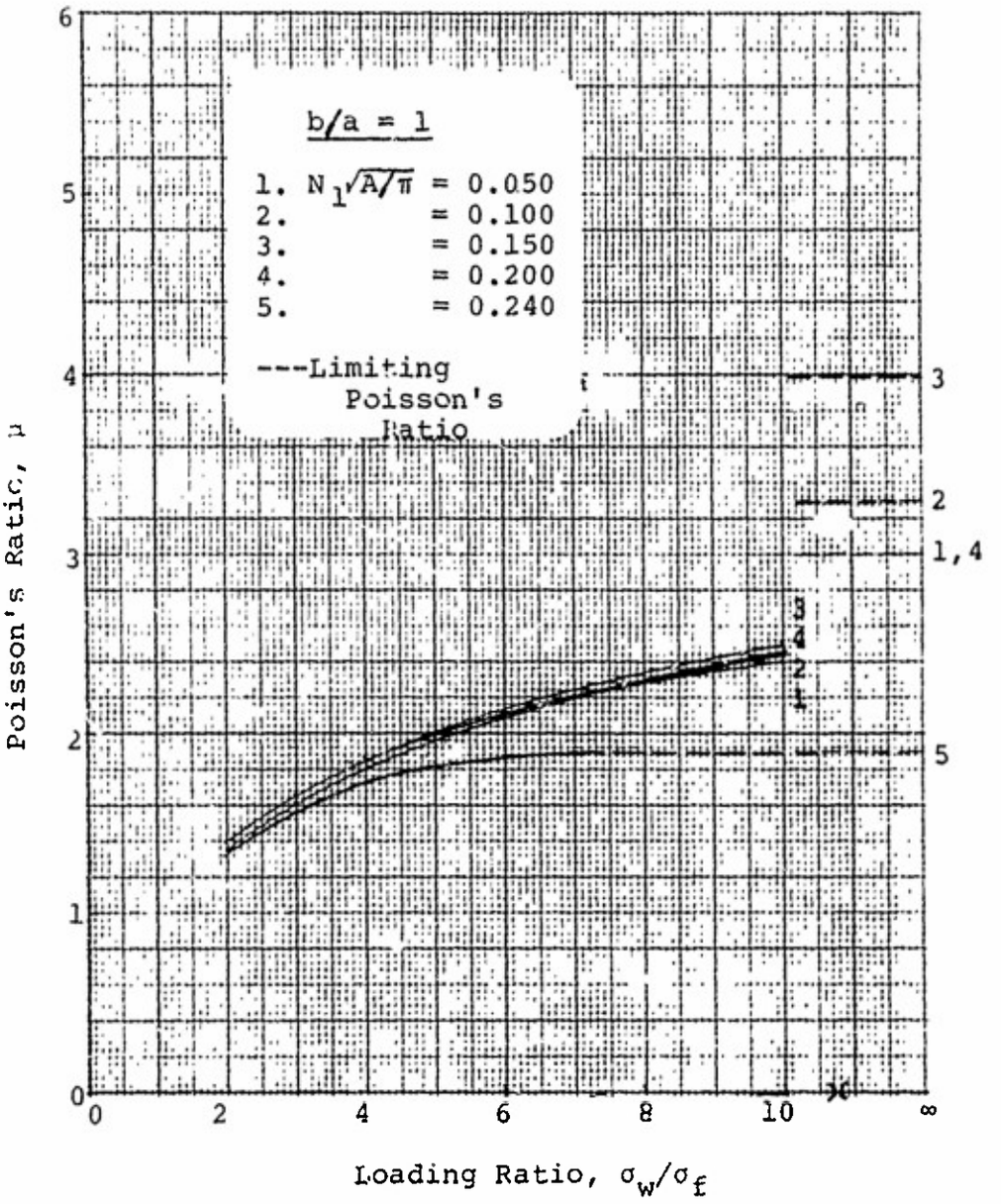

Figure 23(a). Poisson's Ratio: (Aspect Ratio = 1) Inextensible Yarn, Initially Square Fabric

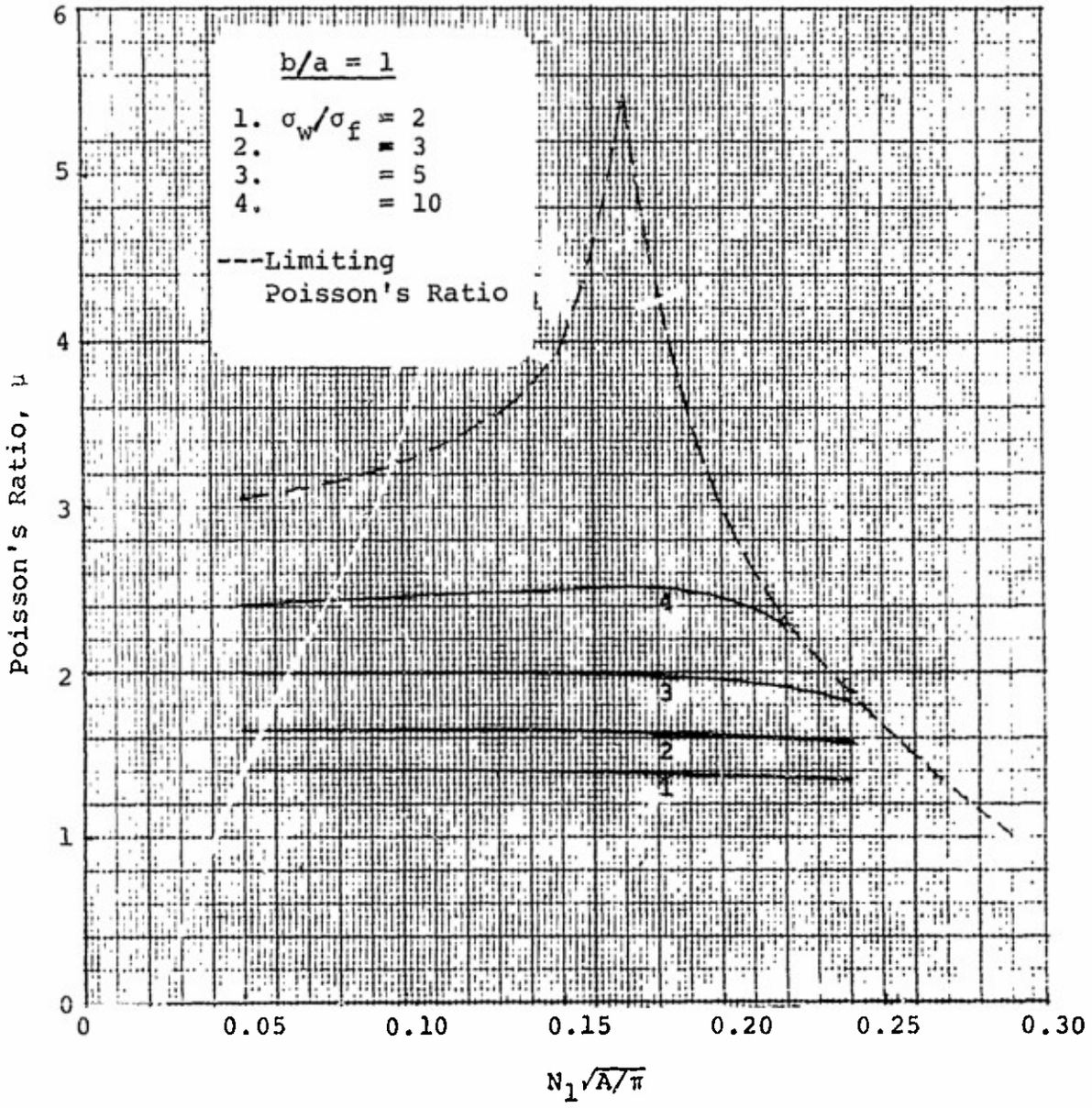

Figure 23(b). Poisson's Ratio: (Aspect Ratio = 1) Inextensible Yarn, Initially Square Fabric

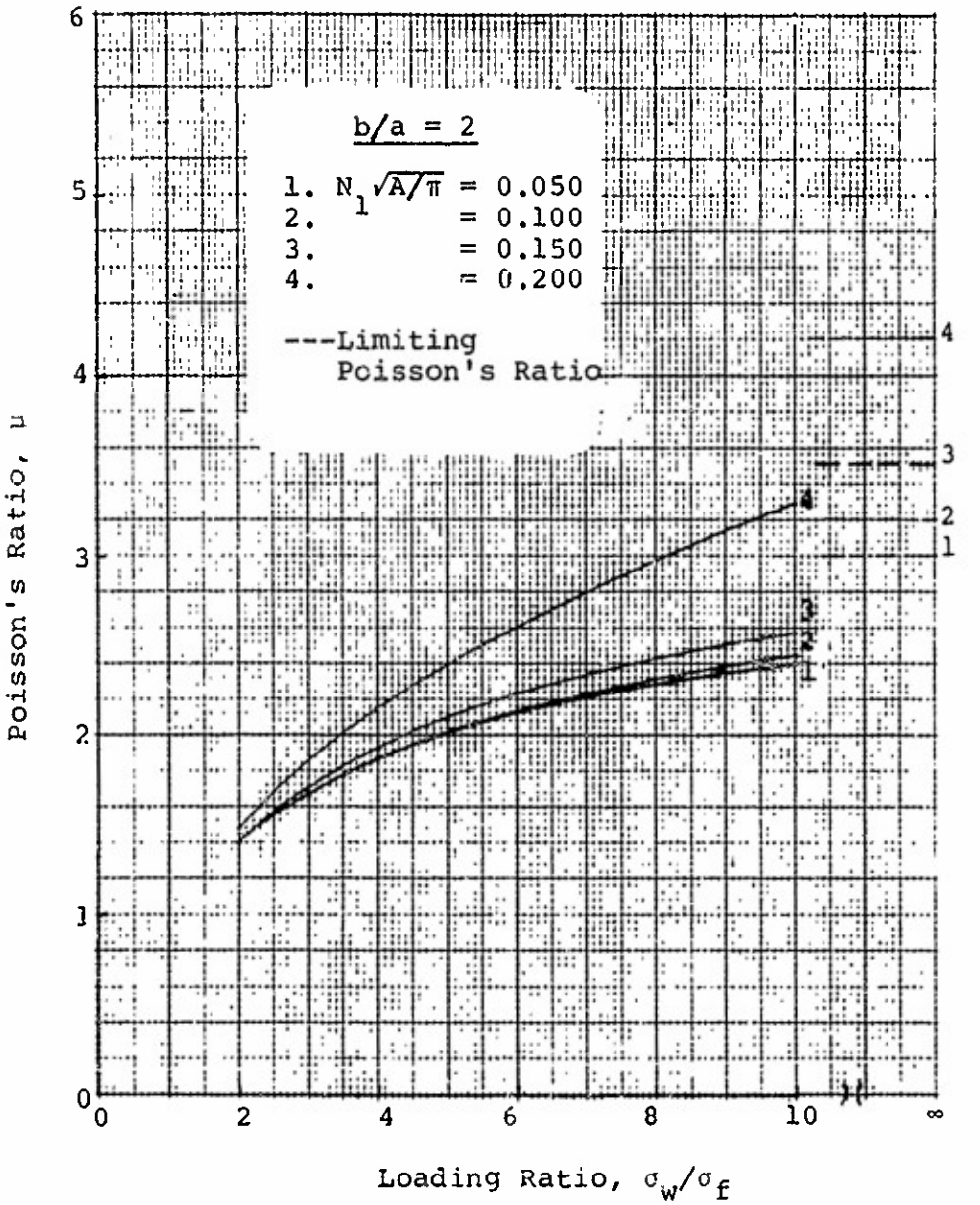

Figure 24(a). Poisson's Ratio: (Aspect Ratio = 2), Inextensible Yarn, Initially Square Fabric

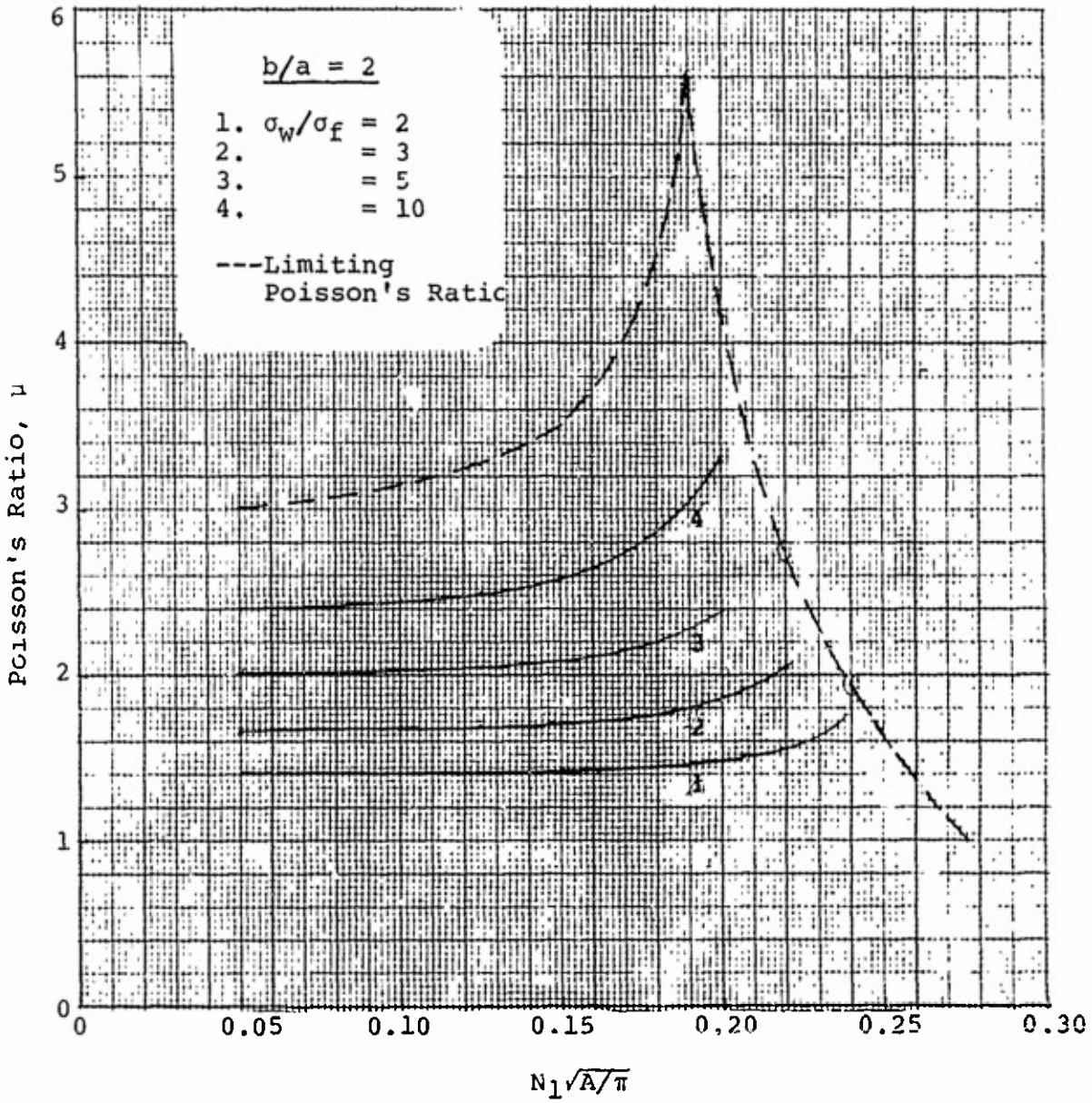

Figure 24(b). Poisson's Ratio: (Aspect Ratio = 2), Inextensible Yarn, Initially Square Fabric

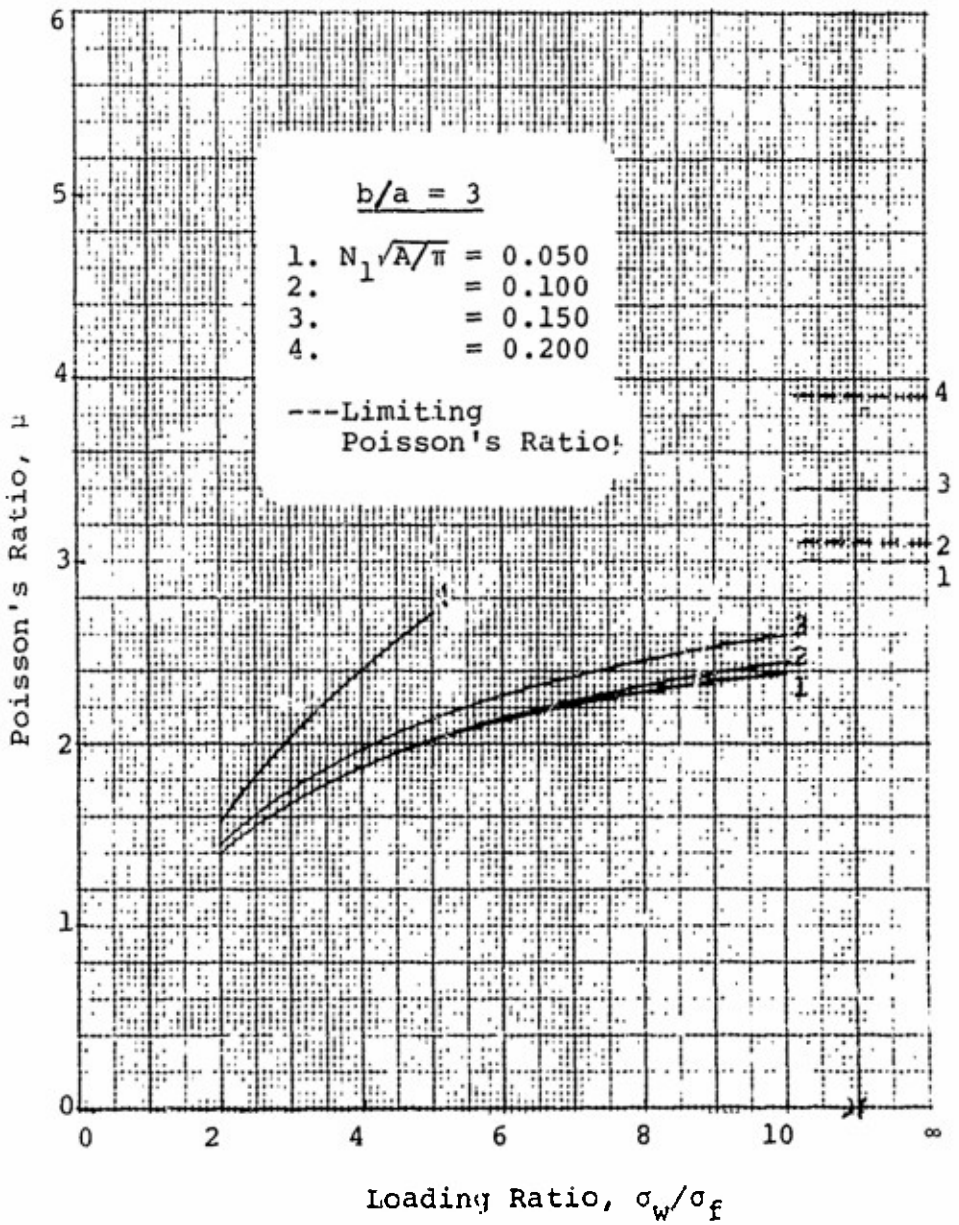

Figure 25(a). Poisson's Ratio: (Aspect Ratio = 3), Inextensible Yarn, Initially Square Fabric

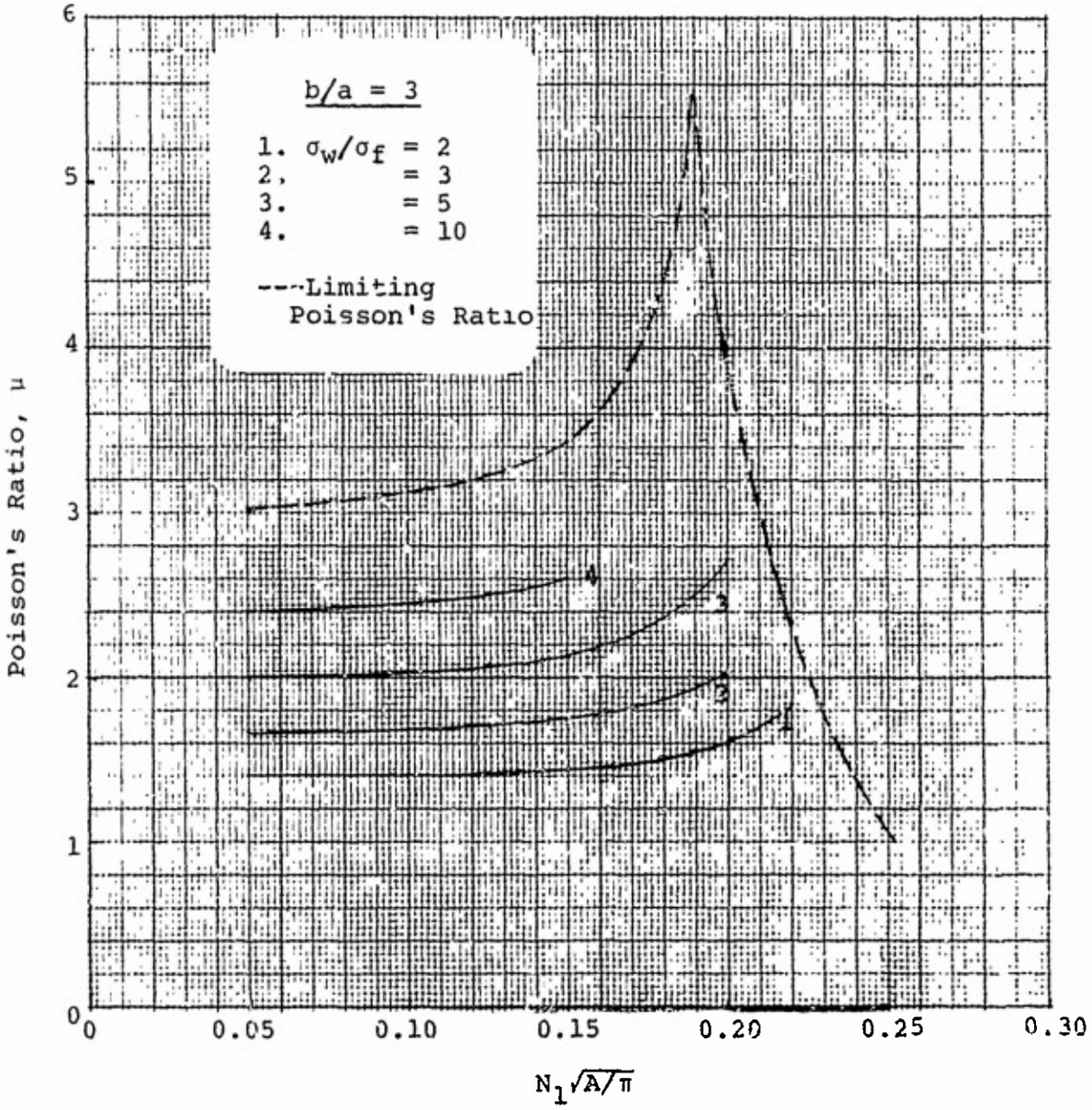

Figure 25(b). Poisson's Ratio: (Aspect Ratio = 3), Inextensible Yarn, Initially Square Fabric

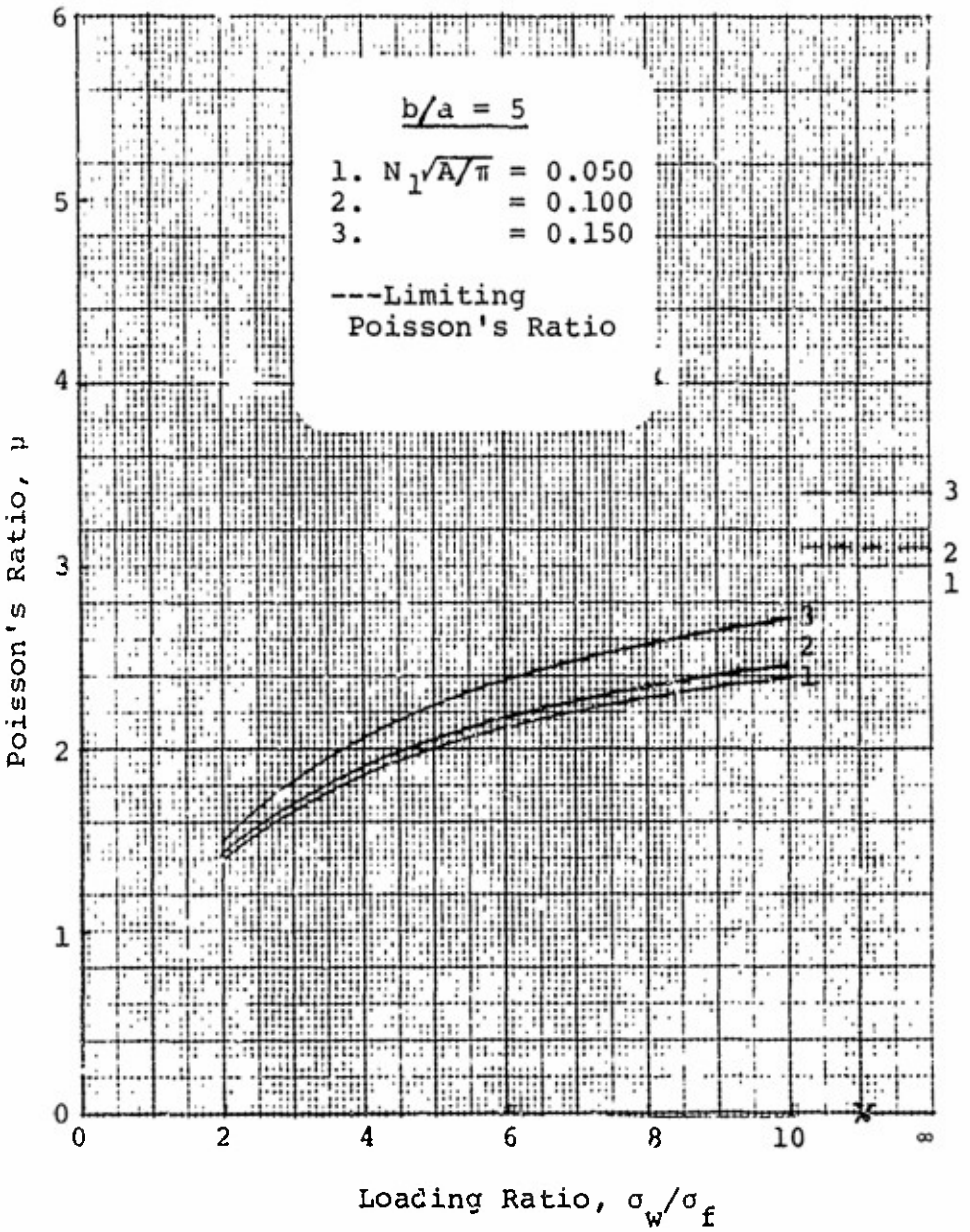

Figure 26(a). Poisson's Ratio: (Aspect Ratio = 5), Inextensible Yarn, Initially Square Fabric

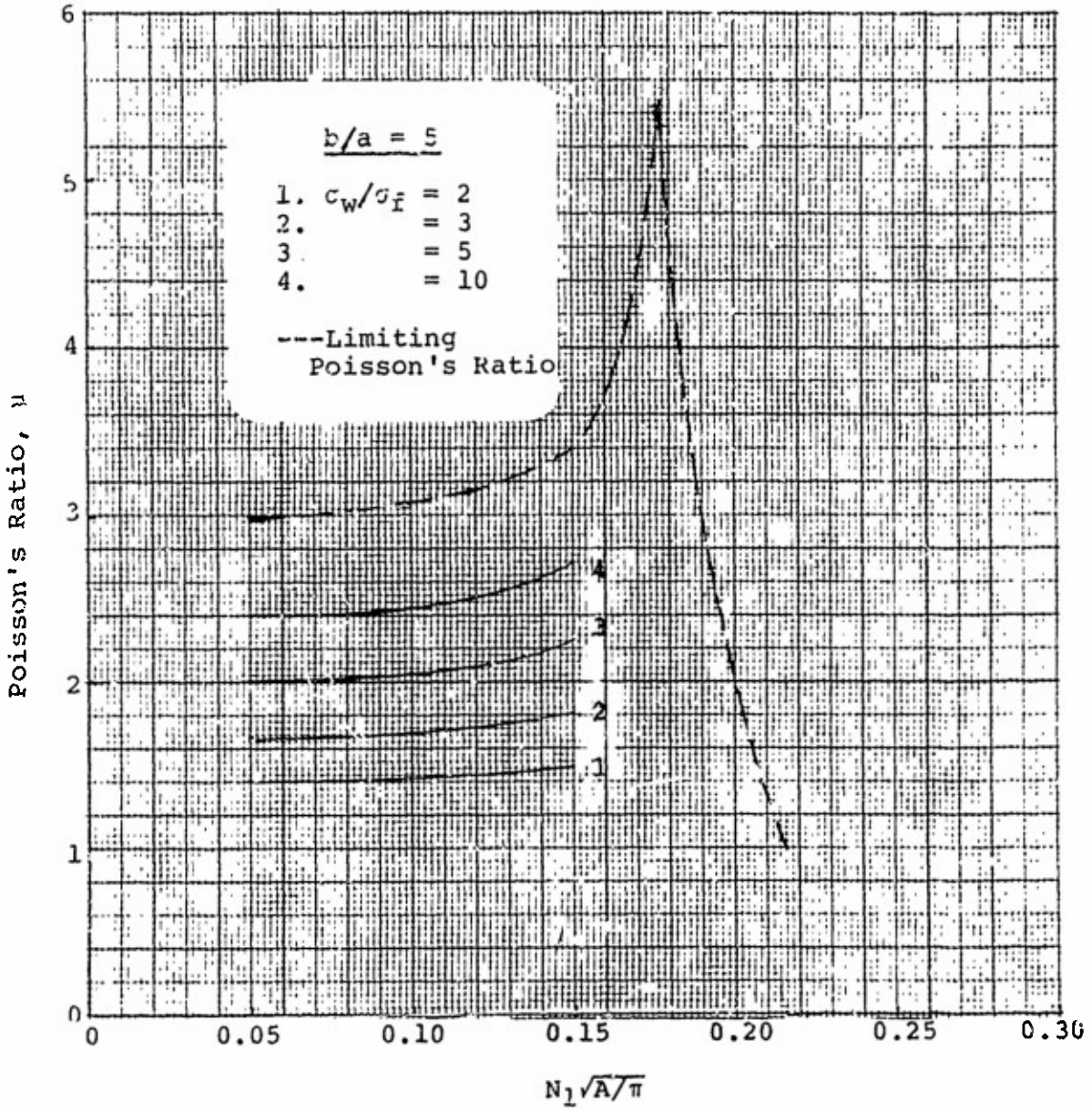

Figure 26(b). Poisson's Ratio (Aspect Ratio = 5), Inextensible Yarn, Initially Square Fabric

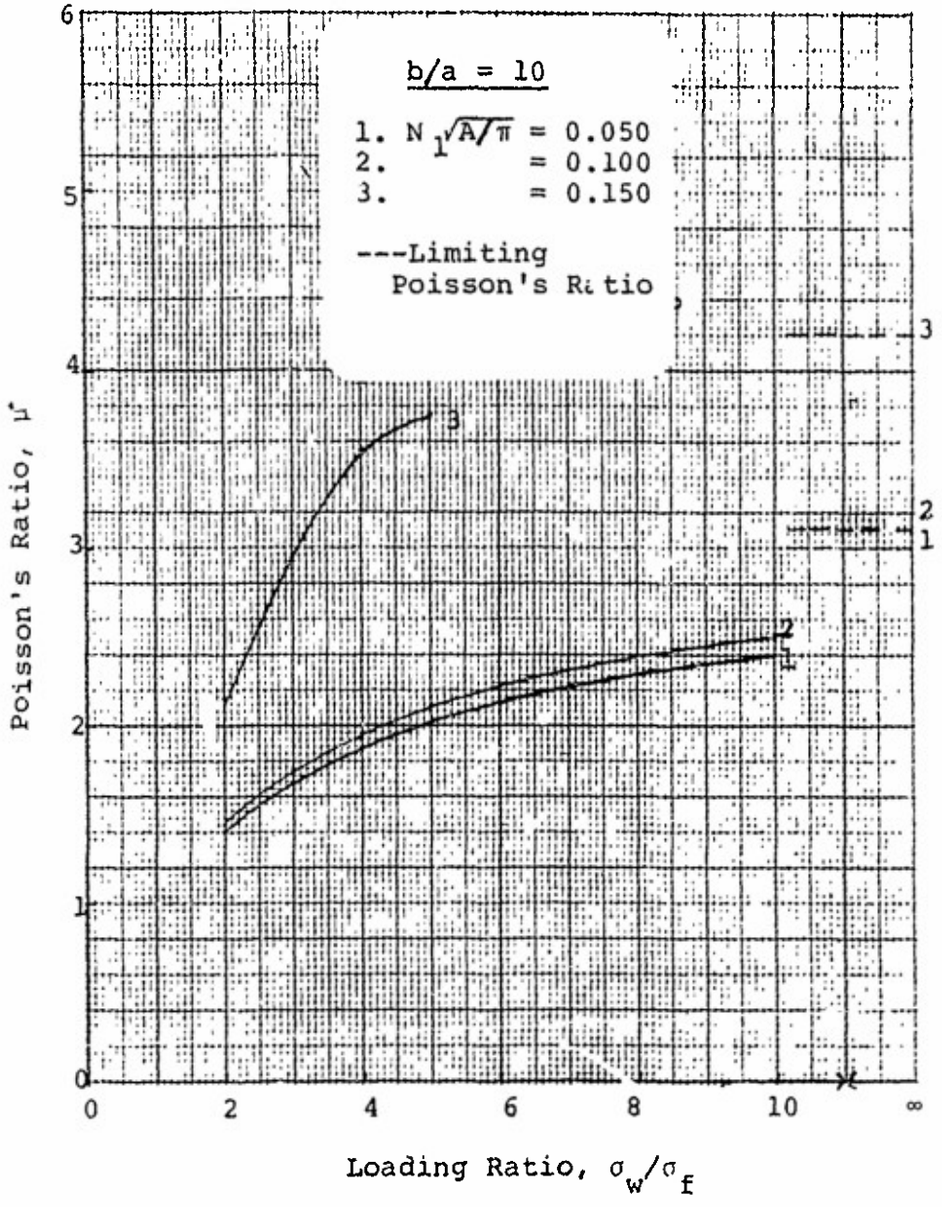

Figure 27(a). Poisson's Ratio: (Aspect Ratio = 10) Inextensible Yarn, Initially Square Fabric

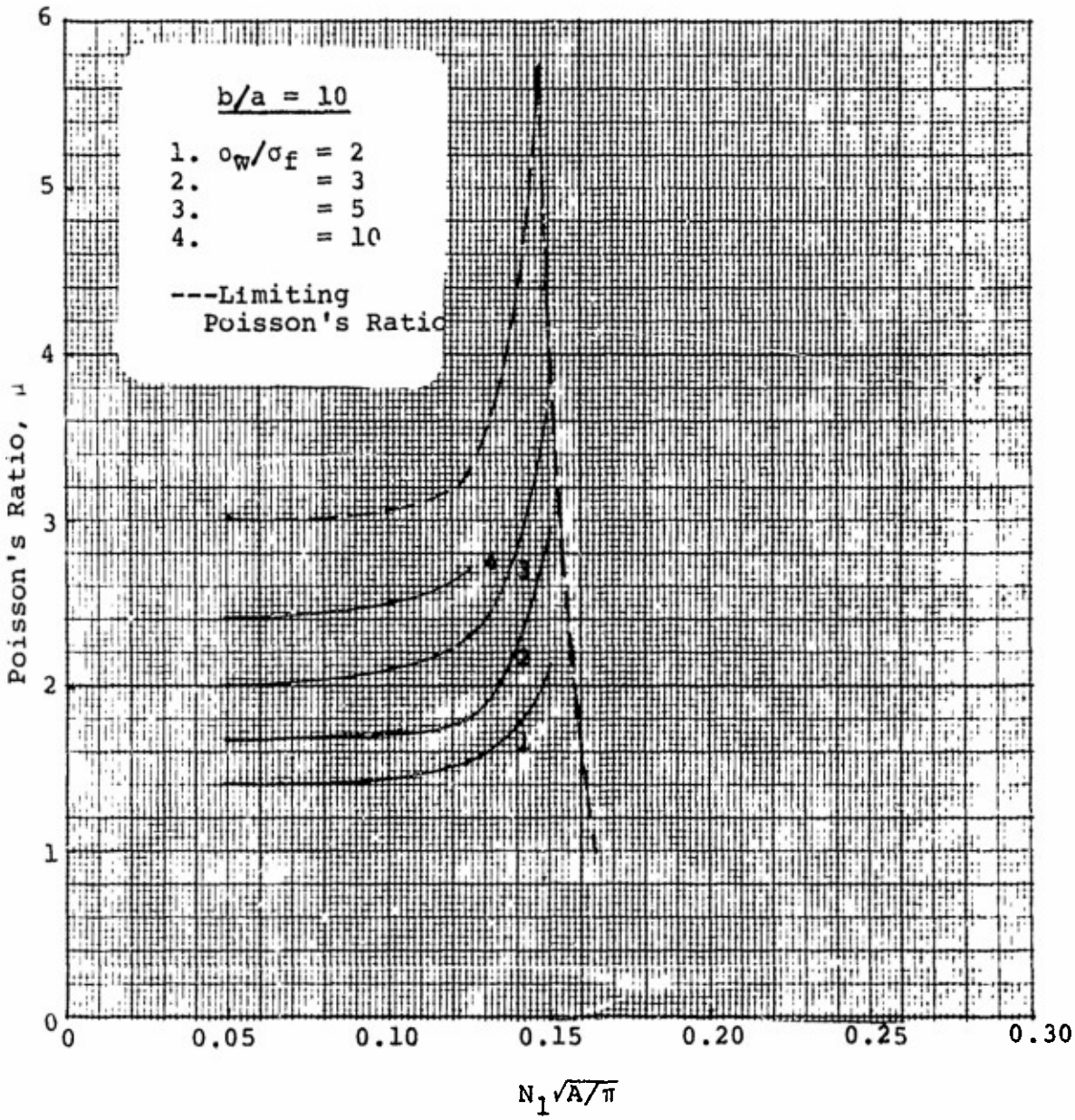

Figure 27(b). Poisson's Ratio: Aspect Ratio = 10), Inextensible Yarn, Initially Square Fabric

II. Filling Yarn Initially Straight, Inextensible, Infinitely Flexible Yarn

For a plain-weave fabric with the same number of identical, infinitely flexible yarns in both the warp and filling directions, and one set of yarns (filling yarns) initially straight (noncrimped)

$$N_{1w} = N_{1f} = N_1$$

$$\theta_{1f} = 0$$

$$L_{1f} = L_{2f} = L_f$$

$$L_{1w} = L_{2w} = L_w$$

and assuming yarn cross-sectional dimensions do not change during loading

$$b_{1w} = b_{1f} = b_{2w} = b_{2f} = b$$

$$a_{1w} = a_{1f} = a_{2w} = a_{2f} = a$$

$$b_w/a_w = b_f/a_f = b/a$$

With these assumptions Equations 3-7 reduce to the following three simplified expressions describing the fabric geometry before loading

$$\frac{1}{N_1 a} = \frac{4}{\sin\theta_{1w}} + 2(b/a-1) \tag{30}$$

$$\frac{L_f}{a} = \frac{1}{N_1 a} \tag{31}$$

$$\frac{L_w}{a} = \frac{4}{\tan\theta_{1w}} + 4\theta_{1w} + 2(b/a-1) \tag{32}$$

$N_1\sqrt{A/\pi}$ vs θ_{1w}, and $L_w/\sqrt{A/\pi}$ and $L_f/\sqrt{A/\pi}$ vs $N_1\sqrt{A/\pi}$ are plotted in Figures 28 and 29 respectively. Figure 28 is similar to the comparable figure for the initially square fabric, Figure 5, and the discussion

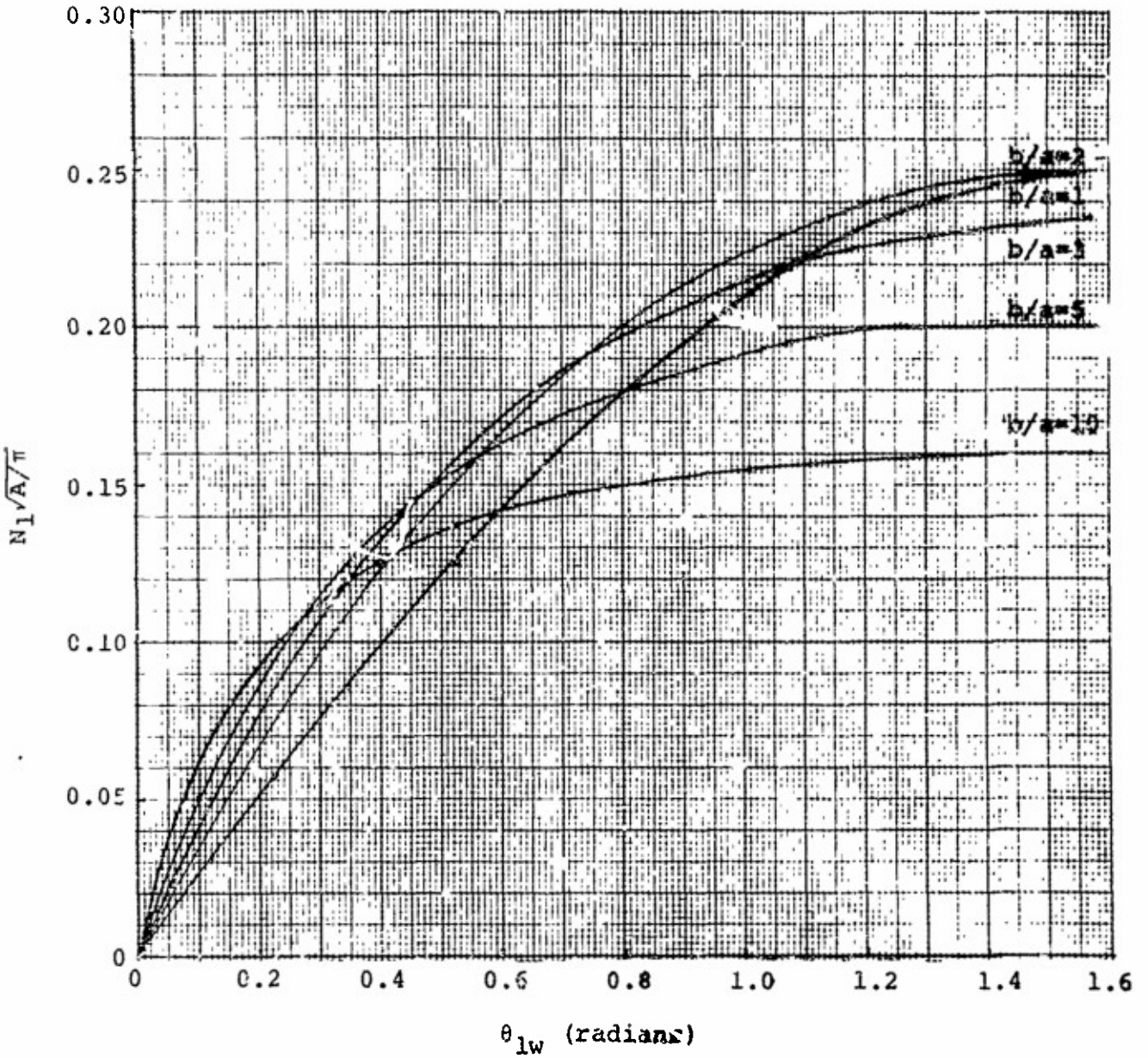

Figure 28. $N_1\sqrt{A/\pi}$ vs θ_{1w} for Fabric with Initially Straight Filling

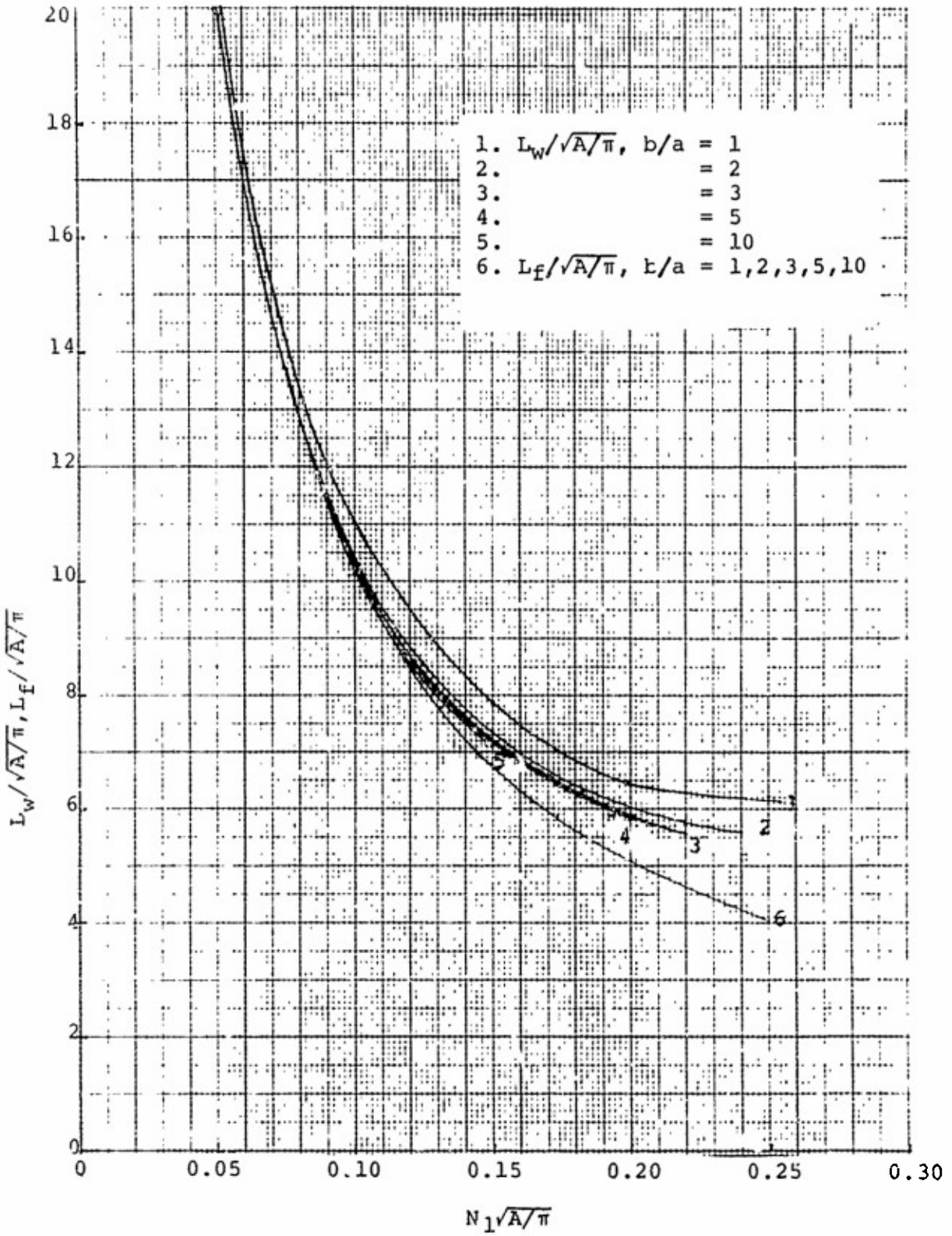

Figure 29. $L/\sqrt{A/\pi}$ vs $N_1\sqrt{A/\pi}$ for Fabric with Initially Straight Filling

or that figure is also applicable to Figure 28. The curves in Figure 28 were terminated at $\theta_{1w} = 1.57$, i.e., $\theta_{1w} = 90°$. This is the maximum achievable angle with the assumed fabric model. Figure 29 shows that the length of filling yarn between yarn crossovers is less than the warp yarn length as expected since the warp yarn is crimped and the filling straight. However, the difference is small at low values of $N_1\sqrt{A/\pi}$, i.e., for open fabric constructions. Also, the lower the yarn aspect ratio, i.e., the more nearly circular the yarns, the greater the difference between the warp and filling yarn lengths.

For infinitely flexible, inextensible yarn, i.e., only taking into account crimp interchange ($L_1 = L_2 = L$), the geometry of the deformed fabric is given by the following four equations derived from Equations 3-7 and 12 after simplification and replacement of subscript "1" by subscript "2".

$$[\frac{L_w}{a} - 2(b/a-1) - 4\theta_{2w}]\sin\theta_{2w} - 4\cos\theta_{2w}$$

$$= 4(\cos\theta_{2f} - 1) - [\frac{L_f}{a} - 2(b/a-1) - 4\theta_{2f}]\sin\theta_{2f} \tag{33}$$

$$\frac{\sigma_w}{\sigma_f} = \frac{\cot\theta_{2w}}{\cot\theta_{2f}} \frac{\{[\frac{L_w}{a} - 2(b/a-1) - 4\theta_{2w}]\cos\theta_{2w} + 4\sin\theta_{2w} + 2(b/a-1)\}}{\{[\frac{L_f}{a} - 2(b/a-1) - 4\theta_{2f}]\cos\theta_{2f} + 4\sin\theta_{2f} + 2(b/a-1)\}} \tag{34}$$

$$\frac{1}{N_{2w}a} = [\frac{L_f}{a} - 2(b/a-1) - 4\theta_{2f}]\cos\theta_{2f} + 4\sin\theta_{2f} + 2(b/a-1) \tag{35}$$

$$\frac{1}{N_{2f}a} = [\frac{L_w}{a} - 2(b/a-1) - 4\theta_{2w}]\cos\theta_{2w} + 4\sin\theta_{2w} + 2(b/a-1) \tag{36}$$

The final crimp angles θ_{2w} and θ_{2f} were determined by solving Equations 33 and 34 simultaneously with specified loading ratios $\sigma_w/\sigma_f \geq 1$ for various values of L_w/a and L_f/a corresponding to a series of values of N_1a and b/a. (Loading ratios less than one were not investigated.) $N_{2w}a$ and $N_{2f}a$ were then determined from Equations 35 and 36 and the resulting fabric strains computed from

Equations 17 and 18. The results of the computations are presented in Figures 30 through 44. The fabric extension in the warp direction and contraction in the filling direction are given in Figures 30(a) through 39(a) as a function of loading ratio for a series of initial fabric constructions, $N_1\sqrt{A/\pi}$ and yarn aspect ratios, b/a. Similarly, the fabric deformations are given in Figures 30(b) through 39(b) as a function of initial construction $N_1\sqrt{A/\pi}$ for a series of loading ratios and yarn aspect ratios. Figures 30 and 31 showing the response of fabric with initially straight filling woven from round yarn (b/a = 1) are reprinted from reference [1]. Additionally, the fabric extensions for uniaxial loading, i.e., $\sigma_w/\sigma_f = \infty$, are given for all cases.

As shown in these figures, the fabric elongates in the warp direction and contracts in the filling direction. The magnitude of these extensions increases with increasing values of the loading ratio, approaching the $\sigma_w/\sigma_f = \infty$ extensions asymptotically. However, unlike the initially square fabrics, fabrics with initially straight filling extend at a loading ratio of one. This occurs in fabric with initially straight filling because, unlike in the initially square fabric the crimp is initially unbalanced and therefore crimp interchange can occur.

The fabric extension in the warp direction increases with increasing $N_1\sqrt{A/\pi}$ at all loading ratios. The contraction in the filling direction also increases with increasing initial fabric tightness for $\sigma_w/\sigma_f \leq 10$. When $\sigma_w/\sigma_f = \infty$, the filling contraction goes through a turning point with increasing $N_1\sqrt{A/\pi}$. The location of the turning point, i.e., the value of $N_1\sqrt{A/\pi}$ for which the filling contraction is a maximum, is the maximum value for which the warp yarns can be pulled straight. These values of $N_1\sqrt{A/\pi}$ are given in Table 5 for the various yarn aspect ratios. The manner in which the data in Table 5 are calculated is similar to the procedure outlined for the initially square fabric.

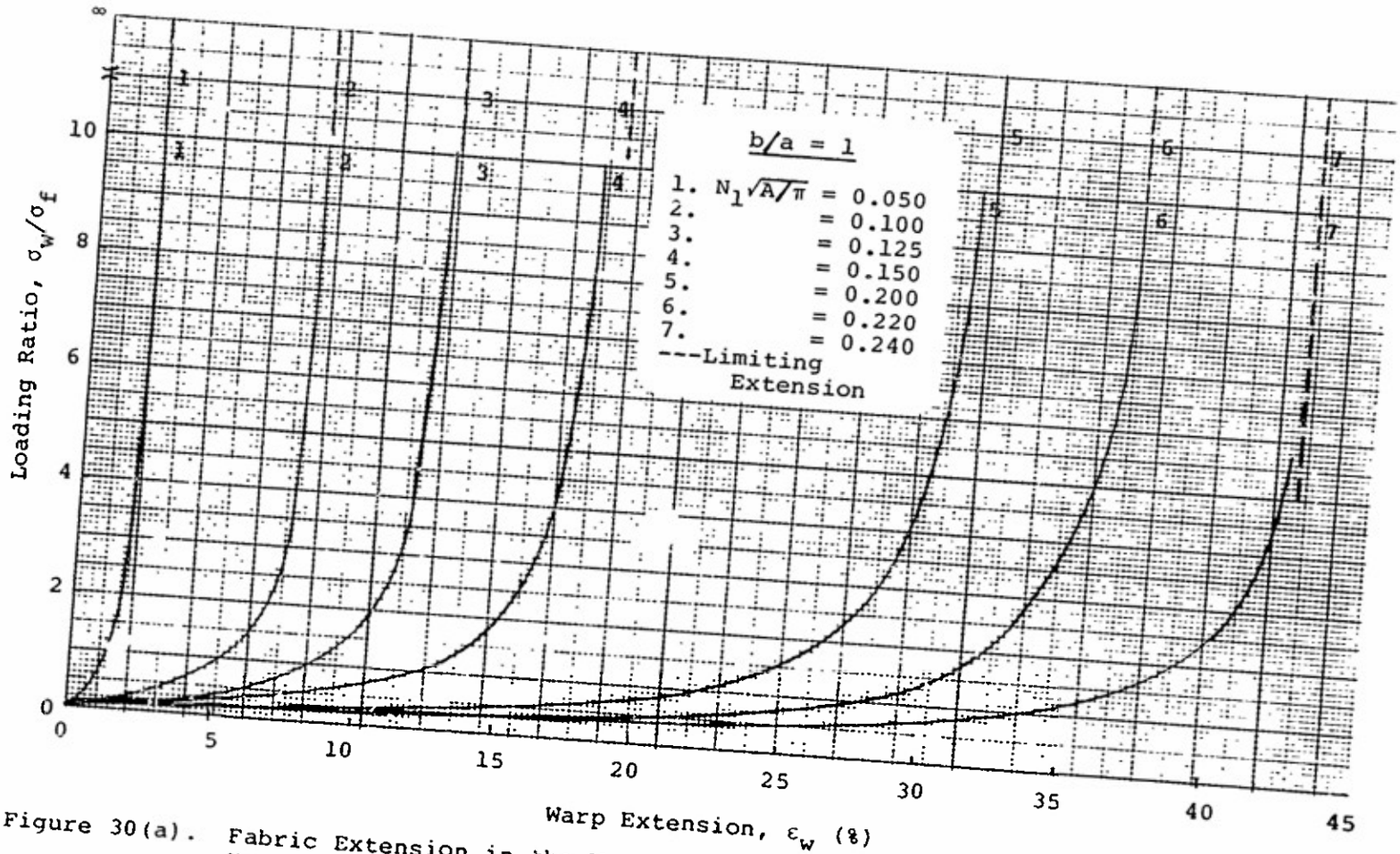

Figure 30(a). Fabric Extension in the Warp Direction: (Aspect Ratio = 1), Inextensible Yarn, Initially Straight Filling

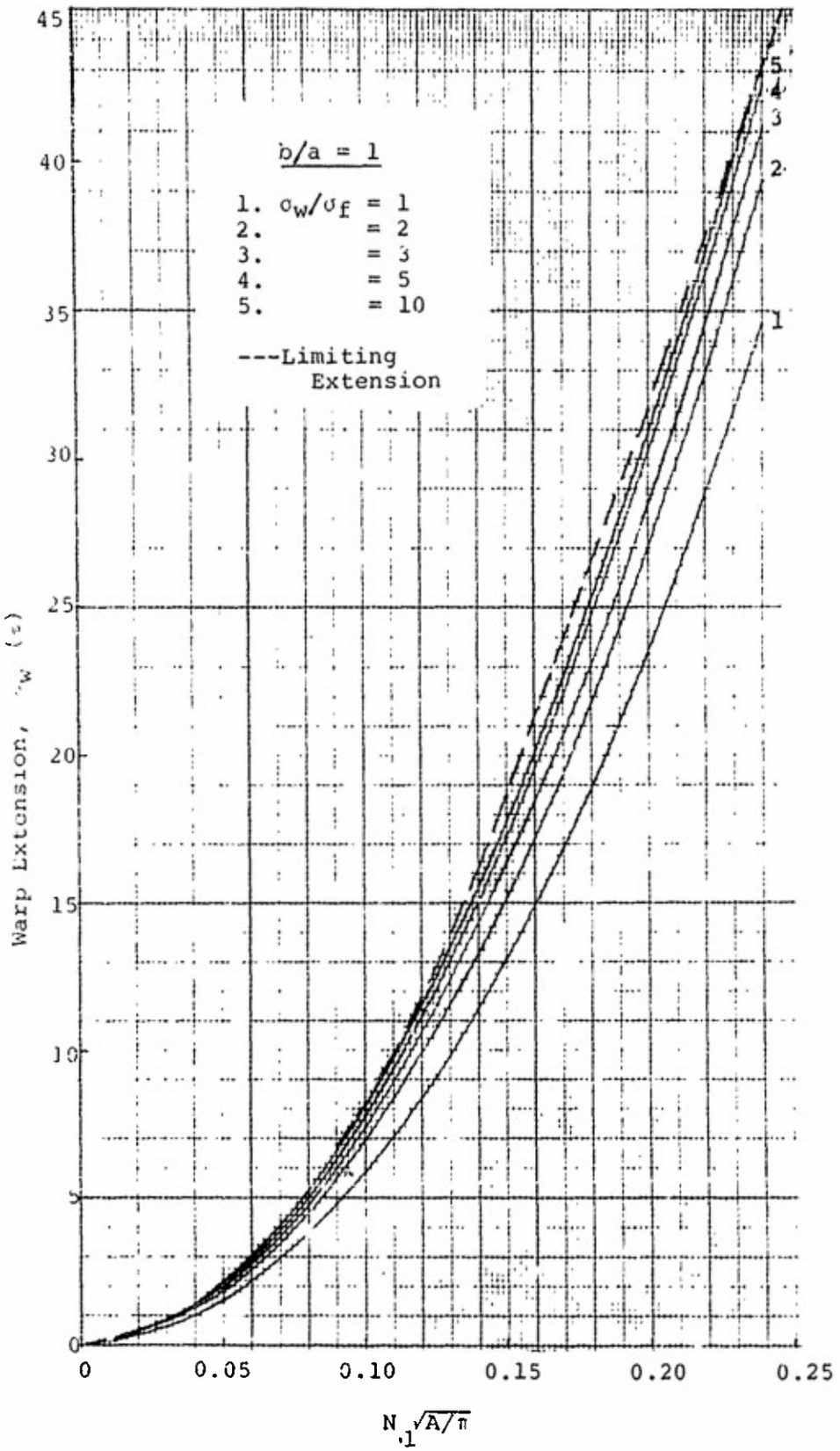

Figure 30(b). Fabric Extension in the Warp Direction: (Aspect Ratio = 1), Inextensible Yarn, Initially Straight Filling

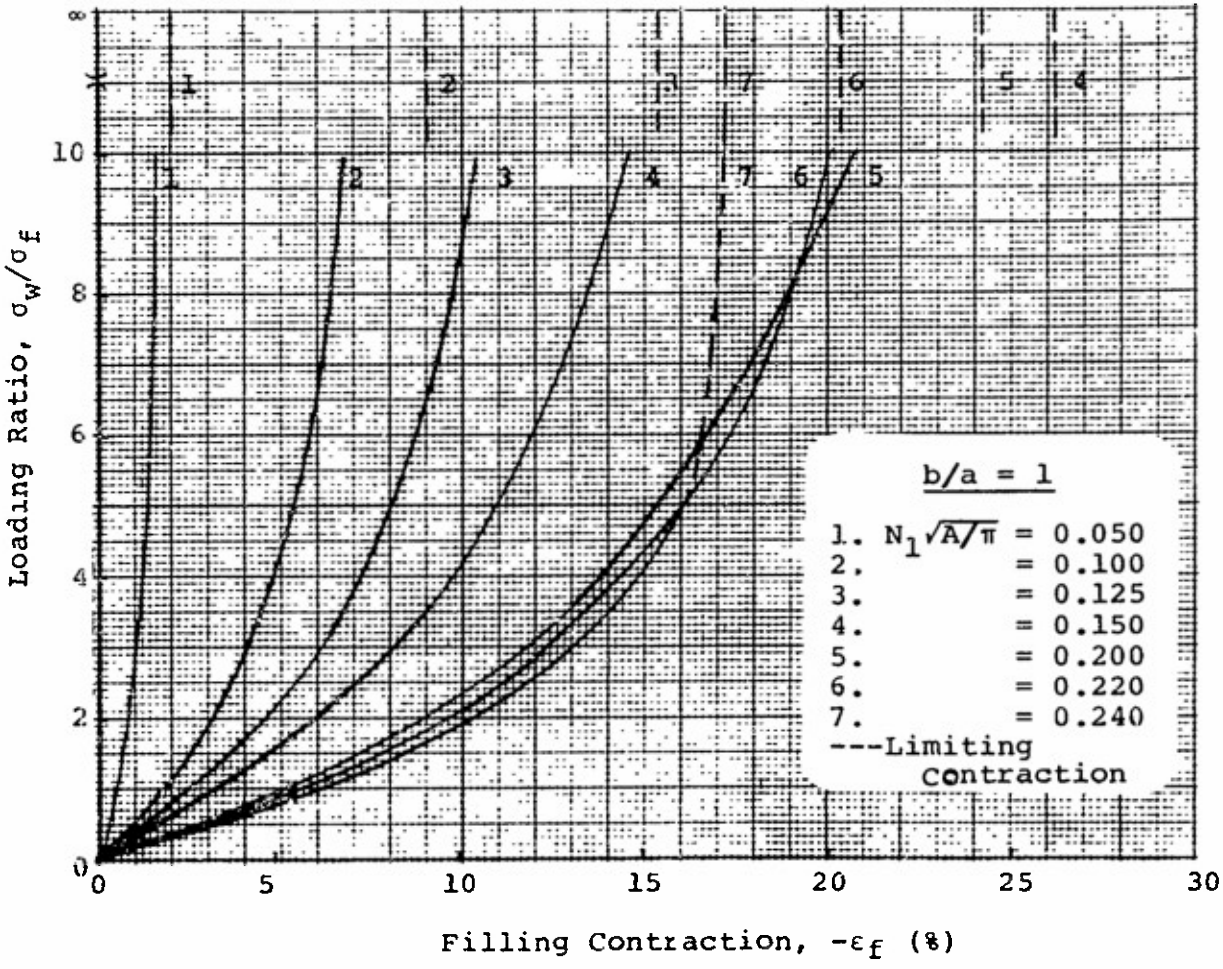

Figure 31(a). Fabric Contraction in the Filling Direction: (Aspect Ratio = 1), Inextensible Yarn, Initially Straight Filling

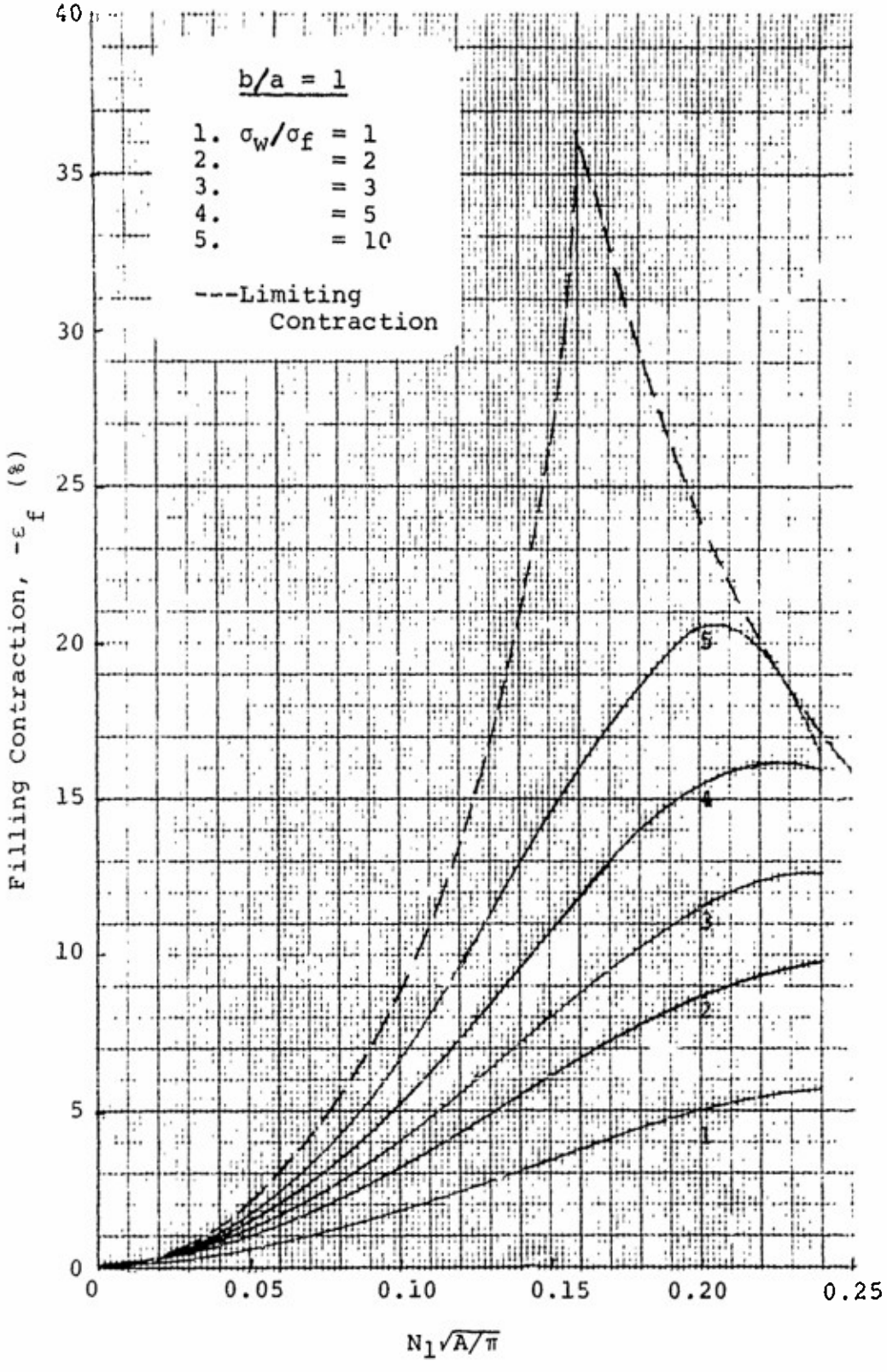

Figure 31(b). Fabric Contraction in the Filling Direction: (Aspect Ratio = 1), Inextensible Yarn, Initially Straight Filling

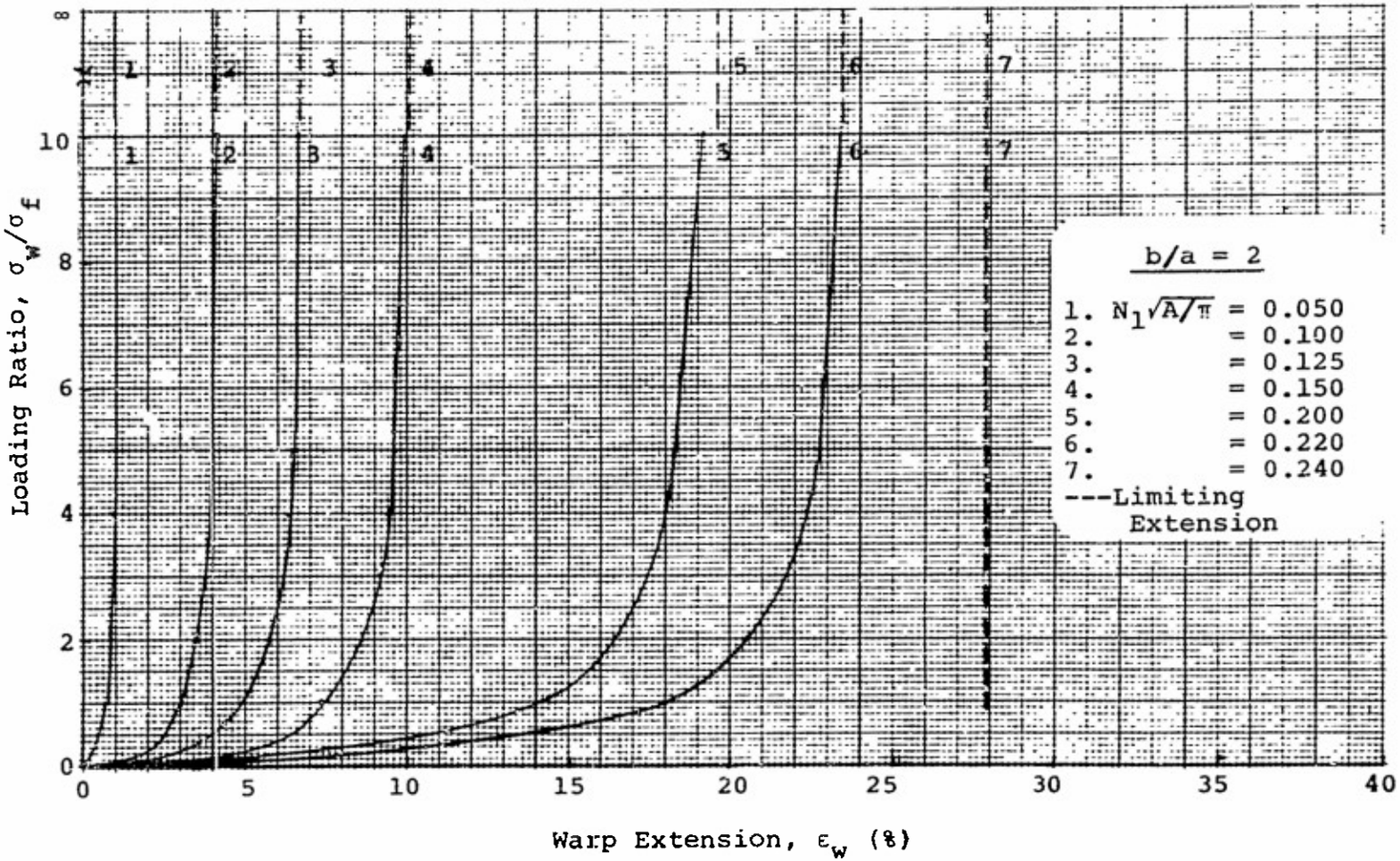

Figure 32(a). Fabric Extension in the Warp Direction: (Aspect Ratio = 2), Inextensible Yarn, Initially Straight Filling

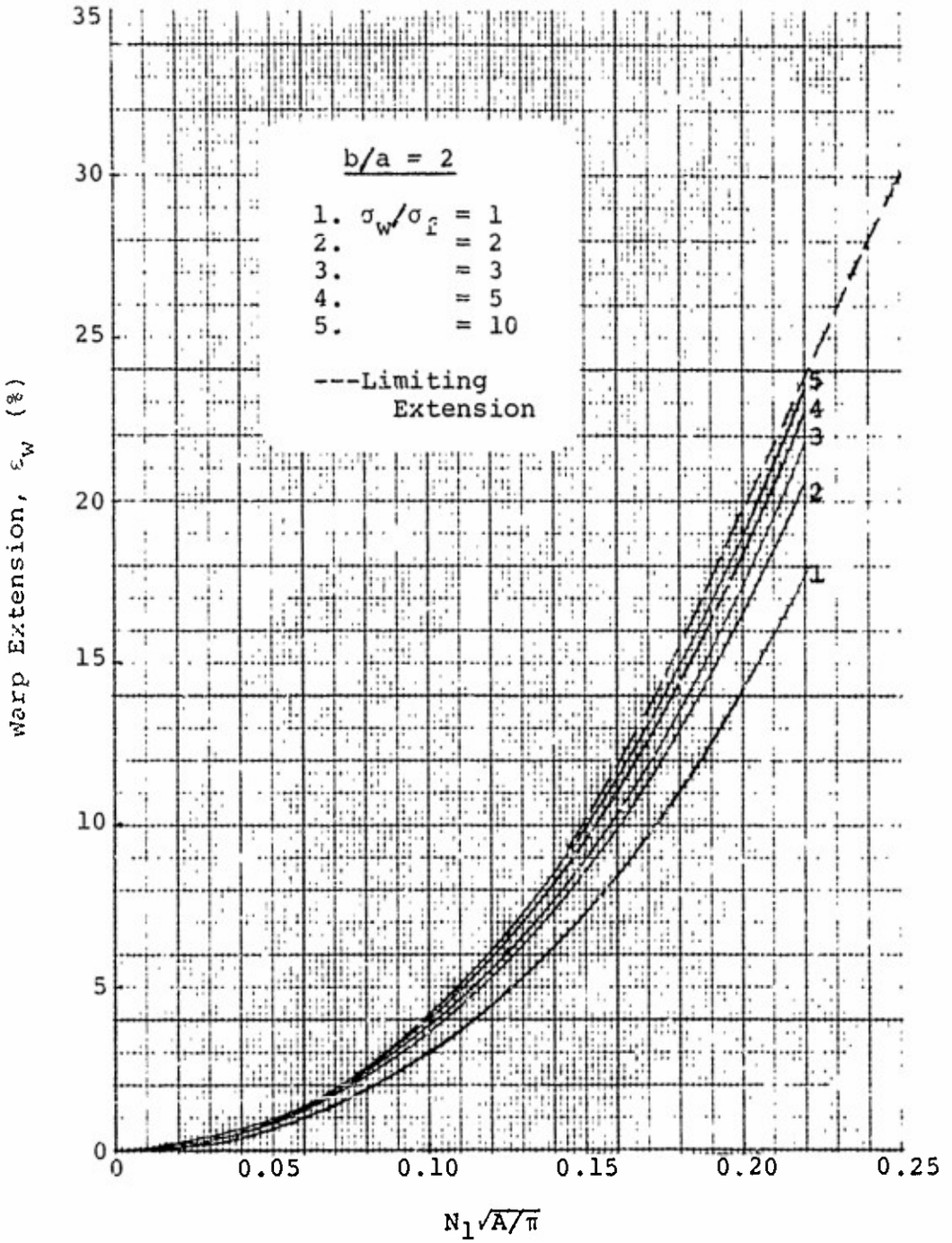

Figure 32(b). Fabric Extension in the Warp Direction: (Aspect Ratio = 2), Inextensible Yarn, Initially Straight Filling

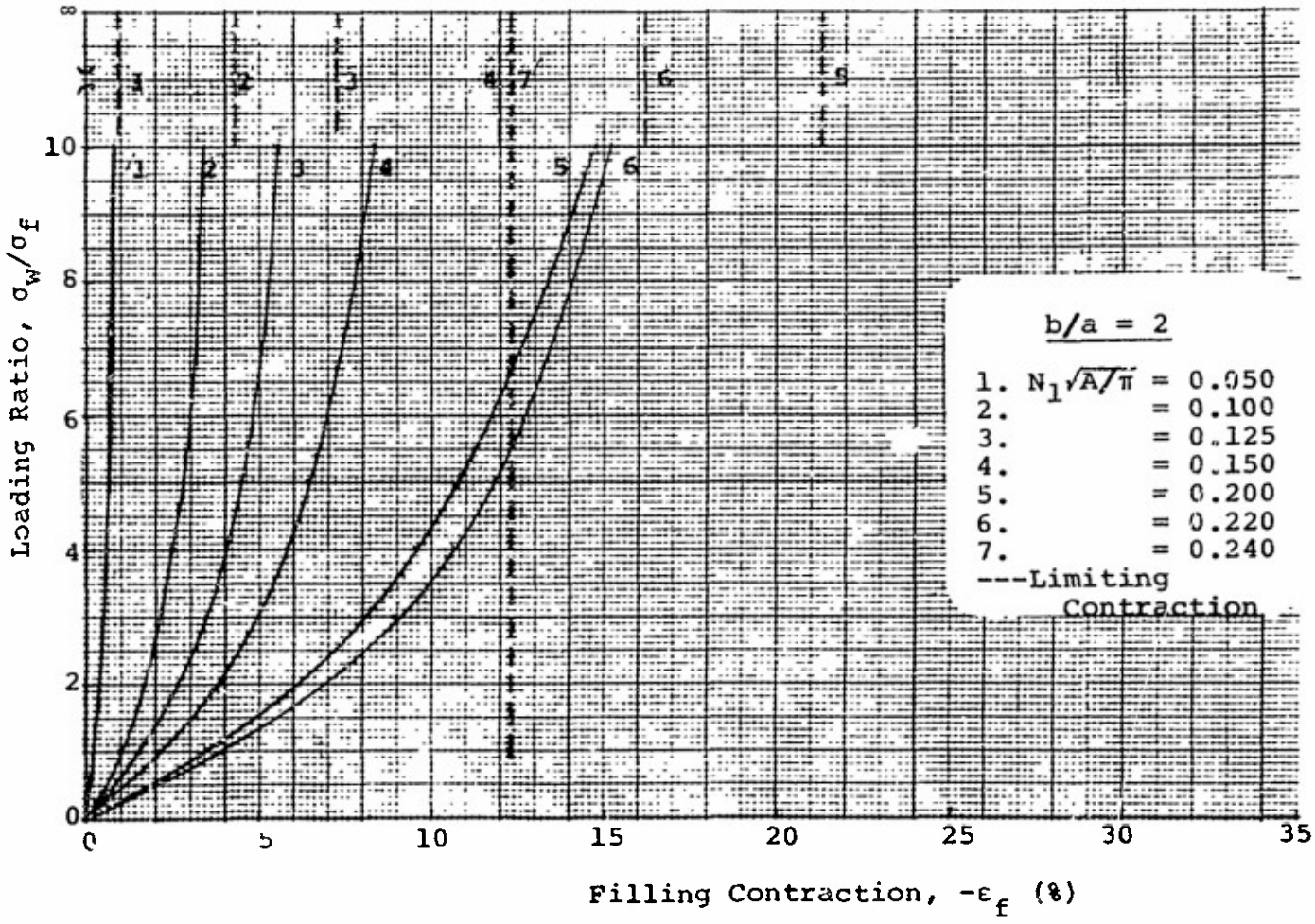

Figure 33(a). Fabric Contraction in the Filling Direction: (Aspect Ratio = 2), Inextensible Yarn, Initially Straight Filling

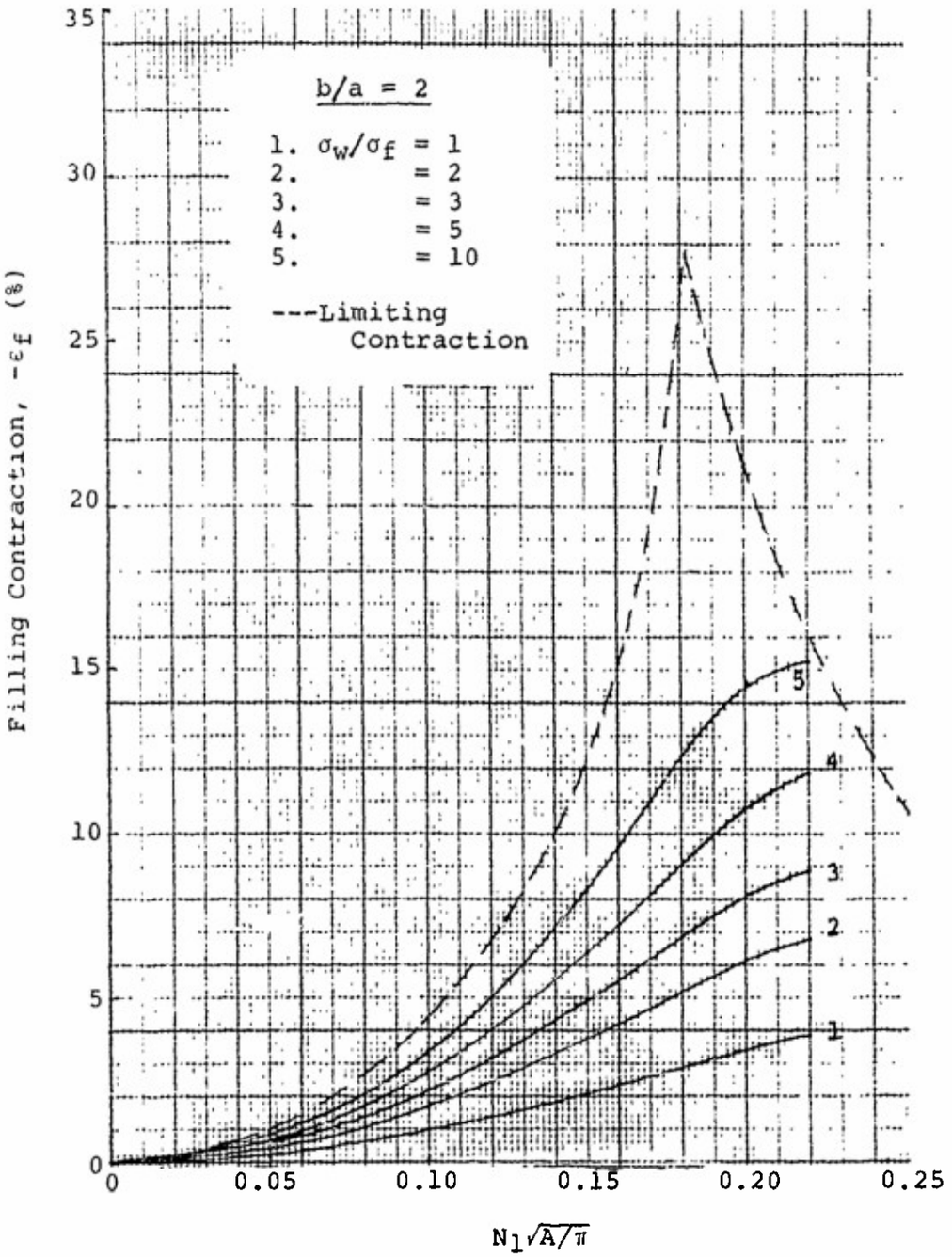

Figure 33(b). Fabric Contraction in the Filling Direction: (Aspect Ratio = 2), Inextensible Yarn, Initially Straight Filling

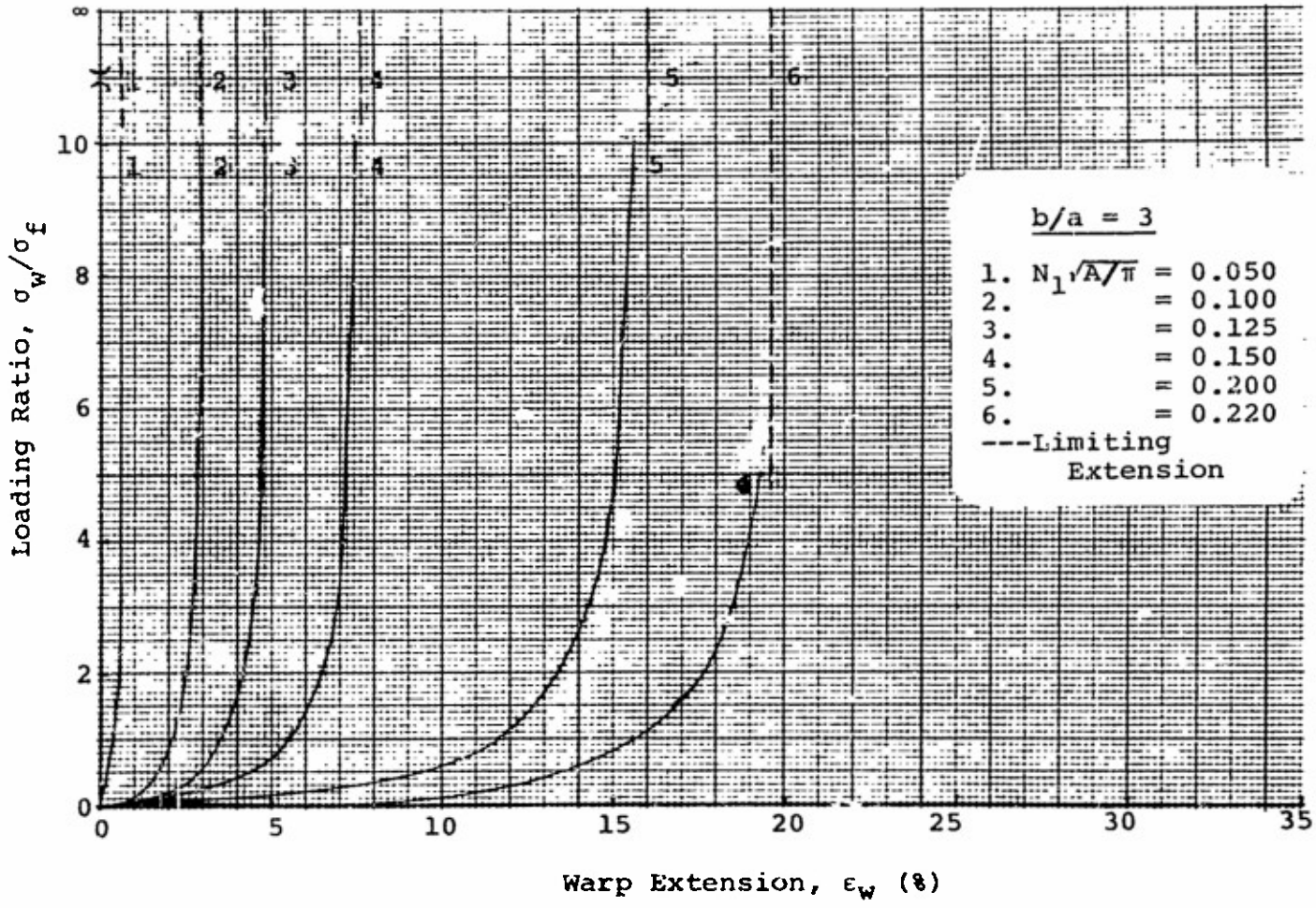

Figure 34(a). Fabr Extension in the Warp Direction (Aspect Ratio = 3), Inex nsible Yarn, Initially Straight Filling

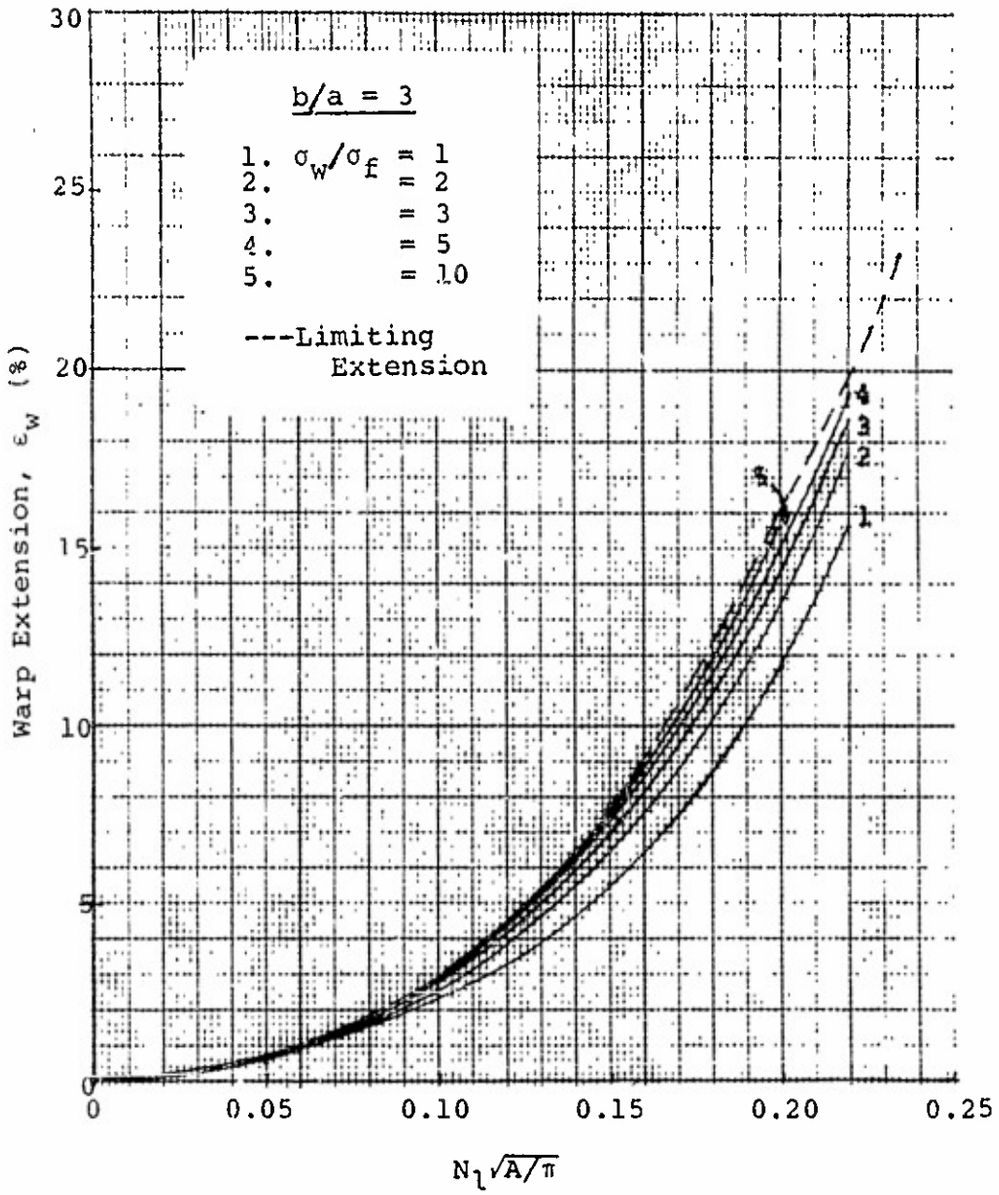

Figure 34(b). Fabric Extension in the Warp Direction: (Aspect Ratio = 3), Inextensible Yarn, Initially Straight Filling

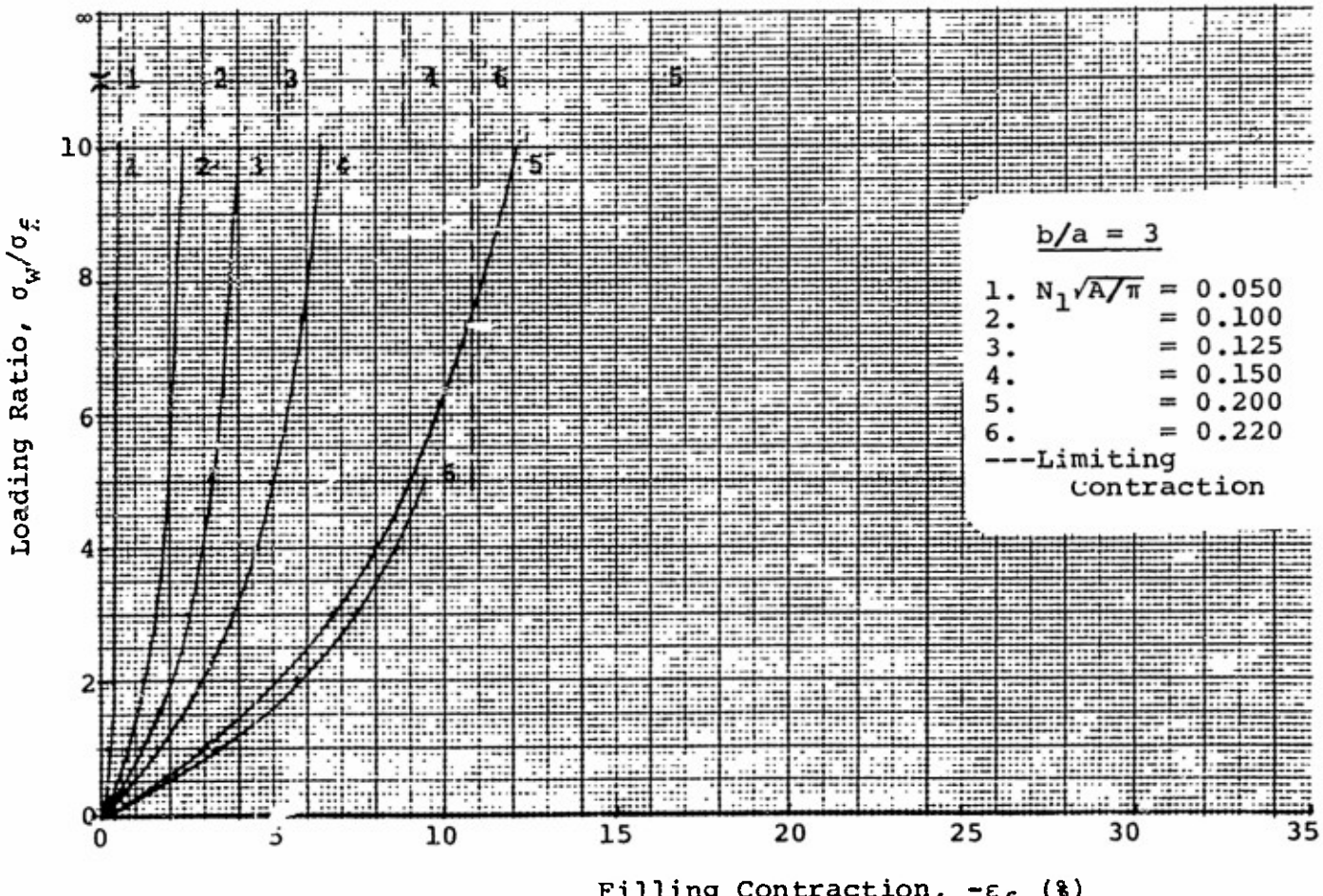

Figure 35(a). Fabric Contraction in the Filling Direction: (Aspect Ratio = 3), Inextensible Yarn, Initially Straight Filling

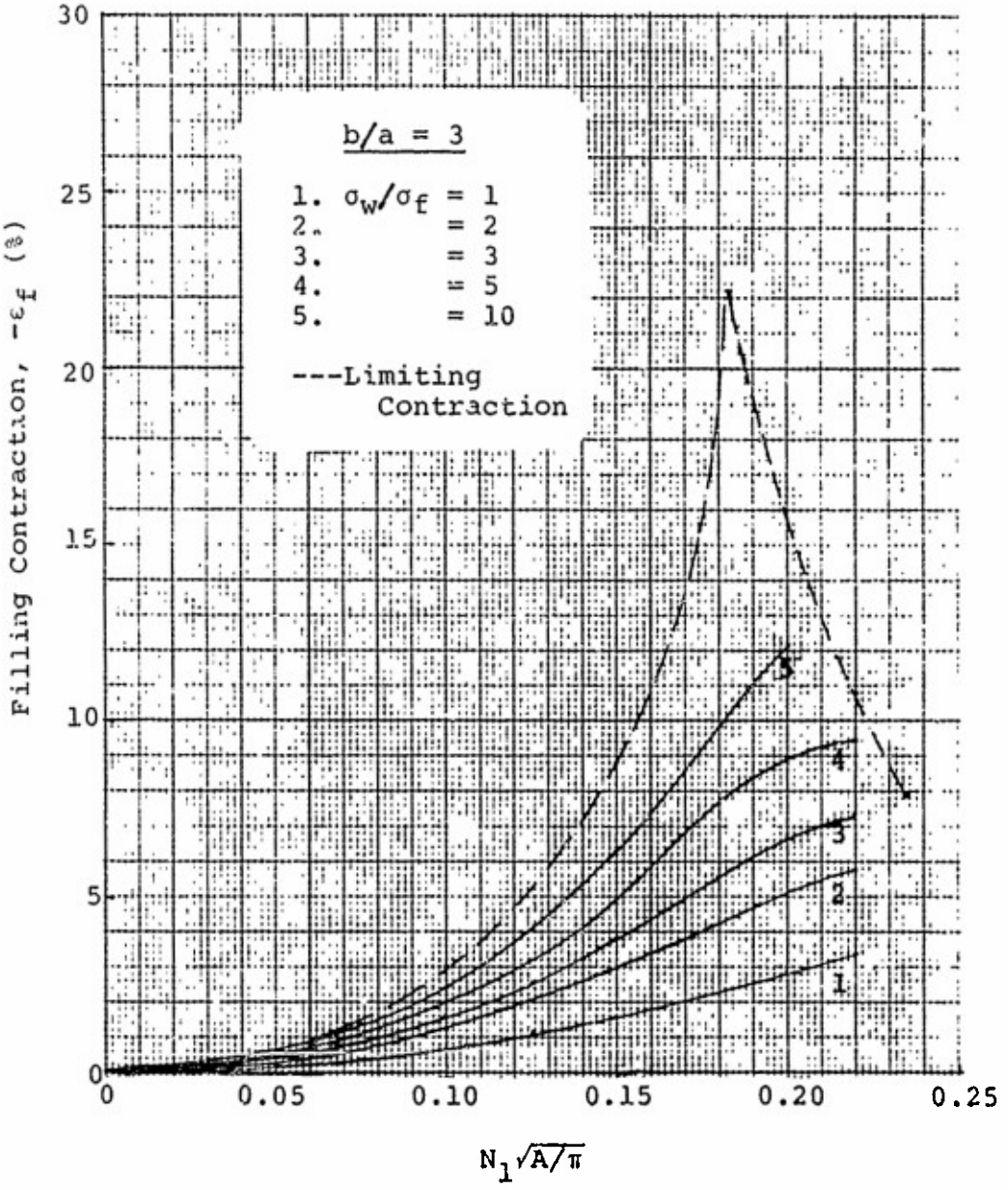

Figure 35(b). Fabric Contraction in the Filling Direction: (Aspect Ratio = 3), Inextensible Yarn, Initially Straight Filling

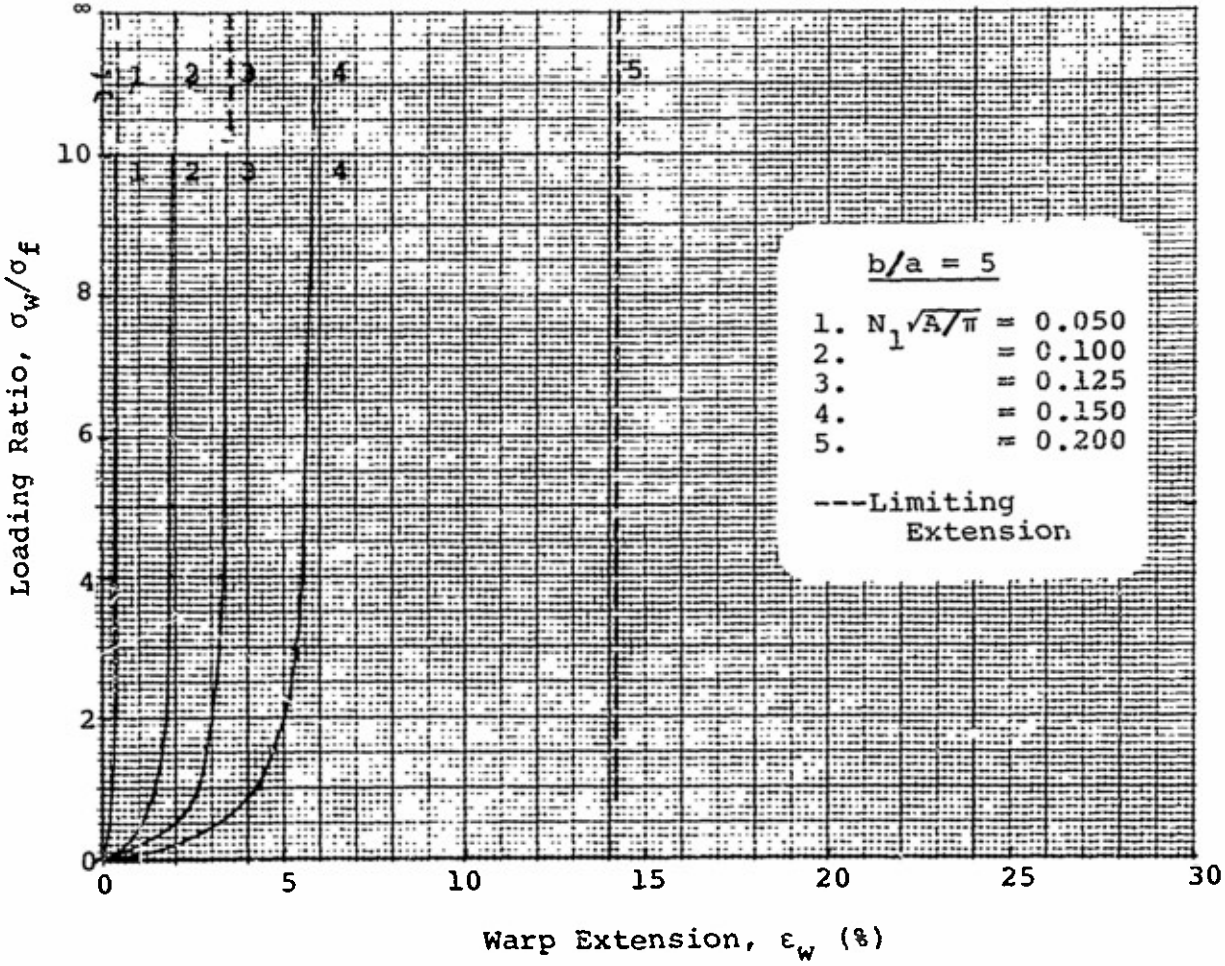

Figure 36(a). Fabric Extension in the Warp Direction: (Aspect Ratio = 5), Inextensible Yarn, Initially Straight Filling

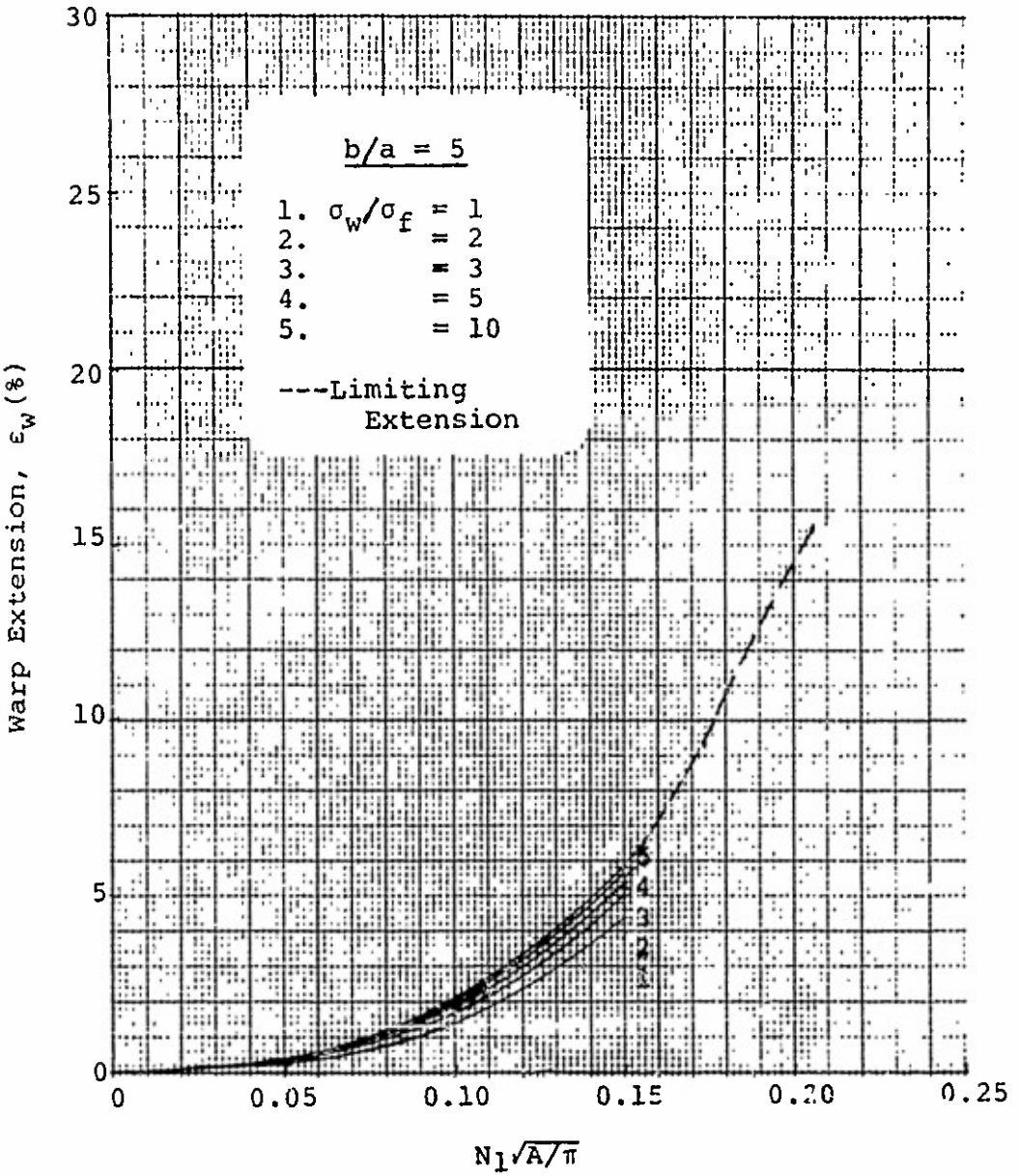

Figure 36(b). Fabric Extension in the Warp Direction: (Aspect Ratio = 5), Inextensible Yarn, Initially Straight Filling

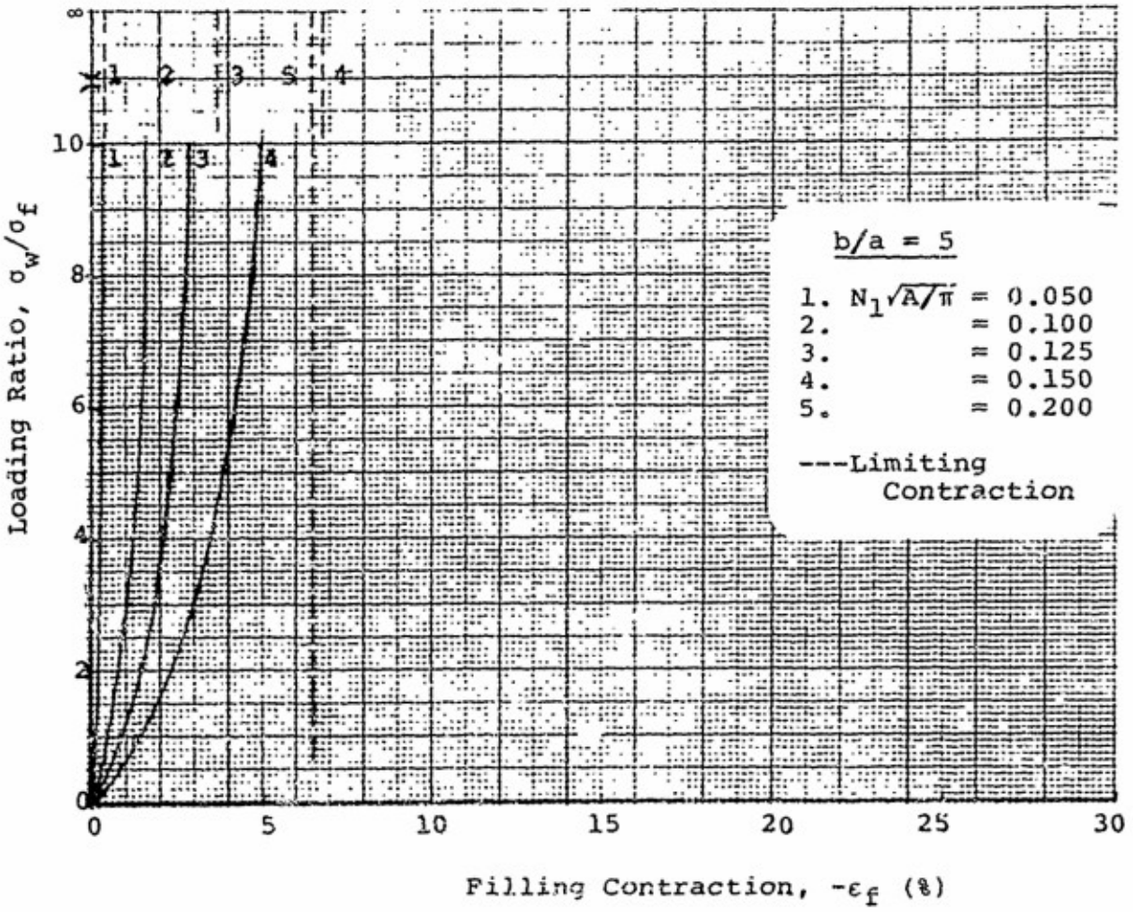

Figure 37(a). Fabric Contraction in the Filling Direction: (Aspect Ratio = 5), Inextensible Yarn, Initially Straight Filling

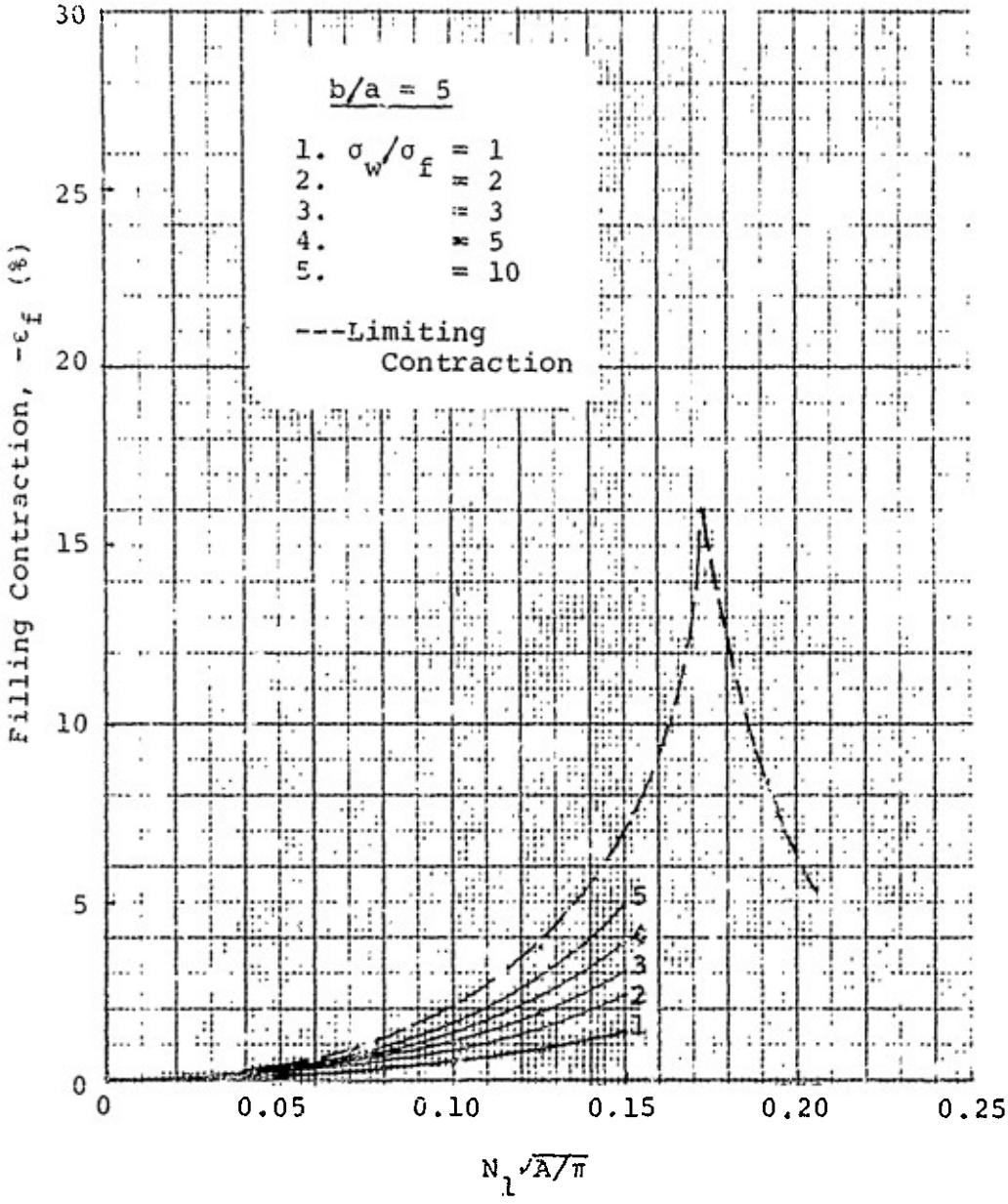

Figure 37(b). Fabric Contraction in the Filling Direction: (Aspect Ratio = 5), Inextensible Yarn, Initially Straight Filling

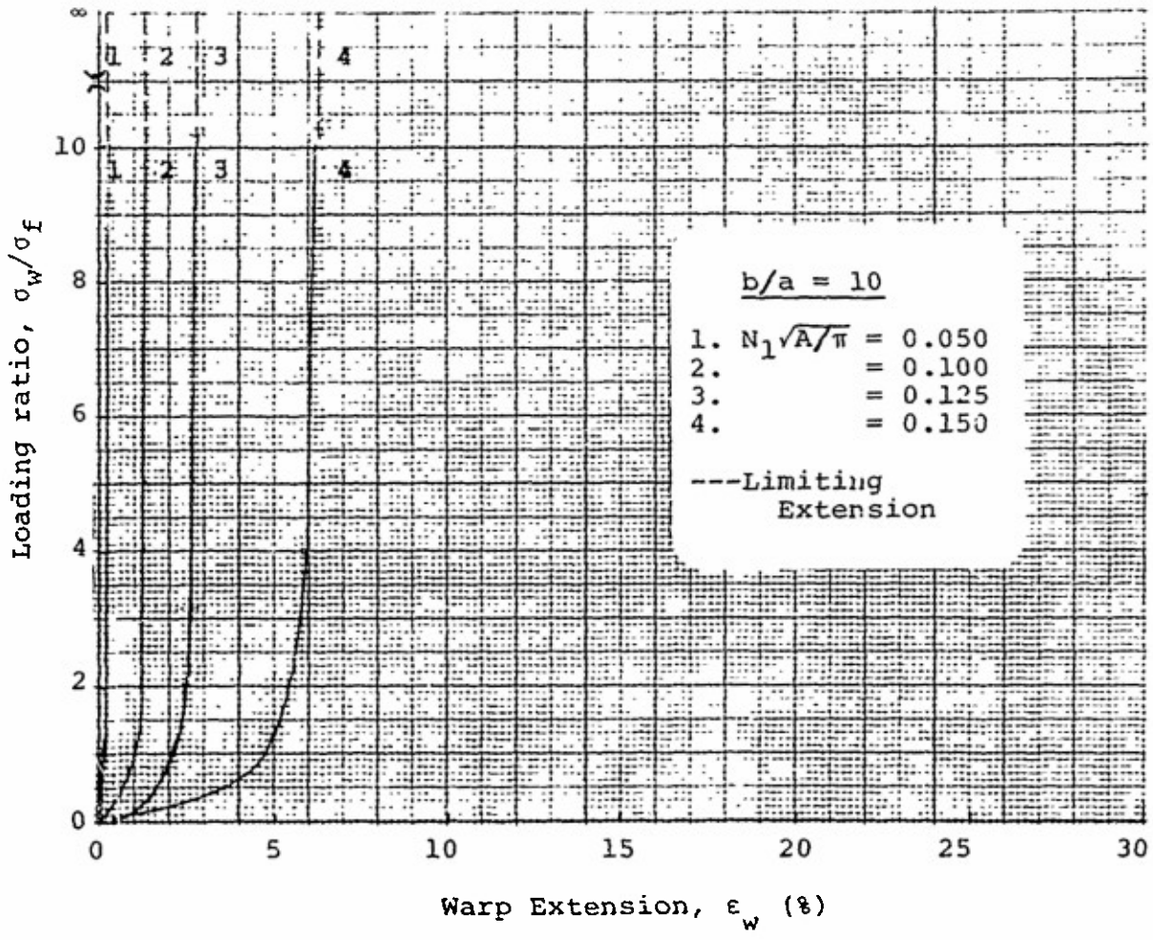

Figure 38(a). Fabric Extension in the Warp Direction: (Aspect Ratio = 10), Inextensible Yarn, Initially Straight Filling

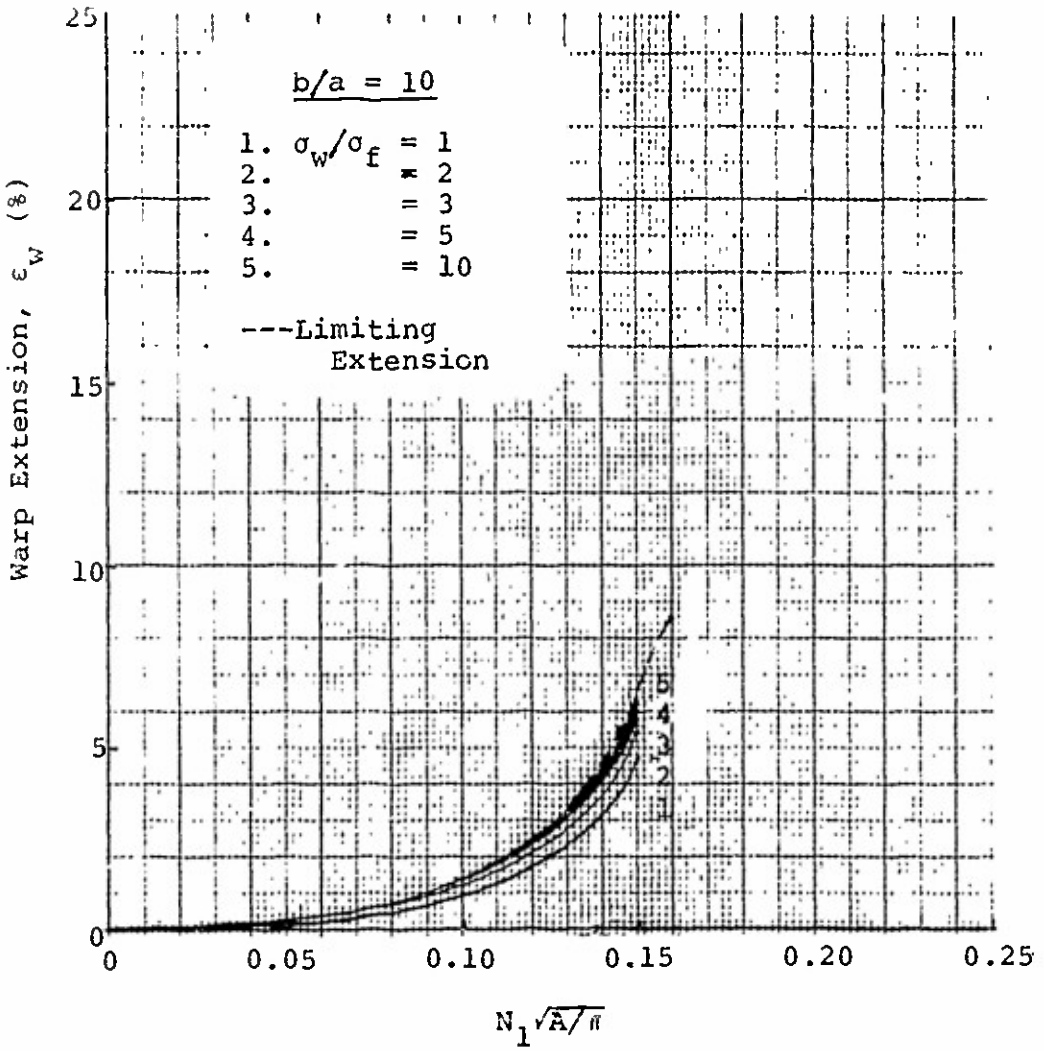

Figure 38(b). Fabric Extension in the Warp Direciton: (Aspect Ratio = 10), Inextensible Yarn, Initially Straight Fabric

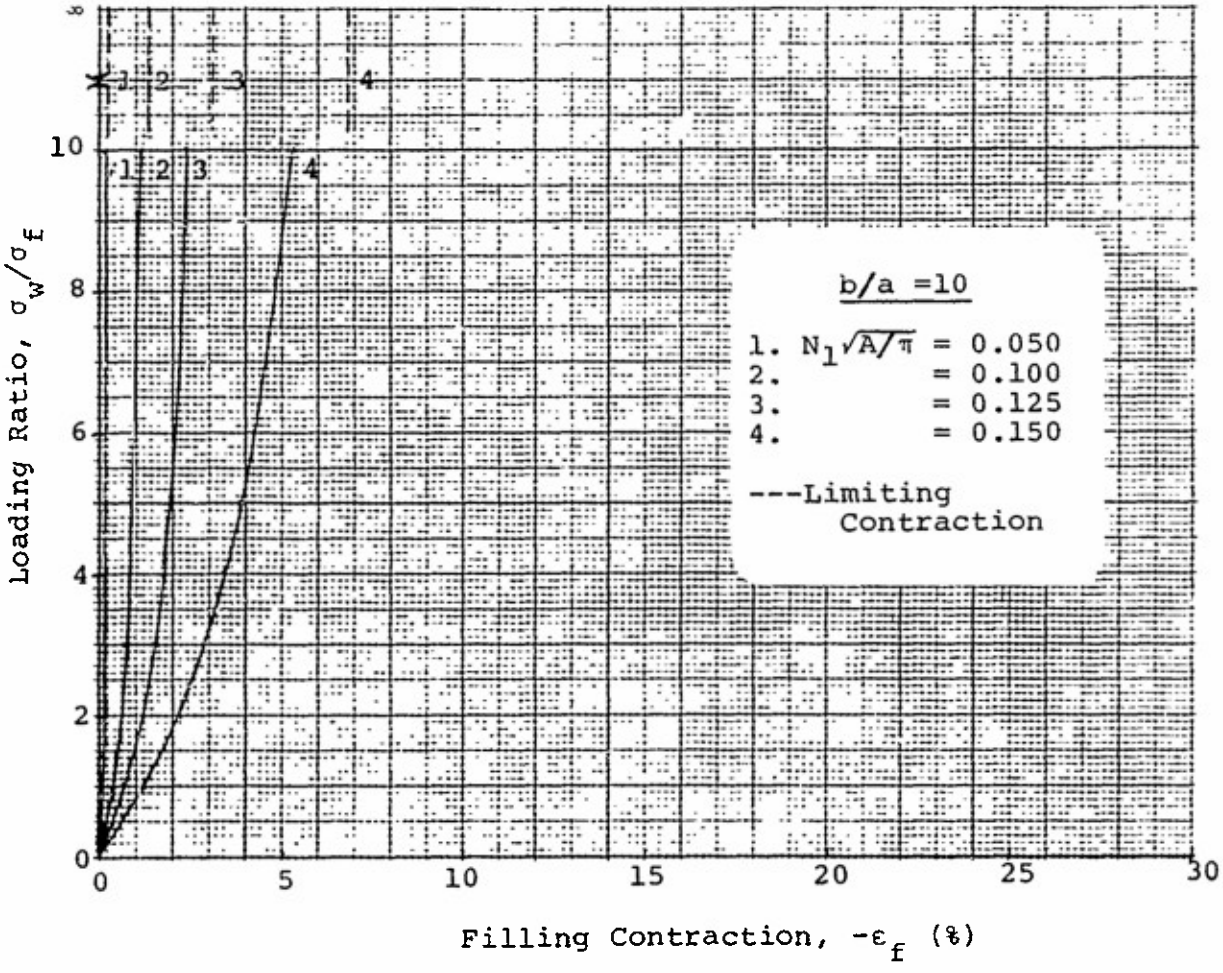

Figure 39(a). Fabric Contraction in the Filling Direction: (Aspect Ratio = 10), Inextensible Yarn, Initially Straight Filling

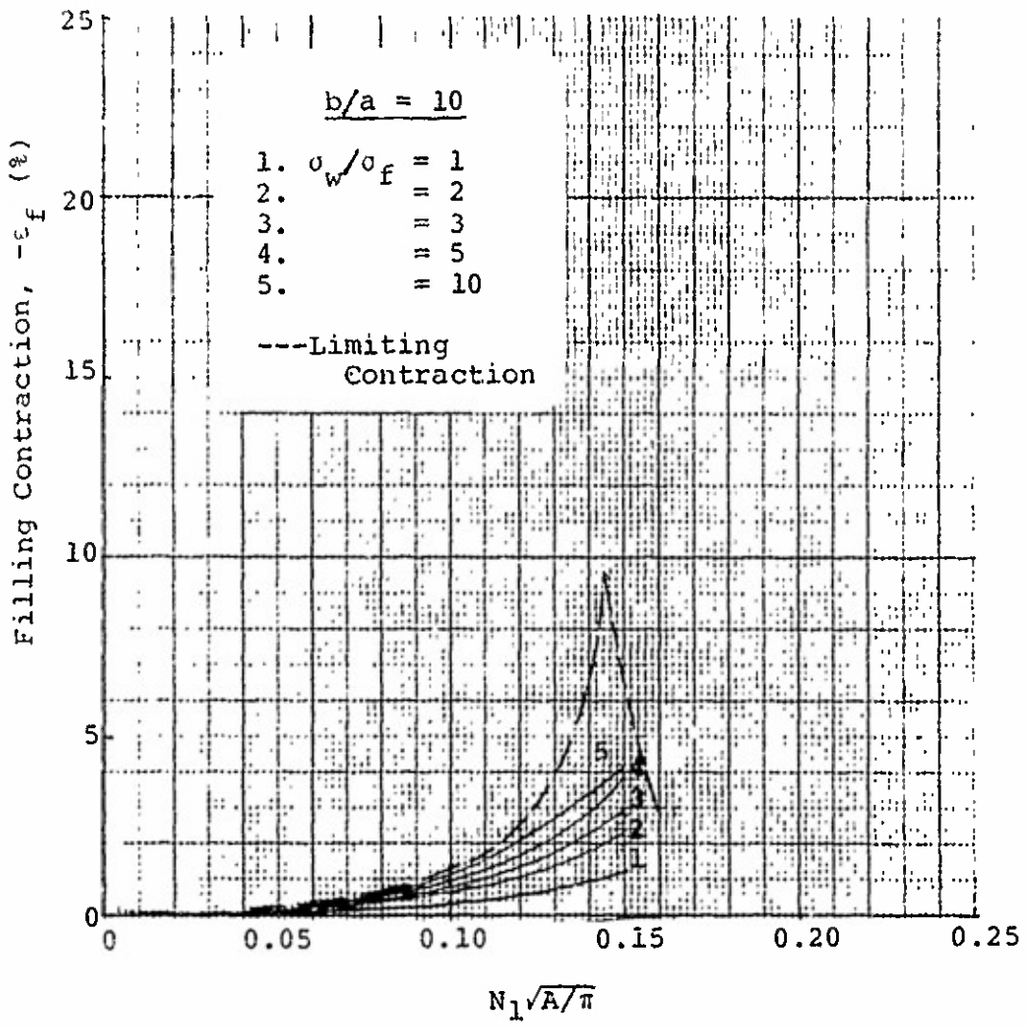

Figure 39(b). Fabric Contraction in the Filling Direction: (Aspect Ratio = 10), Inextensible Yarn, Initially Straight Filling

TABLE 5

MAXIMUM VALUES OF $N_1\sqrt{A/\pi}$ FOR WHICH WARP YARNS CAN BE PULLED STRAIGHT - INITIALLY STRAIGHT FILLING

b/a	Minimum $L_w/\sqrt{A/\pi}$	Maximum $N_1\sqrt{A/\pi}$
1	7.606	0.159
2	6.370	0.182
3	6.164	0.183
5	6.323	0.173
10	7.256	0.145

For values of $N_1\sqrt{A/\pi}$ less than those given in Table 5 for each of the values of yarn aspect ratio b/a, the yarns are pulled straight as $\sigma_w/\sigma_f \to \infty$. However, unlike the case of initially square fabric, the fabric extension in the warp direction continues to increase with increasing $N_1\sqrt{A/\pi}$ for $N_1\sqrt{A/\pi}$ values greater than those given in the table. The fabric extension in the warp direction evidently is not severely limited by the inability of the fabric to contract further in the filling direction as $\sigma_w/\sigma_f \to \infty$, because of the development of the maximum possible crimp in the filling yarn. When $N_1\sqrt{A/\pi}$ is equal to the values given in the table the warp yarns are pulled straight and the maximum crimp is developed in the filling yarn.

The maximum warp extensions possible from crimp interchange are tabulated in Table 6 for various degrees of initial weave tightness and yarn aspect ratios, and values of $N_1\sqrt{A/\pi}$ less than those listed in Table 5. Similarly, the maximum filling contractions possible from crimp interchange are given in Table 7 for values of $N_1\sqrt{A/\pi}$ greater than those listed in Table 5. The corresponding fabric extensions in the orthogonal direction and the effective fabric Poisson's ratios are also given in the tables. The extensions in Tables 6 and 7 are the data plotted in Figures 30 through 39 as the fabrics response at an infinite loading ratio.

A limiting geometry of the third type, i.e., warp yarns touching, does not occur initially in the fabric model with straight filling since an equal number of warp and filling yarns per unit width is specified. Upon loading, the first and second types of limiting geometry are achieved at contractions lower than would be required to achieve this third-type of limitation.

TABLE 6

MAXIMUM WARP EXTENSION POSSIBLE FROM CRIMP INTERCHANGE FOR FABRICS WITH INITIALLY STRAIGHT FILLING

b/a	$N_1\sqrt{A/\pi}$	Maximum Warp Extension, ε_w (%)	Associated Filling Contraction, $-\varepsilon_f$ (%)	Poisson's Ratio, μ
1	0.050	2.0	2.0	1.00
	0.100	8.1	8.9	1.10
	0.125	12.8	15.2	1.19
	0.150	18.6	26.1	1.40
	0.159	21.0	36.3	1.73
2	0.050	0.9	0.9	1.00
	0.100	4.1	4.3	1.05
	0.125	6.7	7.3	1.09
	0.150	10.1	12.0	1.19
	0.182	16.0	27.6	1.73
3	0.050	0.6	0.6	1.00
	0.100	2.9	3.0	1.03
	0.125	4.8	5.2	1.08
	0.150	7.6	8.8	1.16
	0.183	12.9	22.2	1.72
5	0.050	0.4	0.4	1.00
	0.100	2.0	2.0	1.00
	0.125	3.5	3.7	1.06
	0.150	5.8	6.8	1.17
	0.173	9.3	16.0	1.72
10	0.050	0.2	0.2	1.00
	0.100	1.3	1.3	1.00
	0.125	2.8	3.1	1.11
	0.145	5.5	9.4	1.71

TABLE 7

MAXIMUM FILLING CONTRACTION POSSIBLE FROM CRIMP INTERCHANGE FOR FABRICS WITH INITIALLY STRAIGHT FILLING YARNS

b/a	$N_1\sqrt{A/\pi}$	Maximum θ_{2f} (radians)	$N_{2w}\sqrt{A/\pi}$	Maximum Filling Contraction $-\varepsilon_f$ (%)	Associated Warp Extension ε_w (%)	Poisson's Ratio μ
1	0.159	1.5708	0.250	36.3	21.0	1.73
	0.200	1.2500	0.263	24.1	31.7	0.76
	0.220	1.1364	0.276	20.2	36.9	0.55
	0.240	1.0417	0.290	17.1	42.9	0.40
	0.250	1.0000	0.297	15.9	46.6	0.34
2	0.182	1.5708	0.251	27.6	16.0	1.73
	0.200	1.3854	0.254	21.3	19.6	1.09
	0.220	1.2135	0.262	16.2	23.5	0.69
	0.240	1.0704	0.274	12.3	27.9	0.44
	0.251	1.0000	0.281	10.6	31.0	0.34
3	0.183	1.5708	0.235	22.2	12.9	1.72
	0.200	1.3541	0.238	16.0	16.0	1.00
	0.220	1.1404	0.247	10.8	19.6	0.55
	0.235	1.0000	0.256	7.9	23.3	0.34
5	0.173	1.5708	0.206	16.0	9.3	1.72
	0.200	1.0864	0.214	6.5	14.2	0.46
	0.206	1.0000	0.217	5.3	15.5	0.34
10	0.145	1.5708	0.160	9.4	5.5	1.71
	0.150	1.3824	0.161	6.8	6.3	1.08
	0.160	1.0000	0.165	2.9	8.5	0.34

For initially square fabrics the filling contraction is significantly greater than the warpwise extension. However when the filling is initially straight, the warp extension is somewhat greater than the filling contraction. Additionally, a comparison of the extensions in Figures 10 through 19 and Figures 30 through 39 shows that for any value of $N_1\sqrt{A/\pi}$, σ_w/σ_f and b/a the warp extension is considerably greater and the filling contraction somewhat greater when the filling yarns are initially straight. The difference between the extensions decreases as the yarn aspect ratio increases. The filling contraction is greater because larger changes in filling crimp can occur when the filling is initially straight. Similarly, the fabric extension in the warp direction is greater because: (1) the initial crimp in the warp yarns is larger for a given $N_1\sqrt{A/\pi}$ when the filling yarns are initially straight; (2) there is greater crimp interchange between the warp and filling yarns when the filling yarns are initially straight. The difference between the extensions and contractions for the initially square and filling straight fabrics decreases with increasing yarn aspect ratio because the larger b/a the less the initial yarn crimp.

The effective Poisson's ratio for fabrics with initially straight filling is given in Figures 40(a), 41(a)---44(a) as a function of loading ratio for various values of b/a and $N_1\sqrt{A/\pi}$, and similarly in Figures 40(b), 41(b)---44(b) as a function of $N_1\sqrt{A/\pi}$ for various values of b/a and σ_w/σ_f. The values for an infinite loading ratio are also plotted. These latter data were taken from Tables 6 and 7.

As shown, μ increases with increasing loading ratio for all values of b/a and $N_1\sqrt{A/\pi}$. For $\sigma_w/\sigma_f < 10$ and low values of b/a the Poisson's ratio decreases with increasing $N_1\sqrt{A/\pi}$; for larger b/a, μ is constant for small $N_1\sqrt{A/\pi}$ but decreases moderately at large values of $N_1\sqrt{A/\pi}$. At $\sigma_w/\sigma_f = \infty$, μ increases up to a maximum at the $N_1\sqrt{A/\pi}$ value given in Table 5 for the appropriate b/a and then decreases with increasing values above those given in the table.

The Poisson's ratio for $\sigma_w/\sigma_f = \infty$ does not have a value of one at that $N_1\sqrt{A/\pi}$ for which the fabric is initially jammed as was the case for initially square fabric. In the initially square jammed fabric

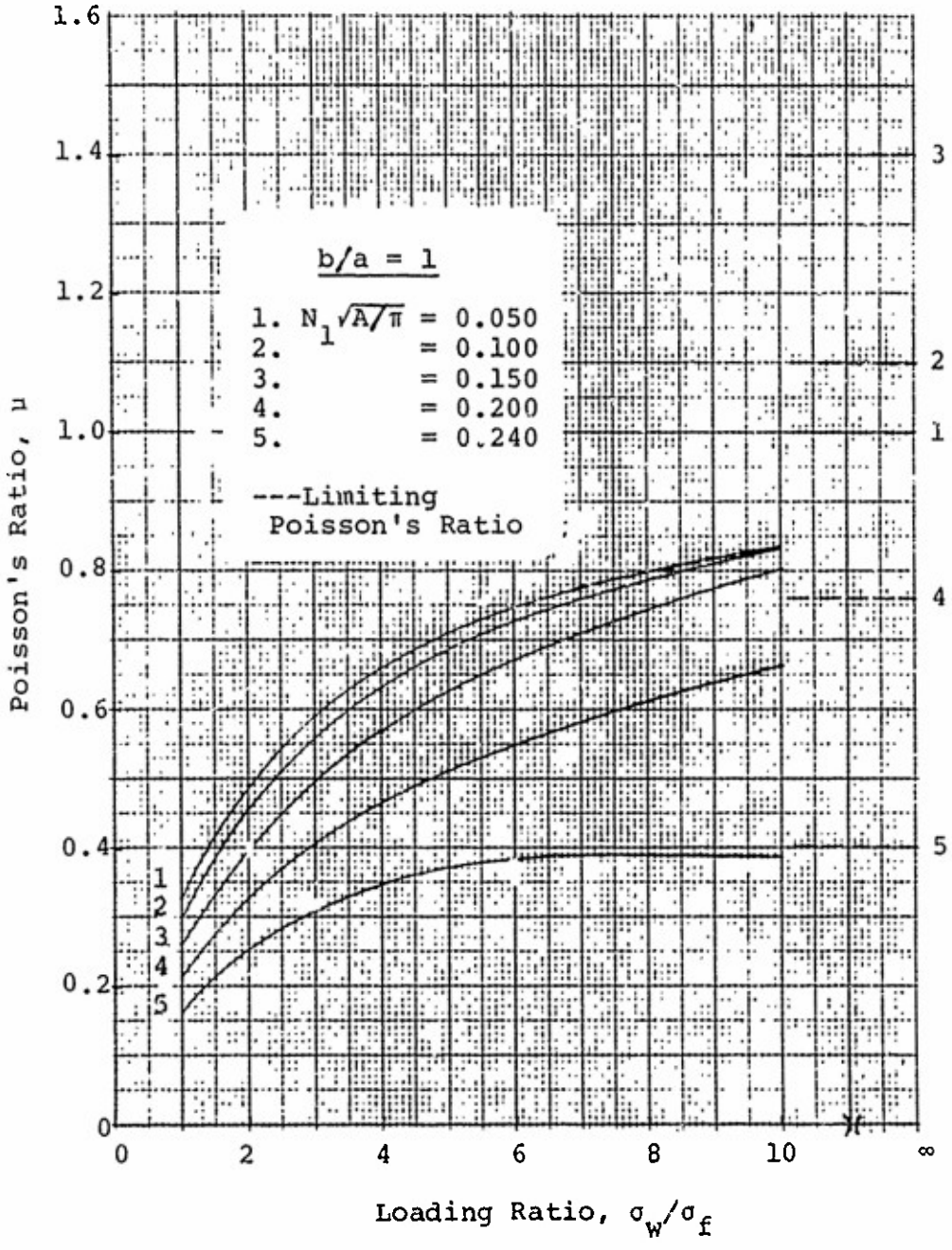

Figure 40(a). Poisson's Ratio:(Aspect Ratio = 1), Inextensible Yarn, Initially Straight Filling

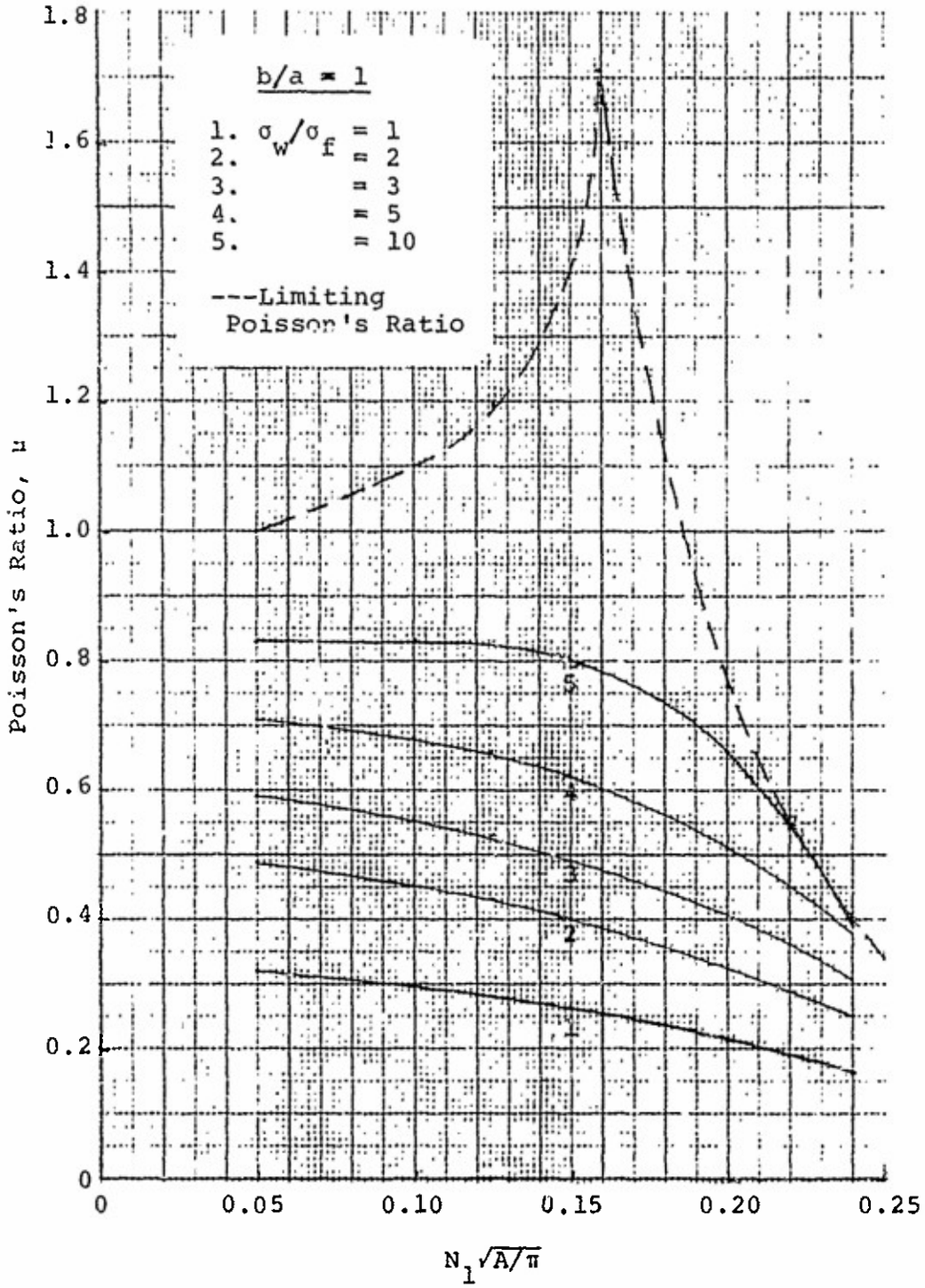

Figure 40(b). Poisson's Ratio:(Aspect Ratio = 1), Inextensible Yarn, Initially Straight Filling

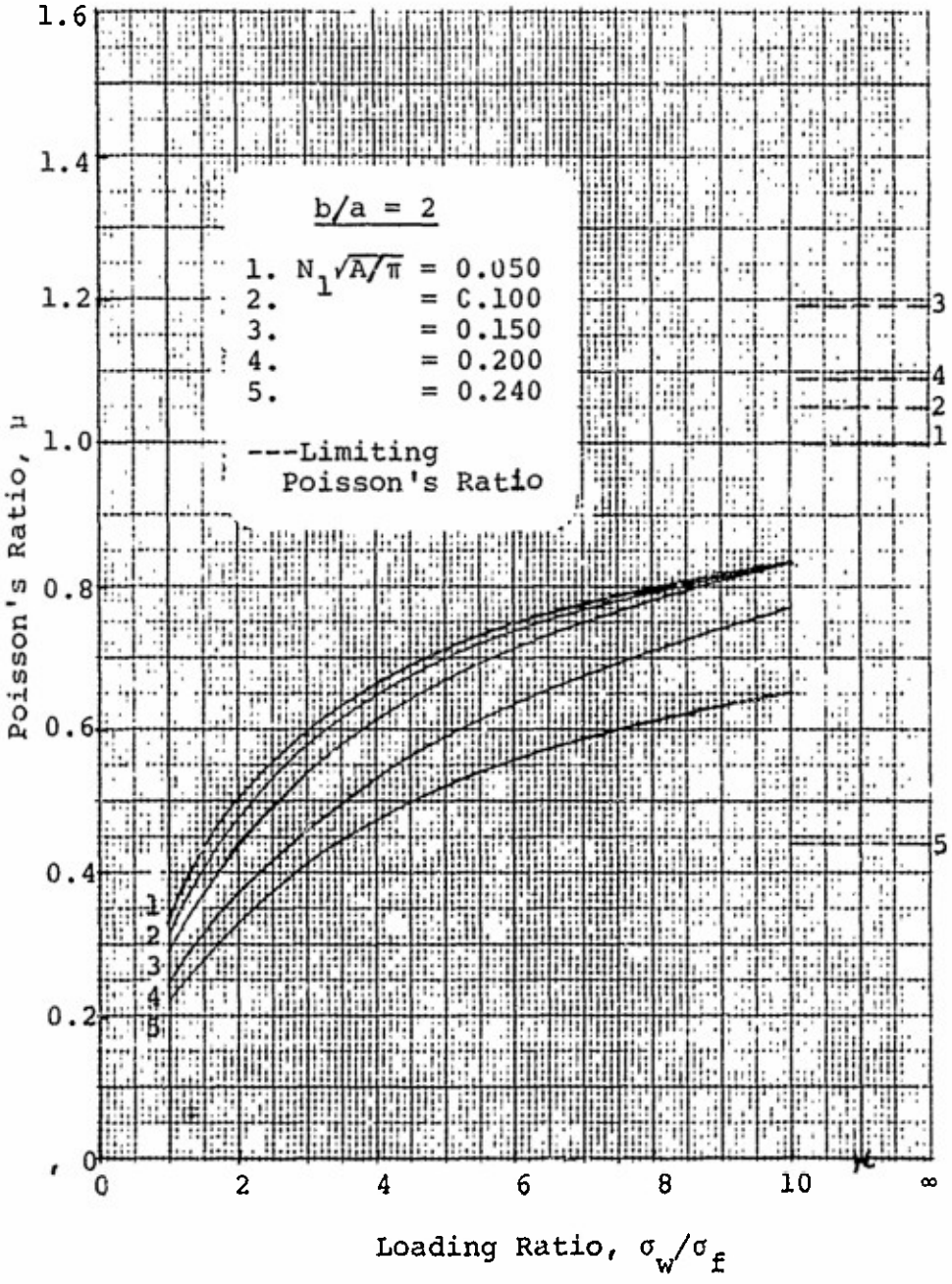

Figure 41(a). Poisson's Ratio:(Aspect Ratio = 2), Inextensible Yarn, Initially Straight Filling

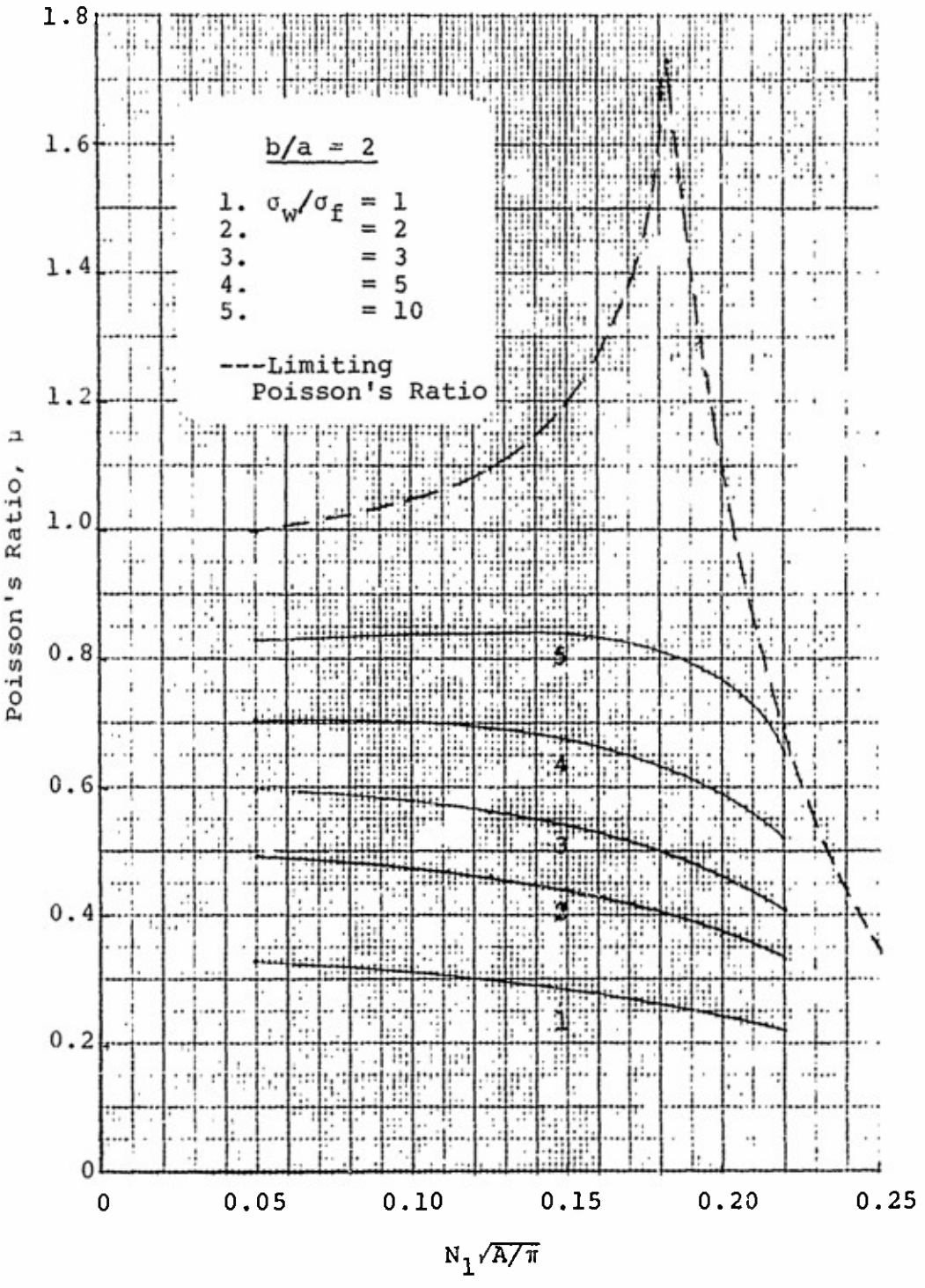

Figure 41(b). Poisson's Ratio: (Aspect Ratio = 2), Inextensible Yarn, Initially Straight Filling

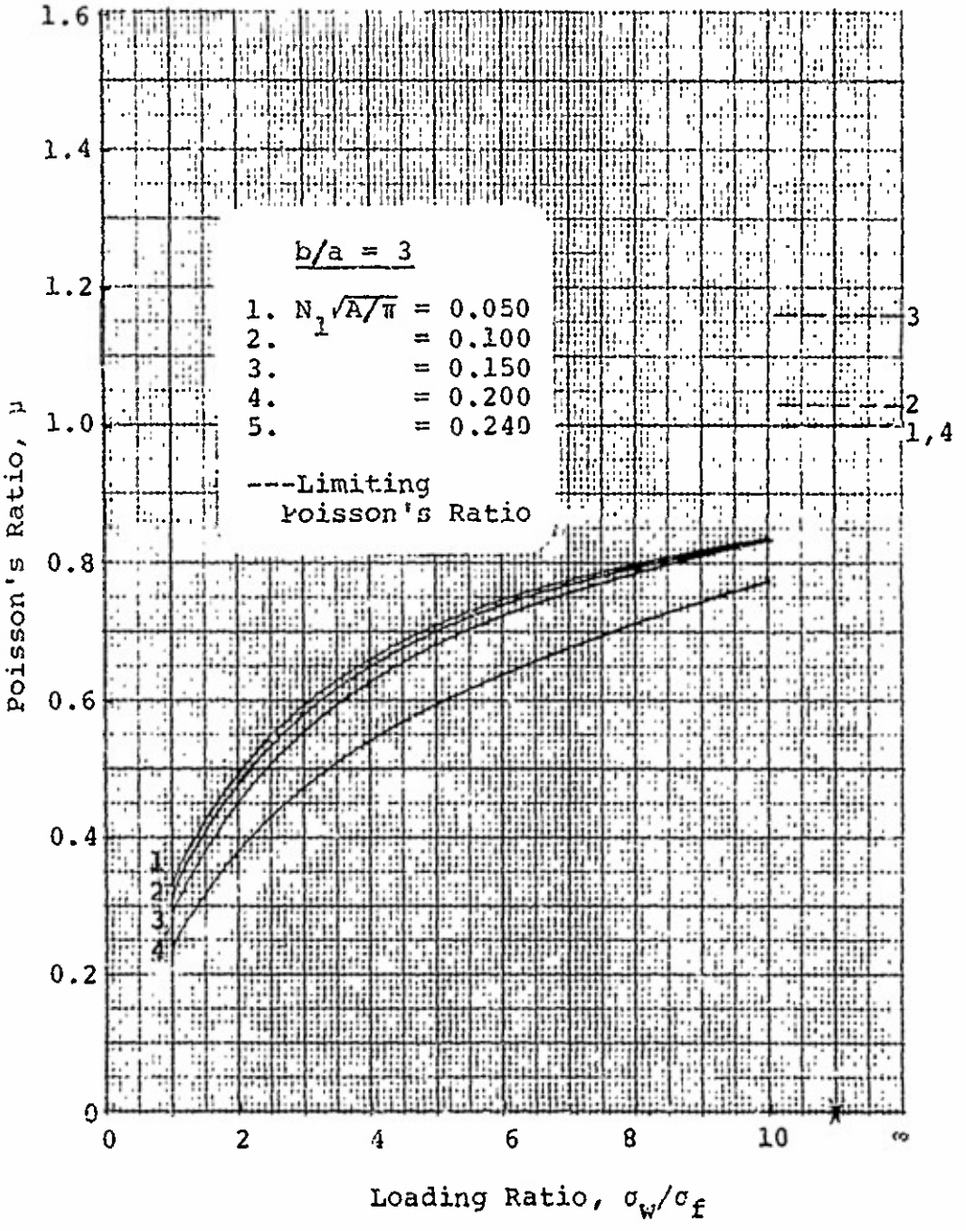

Figure 42(a). Poisson's Ratio: (Aspect Ratio = 3), Inextensible Yarn, Initially Straight Filling

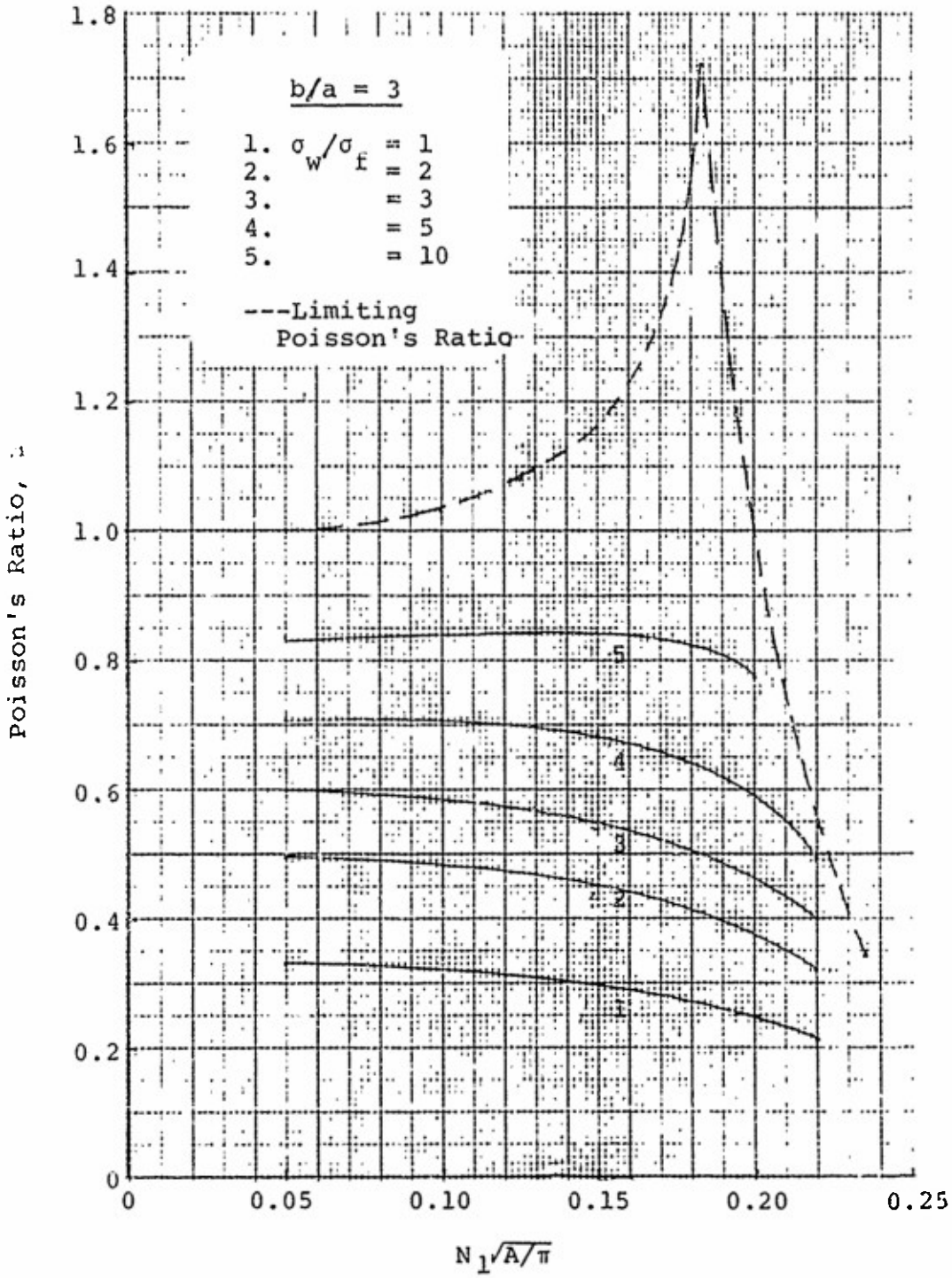

Figure 42(b). Poisson's Ratio:(Aspect Ratio = 3), Inextensible Yarn, Initially Straight Filling

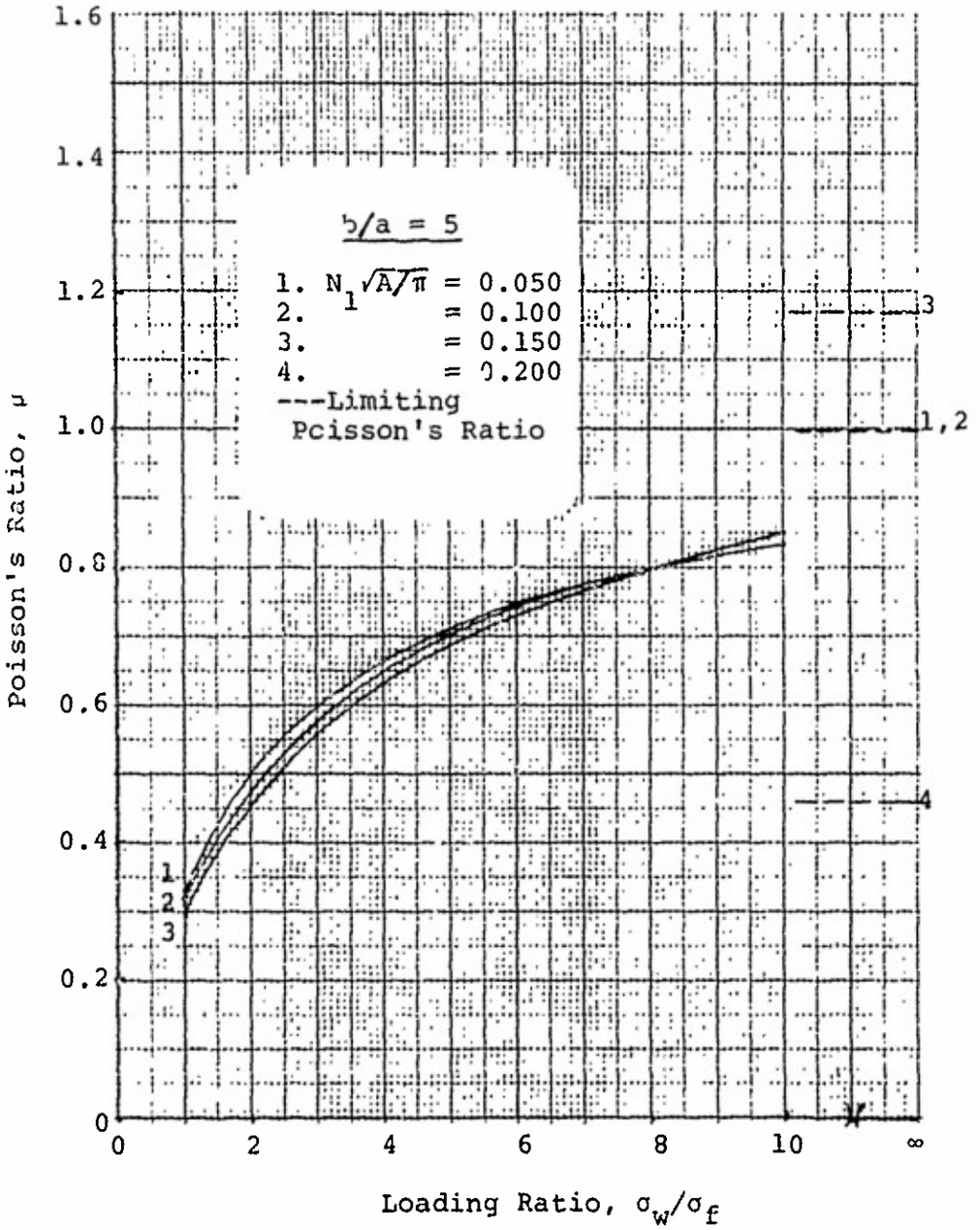

Figure 43(a). Poisson's Ratio: (Aspect Ratio = 5), Inextensible Yarn, Initially Straight Filling

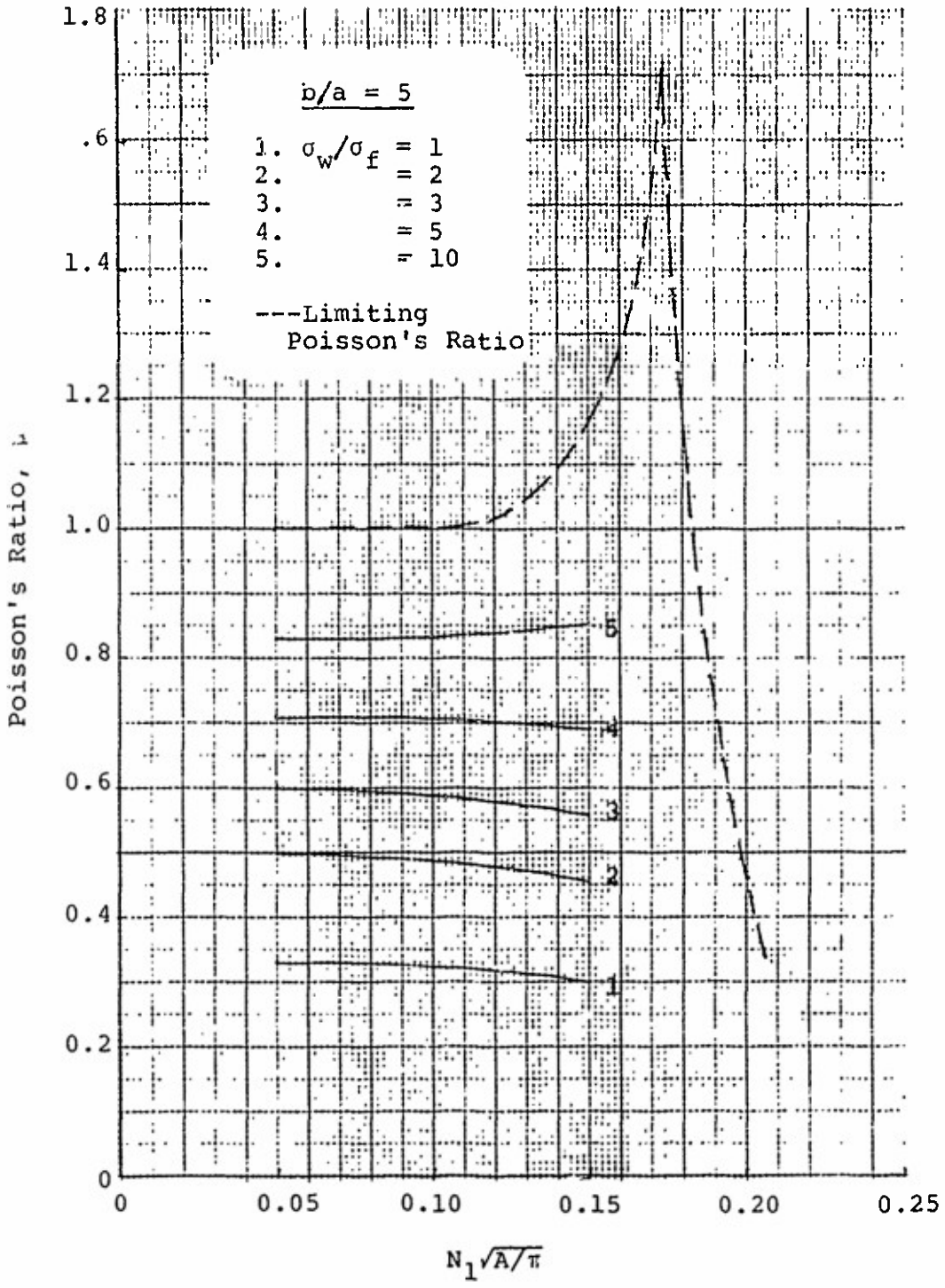

Figure 43(b). Poisson's Ratio: (Aspect Ratio = 5), Inextensible Yarn, Initially Straight Filling

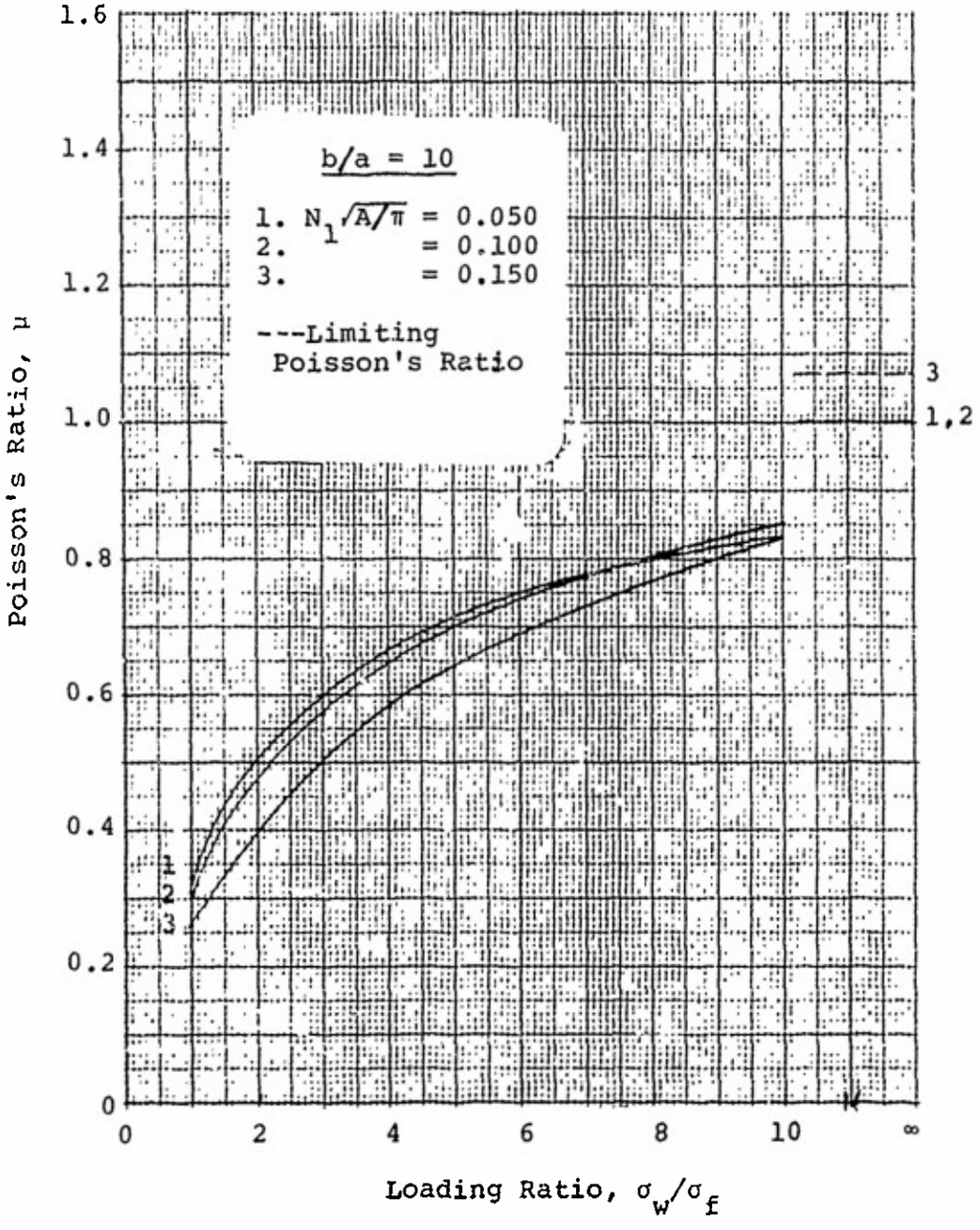

Figure 44(a). Poisson's Ratio: (Aspect Ratio = 10), Inextensible Yarn, Initially Straight Filling

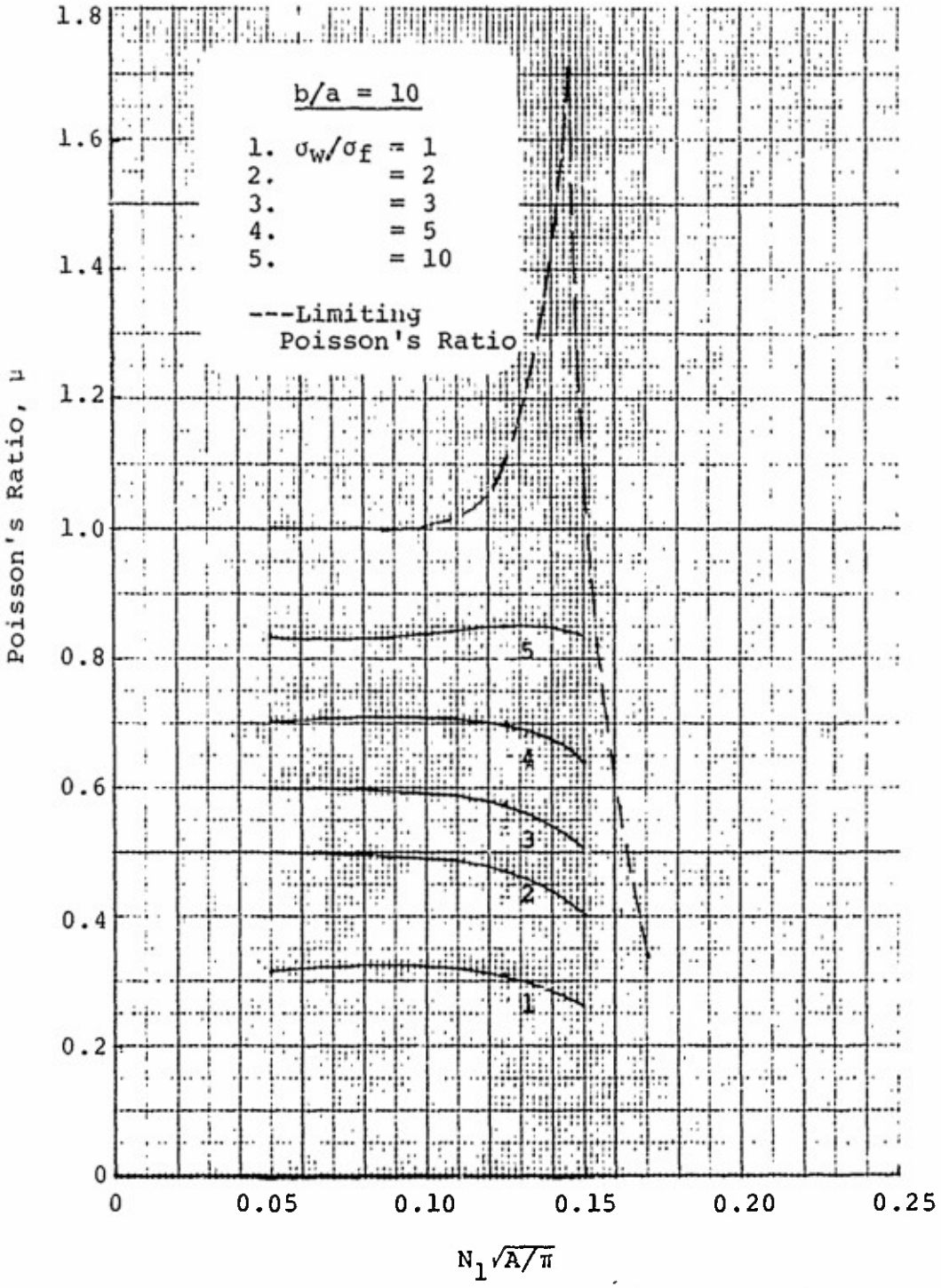

Figure 44(b). Poisson's Ratio: (Aspect Ratio = 10), Inextensible Yarn, Initially Straight Filling

the filling yarns have already attained maximum achievable crimp. However, in the initially jammed fabric with straight filling (with the same number of yarns per unit width in the warp and filling directions), as a force is applied in the warpwise direction, crimp can develop in the filling yarns.

As can be seen by comparing the data in Figures 40 through 44, the Poisson's ratio changes little with yarn aspect ratio.

Comparison of the data in Figures 23-27 and 40-44 shows that the Poisson's ratio for fabric with initially straight filling is roughly one third that for initially square fabric.

The maximum number of yarns accommodatable in fabric with straight filling is given in Figure 45 as a function of yarn aspect ratio. This curve is determined from Equation 30 letting $\theta_{1w} = 90°$, the maximum angle achievable with the assumed initial fabric geometry.

Comparing Figures 22 and 45, it can be seen that for a given yarn aspect ratio the maximum $N_1\sqrt{A/\pi}$ is approximately the same for both initially square fabric and fabric with initially straight filling at the larger b/a's. However, as the yarns become more nearly circular, the maximum permissible $N_1\sqrt{A/\pi}$ is somewhat larger for the initially square fabric.

III. Simplified Procedure; Any Yarn Aspect Ratio

The response to loading of racetrack-yarn fabrics of any aspect ratio, b/a, woven from inextensible yarns is identical to that of round-yarn fabrics of radius "a" with respect to the final yarn angles, θ_{2w} and θ_{2f}, and changes in the yarn spacing $\Delta\, 1/N_w$ and $\Delta\, 1/N_f$ achieved for any particular loading ratio

where $$\Delta\frac{1}{N_w} = \frac{1}{N_{2w}} - \frac{1}{N_{1w}}$$

and $$\Delta\frac{1}{N_f} = \frac{1}{N_{2f}} - \frac{1}{N_{1f}}.$$

As illustrated in Figure 1, that portion of the fabric model between sections A-A and B-B is the same as that for a fabric woven from circular yarns of radius a. For b/a > 1 only the straight

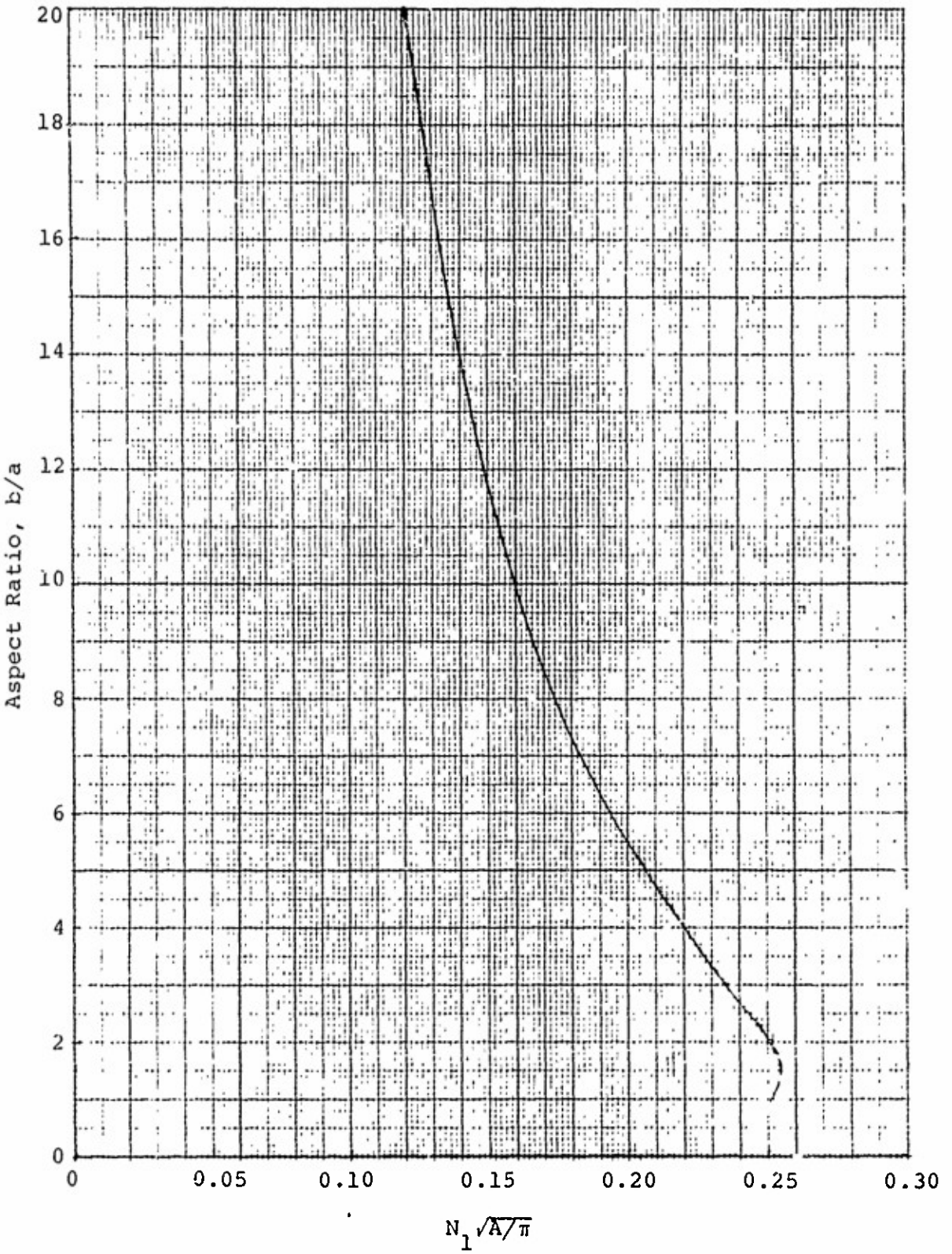

Figure 45. Maximum Number of Yarns Accommodatable in Fabric with Initially Straight Filling as a Function of Yarn Aspect Ratio

segment of the yarn cross-section is outside the sections A-A and B-E, and this portion of the model does not change with increasing load.

Letting N_1' and N_2' denote the number of yarns per unit width in a fabric comprised of inextensible circular yarns (b/a = 1) before and after application of the external loads respectively, and N_1 and N_2, the number of yarns per unit width in a fabric comprised of racetrack yarns of any aspect ratio as before, it can be seen from Figure 1 that

$$\frac{1}{N_1} = \frac{1}{N_1'} + 2(b-a)$$

$$\frac{1}{N_2} = \frac{1}{N_2'} + 2(b-a) \qquad (37)$$

Therefore, the fabric extension ε is given by

$$\varepsilon = \frac{1/N_2 - 1/N_1}{1/N_1} = \frac{\varepsilon'}{1+2(b/a-1)N_1'a}$$

where

$$\varepsilon' = \frac{N_1'}{N_2'} - 1$$

Consequently, the response of both initially square fabric and fabric with initially straight filling woven from inextensible yarn having any yarn aspect ratio b/a can be determined from the diagrams giving the response of fabric comprised of circular yarns (b/a = 1). The procedure is as follows:

Given b/a and $N_1\sqrt{A/\pi}$ calculate N_1a (Equation 22) and $N_1'a$

$$\frac{1}{N_1'a} = \frac{1}{N_1a} - 2(b/a-1) \qquad (38)$$

(note: $N_1'a \approx N_1'\sqrt{A/\pi}$ for round yarns). Obtain ε'_w and ε'_f from the load-extension diagrams for b/a = 1 at the specified loading ratio σ_w/σ_f and calculated value

of $N_1'\sqrt{A/\pi}$. The actual extensions of the racetrack-yarn fabric having yarn with b/a > 1 are then determined from the following expressions

$$\varepsilon_w = \frac{\varepsilon'_w}{[1+2(b/a-1)(N_1'a)]} \tag{39}$$

$$\varepsilon_f = \frac{\varepsilon'_w}{[1+2(b/a-1)(N_1'a)]} \tag{40}$$

IV. Initially Square Fabric, Infinitely Flexible, Extensible Yarn (Linearly Elastic, $\nu = 0$), $\sigma_w/\sigma_f \geq 1$

Equations 20 and 21 describe the geometry of the fabric in the unloaded state with $L = L_1$. Then, assuming that the yarn cross-sectional dimensions do not change during loading, i.e., that the Poisson's ratio of the yarn is zero

$$b_{1w} = b_{1f} = b_{2w} = b_{2f} = b$$

$$a_{1w} = a_{1f} = a_{2w} = a_{2f} = a$$

The geometry of the deformed fabric is given by the following six equations derived from Equations 3-7 after simplification and replacement of subscript "1" by subscript "2", and Equation ? and Equations 15 and 16, assuming the fabric is woven from linearly elastic yarns.

$$\frac{\sigma_w}{K} = \frac{[\frac{L_{2w/a}}{L_1/a} - 1]\cos\theta_{2w}}{[\frac{L_{2f}}{a} - 2(b/a-1) - 4\theta_{2f}]\cos\theta_{2f} + 4\sin\theta_{2f} + 2(b/a-1)} \tag{41}$$

$$\frac{\sigma_f}{K} = \frac{[\frac{L_{2f}/a}{L_1/a} - 1]\cos\theta_{2f}}{[\frac{L_{2w}}{a} - 2(b/a-1) - 4\theta_{2w}]\cos\theta_{2w} + 4\sin\theta_{2w} + 2(b/a-1)} \tag{42}$$

$$\left[\frac{L_{2w}}{a} - 2(b/a-1)-4\theta_{2w}\right] \sin\theta_{2w}-4\cos\theta_{2w}$$

$$= 4(\cos\theta_{2f}-1)-\left[\frac{L_{2f}}{a} -2(b/a-1)-4\theta_{2f}\right]\sin\theta_{2f} \tag{43}$$

$$\frac{\sigma_w}{\sigma_f} = \frac{\cot\theta_{2w}\left\{\left[\frac{L_{2w}}{a} -2(b/a-1)-\theta_{2w}\right]\cos\theta_{2w}+4\sin\theta_{2w}+2(b/a-1)\right\}}{\cot\theta_{2f}\left\{\left[\frac{L_{2f}}{a} -2(b/a-1)-\theta_{2f}\right]\cos\theta_{2f}+4\sin\theta_{2f}+2(b/a-1)\right\}} \tag{44}$$

$$\frac{1}{N_{2w}a} = \left[\frac{L_{2f}}{a} -2(b/a-1)-4\theta_{2f}\right]\cos\theta_{2f}+4\sin\theta_{2f}+2(b/a-1) \tag{45}$$

$$\frac{1}{N_{2f}a} = \left[\frac{L_{2w}}{a} -2(b/a-1)-4\theta_{2w}\right]\cos\theta_{2w}+4\sin\theta_{2w}+2(b/a-1) \tag{46}$$

where $K = pE_fA/a$.

L_{2w}/a, L_{2f}/a, θ_{2w} and θ_{2f} were obtained from Equations 41 through 44 for a series of values of L_1/a, N_1a, σ_w/σ_f and $\sigma_w/(N_1a)K$. (Although only values of $\sigma_w/\sigma_f \geq 1$ were used, the results are also valid for $\sigma_w/\sigma_f < 1$ if the subscripts "w" and "f" are reversed.) $N_{2w}a$ and $N_{2f}a$ were then computed for each of the sets of values of L_{2w}/a, L_{2f}/a, θ_{2w} and θ_{2f} using Equations 45 and 46, and the corresponding fractional fabric extensions in the warp and filling directions computed with Equations 17 and 18. The results of the computations are plotted in Figures 46 through 70. These results encompass combinations of the following range of values for each of the parameters: $N_1\sqrt{A/\pi} = 0.050 - 0.240$; applied load $\sigma = 10 - 500$ lbs/inch width; yarn cross-sectional area $A = 0.785 \times 10^{-3} - 3.14 \times 10^{-3}$ square inches (for circular yarns this is a yarn radius of 0.005 - 0.010 inch); fiber modulus $E_f = 2 \times 10^5 - 30 \times 10^6$ lbs/square inch.

The fabric extensions in the warp and filling direction are given in Figures 46 through 65 as a function of the load applied in the warp direction for specific loading ratios and yarn aspect ratios and various values of $N_1\sqrt{A/\pi}$. Similarly, the fabric extensions are given in Figures 66 through 70 as a function of the load applied in the warp direction for specific values of b/a and $N_1\sqrt{A/\pi}$,

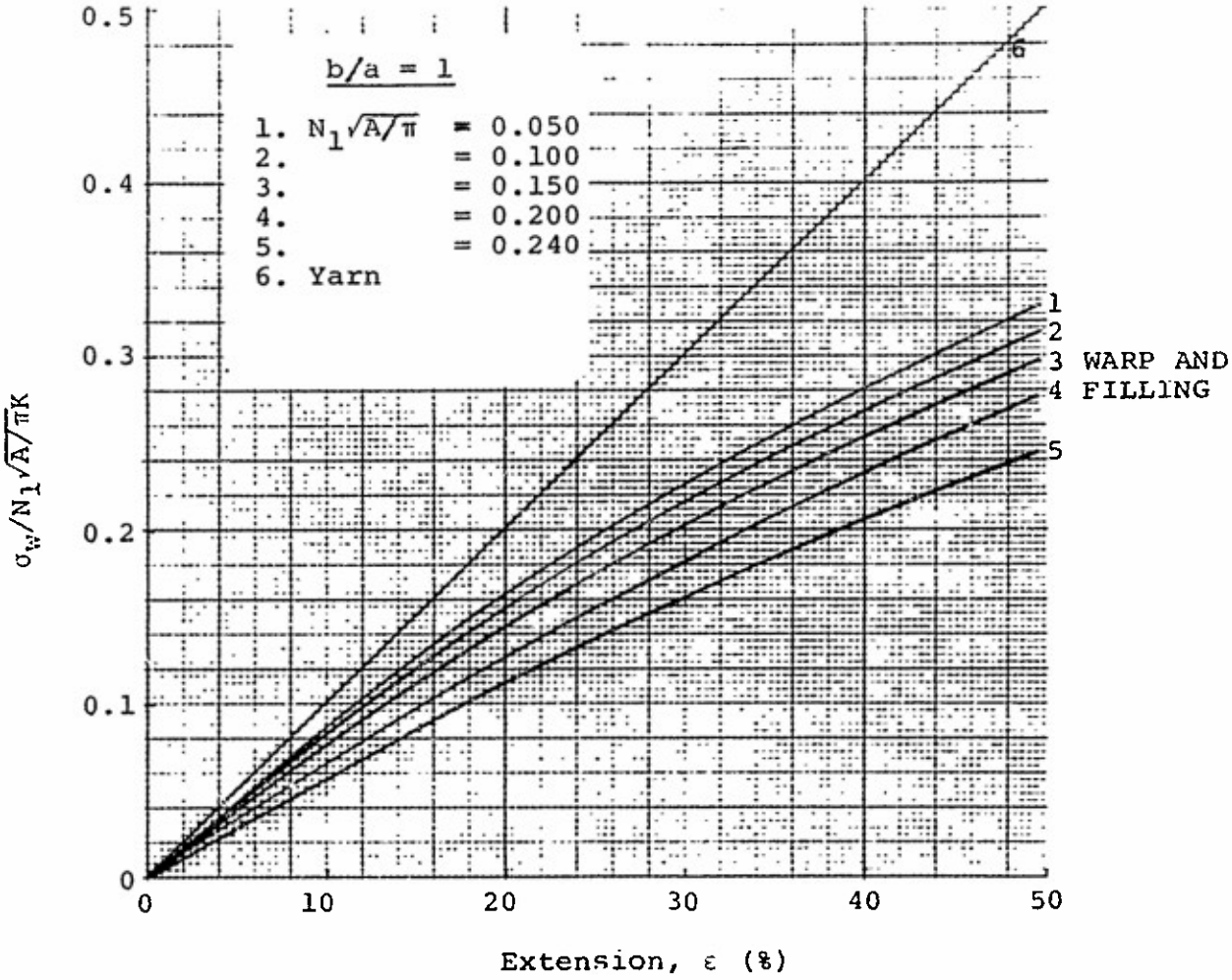

Figure 46. Fabric Extension: Linearly Elastic Yarn Initially Square Fabric, $\sigma_w/\sigma_f = 1$, b/a = 1

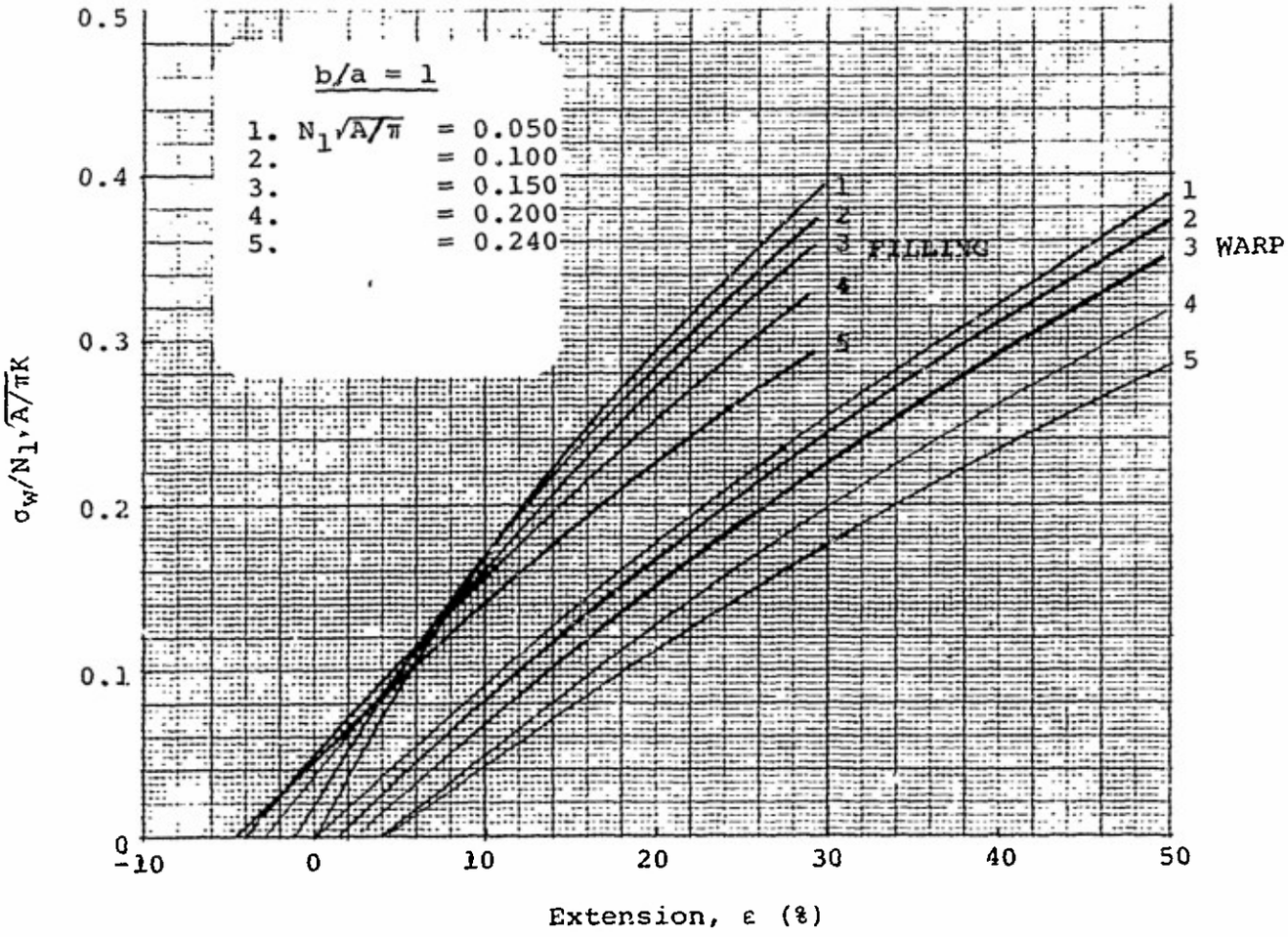

Figure 47. Fabric Extension: Linearly Elastic Yarn Initially Square Fabric, $\sigma_w/\sigma_f = 2$, b/a = 1

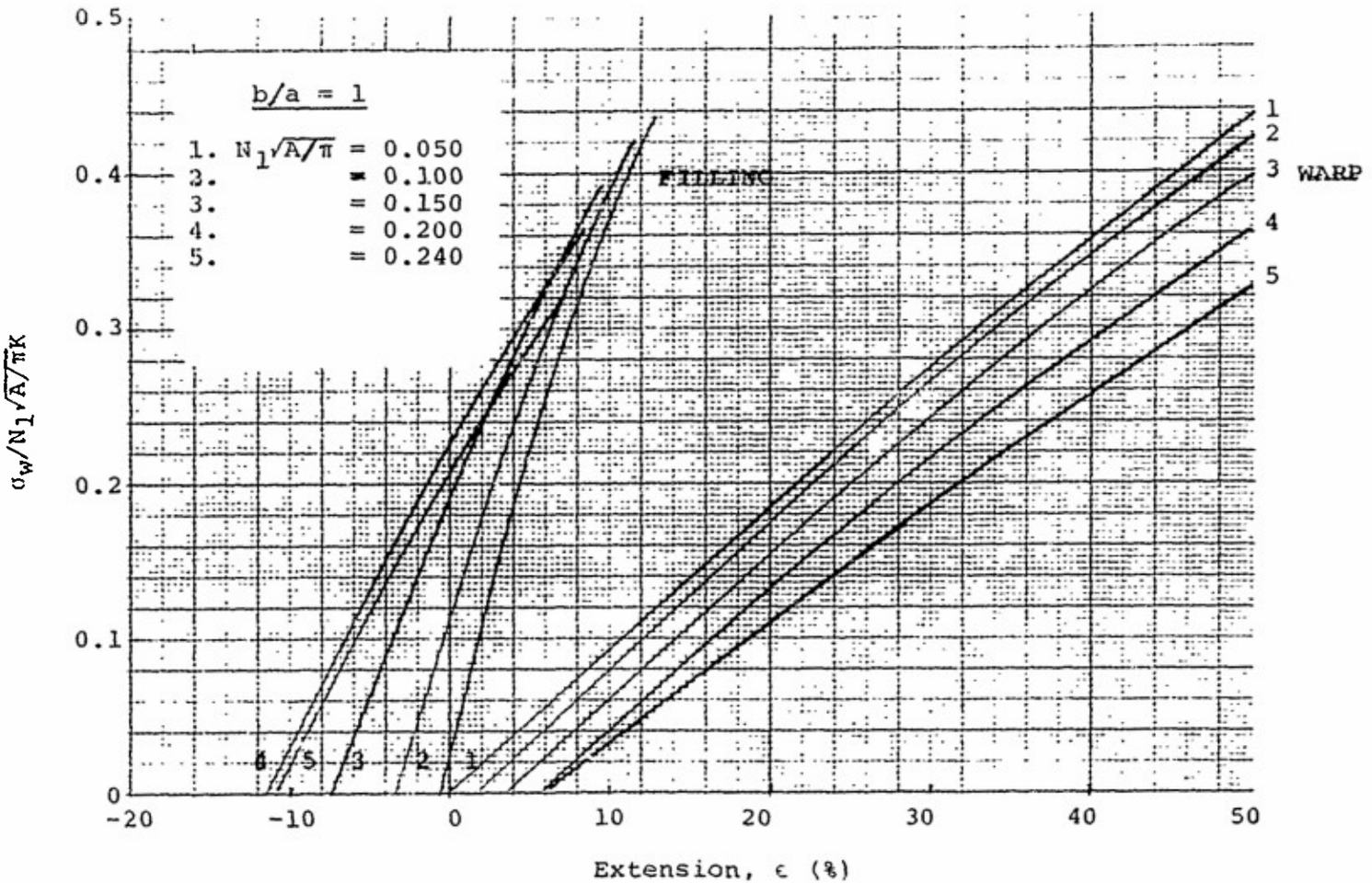

Figure 48. Fabric Extension: Linearly Elastic Yarn Initially Square Fabric, $\sigma_w/\sigma_f = 5$, b/a = 1

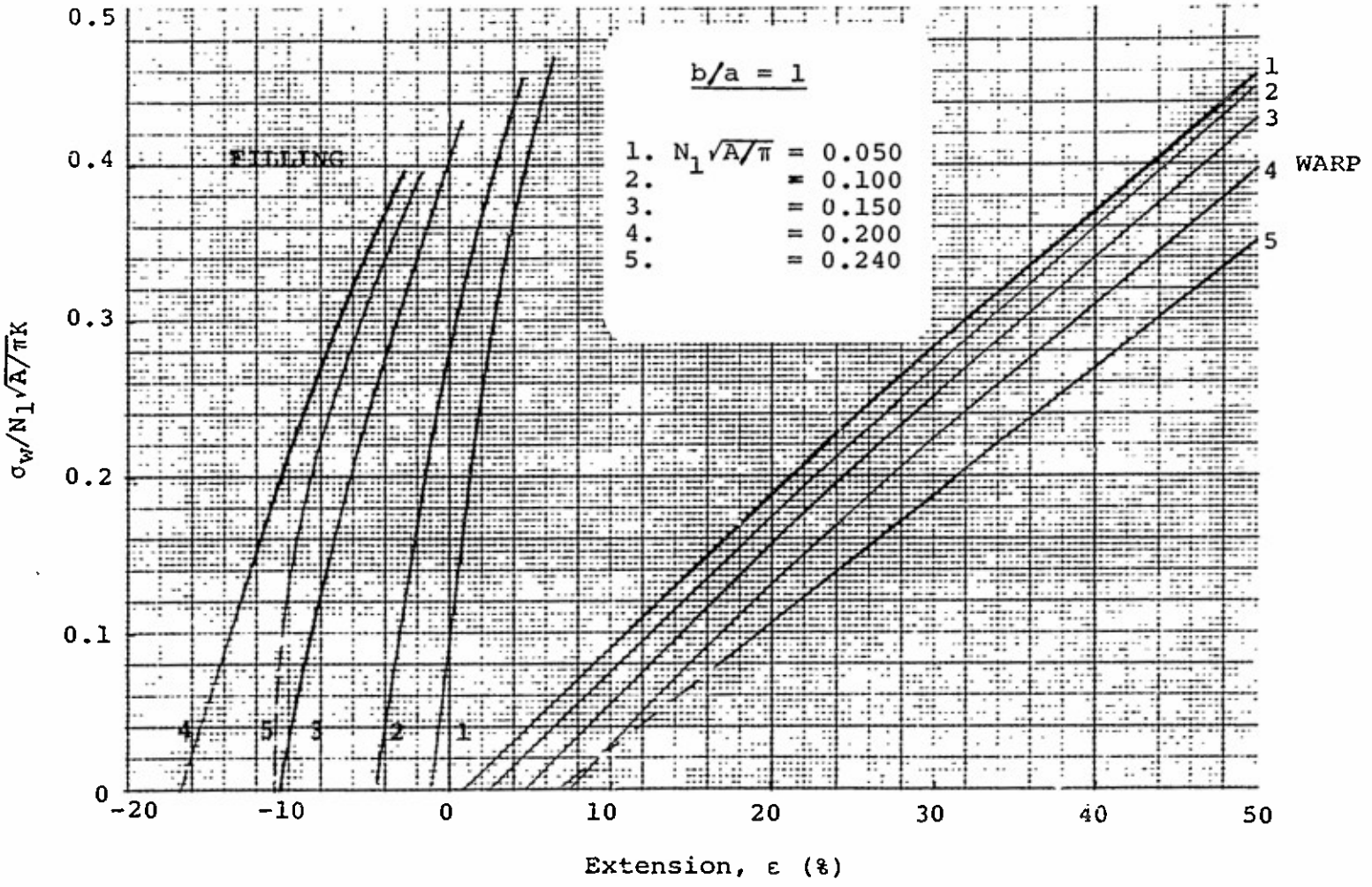

Figure 49. Fabric Extension: Linearly Elastic Yarn
Initially Square Fabric, σ_w/σ_f = 10, b/a = 1

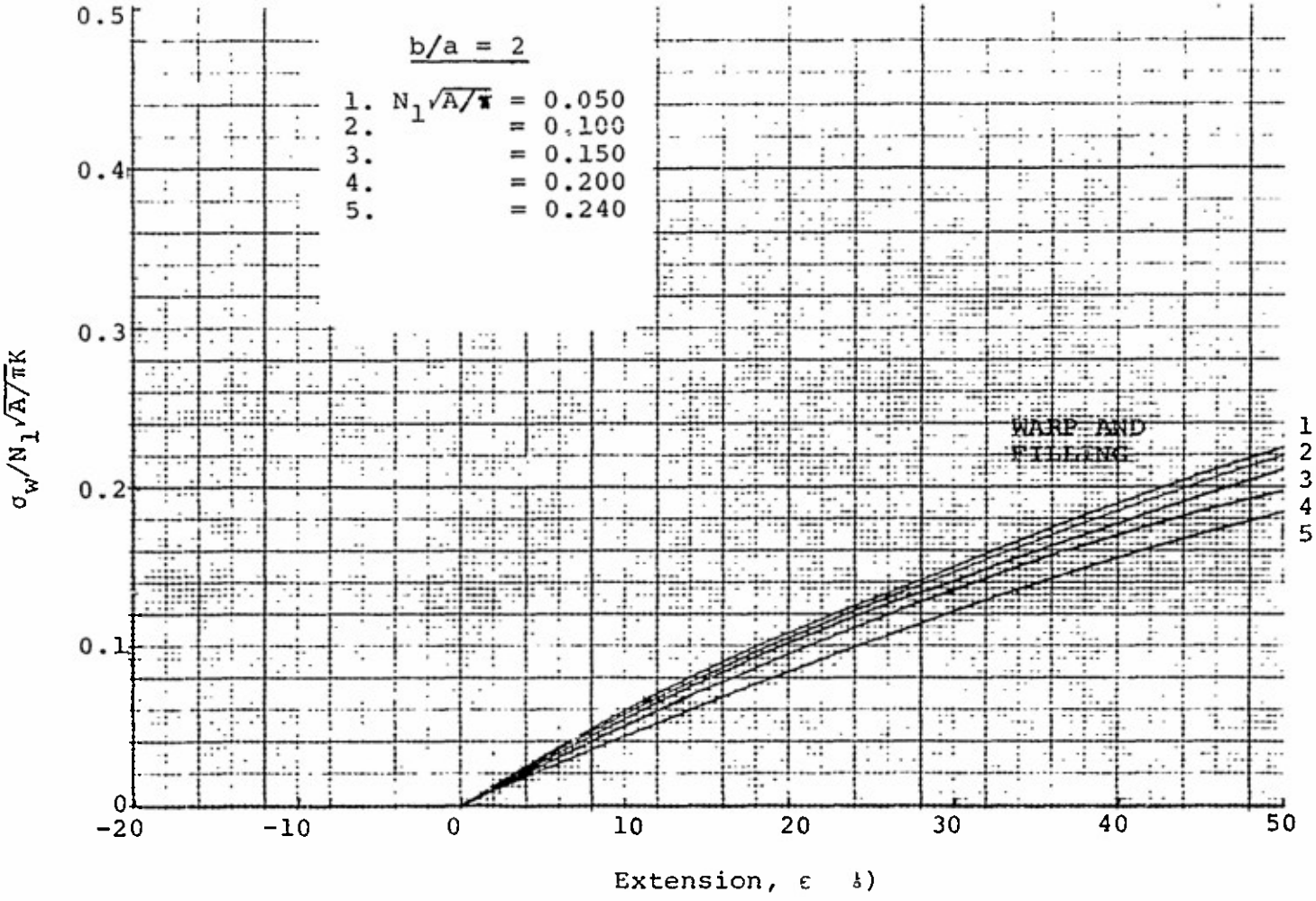

Figure 50. Fabric Extension: Linearly Elastic Yarn, Initially Square Fabric, $\sigma_w/\sigma_f = 1$, b/a = 2

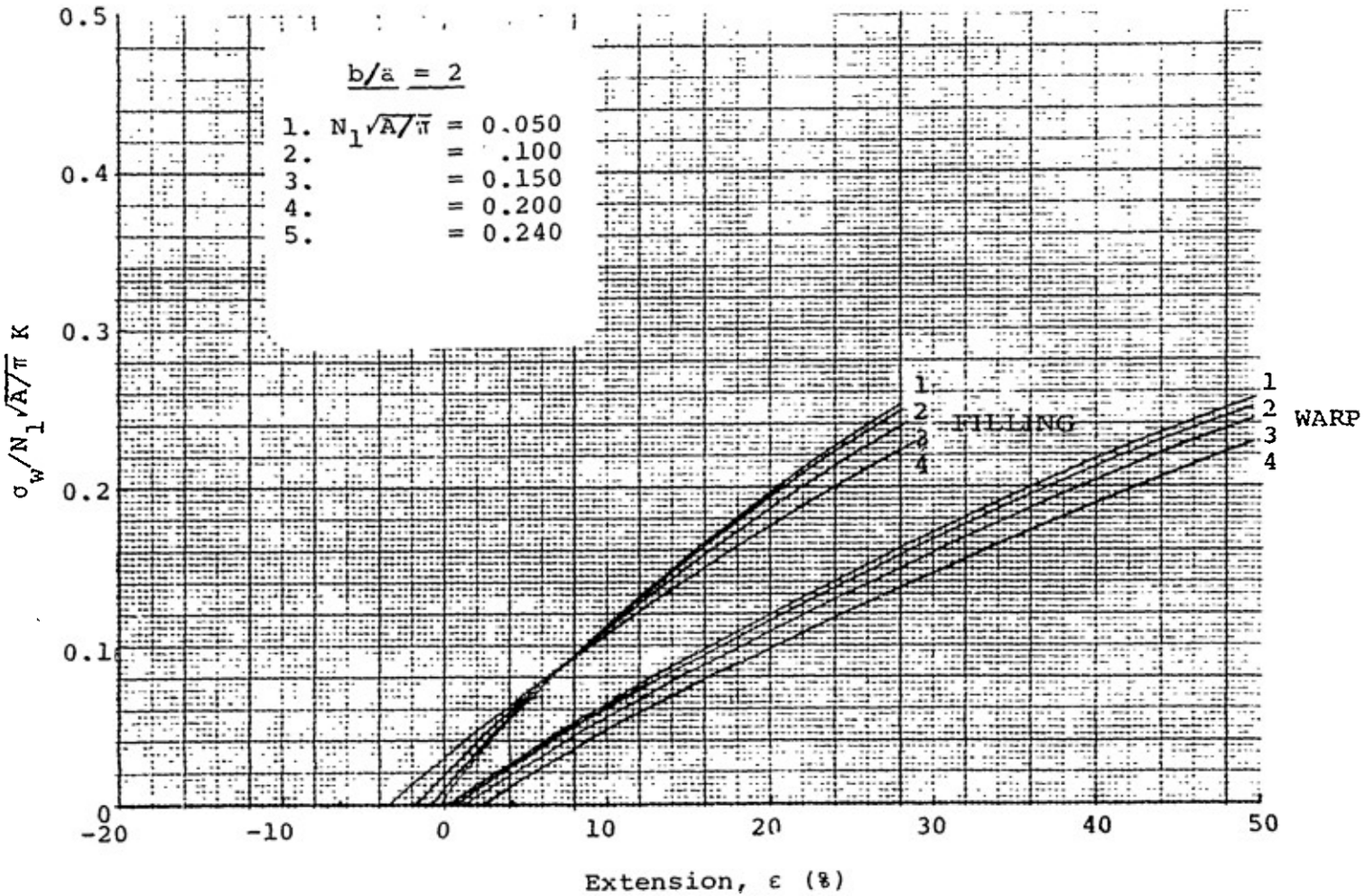

Figure 51. Fabric Extension: Linearly Elastic Yarn, Initially Square Fabric $\sigma_w/\sigma_f = 2$, b/a = 2

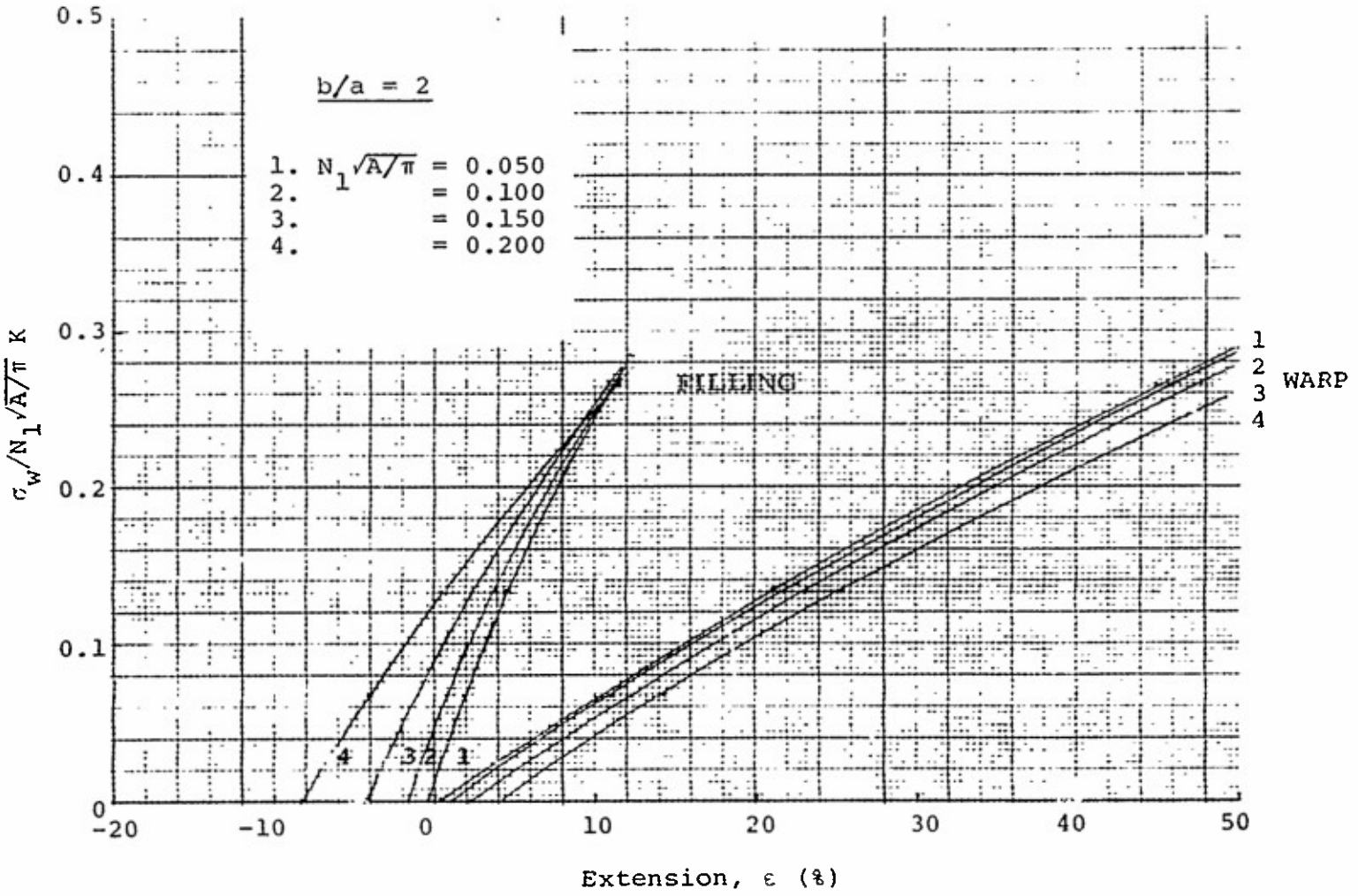

Figure 52. Fabric Extension: Linearly Elastic Yarn, Initially Square Fabric $\sigma_w/\sigma_f = 5$, b/a = 2

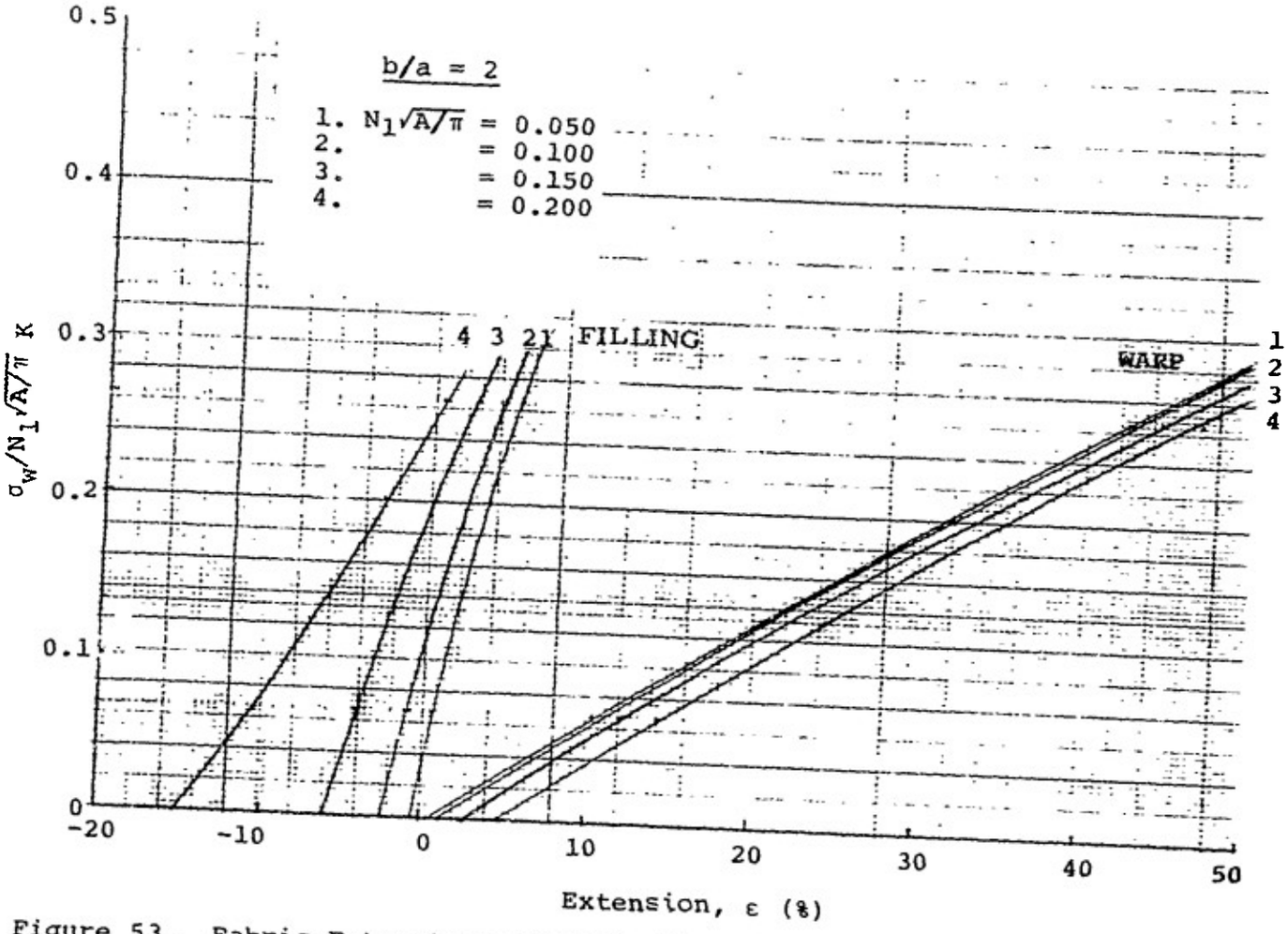

Figure 53. Fabric Extension: Linearly Elastic Yarn, Initially Square Fabric $\sigma_w/\sigma_f = 10$, b/a = 2

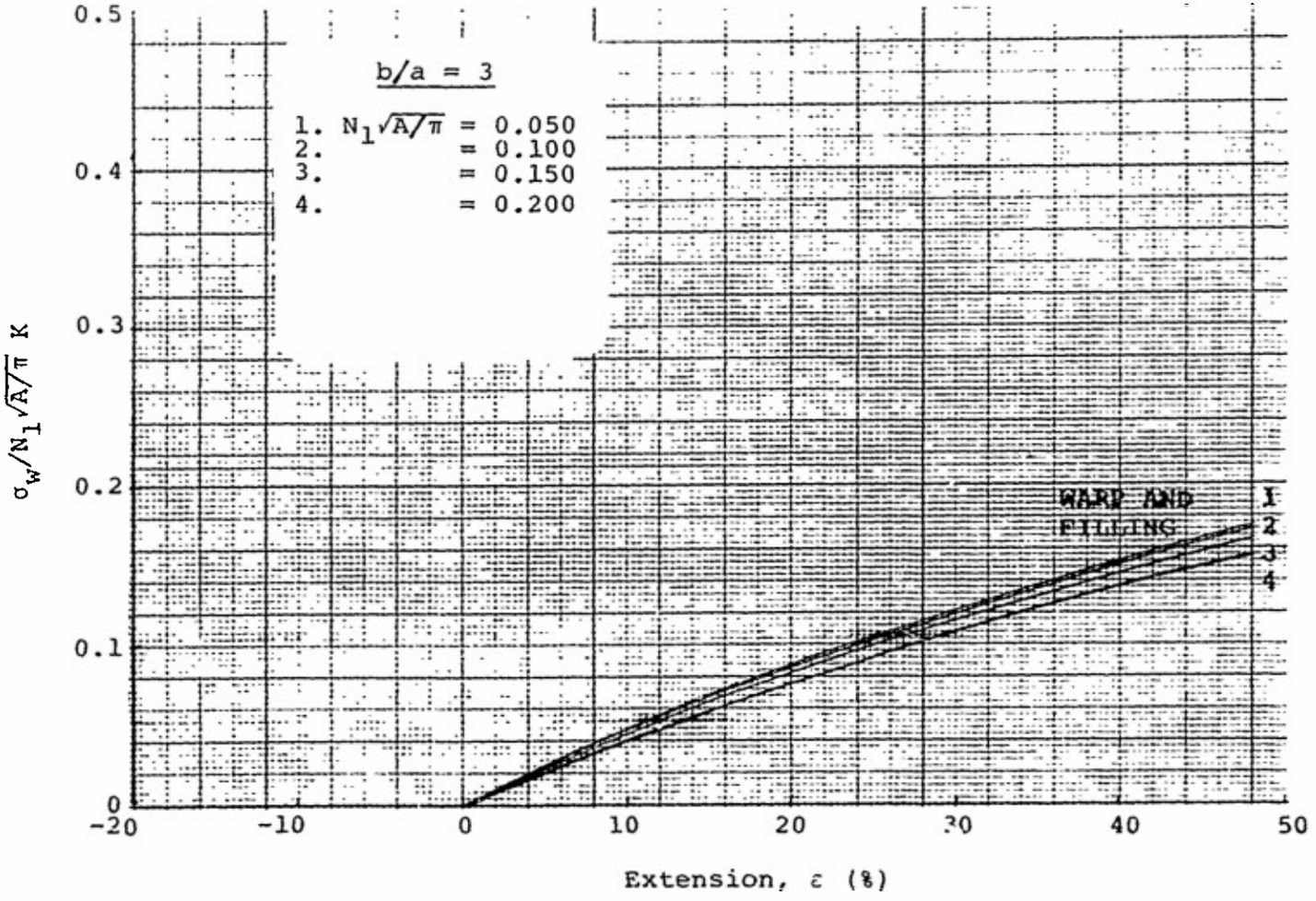

Figure 54. Fabric Extension: Linearly Elastic Yarn, Initially Square Fabric $\sigma_w/\sigma_f = 1$, b/a = 3

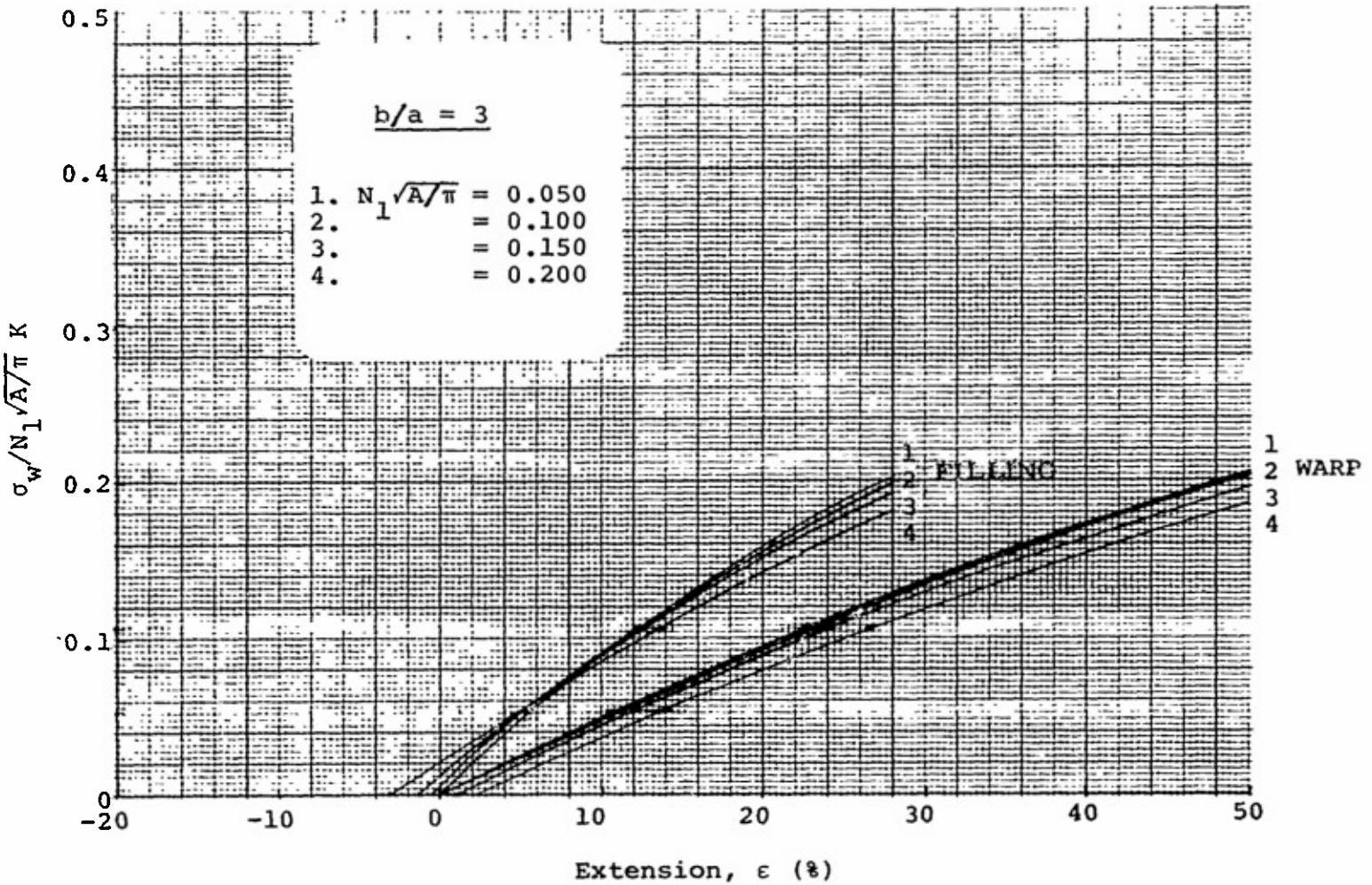

Figure 55. Fabric Extension: Linearly Elastic Yarn, Initially Square Fabric $\sigma_w/\sigma_f = 2$, b/a = 3

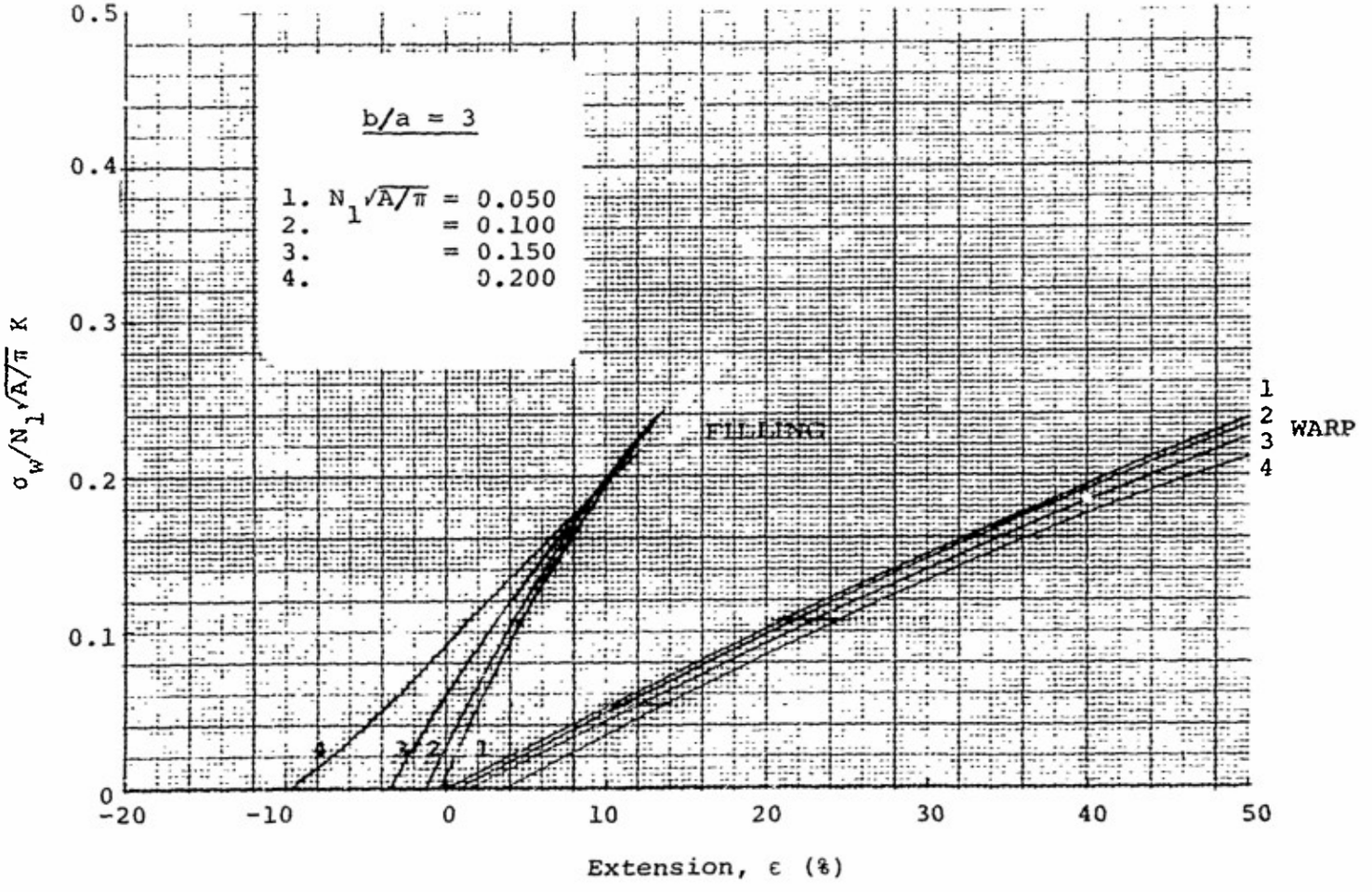

Figure 56. Fabric Extension: Linearly Elastic Yarn, Initially Square Fabric $\sigma_w/\sigma_f = 5$, b/a = 3

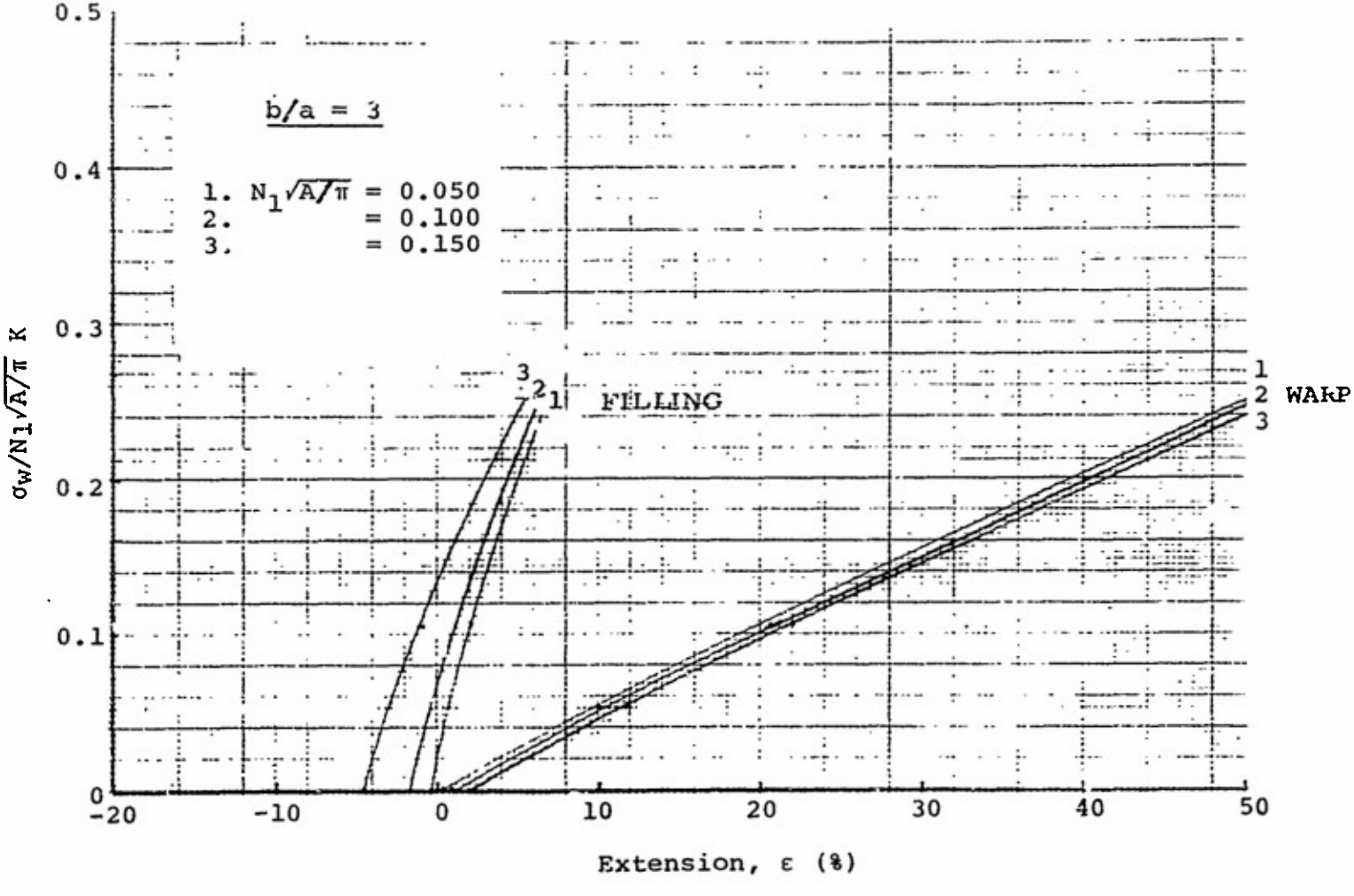

Figure 57. Fabric Extension: Linearly Elastic Yarn, Initially Square Fabric $\sigma_w/\sigma_f = 10$, b/a = 3

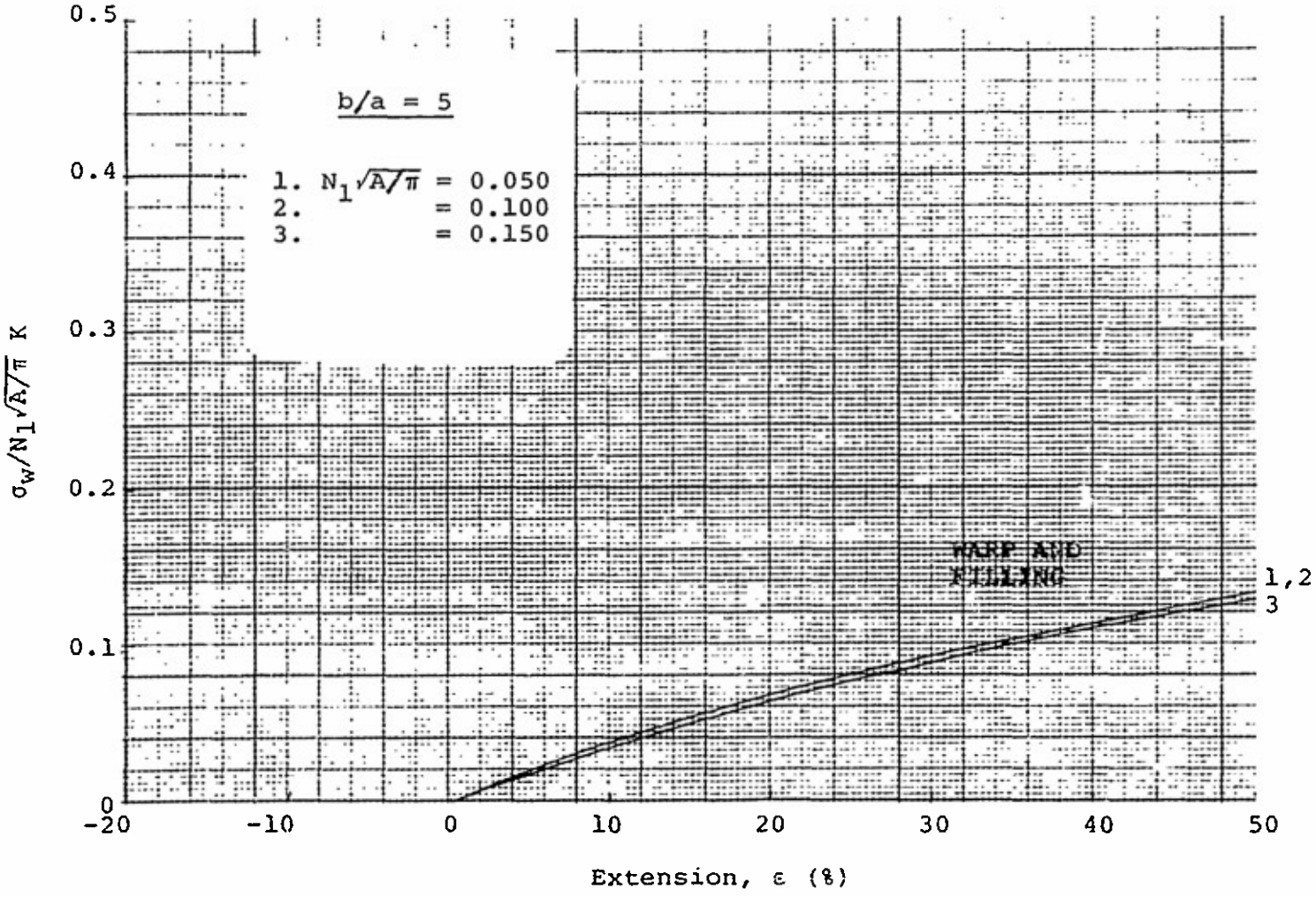

Figure 58. Fabric Extension: Linearly Elastic Yarn, Initially Square Fabric $\sigma_w/\sigma_f = 1$, b/a = 5

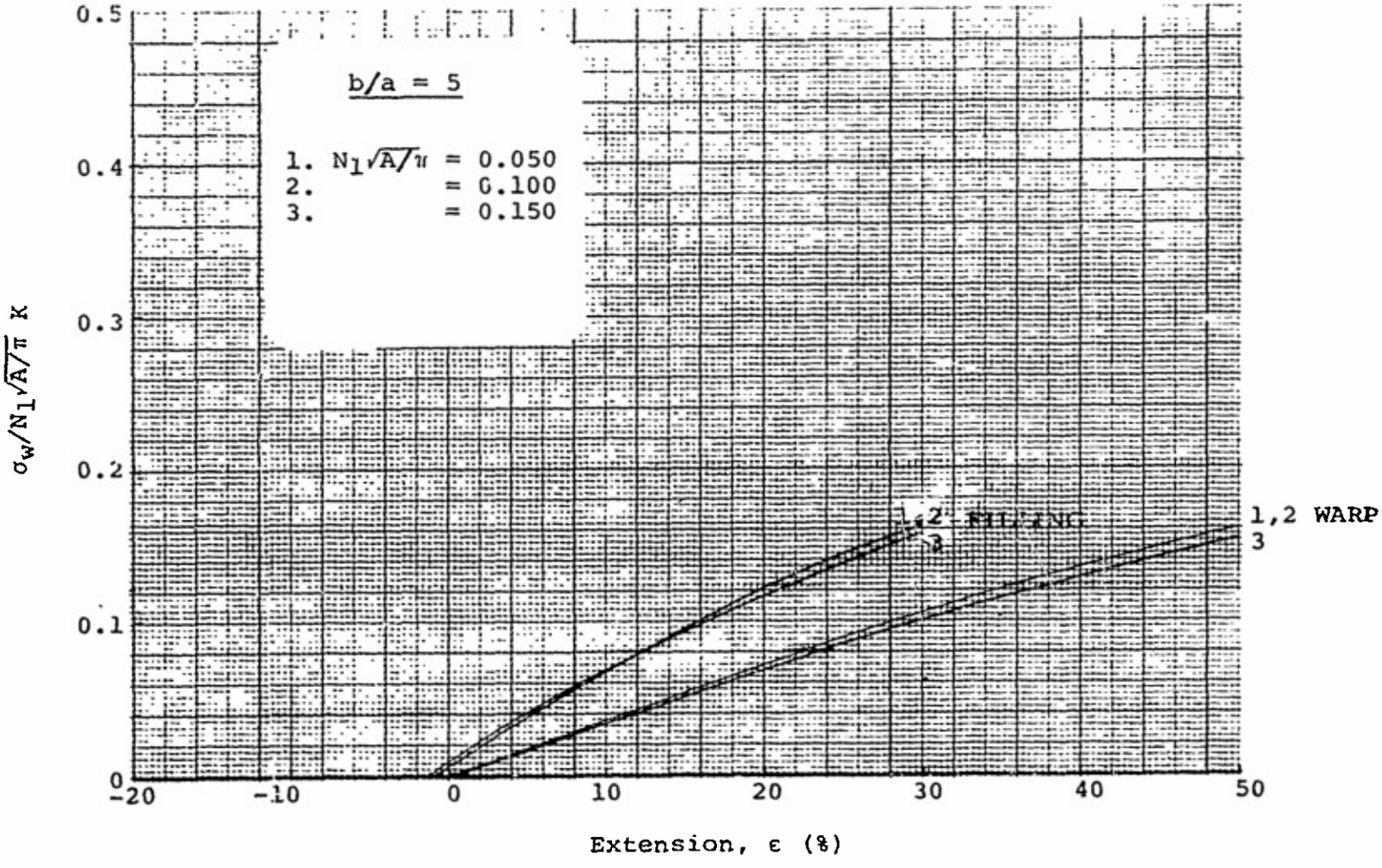

Figure 59. Fabric Extension: Linearly Elastic Yarn, Initially Square Fabric $\sigma_w/\sigma_f = 2$, b/a = 5

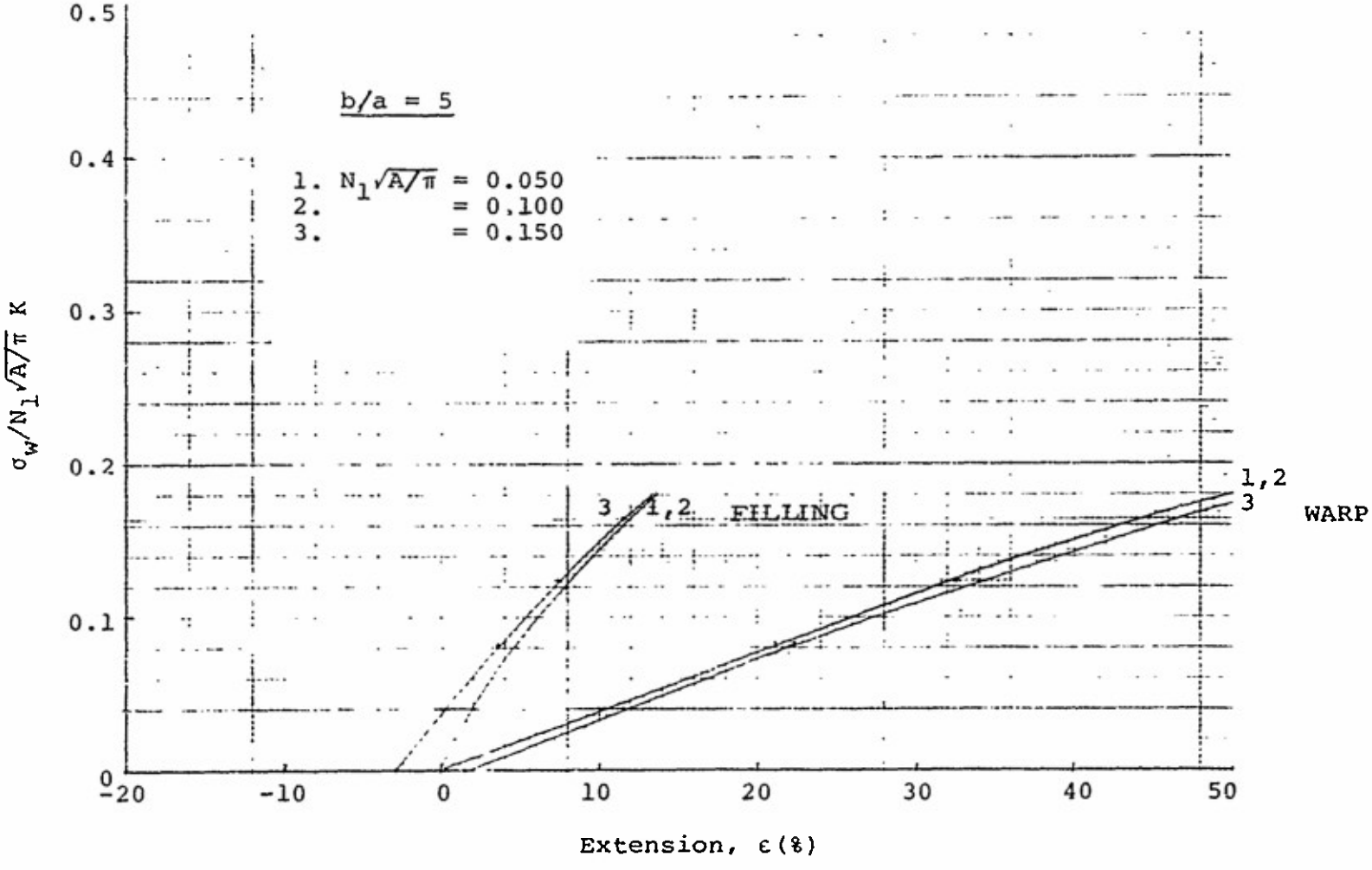

Figure 60. Fabric Extension: Linearly Elastic Yarn, Initially Square Fabric $\sigma_w/\sigma_f = 5$, b/a = 5

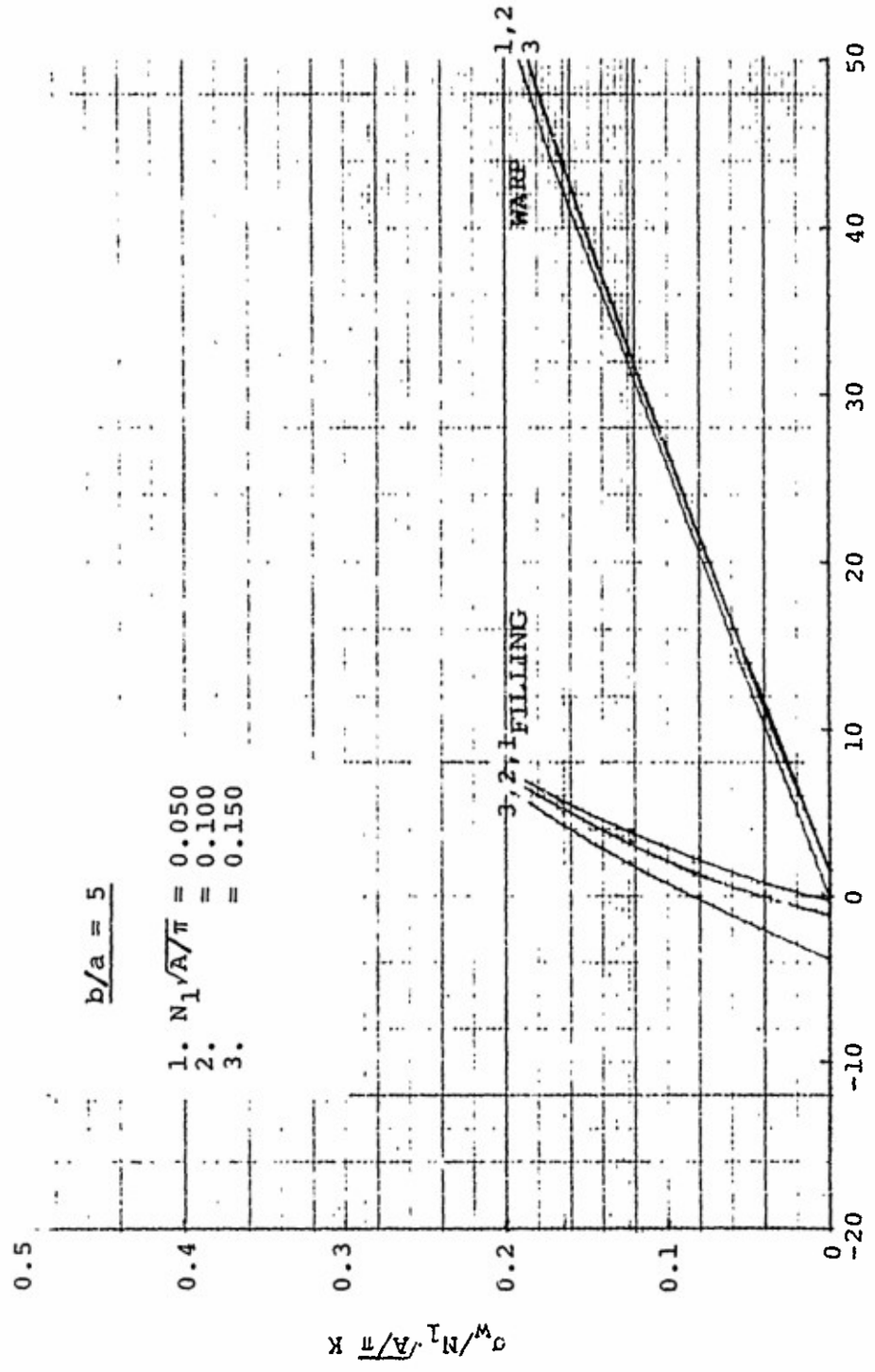

Figure 61. Fabric Extension: Linearly Elastic Yarn, Initially Square Fabric
σ_w/σ_f = 10, b/a = 5

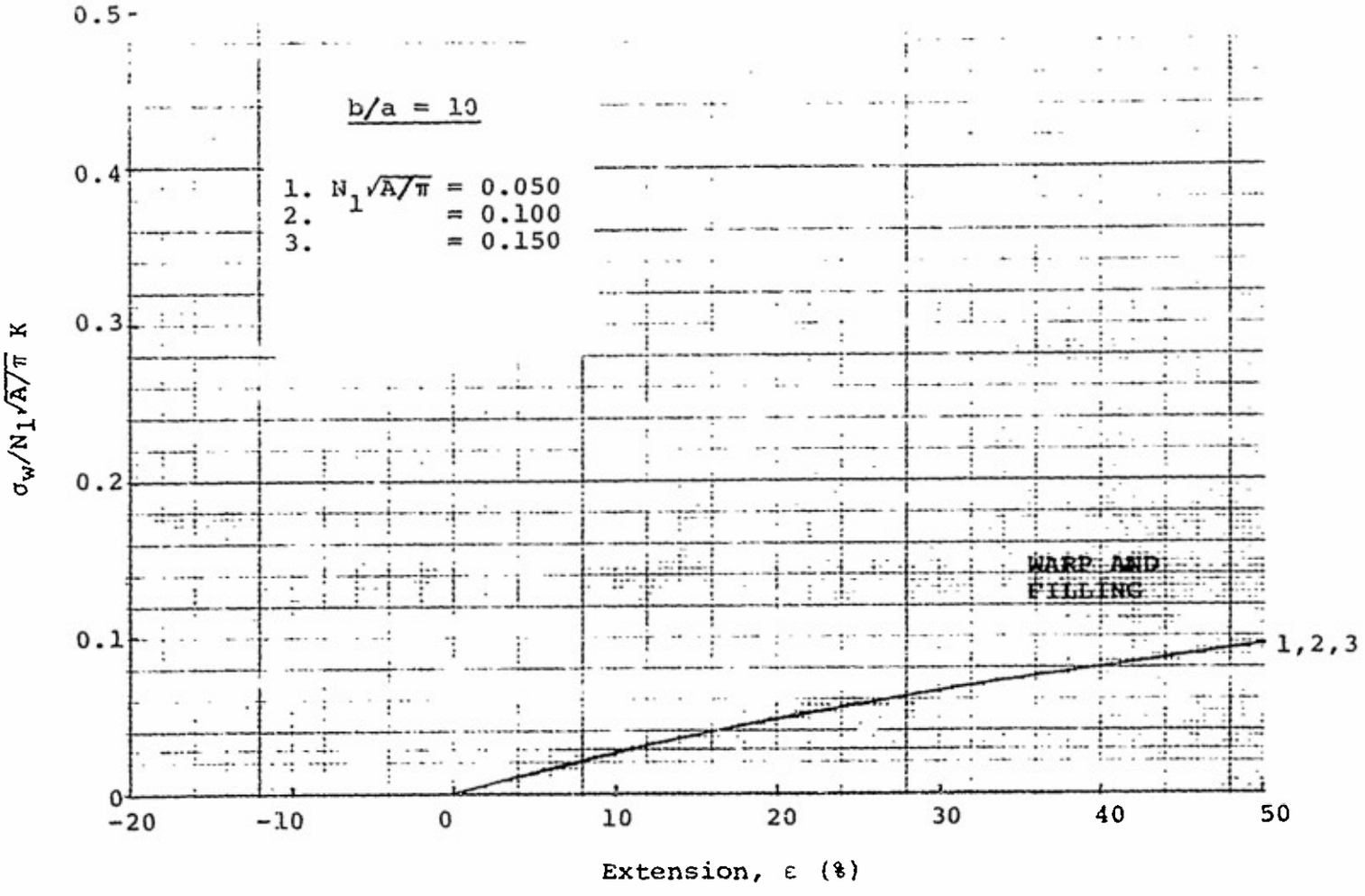

Figure 62. Fabric Extension: Linearly Elastic Yarn, Initially Square Fabric $\sigma_w/\sigma_f = 1$, b/a = 10

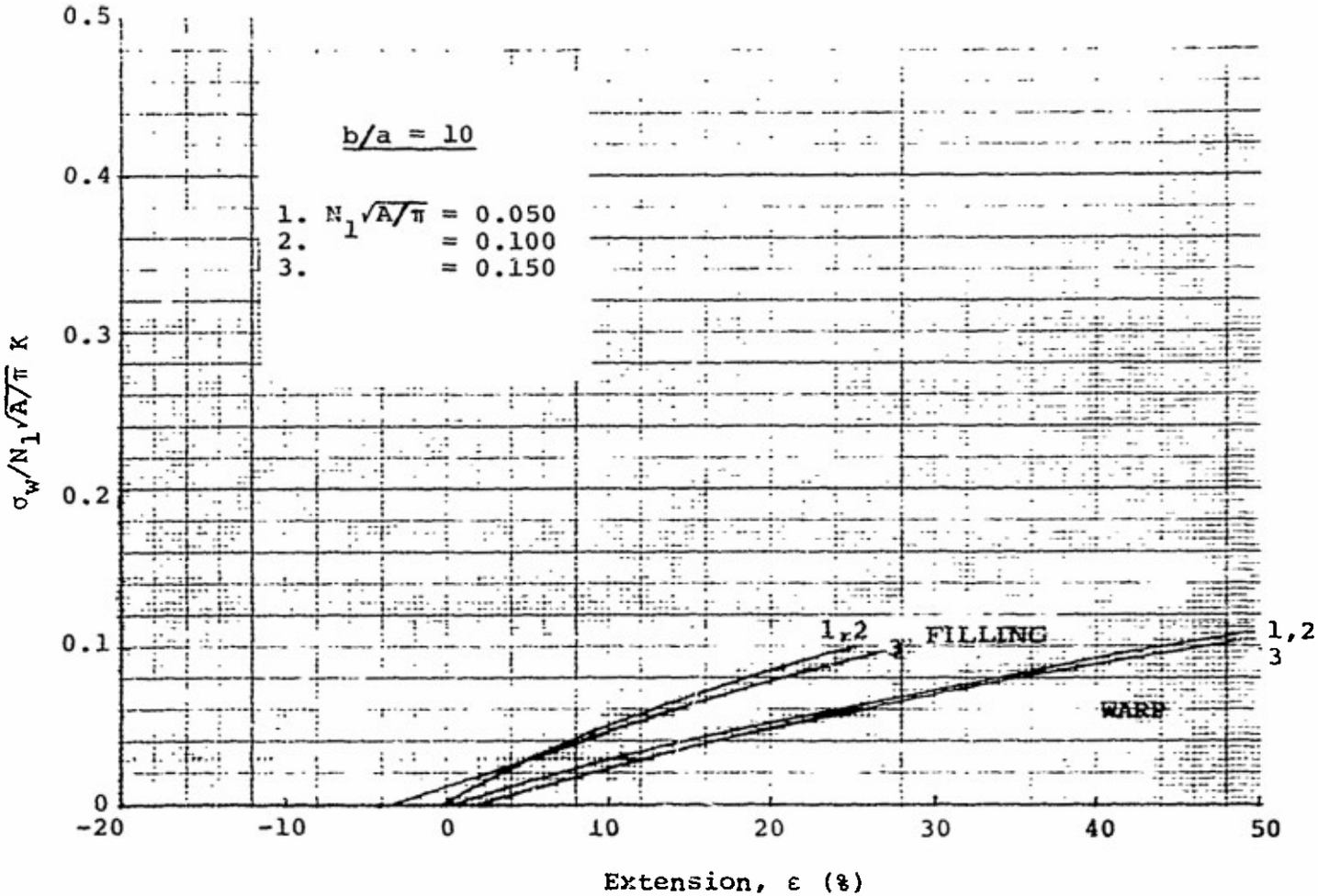

Figure 63. Fabric Extension: Linearly Elastic Yarn, Initially Square Fabric $\sigma_w/\sigma_f = 2$, $b/a = 10$

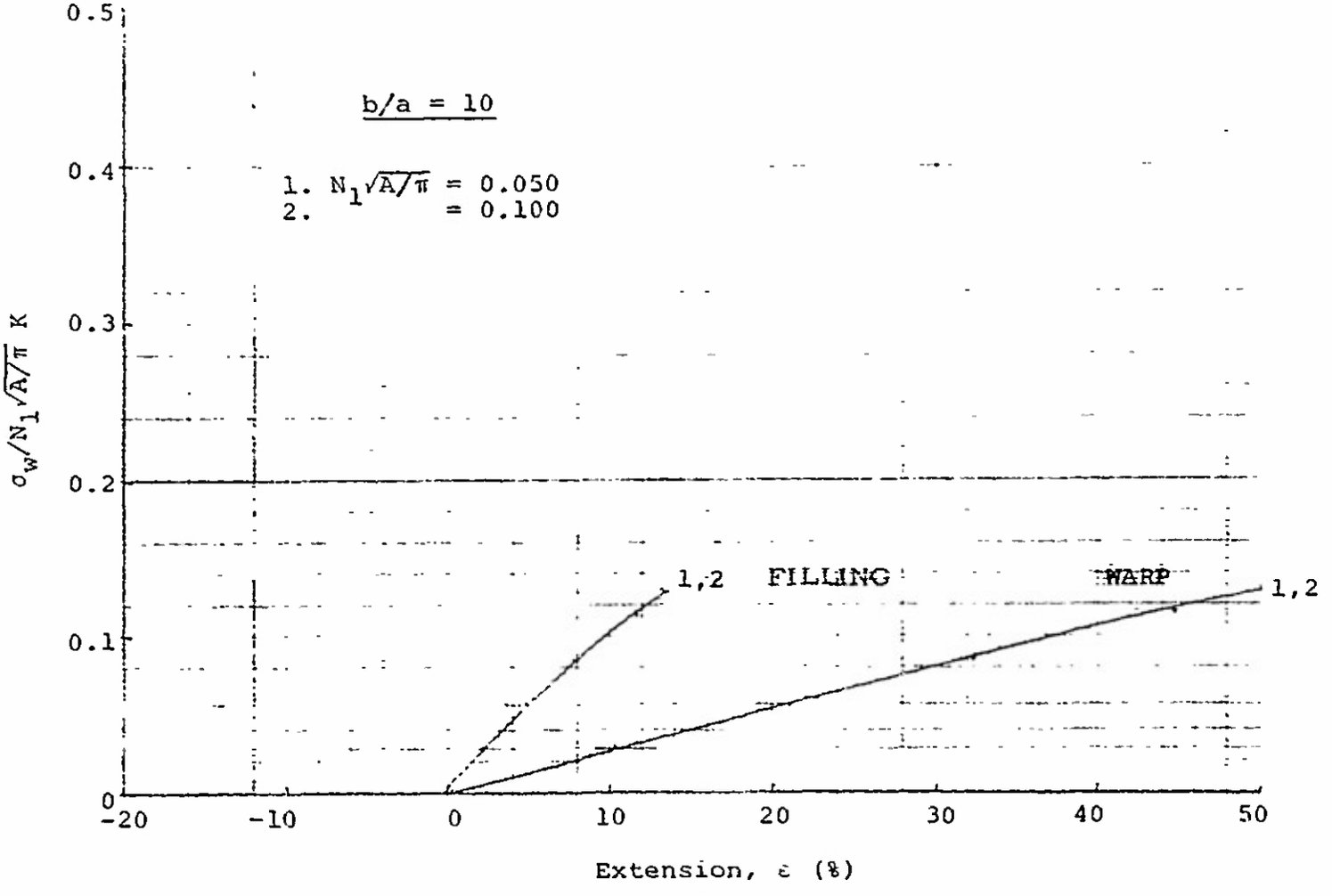

Figure 64. Fabric Extension: Linearly Elastic Yarn, Initially Square Fabric σ_w/σ_f = 5, b/a = 10

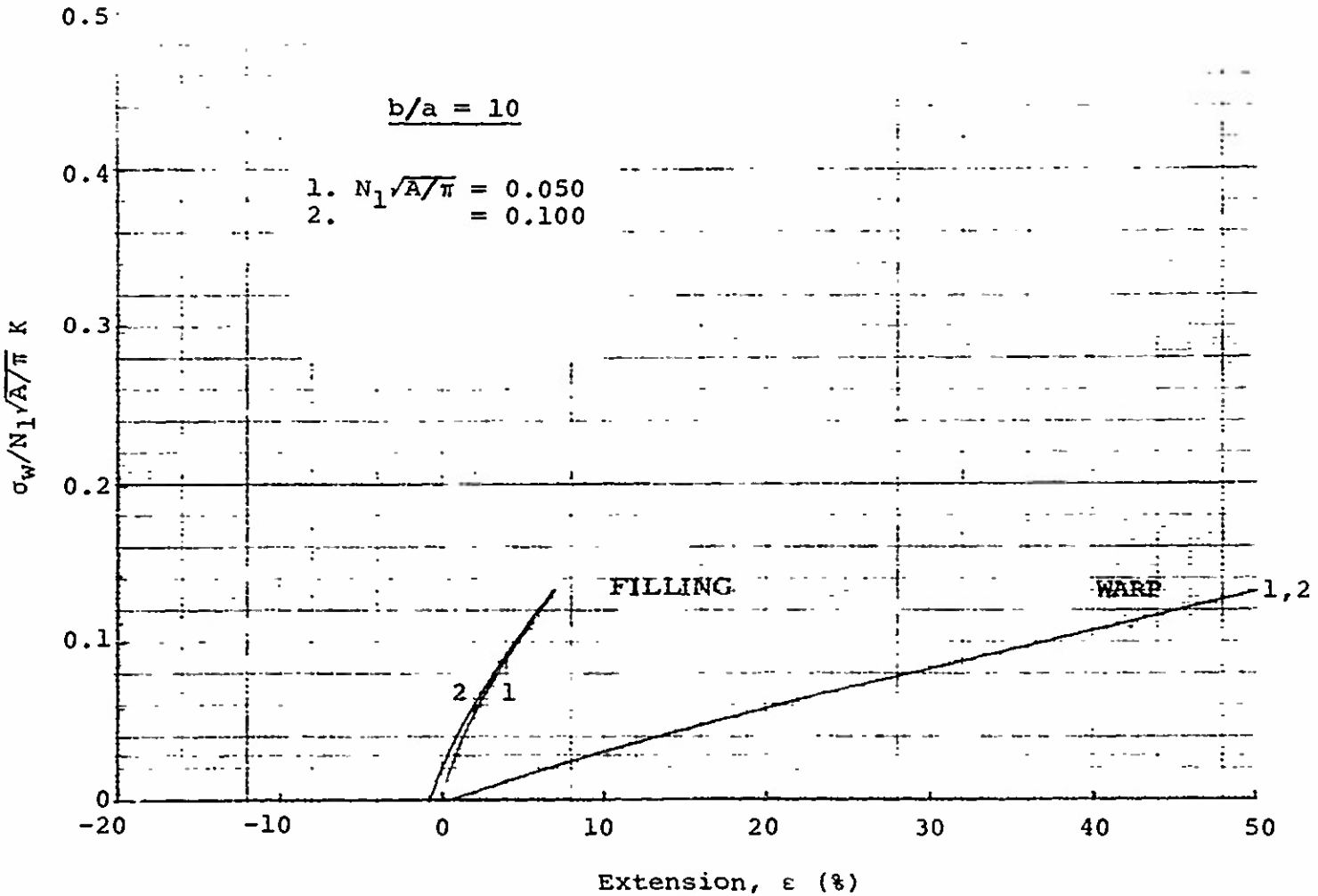

Figure 65. Fabric Extension: Linearly Elastic Yarn, Initially Square Fabric $\sigma_w/\sigma_f = 10$, b/a = 10

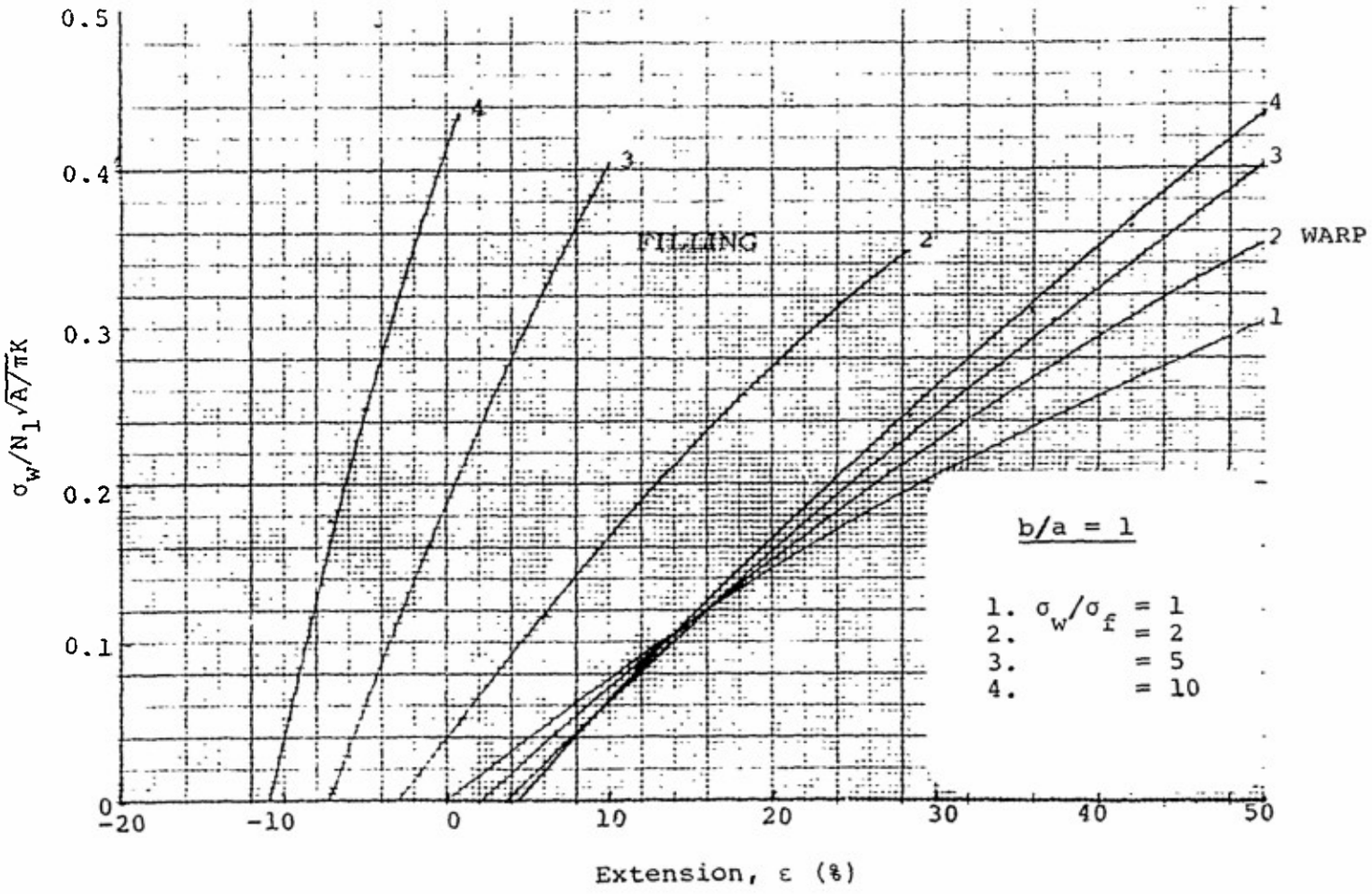

Figure 66. Fabric Extension: Linearly Elastic Yarn
Initially Square Fabric, $N_1\sqrt{A/\tau}$ = 0.15, b/a = 1

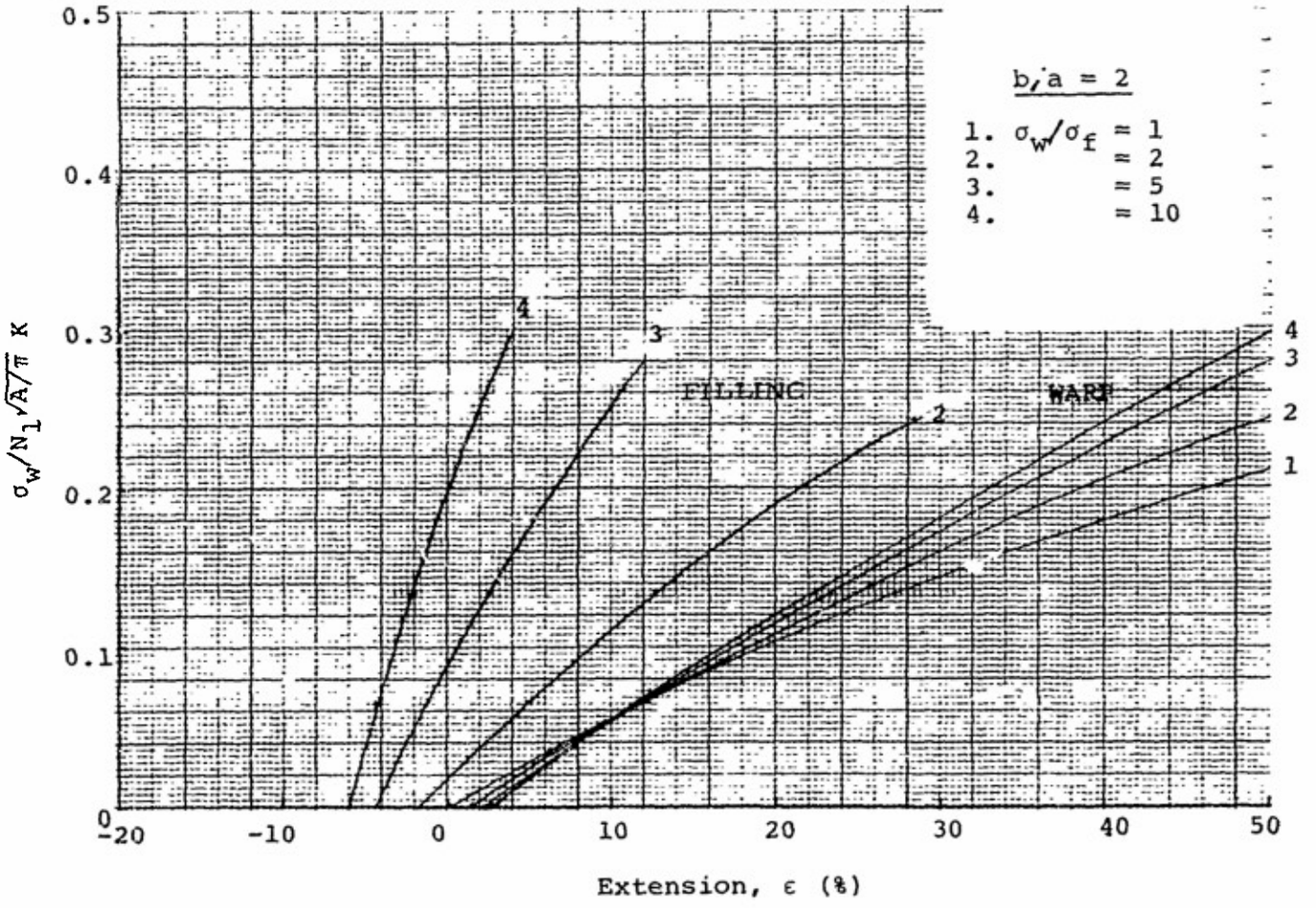

Figure 67. Fabric Extension: Linearly Elastic Yarn, Initially Square Fabric $N_1\sqrt{A/\pi} = 0.15$, b/a = 2

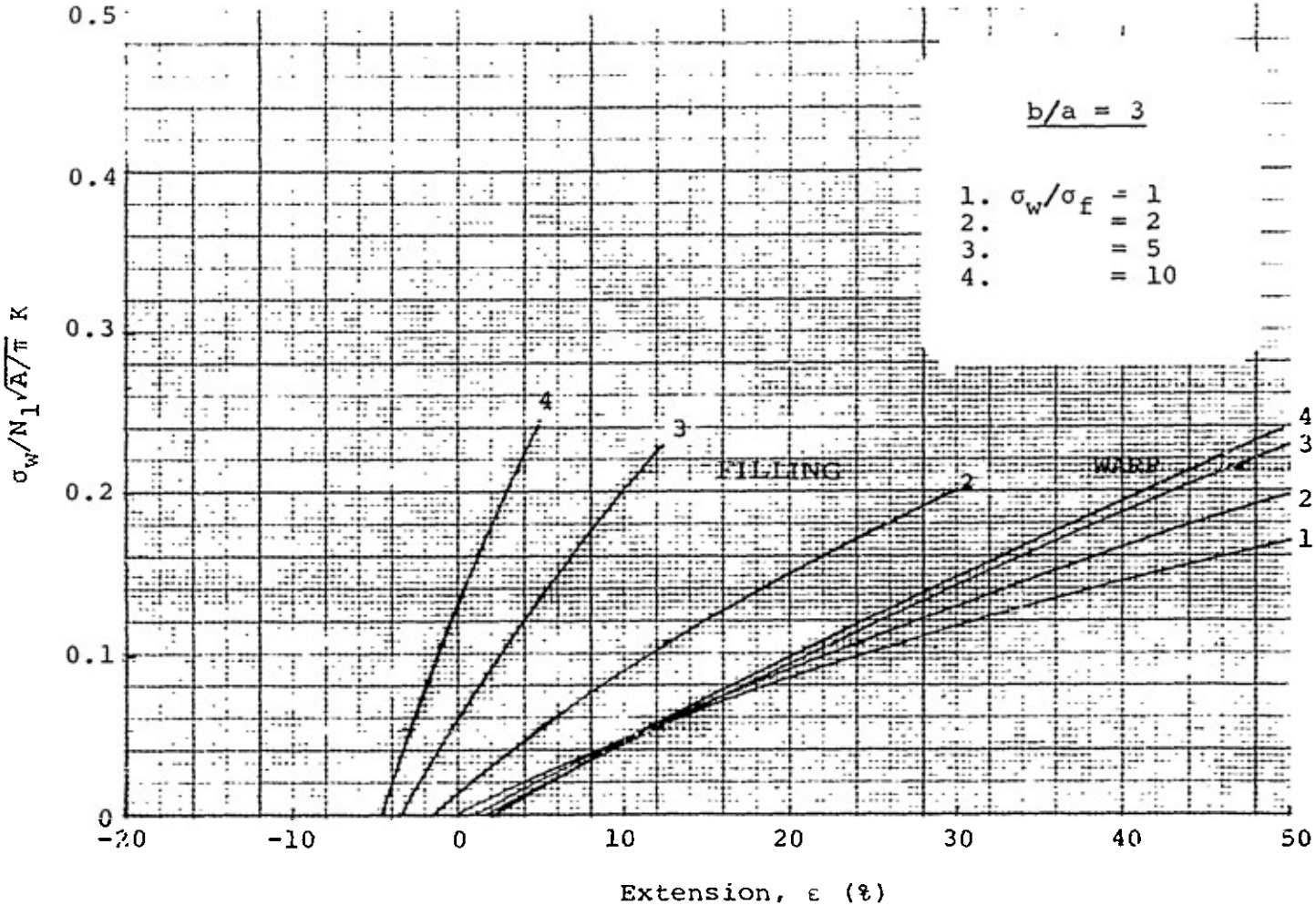

Figure 68. Fabric Extension: Linearly Elastic Yarn, Initially Square Fabric $N_1\sqrt{A/\pi}$ = 0.15, b/a = 3

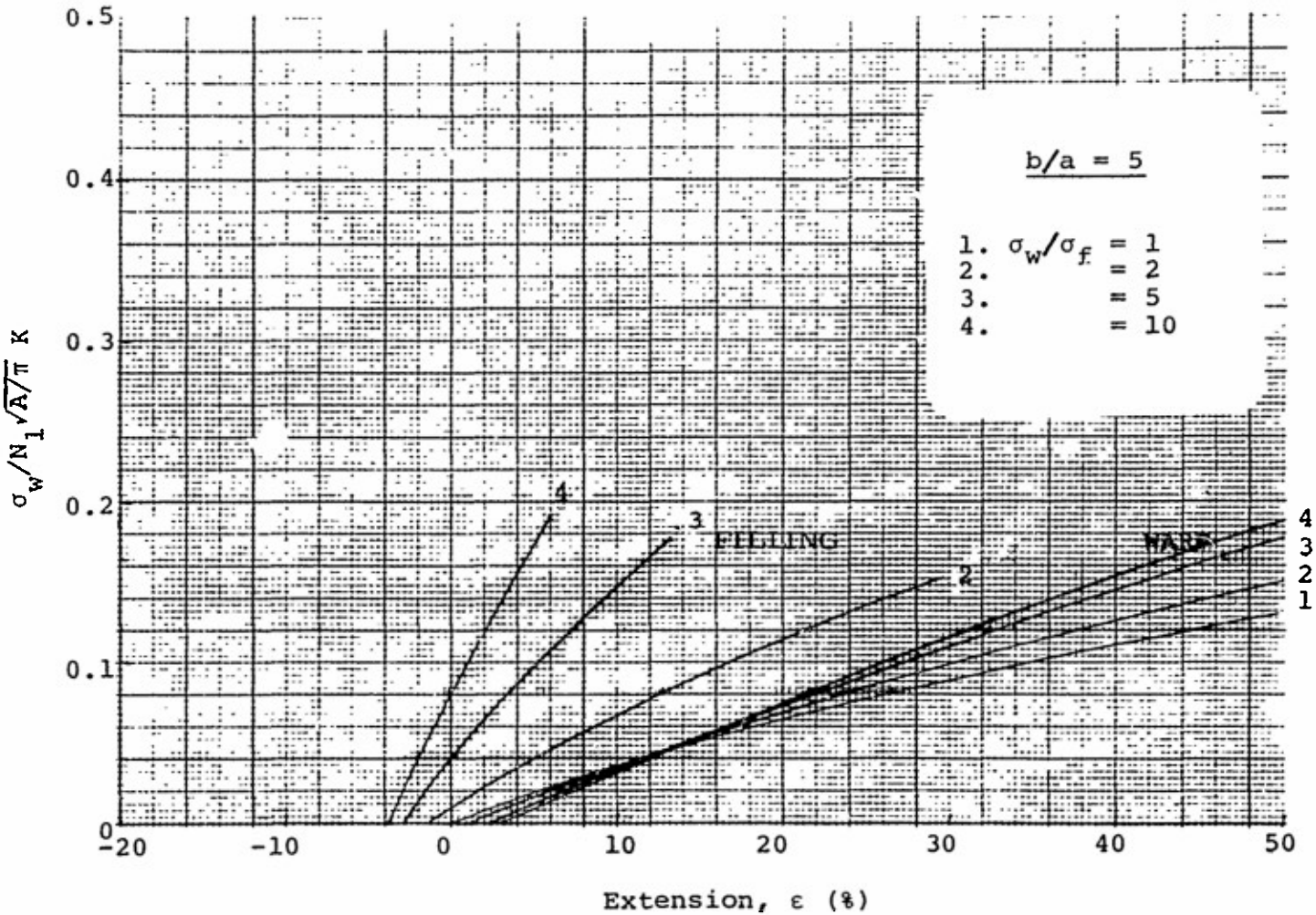

Figure 69. Fabric Extension: Linearly Elastic Yarn, Initially Square Fabric $N_1\sqrt{A/\pi}$ = 0.15, b/a = 5

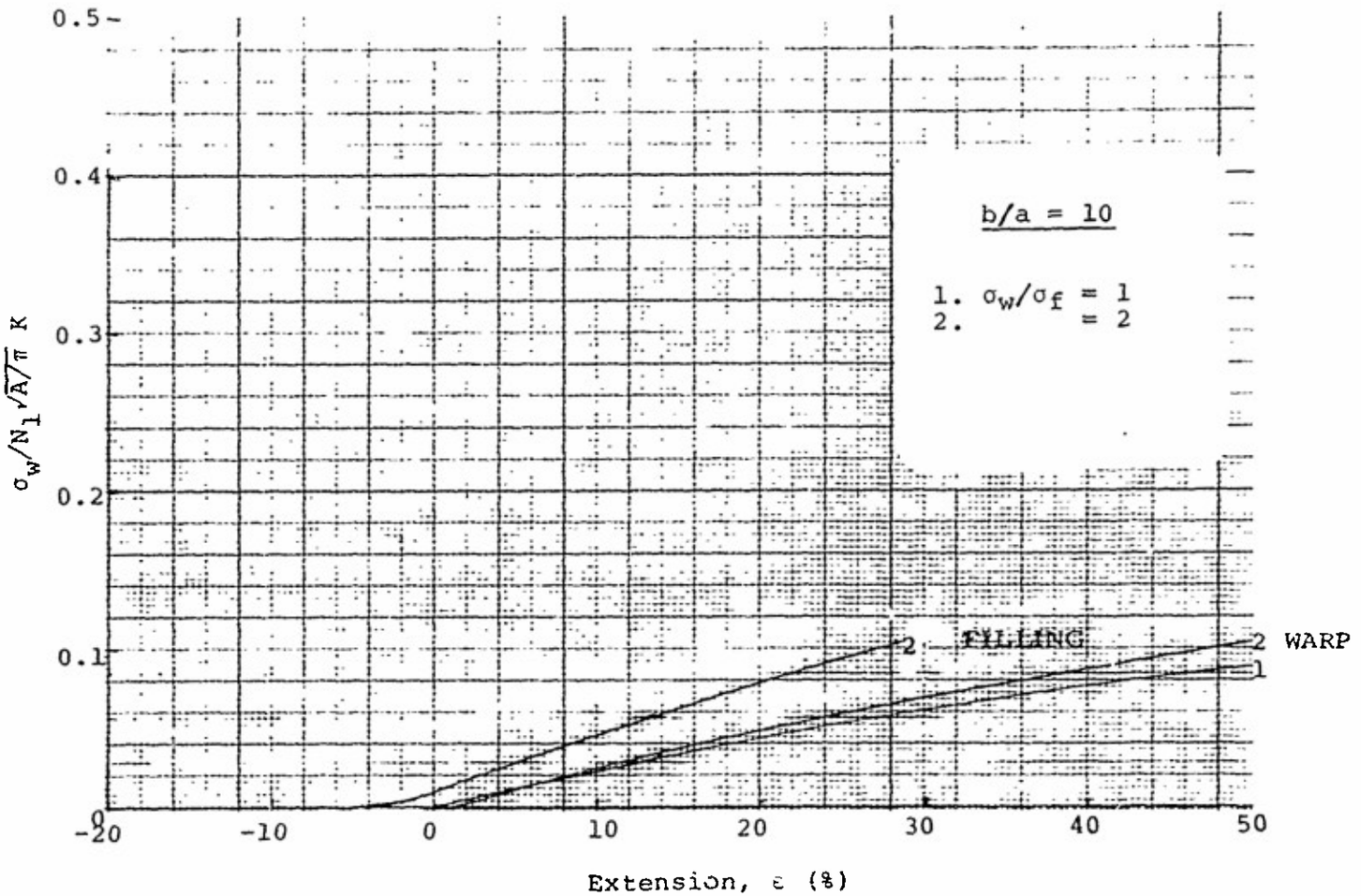

Figure 70. Fabric Extension: Linearly Elastic Yarn, Initially Square Fabric $N_1\sqrt{A/\pi} = 0.15$, b/a = 10

and various values of σ_w/σ_f. All the filling load-extension diagrams are terminated at the point corresponding to 50% extension in the warp direction.

The extension at constant radius of a straight, linearly elastic, twisted yarn is also given in Figure 46 as a function of the same parameters. This can be done since σ/N_1 represents the load applied to each yarn in the fabric and, from Equation 14, the extension, ε_y, of a linearly elastic yarn is given by

$$\varepsilon_y = \frac{P_y}{pE_fA} = \frac{\sigma}{N_1 E_f A}$$

where P_y is the load applied to the yarn. As shown in Figure 46, the fabric is more easily extended than a straight yarn identical to those from which the fabric is woven. This is because of the crimp in the fabric yarns.

In Figures 46 through 65, curves are given only for the lower values of $N_1\sqrt{A/\pi}$ at the larger yarn aspect ratios, i.e., for those values of $N_1\sqrt{A/\pi}$ for which the fabric is neither initially jammed, nor reaches the jammed state at low levels of load.

All the analytical results were examined to check that none of the solutions gave a physically impossible fabric deformation, i.e., a deformation that violated the second or third types of limiting geometries discussed previously. L_{2f}/a was found to be less than $2b/a+4\theta_{2f}$ only over a narrow range of the loading parameter $\sigma/(N_1\sqrt{A/\pi})K$ when $N_1\sqrt{A/\pi} = 0.24$, $\sigma_w/\sigma_f = 10$ and $b/a = 1$. The corresponding portions of the $N_1\sqrt{A/\pi} = 0.240$ curves in Figure 49 are therefore dotted. Although the actual deformations must be less than that predicted by the dotted curves, the difference is probably small.

No solutions were found where contact between adjacent warp yarns was indicated, i.e., where $1/N_{2w} \leq 2b$.

As shown in Figures 46 through 66, the fabric load-extension curves appear to intersect the zero-load axes at finite strains. This results from the assumption that the yarns are infinitely flexible, have zero bending rigidity. The strain values at these apparent intercepts are roughly the same as those given for initially square fabrics woven from inextensible yarn at the corresponding loading ratios (see Figures 10 through 19).

It can be shown that for any specific load, σ_f (lbs/inch width of fabric) applied to the fabric, the fabric extension increases with decreasing $N_1\sqrt{A/\pi}$. The smaller $N_1\sqrt{A/\pi}$, the fewer are the number of yarns available for supporting the applied load and thus, the greater each yarn's share of the total load applied to the fabric. The fabric extension also increases with decreasing yarn cross-sectional area and decreasing yarn modulus

The fabrics contract in the filling direction at low levels of applied loads; the contraction is greater at the higher loading ratios and lower yarn aspect ratios. However, the fabric extends from the contracted state as the applied load is increased. The level of load that must be applied in the warp direction to eliminate the filling contraction increases with increasing loading ratio and decreasing yarn aspect ratio For a given applied load and loading ratio, the magnitude of the fabric extension in the warp direction is considerably greater than the extension (or contraction) in the filling direction; the difference increases with increasing loading ratio and increasing yarn aspect ratio.

The slope of the fabric warp and filling load-extension curves subsequent to the extension that occurs instantaneously upon application of infinitesimal loads (when σ_w/σ_f = 1) decreases as the yarn aspect ratio increases. This occurs because the initial angulation of the fabric yarns to the fabric mid-plane decreases, in the cases for which solutions were obtained, with increasing yarn aspect ratio. Consequently, the component of the applied load parallel to the yarn axis at the fabric mid-plane increases with increasing yarn aspect ratio. Therefore, the yarn extension and resultant fabric extension increases with increasing yarn aspect ratio for a given applied load.

Additionally, the slopes of the fabric load-extension curves increase with increasing loading ratio. The reason for this bend is not readily apparent.

Figures 66 through 70 show that at low levels of applied load the fabrics exhibit roughly the same extension in the warp direction at all loading ratios σ_w/σ_f = 10. However, the fabric contraction in the filling direction does vary significantly with loading ratio. Additionally, the fabric response in the two

directions is different for the various loading ratios at the higher levels of applied load.

As also shown in these figures the initial "instantaneous" fabric extension in the warp direction increases with increasing loading ratio. However, the extension at the lower loading ratios increases at a faster rate with increasing applied load so that the curves cross. At load levels resulting in extensions larger than those at which the curves cross the fabric extension in the warp direction increases with decreasing loading ratio; the loading ratio $\sigma_w/\sigma_f = 1$ gives the greatest fabric extension. The latter evidently is the result of the greater filling extension that occurs when the load applied in the filling direction approaches that applied in the warp direction. Increased filling yarn extension permits a decrease in filling yarn crimp, and, consequently, through the balance of the vertical components of the forces in the two orthogonal systems of yarns, a decrease in warp yarn crimp, thereby permitting increased fabric extension in the warp direction.

The effective fabric Poisson's ratio, μ is given in Figures 71 through 90 as a function of the dimensionless loading parameter $\sigma_w/(N_1\sqrt{A/\pi})K$ for various values of initial fabric geometry $N_1\sqrt{A/\pi}$, yarn aspect ratio a/b and loading ratio σ_w/σ_f. The curves have been terminated at a fabric warp extension of about 50%. For a loading ratio of one, $\mu = -1$ at all loads and for all initial fabric geometries. For $\sigma_w/\sigma_f \geq 2$ the Poisson's ratio is positive and greater than one at small values of the loading parameter, decreases with increasing values of the loading parameter becoming negative over a large portion of the load-parameter range. Also, μ is slightly larger throughout the load-parameter range for $N_1\sqrt{A/\pi} = 0.240$ than for $N_1\sqrt{A/\pi} = 0.050$. The Poisson's ratio does not vary greatly with yarn aspect ratio. However, Figures 71 through 85 show μ to increase positively with decreasing yarn aspect ratio. Additionally, as shown in Figures 86 through 90, μ increases positively with increasing loading ratio.

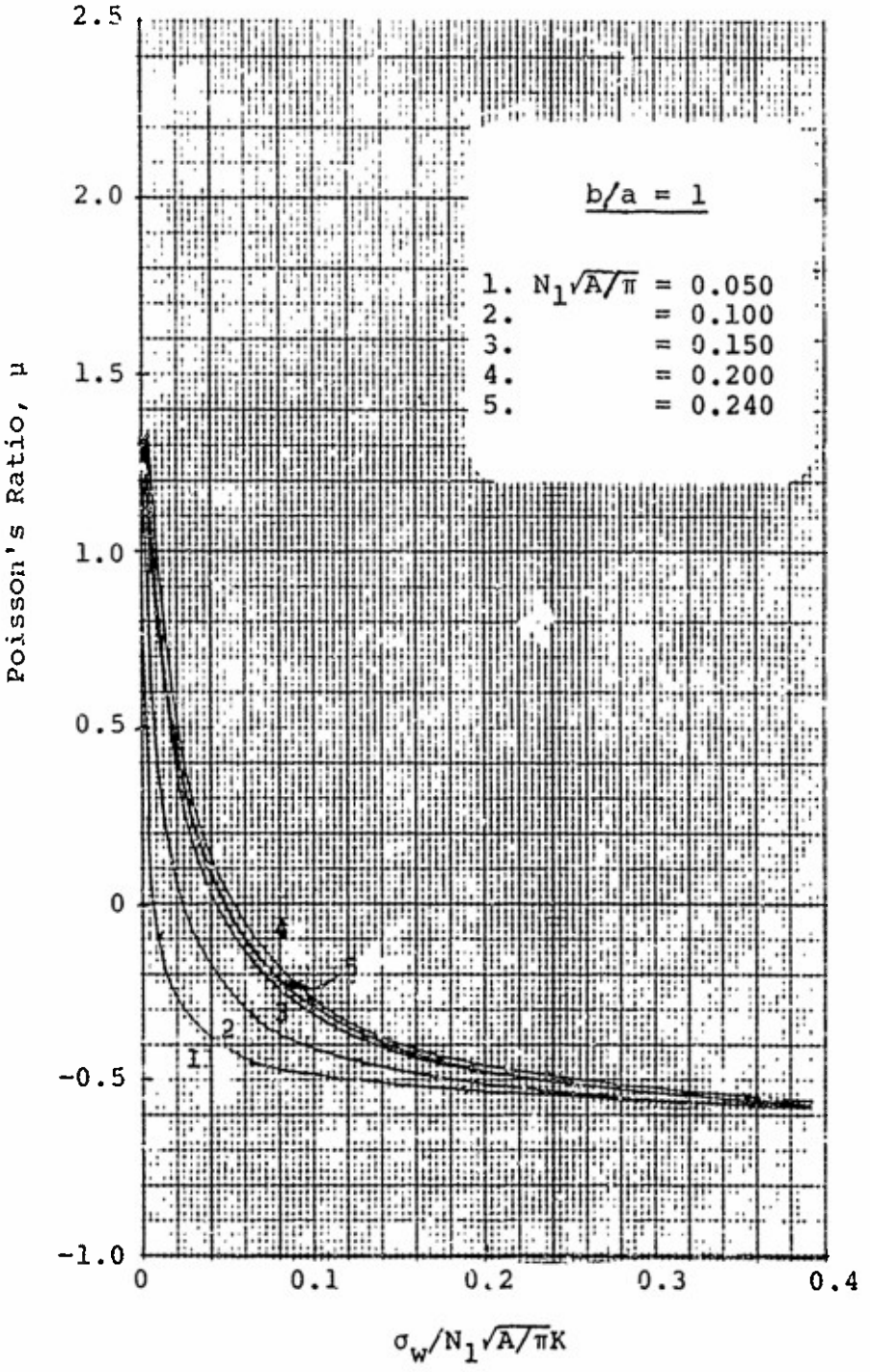

Figure 71. Poisson's Ratio (Aspect Ratio = 1): Linearly Elastic Yarn, Initially Square Fabric, $\sigma_w/\sigma_f = 2$, b/a = 1

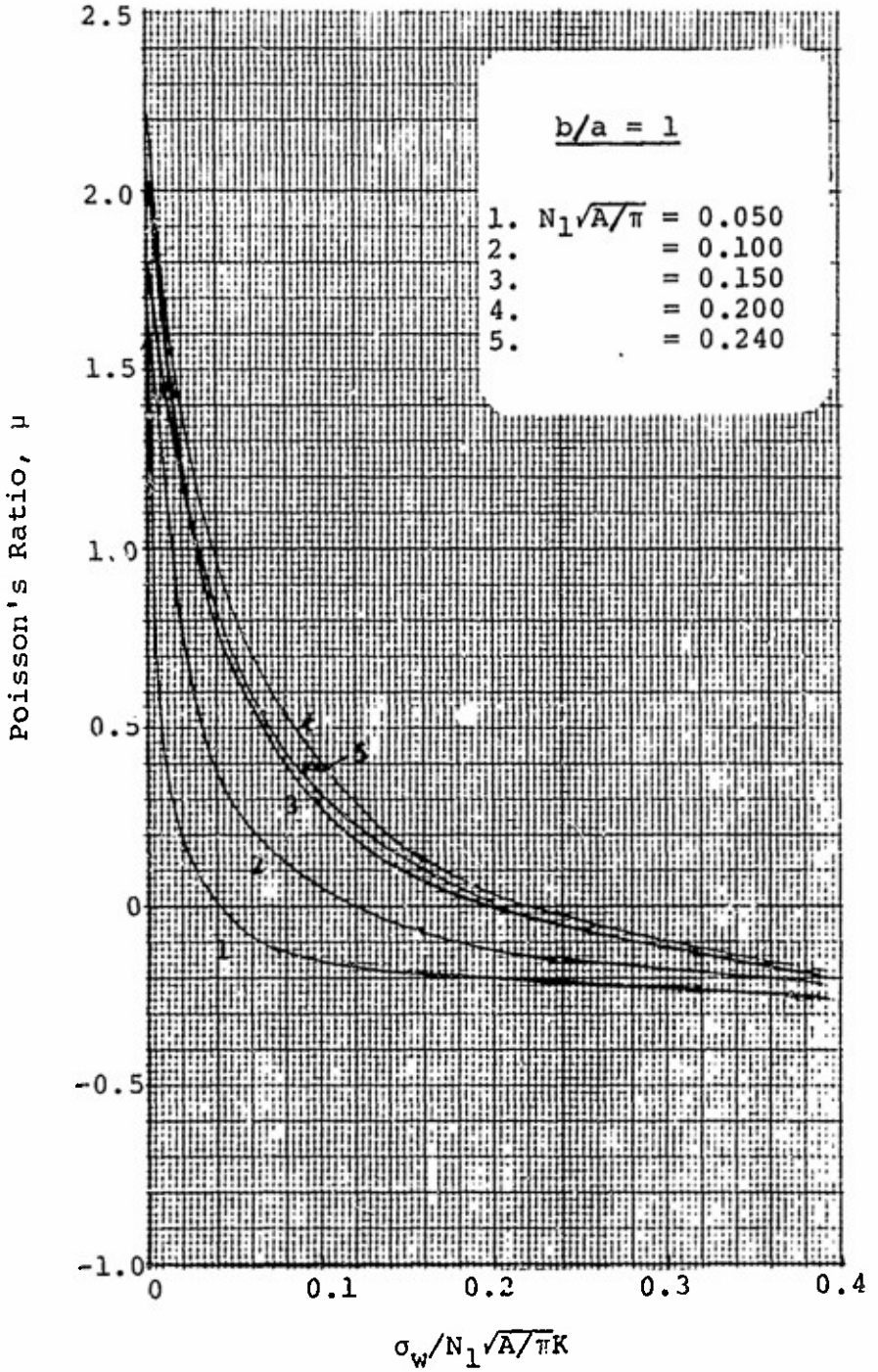

Figure 72. Poisson's Ratio (Aspect Ratio = 1): Linearly Elastic Yarn, Initially Square Fabric, $\sigma_w/\sigma_f = 5$, b/a = 1

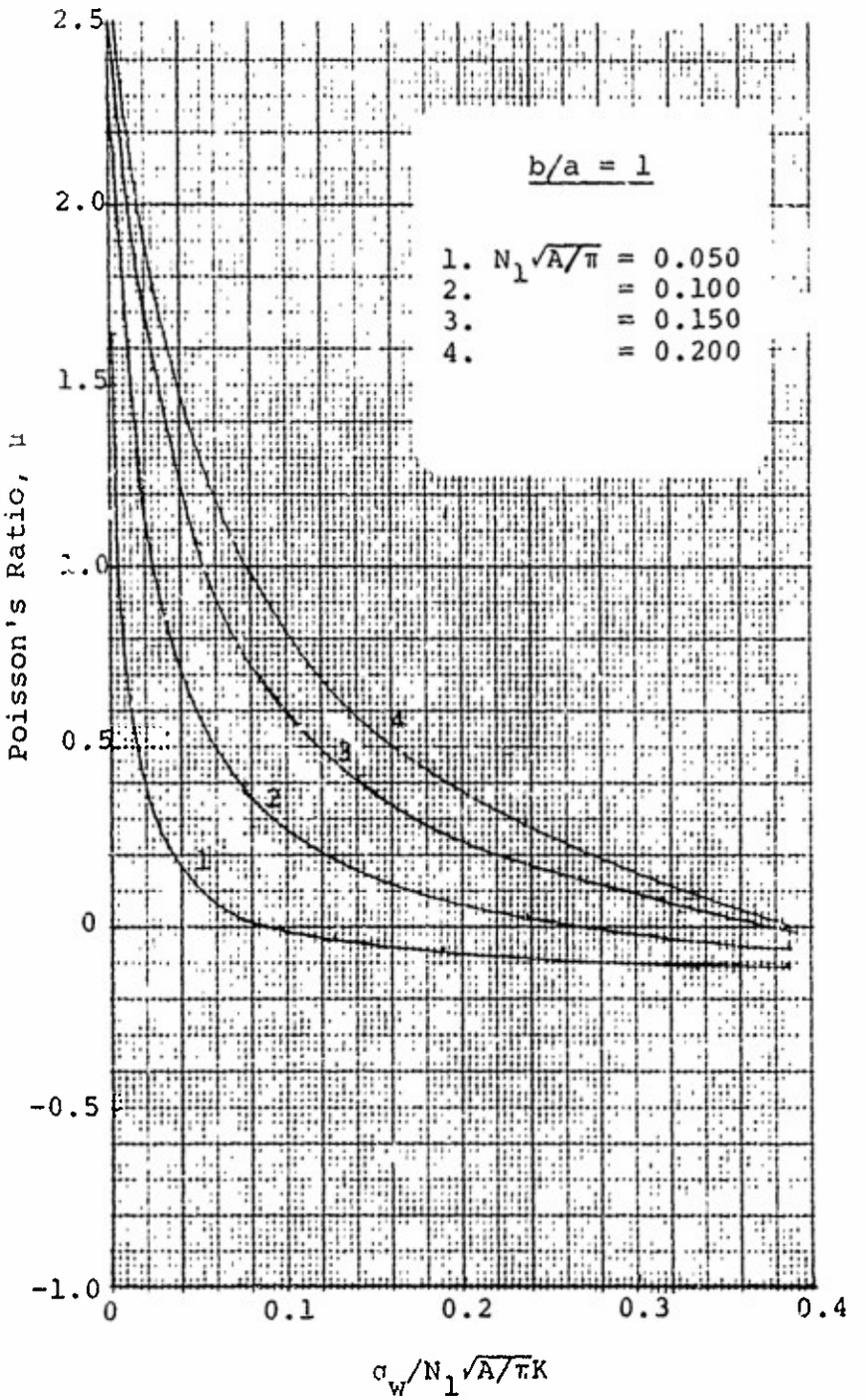

Figure 73. Poisson's Ratio (Aspect Ratio = 1): Linearly Elastic Yarn, Initially Square Fabric, σ_w/σ_f = 10, b/a = 1

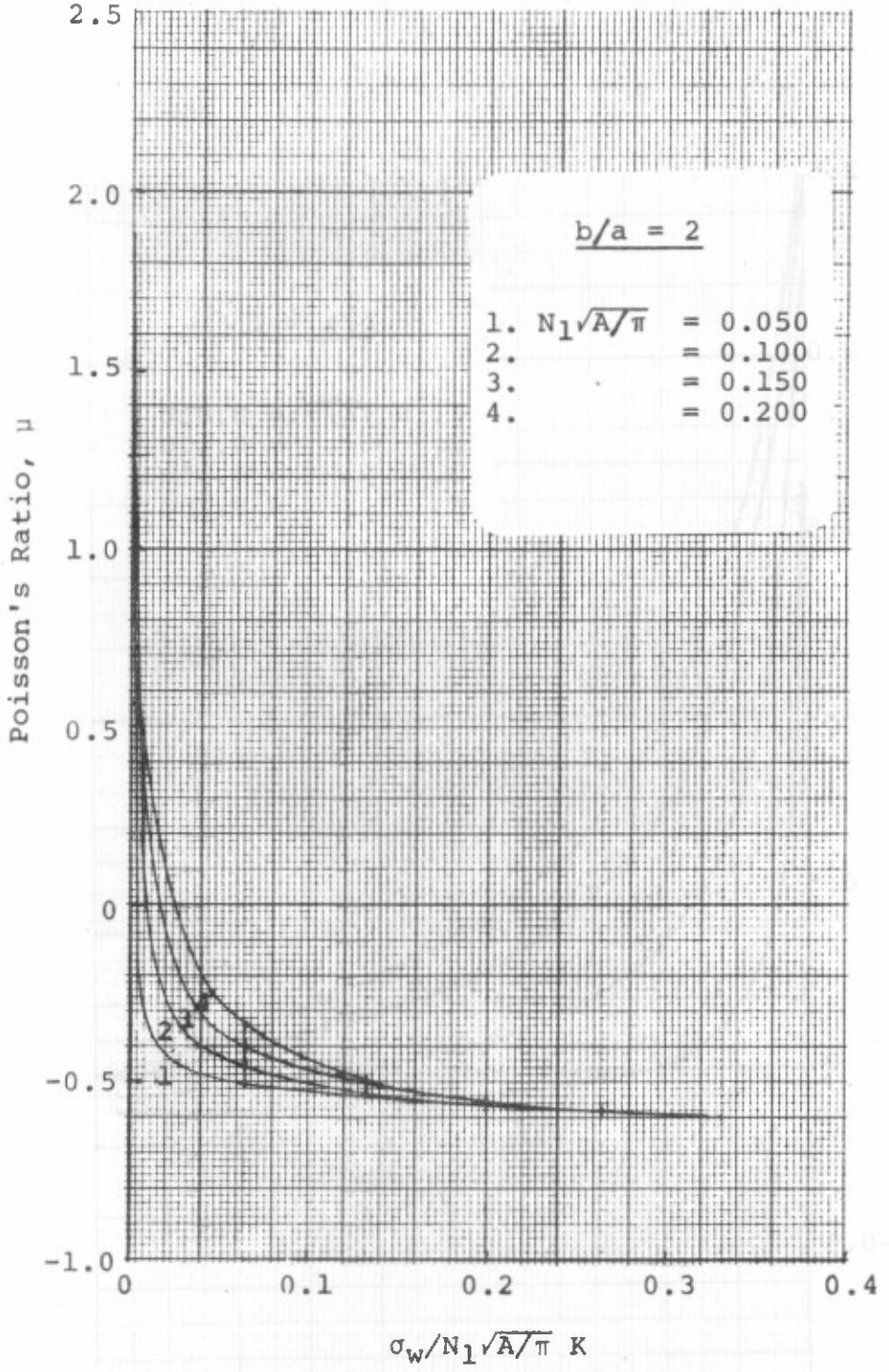

Figure 74. Fabric Poisson's Ratio: Linearly Elastic Yarn, Initially Square Fabric $\sigma_w/\sigma_f = 2$, b/a = 2

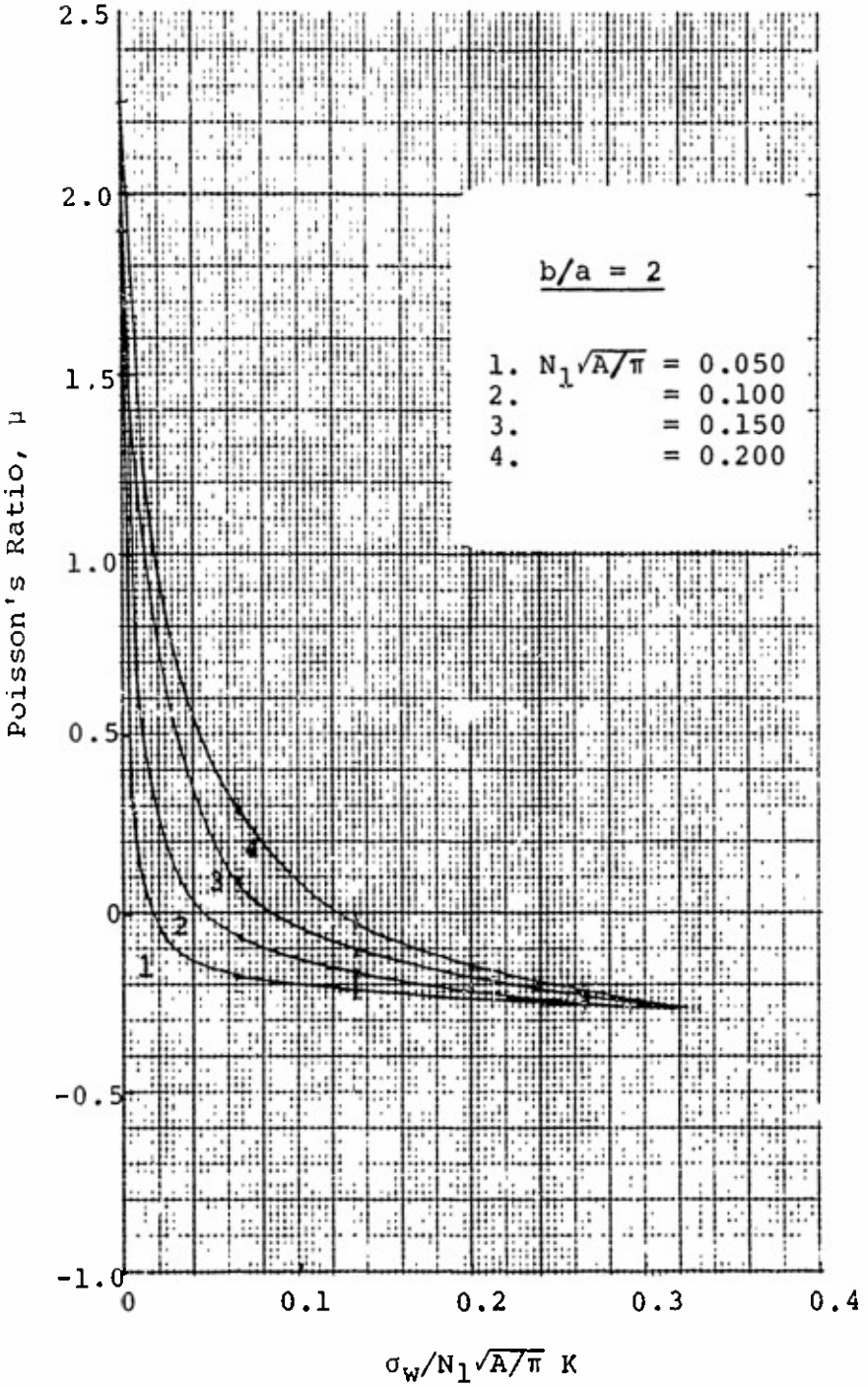

Figure 75. Fabric Poisson's Ratio: Linearly Elastic Yarn, Initially Square Fabric
σ_w/σ_f = 5, b/a = 2

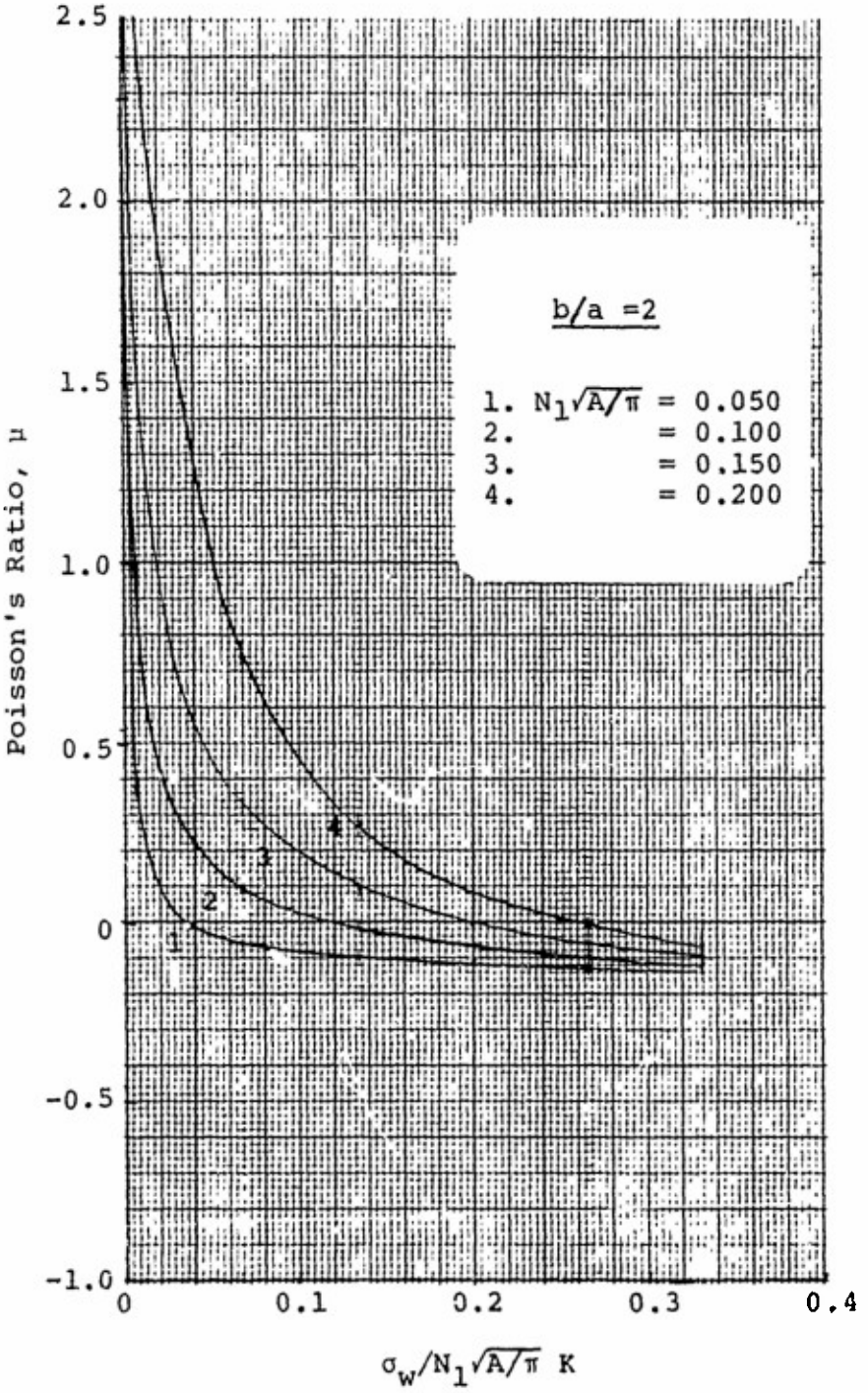

Figure 76. Fabric Poisson's Ratio: Linearly Elastic Yarn, Initially Square Fabric σ_w/σ_f = 10, b/a = 2

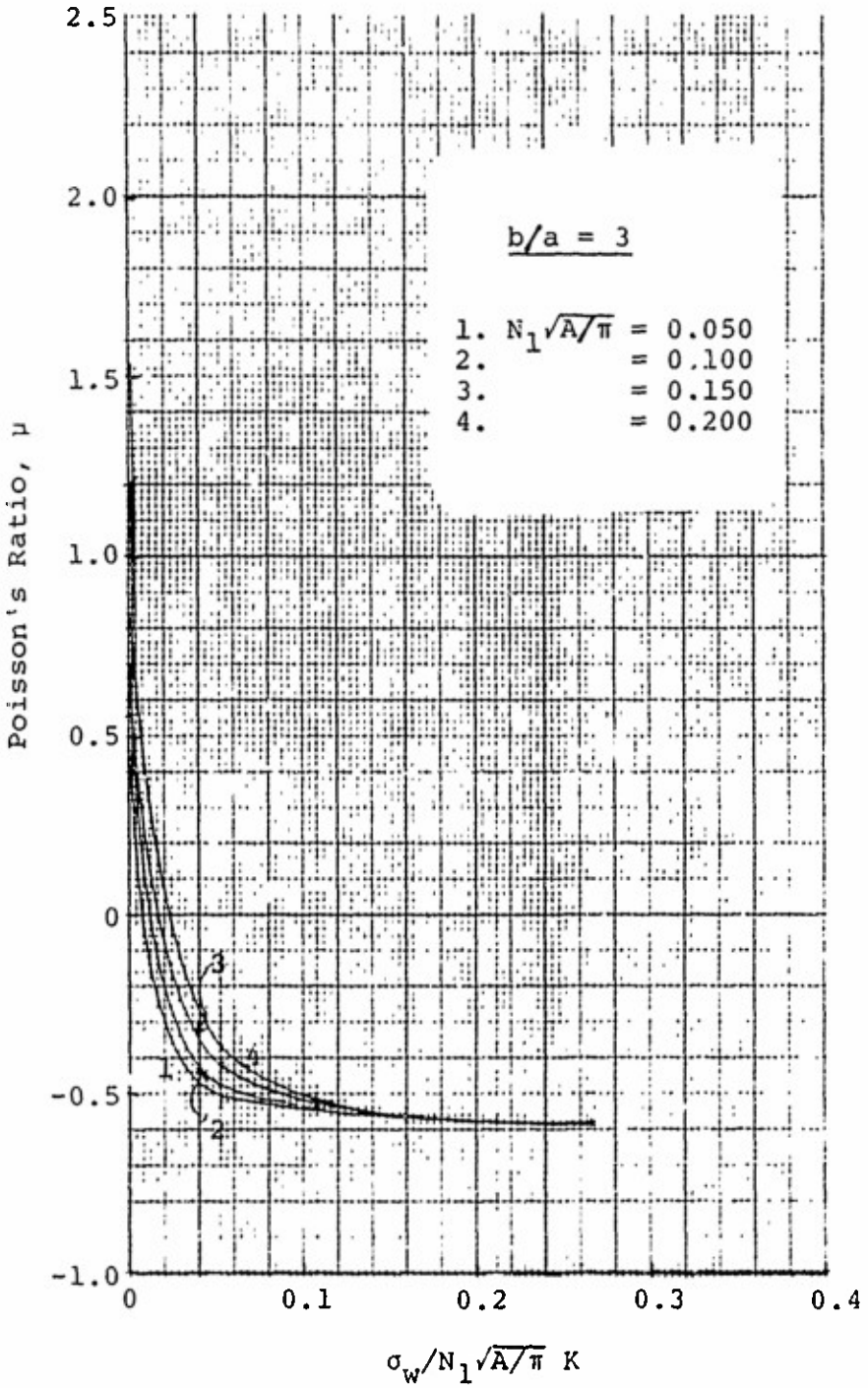

Figure 77. Fabric Poisson's Ratio: Linearly Elastic Yarn, Initially Square Fabric $\sigma_w/\sigma_f = 2$, b/a = 3

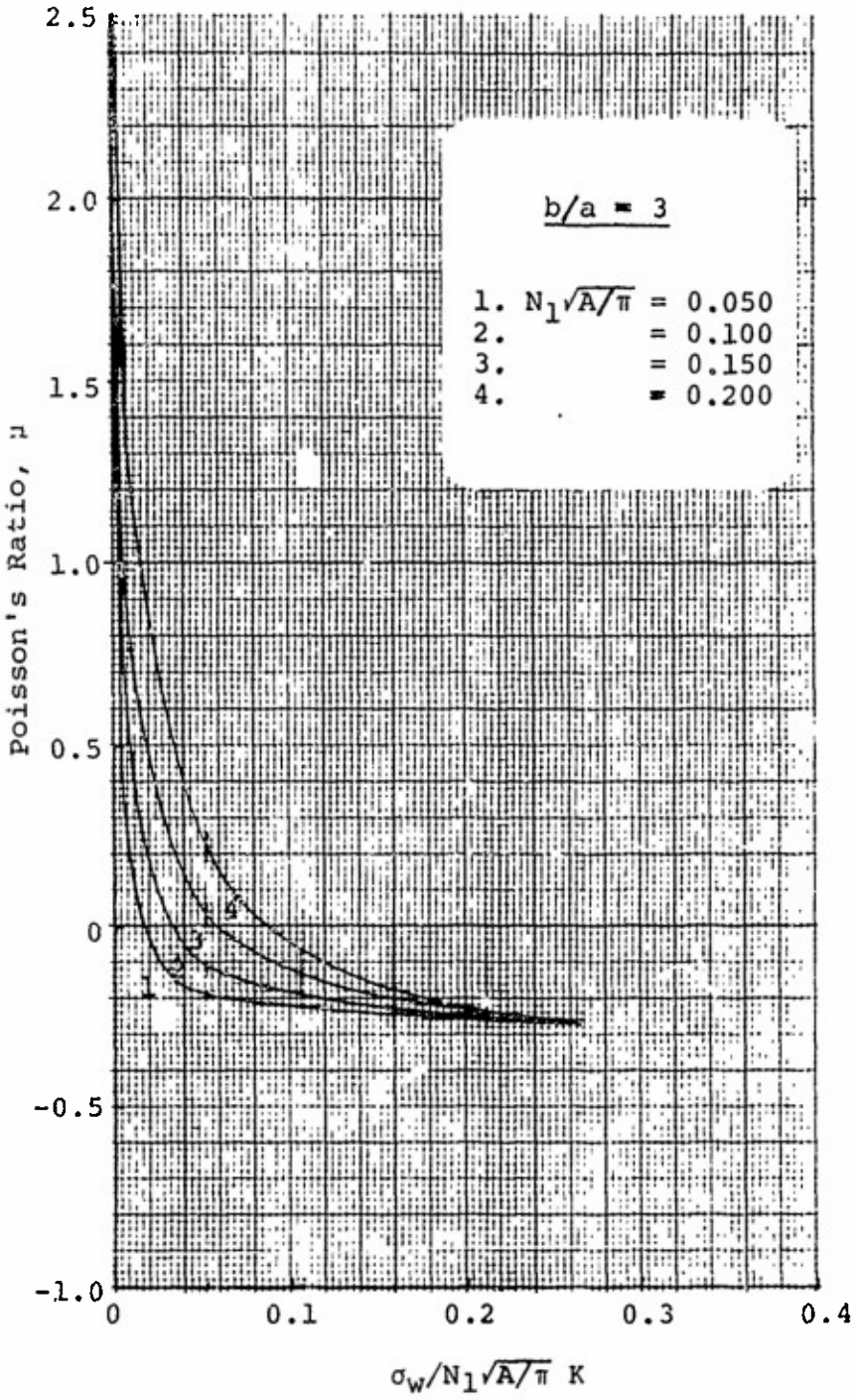

Figure 78. Fabric Poisson's Ratio: Linearly Elastic Yarn, Initially Square Fabric $\sigma_w/\sigma_f = 5$, b/a = 3

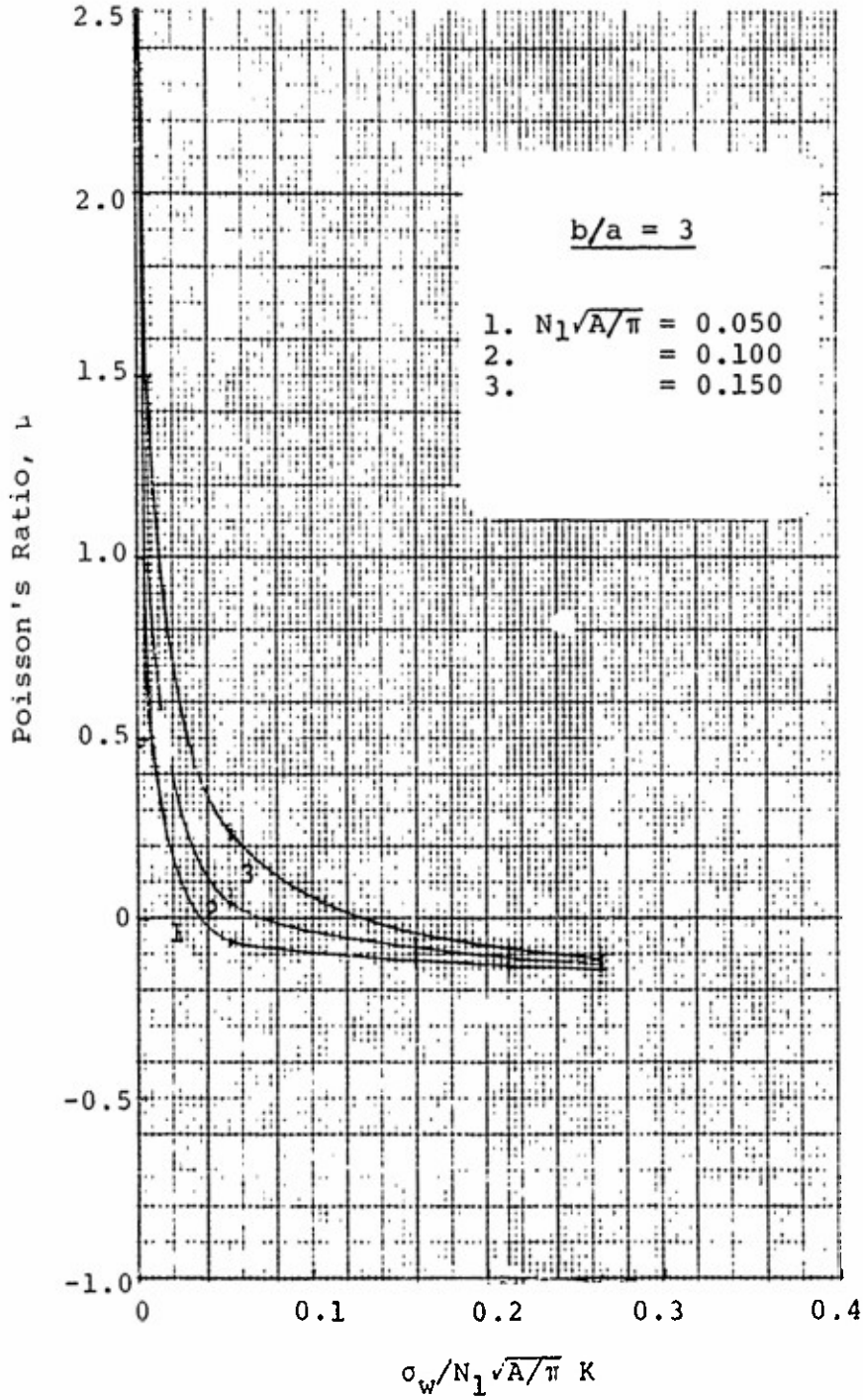

Figure 79. Fabric Poisson's Ratio: Linearly Elastic Yarn, Initially Square Fabric $\sigma_w/\sigma_f = 10$, b/a = 3

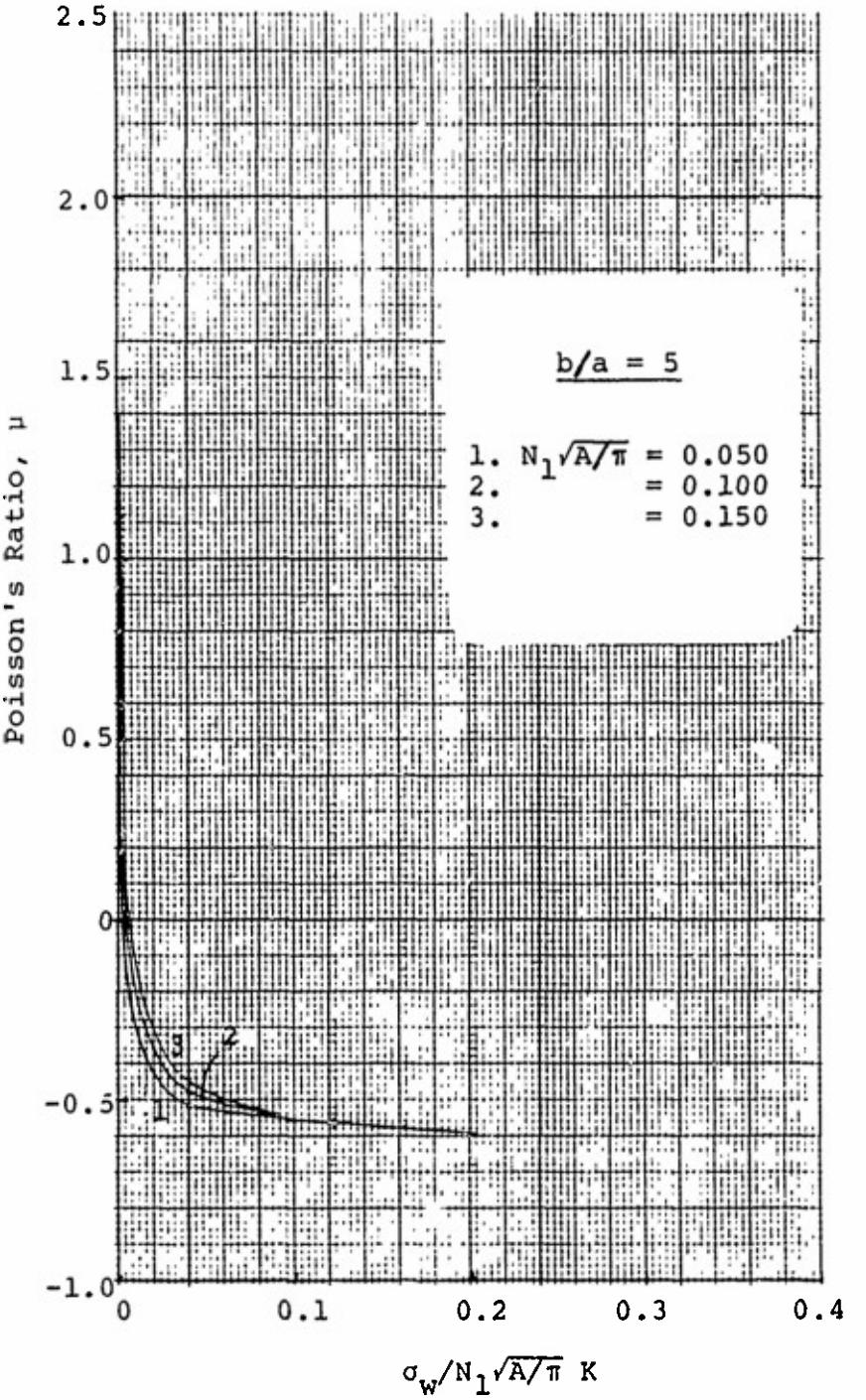

Figure 80. Fabric Poisson's Ratio: Linearly Elastic Yarn, Initially Square Fabric $\sigma_w/\sigma_f = 2$, b/a = 5

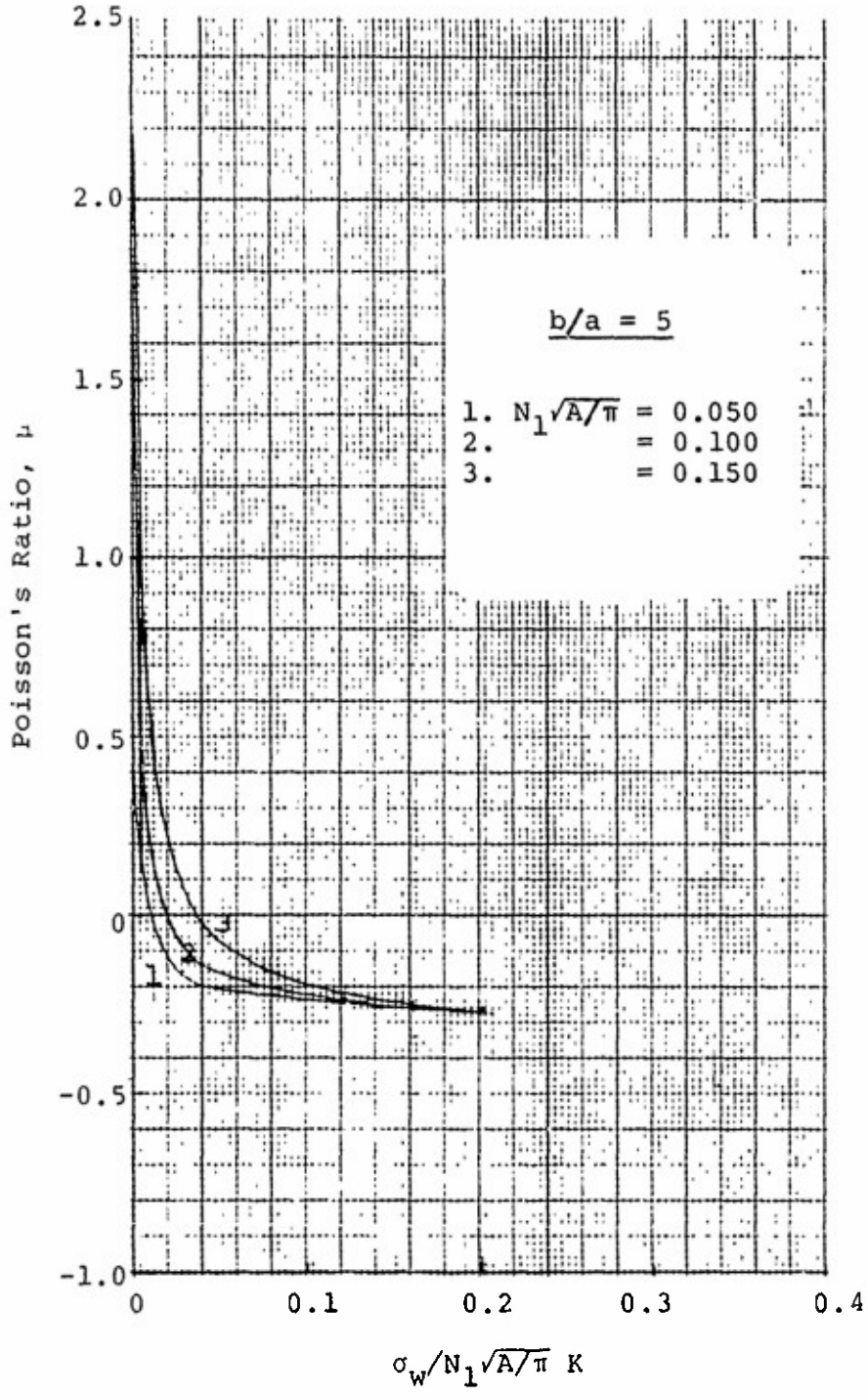

Figure 81. Fabric Poisson's Ratio: Linearly Elastic Yarn, Initially Square Fabric $\sigma_w/\sigma_f = 5$, $b/a = 5$

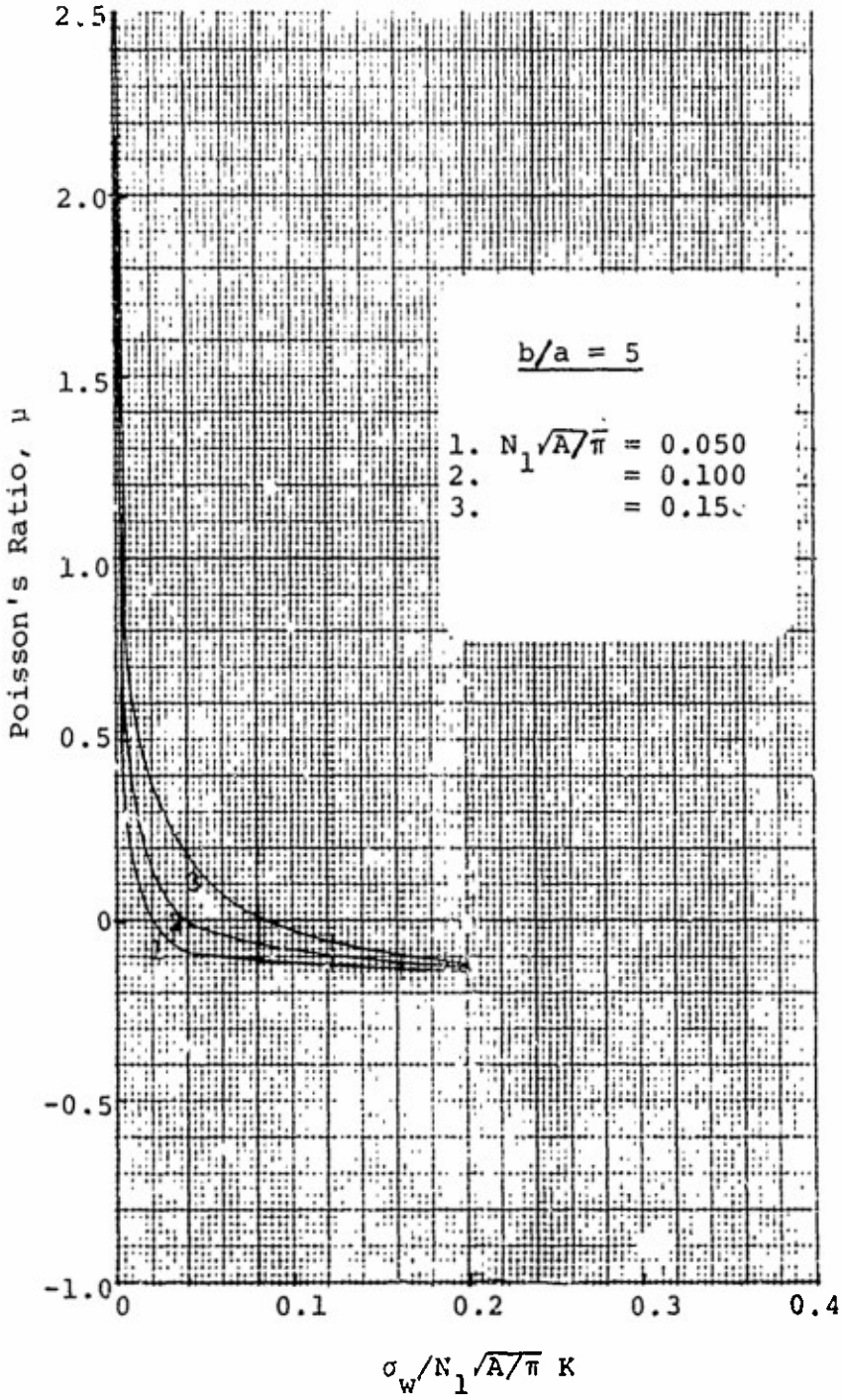

Figure 82. Fabric Poisson's Ratio: Linearly Elastic Yarn, Initially Square Fabric $\sigma_w/\sigma_f = 10$, b/a = 5

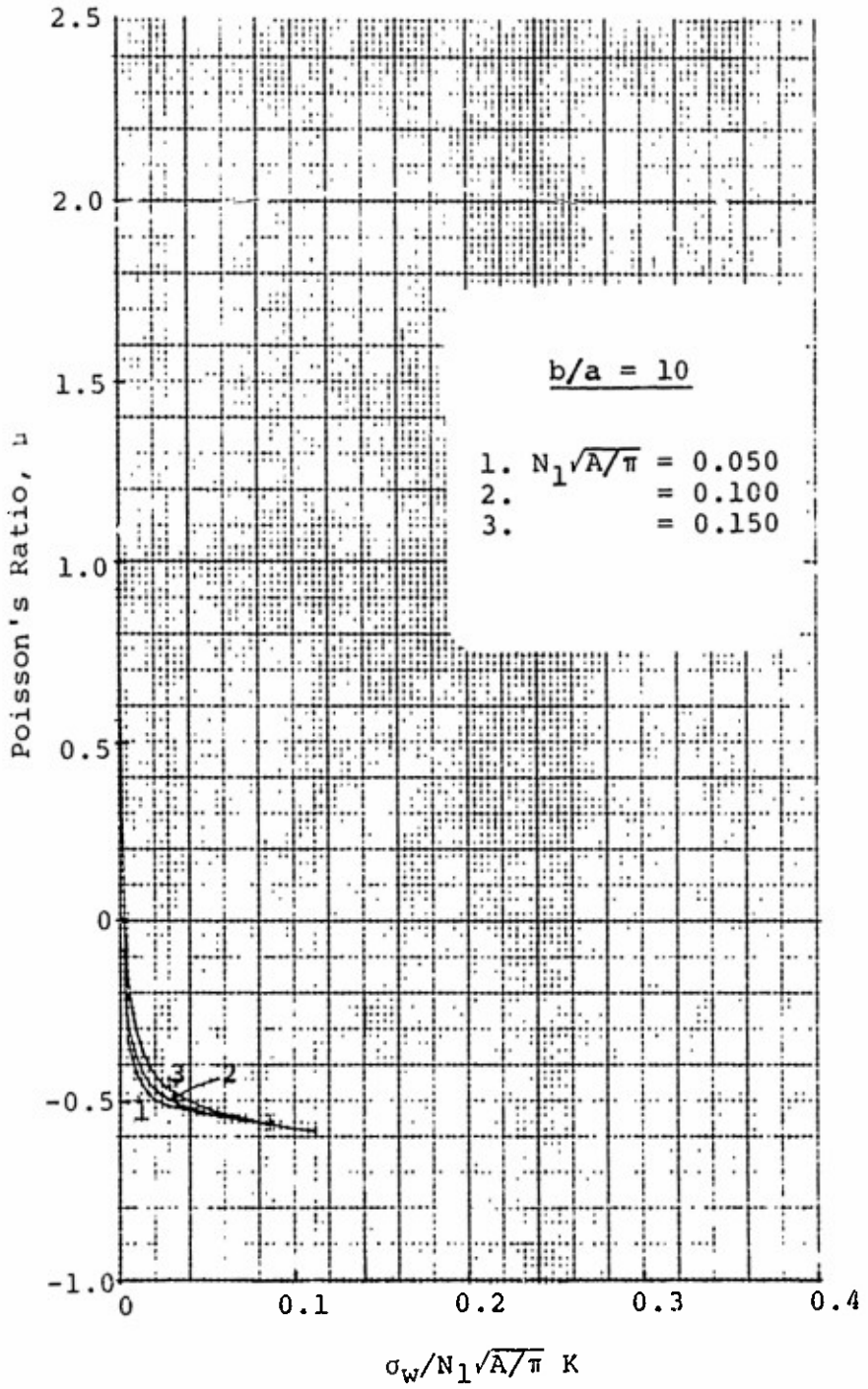

Figure 83. Fabric Poisson's Ratio: Linearly Elastic Yarn, Initially Square Fabric $\sigma_w/\sigma_f = 2$, b/a = 10

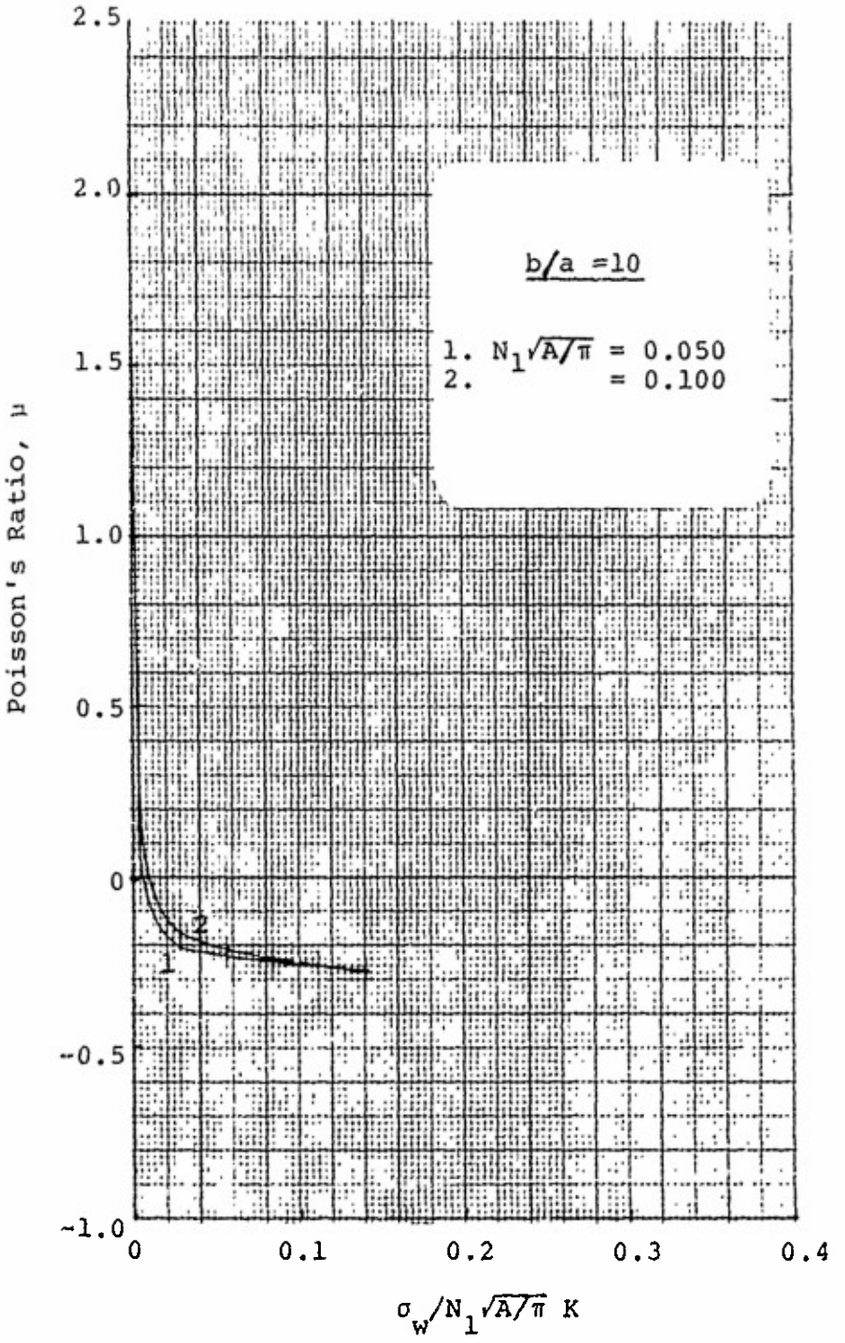

Figure 84. Fabric Poisson's Ratio: Linearly Elastic Yarn, Initially Square Fabric σ_w/σ_f = 5, b/a = 10

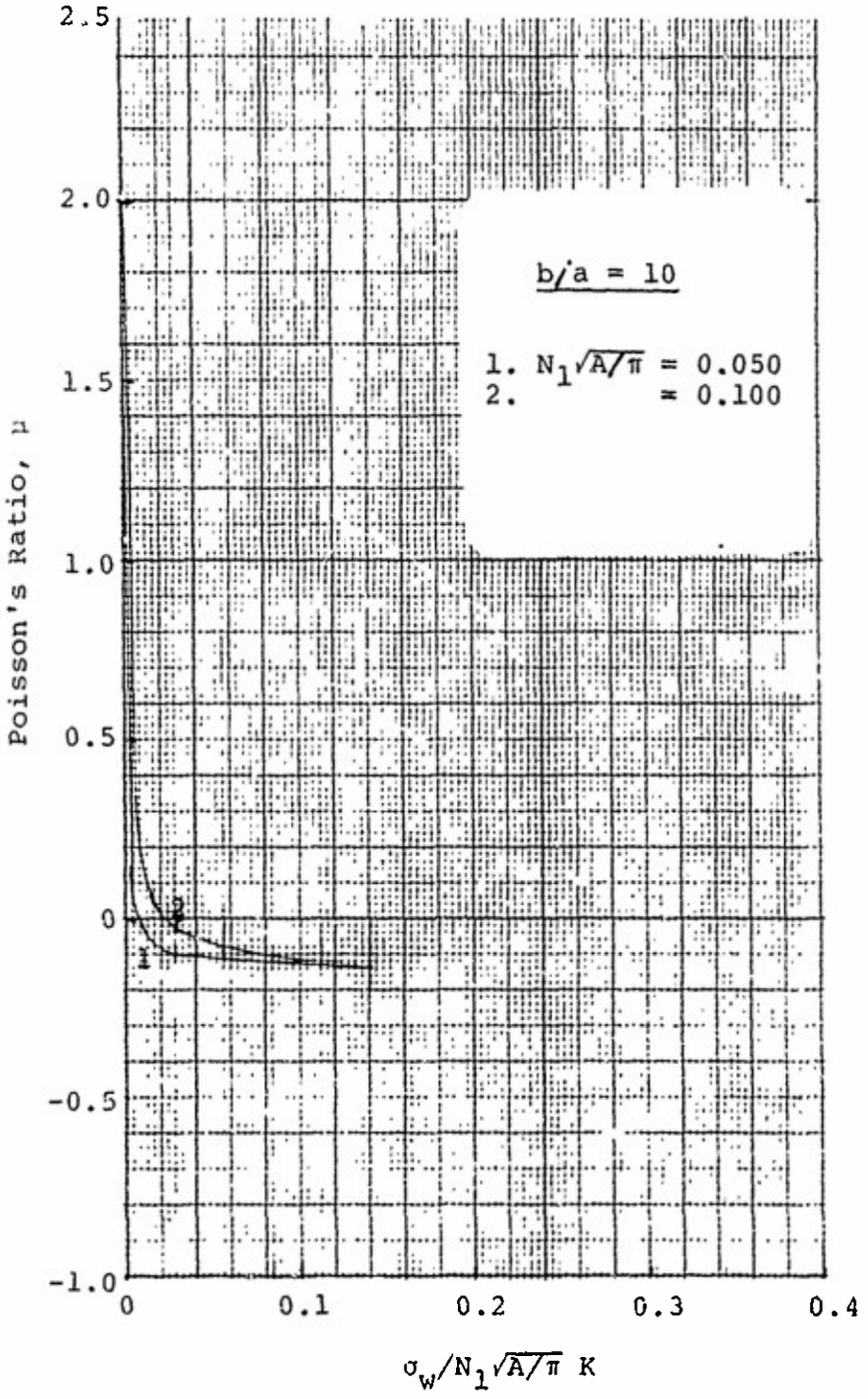

Figure 85. Fabric Poisson's Ratio, Linearly Elastic Yarn, Initially Square Fabric σ_w/σ_f = 10, b/a = 10

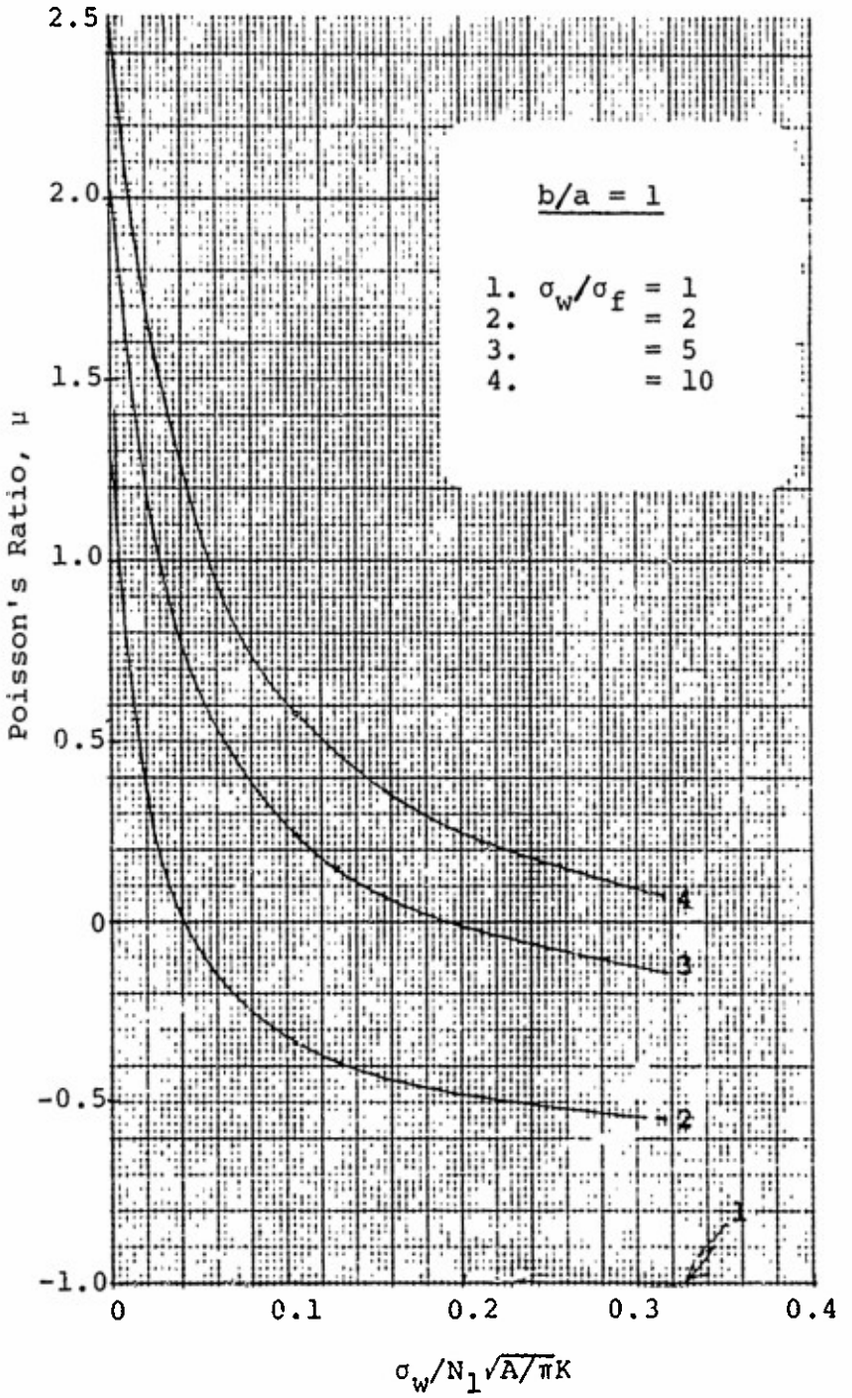

Figure 86. Poisson's Ratio (Aspect Ratio = 1): Linearly Elastic Yarn, Initially Square Fabric, $N_1\sqrt{A/\pi} = 0.15$. b/a = 1

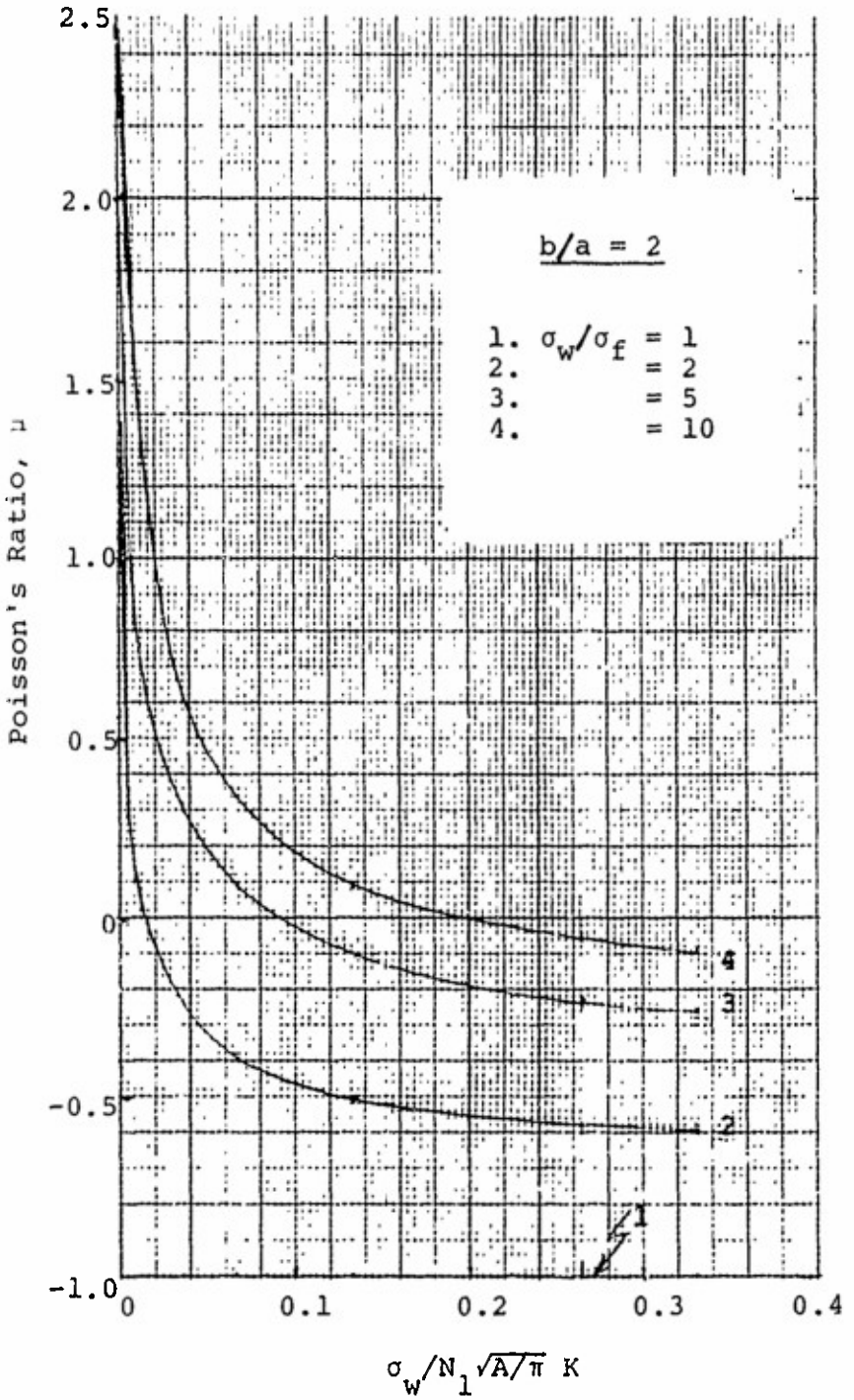

Figure 87. Fabric Poisson's Ratio: Linearly Elastic Yarn, Initially Square Fabric
$N_1\sqrt{A/\pi} = 0.15$, b/a = 2

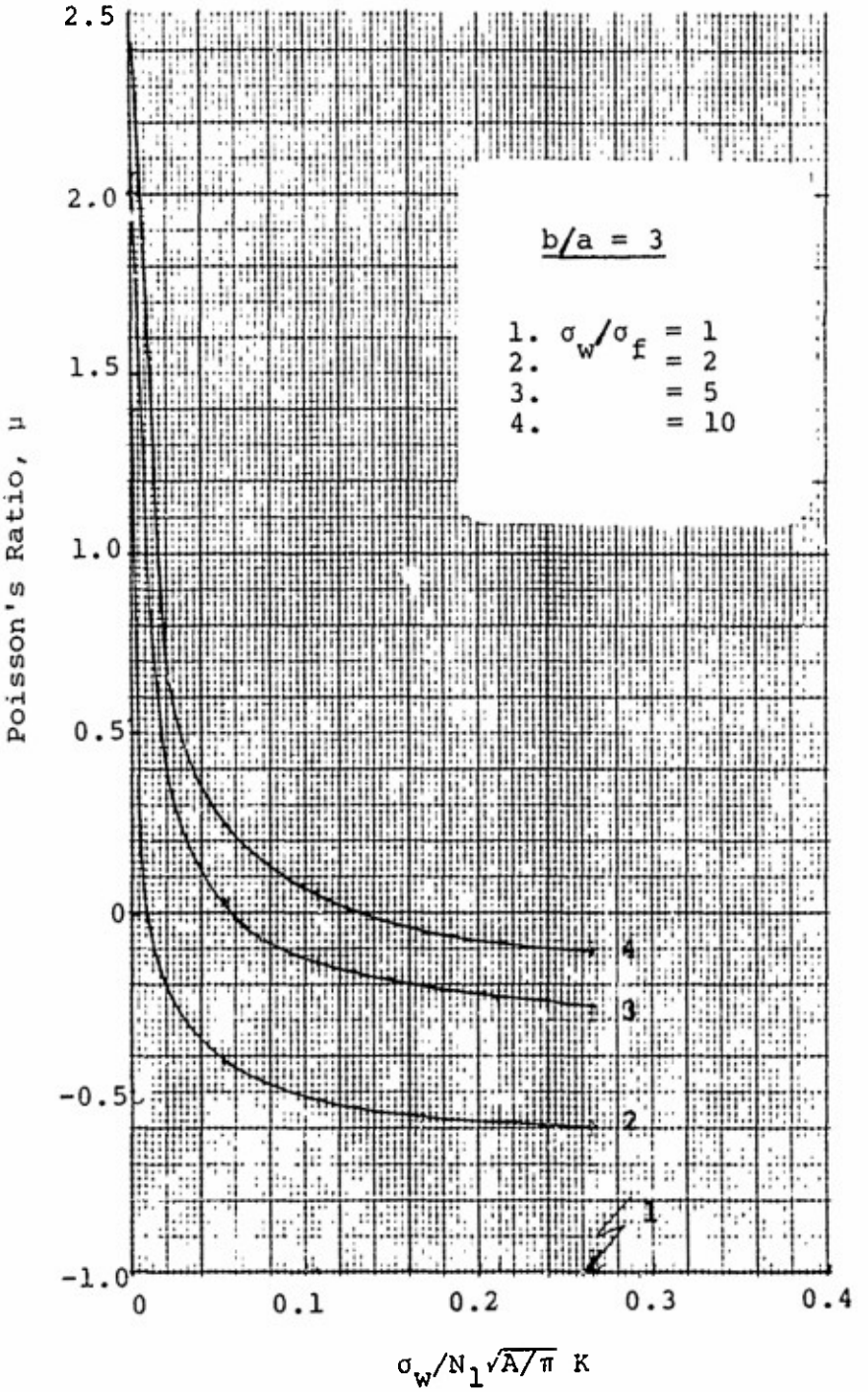

Figure 88. Fabric Poisson's Ratio: Linearly Elastic Yarn, Initially Square Fabric $N_1\sqrt{A/\pi} = 0.15$, $b/a \approx 3$

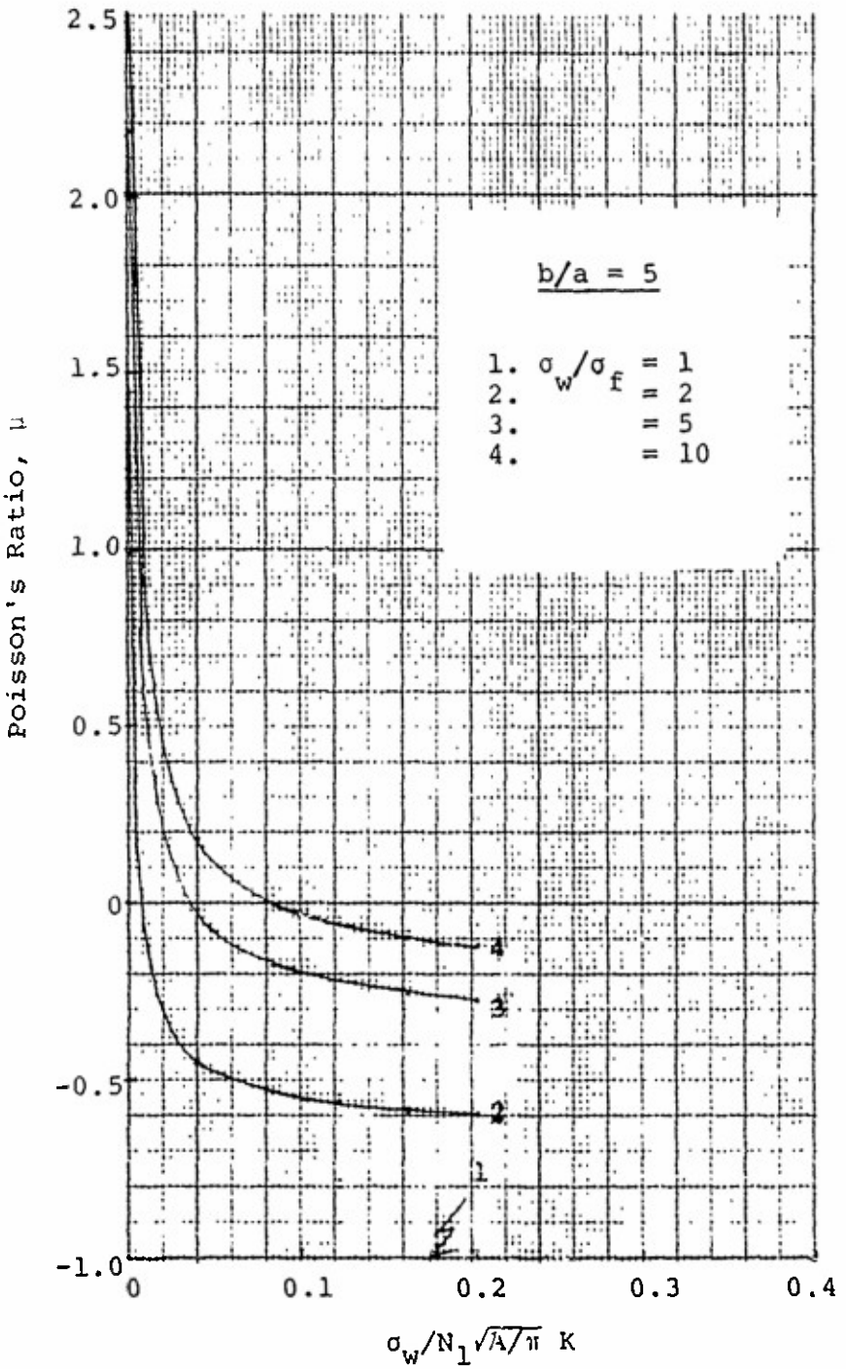

Figure 89. Fabric Poisson's Ratio: Linearly Elastic Yarn, Initially Square Fabric $N_1\sqrt{A/\pi} = 0.15$, b/a = 5

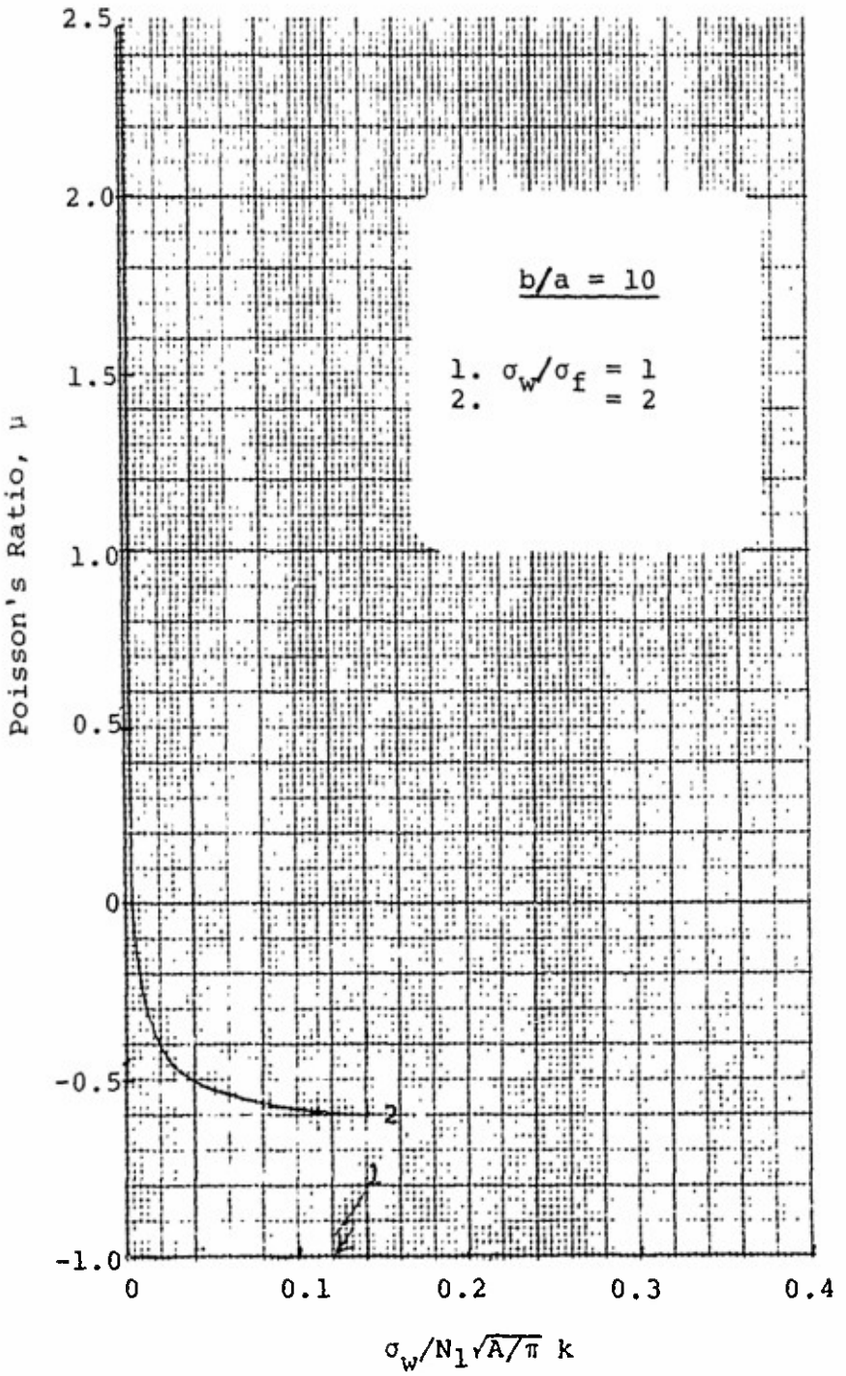

Figure 90. Fabric Poisson's Ratio: Linearly Elastic Yarn, Initially Square Fabric $N_1\sqrt{A/\pi} = 0.15$, b/a = 10

A simplified procedure for determining the load-extension response of a fabric comprised of linearly elastic yarns with b/a > 1 analogous to that outlined for fabric comprised of inextensible yarn is not possible. This is because it is assumed that there is no friction between yarns at crossovers. Therefore, the yarn length 2(b-a) in contact with the crossing yarn at the crossovers extends into the region between crossovers. This alters the response of this region so that it is not identical to that for a round-yarn fabric of yarn radius a.

V. Fabric Strength

The design engineer is usually concerned with predicting not only the load-extension behavior of the fabric but also the ultimate strength of the fabric. Assuming the load applied in the warp direction is greater than or equal to that applied in the filling direction $\sigma_w \geq \sigma_f$, the fabric strength is given by the following expression (see Equation 9).

$$(\sigma)_{ult} = N_2 \cos\theta_2 (P_y)_{ult} \tag{47}$$

where $(P_y)_{ult}$ is the rupture strength of the yarn from which the fabric is woven. If it is assumed that the fabric is comprised of linearly elastic yarns having a modulus E_y and known rupture extension $(\varepsilon_y)_{rupt}$

$$(P_y)_{ult} = E_y(\varepsilon_y)_{rupt} = \rho E_f A(\varepsilon_y)_{rupt} \tag{48}$$

The extended length of the yarn between crossovers in the fabric can be determined from the following expression

$$L_2 = (1+\varepsilon_y)L_1 \tag{49}$$

For the case of initially square fabrics with $\sigma_w \geq \sigma_f$, the load and also the yarn extension are greater in the warp direction. Therefore, the ultimate strength of the fabric is governed by the load σ_w and the fabric will fail in the warp direction. For this case

L_{1w} is determined from Equations 20, 21 and 22 for specific initial parameters $N_1\sqrt{A/\pi}$ and b/a. Then $\sigma_{w(ult)}$ can be found from Equations 41-44 for a specific loading ratio.

Although the design engineer may only be interested in the strength or strength-to-weight ratio of a fabric, industrial fabrics are often rated by the efficiency with which the yarn strength is translated into fabric strength. This efficiency, E_w, in the warp direction is given by (see Equation 47)

$$E_w = \frac{(\sigma_w)_{ult}}{N_{2w}(P_y)_{ult}} \times 100 = \cos\theta_{2w} \times 100 \qquad (50)$$

This quantity is plotted for initially square fabric woven from linearly elastic yarns in Figures 91 through 104 as a function of yarn rupture strain determined according to Equation 49 for various initial fabric constructions, degrees of yarn flattening and loading ratios. Results are not plotted for σ_w/σ_f = 10 with b/a = 2 and 3, nor for σ_w/σ_f = 5 and 10 with b/a = 5 and 10 because the efficiency in these cases is greater than 99.5% for all values of $N_1\sqrt{A/\pi}$. As shown, the efficiency increases with increasing loading ratio, yarn aspect ratio, and yarn rupture strain. Additionally, the more open the fabric, i.e., the lower $N_1\sqrt{A/\pi}$, the higher the efficiency. All of these trends toward increased efficiency are the result of decreasing warp yarn crimp - yarn angulation with the fabric mid-plane - with increasing loading ratio, aspect ratio, yarn rupture strain and decreasing $N_1\sqrt{A/\pi}$.

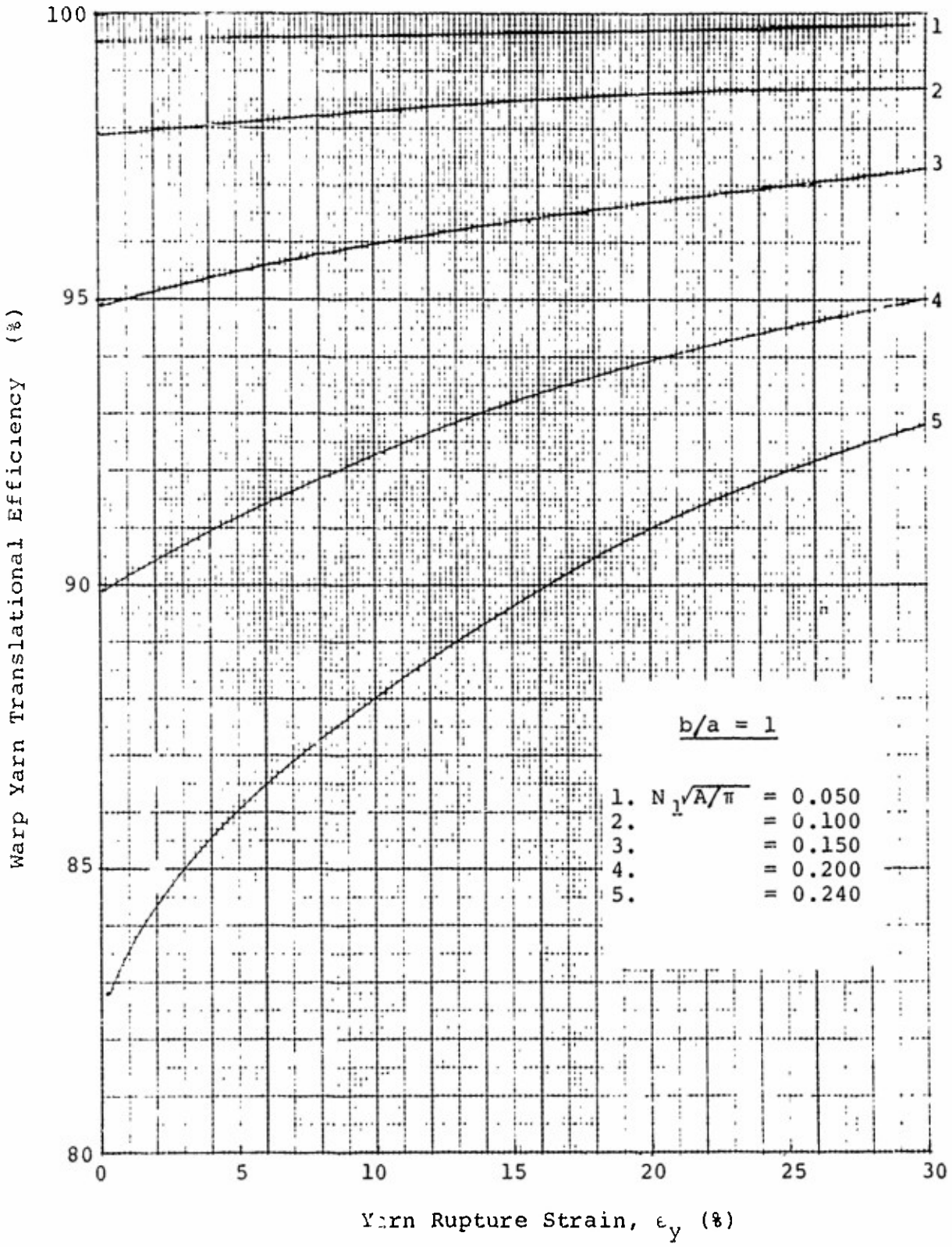

Figure 91. Yarn Translation Efficiency (Aspect Ratio = 1): Linearly Elastic Yarn, Initially Square Fabric $\sigma_w/\sigma_f = 1$, b/a = 1

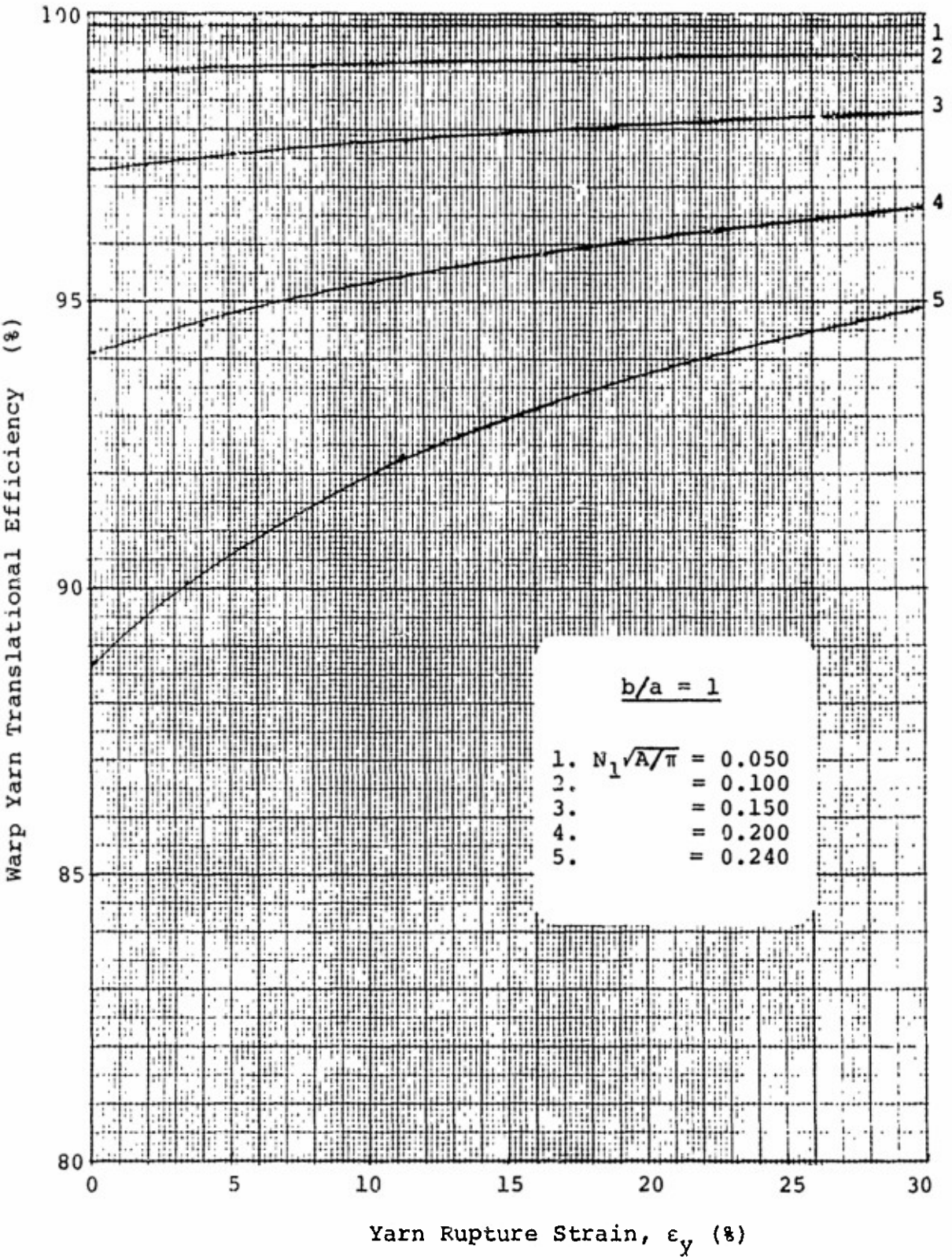

Figure 92. Yarn Translational Efficiency (Aspect Ratio = 1); Linearly Elastic Yarn, Initially Square Fabric $\sigma_w/\sigma_f = 2$, b/a = 1

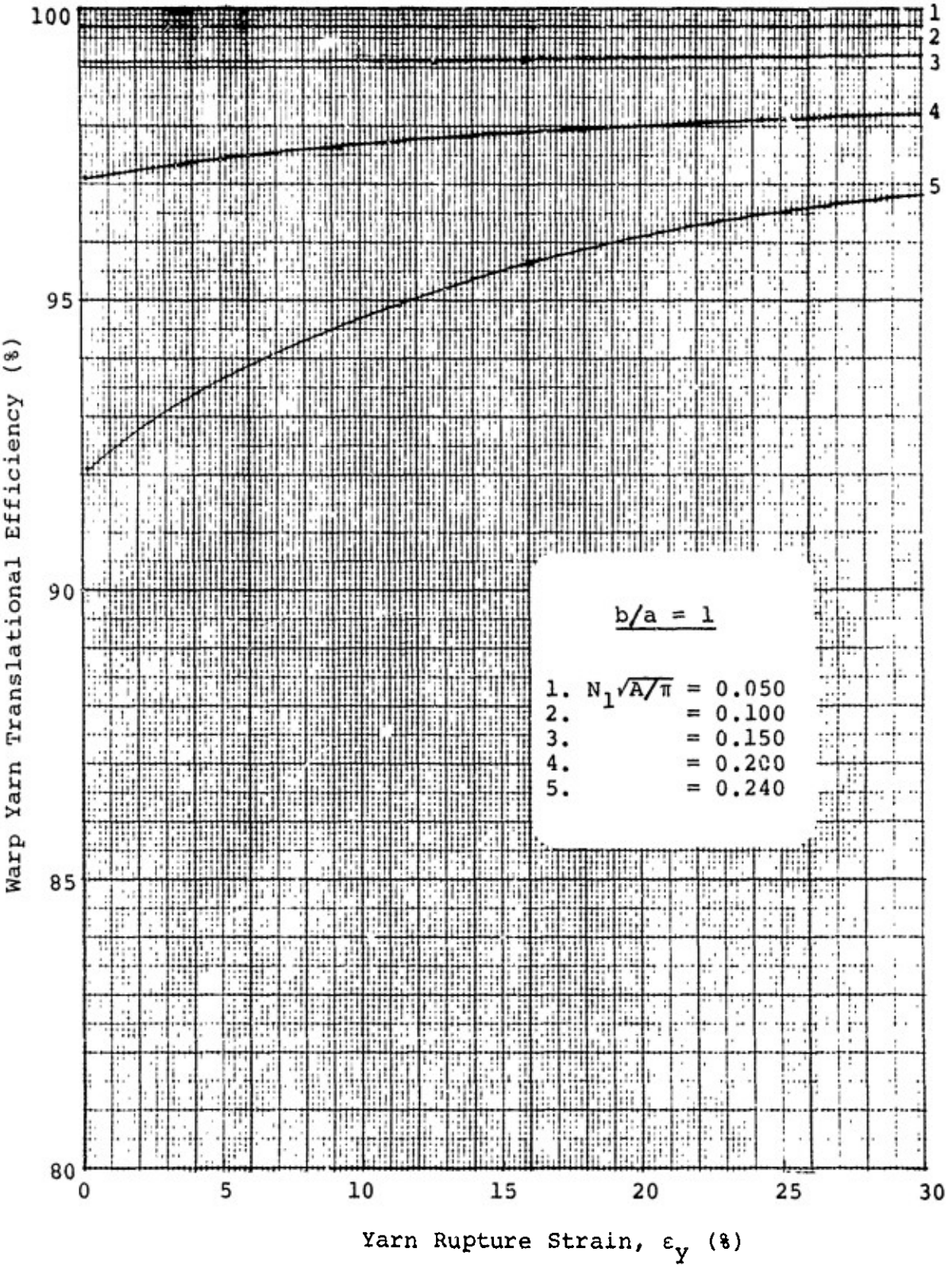

Figure 93. Yarn Translational Efficiency (Aspect Ratio = 1): Linearly Elastic Yarn, Initially Square Fabric $\sigma_w/\sigma_f = 5$, b/a = 1

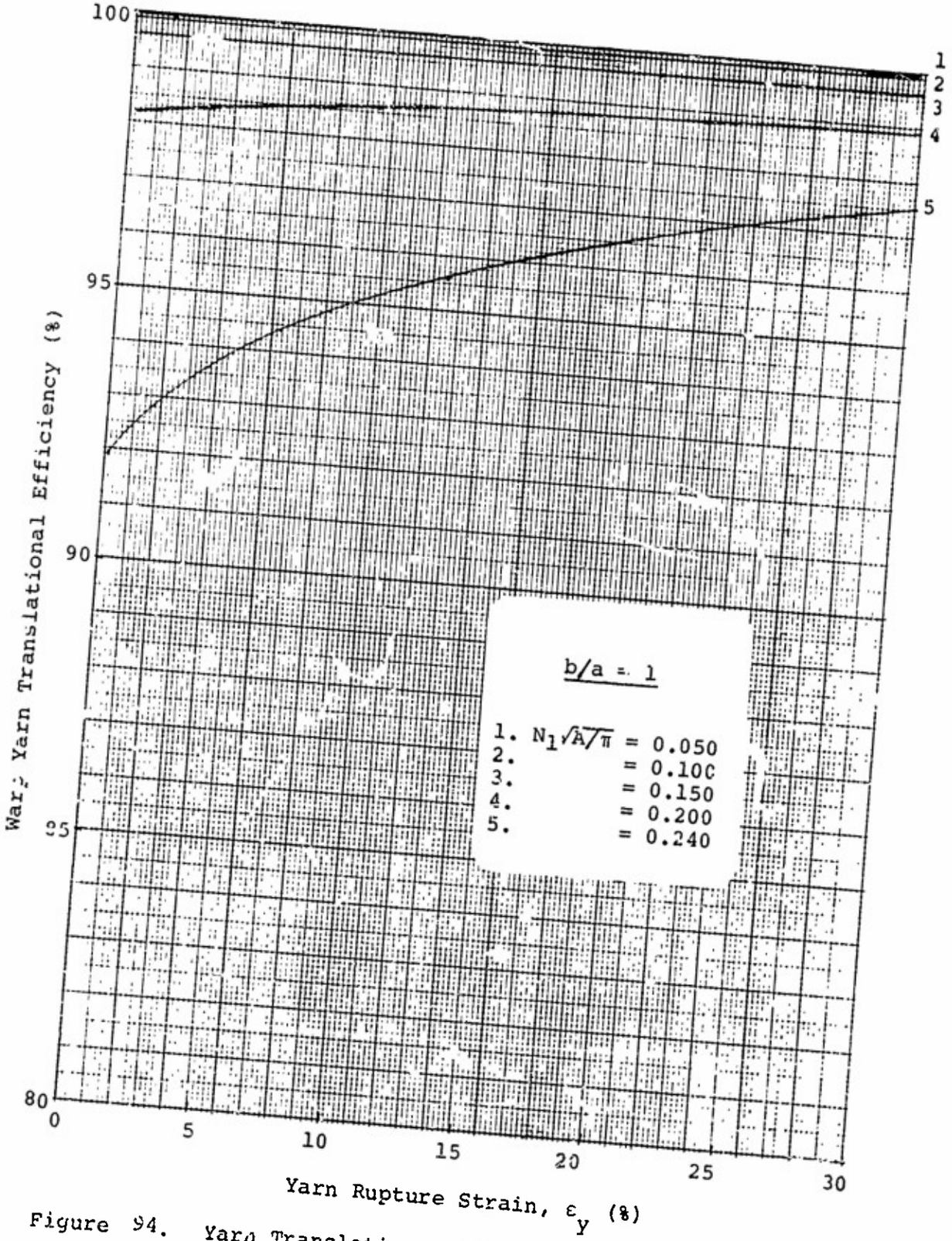

Figure 94. Yarn Translational Efficiency (Aspect Ratio = 1): Linearly Elastic Yarn, Initially Square Fabric $\sigma_w/\sigma_f = 10$, b/a = 1

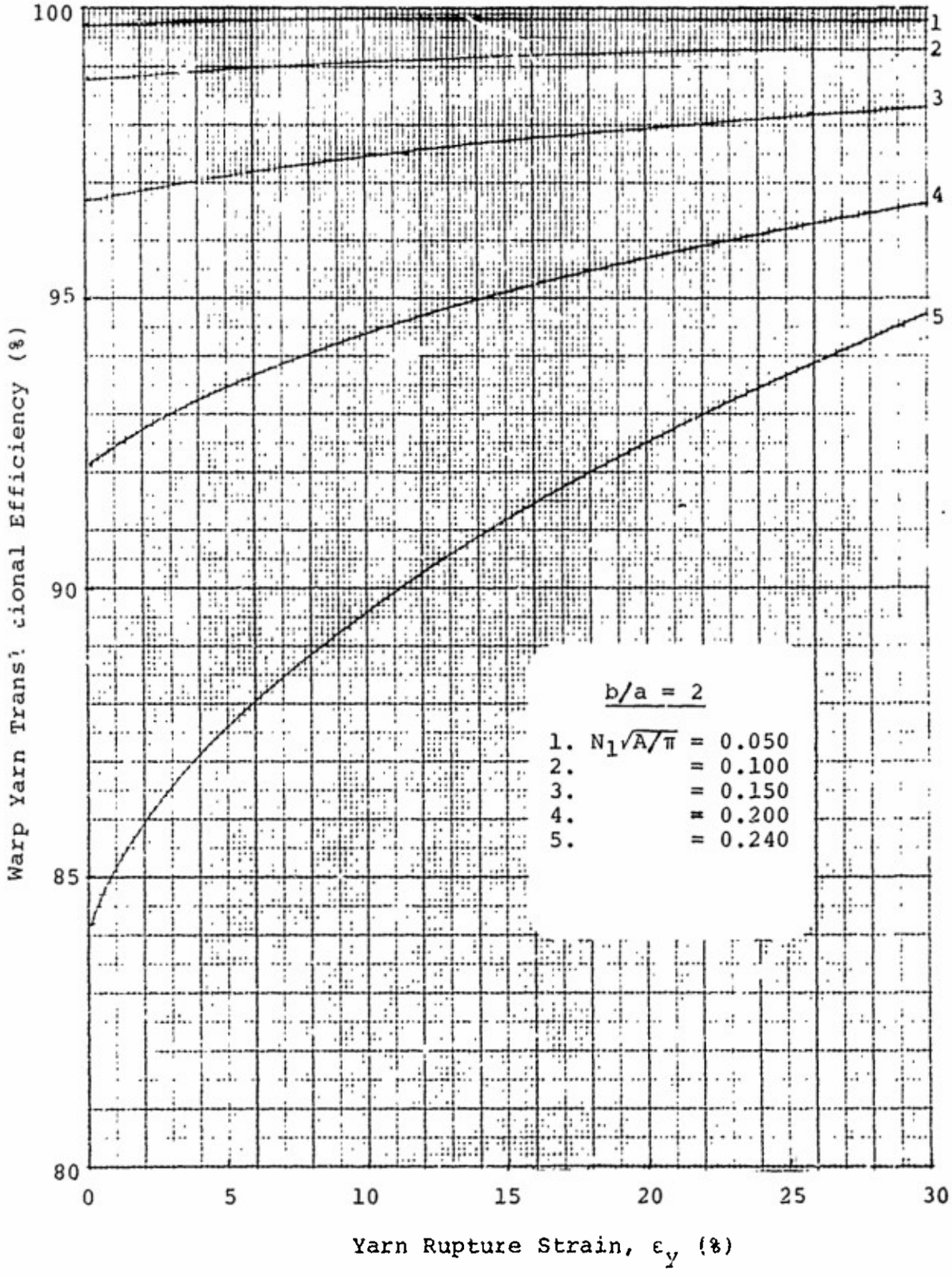

Figure 95. Yarn Translational Efficiency: Linearly Elastic Yarn, Initially Square Fabric, $\sigma_w/\sigma_f = 1$, $b/a = 2$

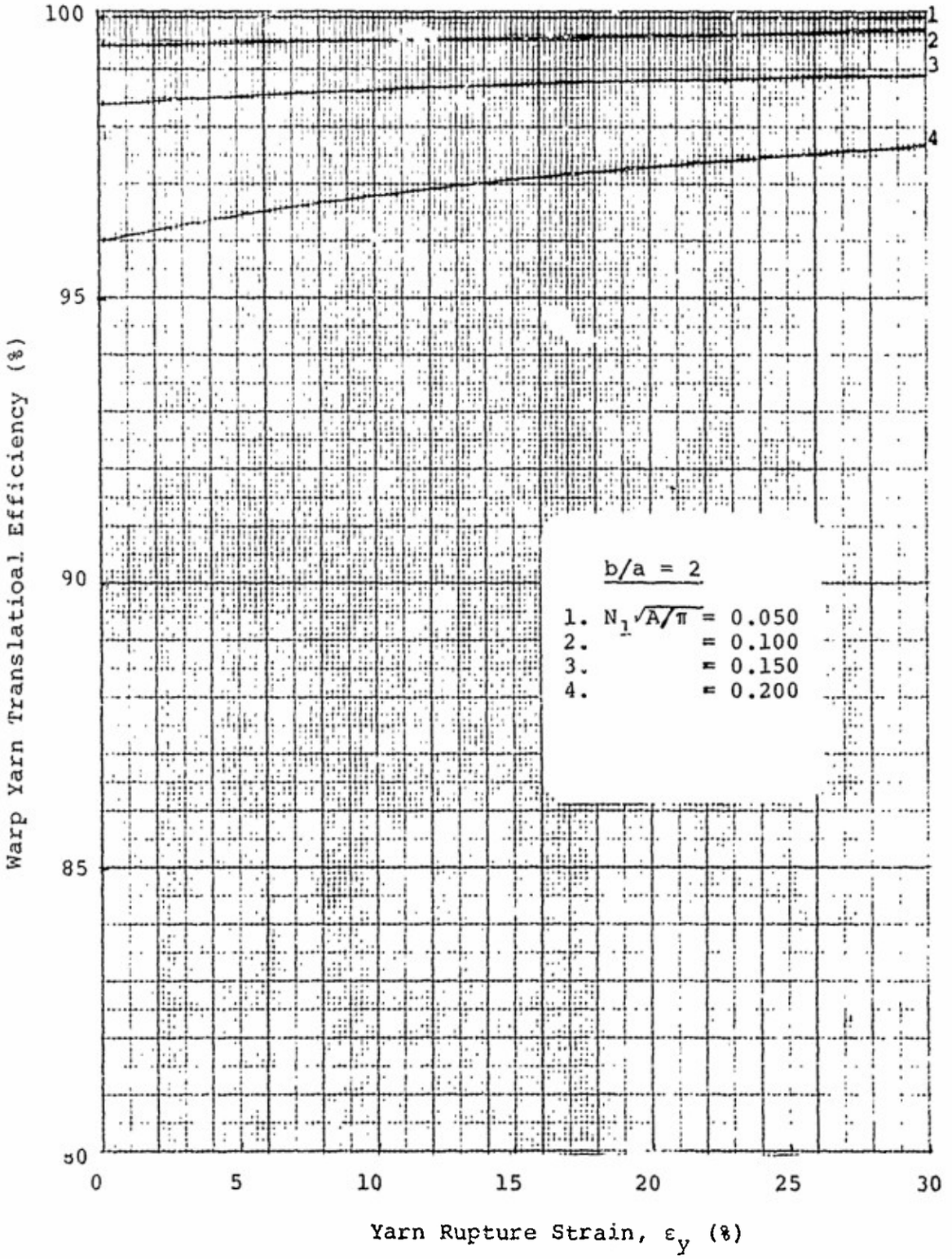

Figure 96. Yarn Translational Efficiency: Linearly Elastic Yarn, Initially Square Fabric, $\sigma_w/\sigma_f = 2$, b/a = 2

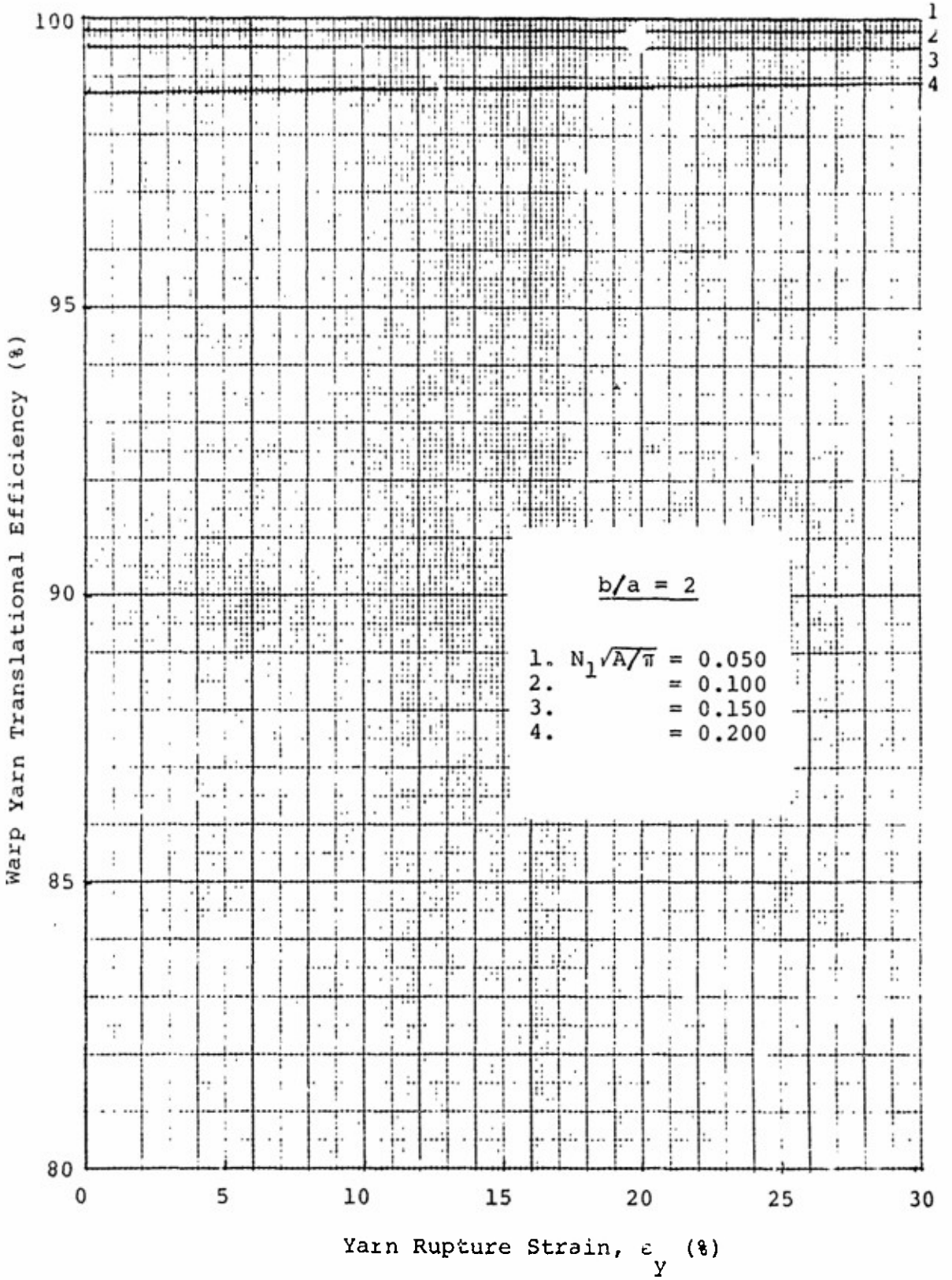

Figure 97 Yarn Translational Efficiency: Linearly Elastic Yarn, Initially Square Fabric, $\sigma_w/\sigma_f = 5$, b/a = 2

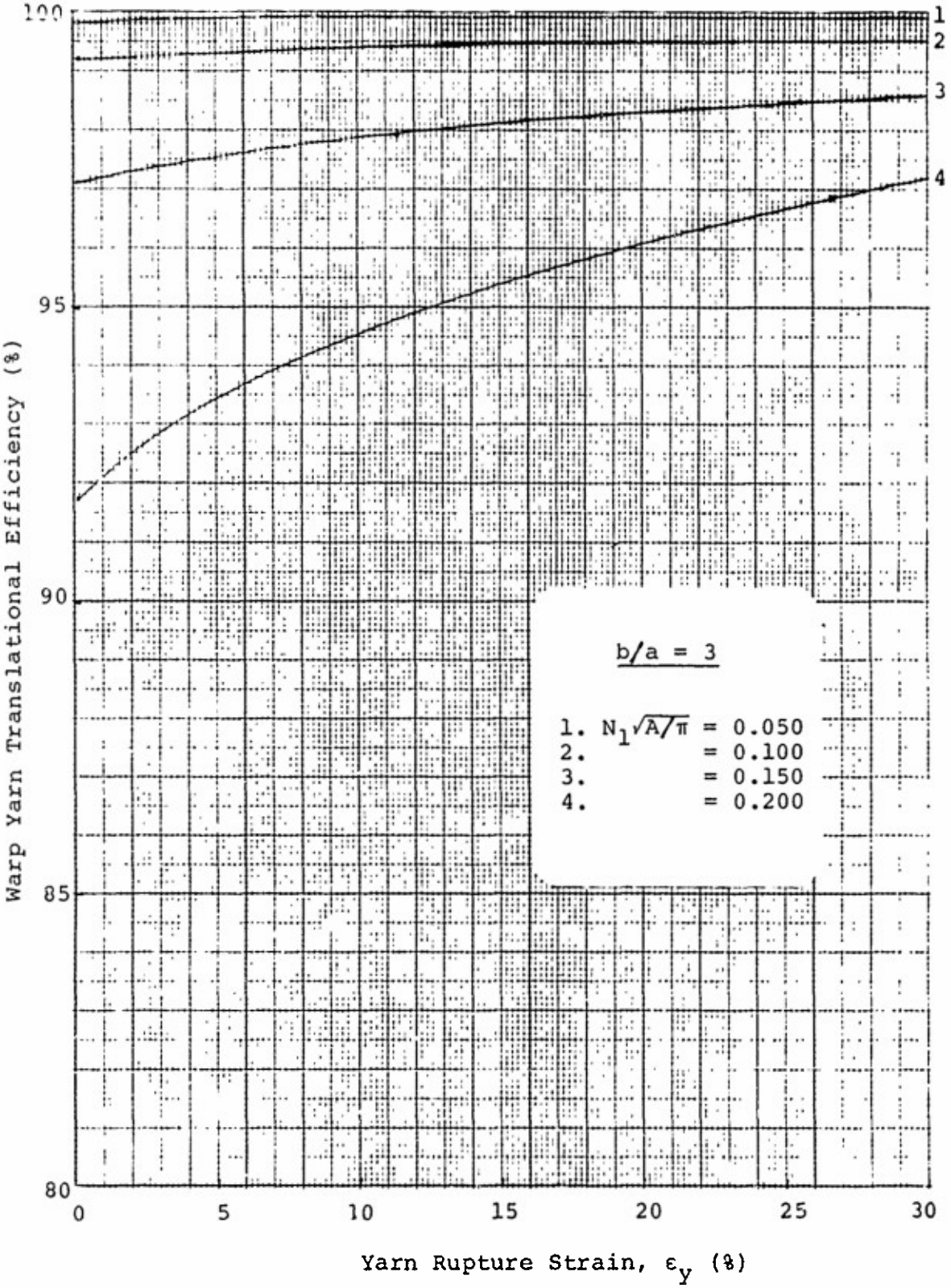

Figure 98. Yarn Translational Efficiency: Linearly Elastic Yarn, Initially Square Fabric, $\sigma_w/\sigma_f = 1$, b/a = 3

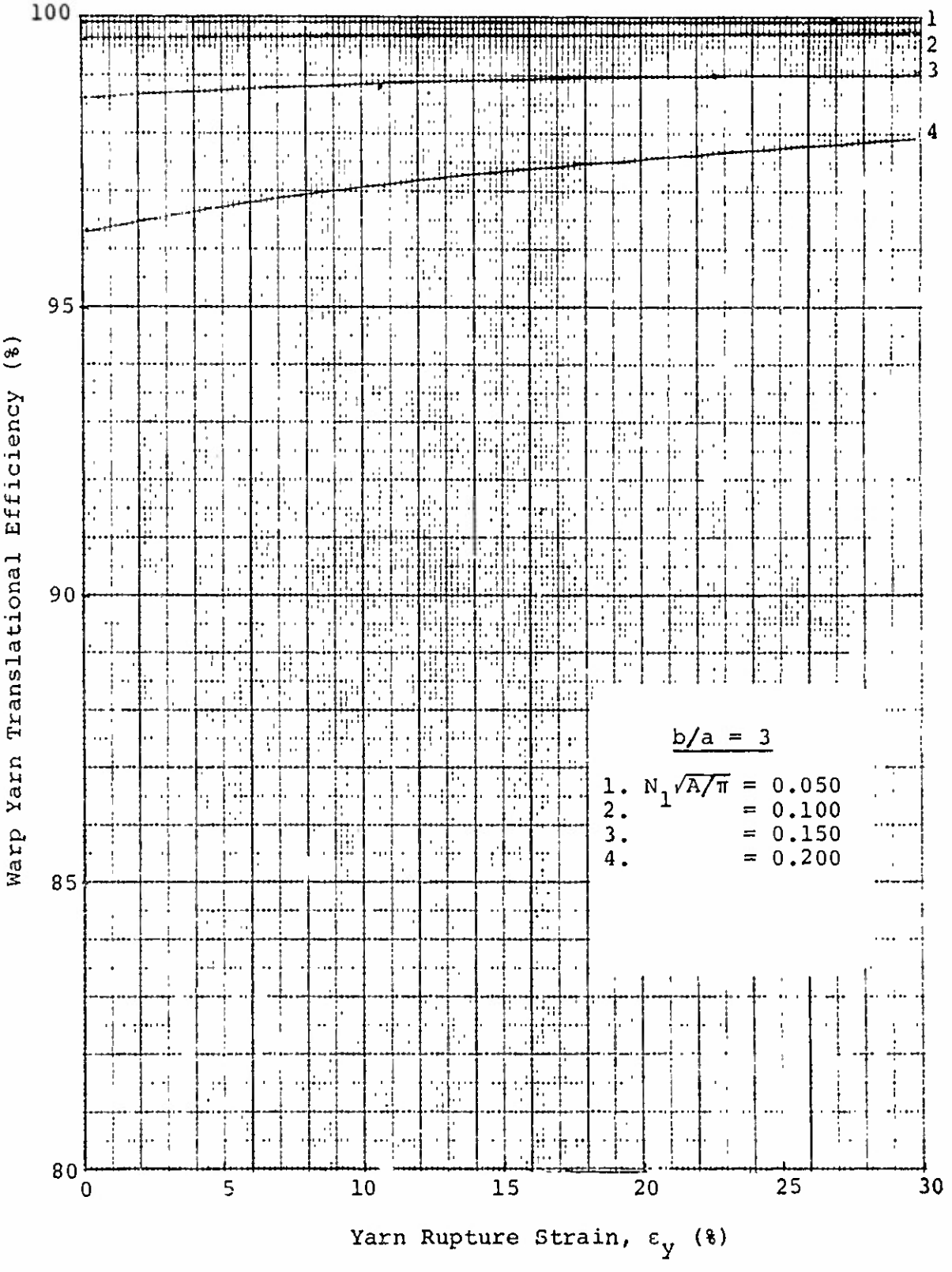

Figure 99. Yarn Translational Efficiency: Linearly Elastic Yarn, Initially Square Fabric, σ_w/σ_f = 2, b/a = 3

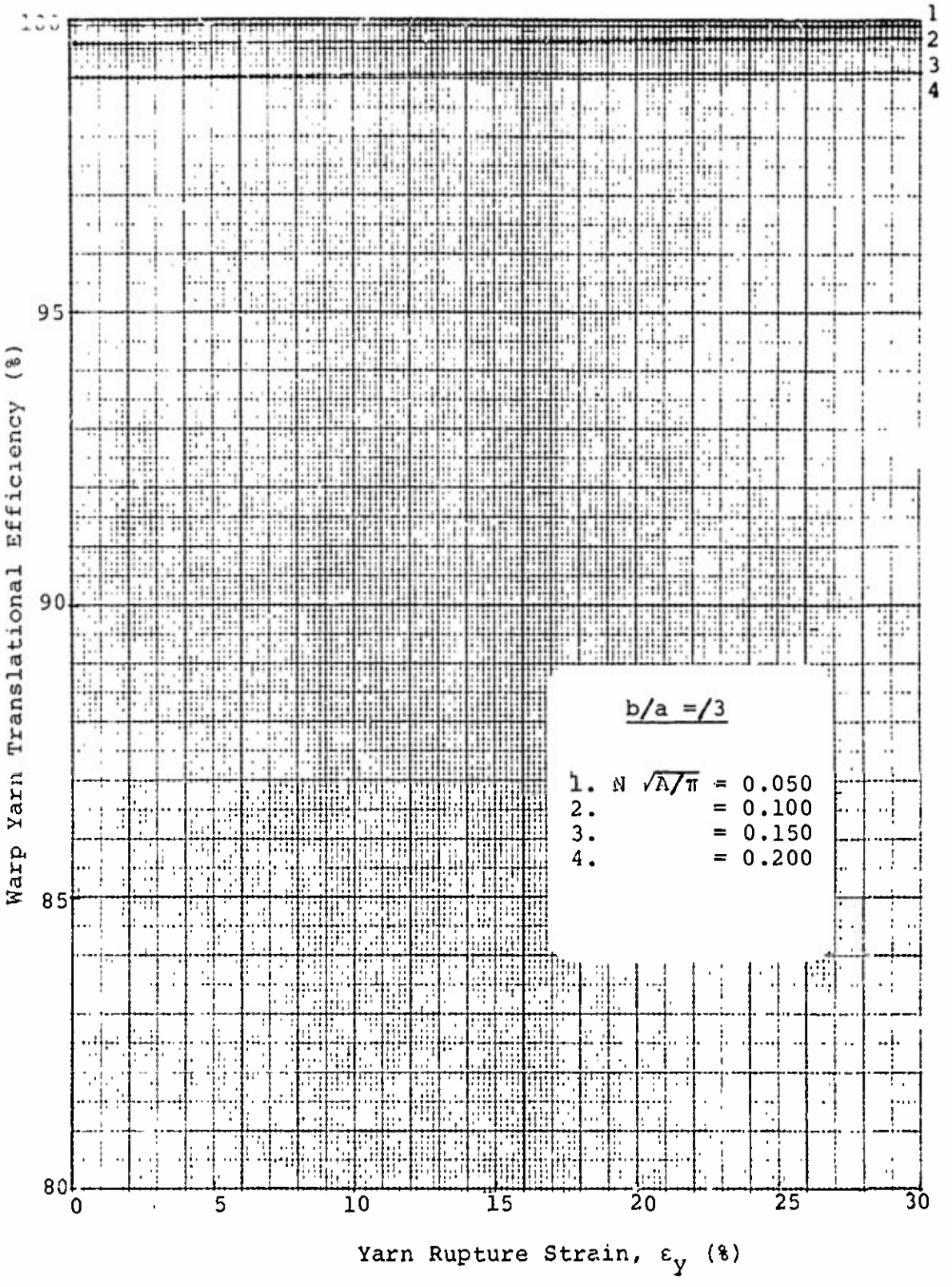

Figure 100. Yarn Translational Efficiency: Linearly Elastic Yarn, Initially Square Fabric, $\sigma_w/\sigma_f = 5$, b/a = 3

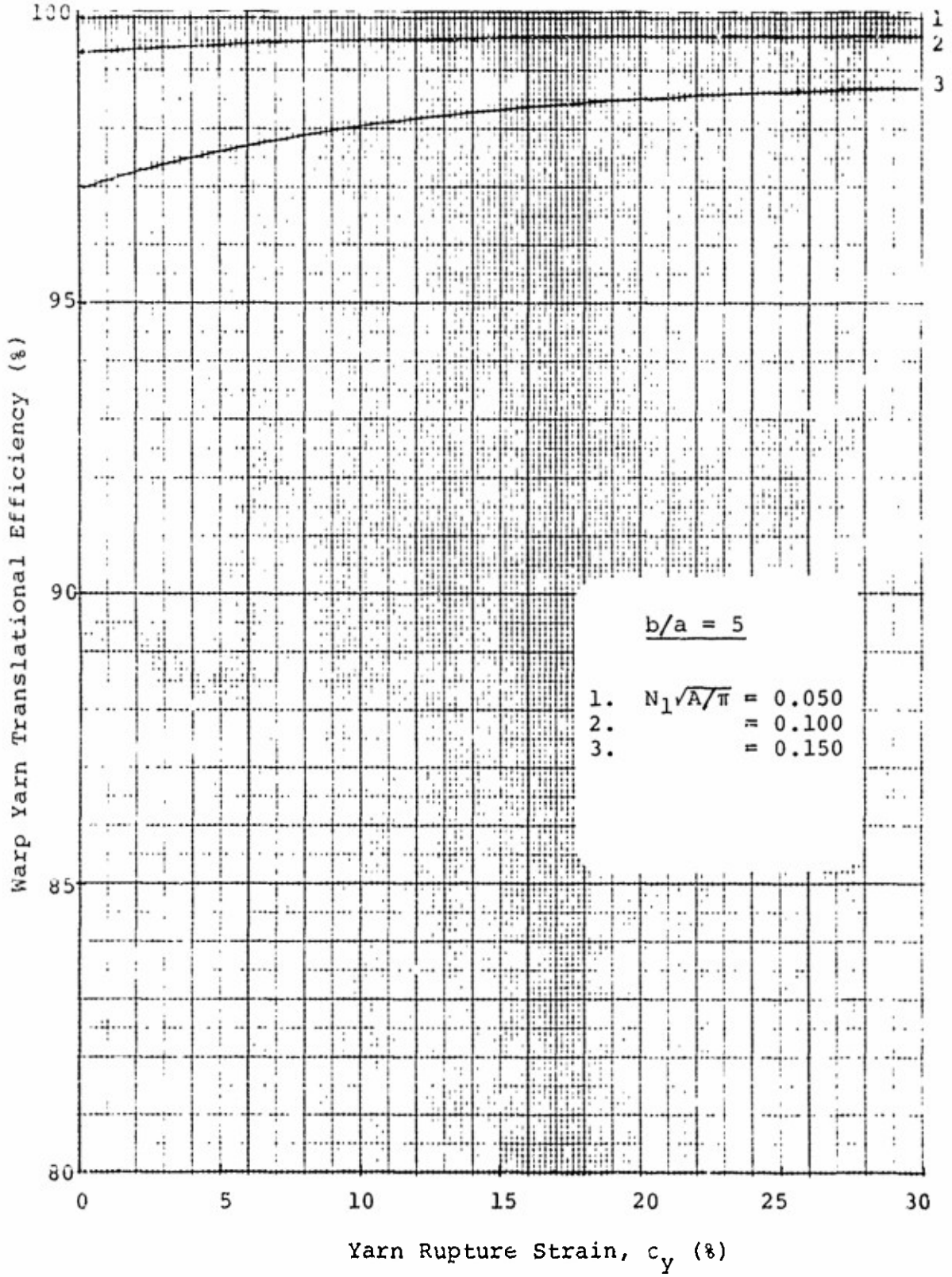

Figure 101. Yarn Translational Efficiency: Linearly Elastic Yarn, Initially Square Fabric, $\sigma_w/\sigma_f = 1$, b/a = 5

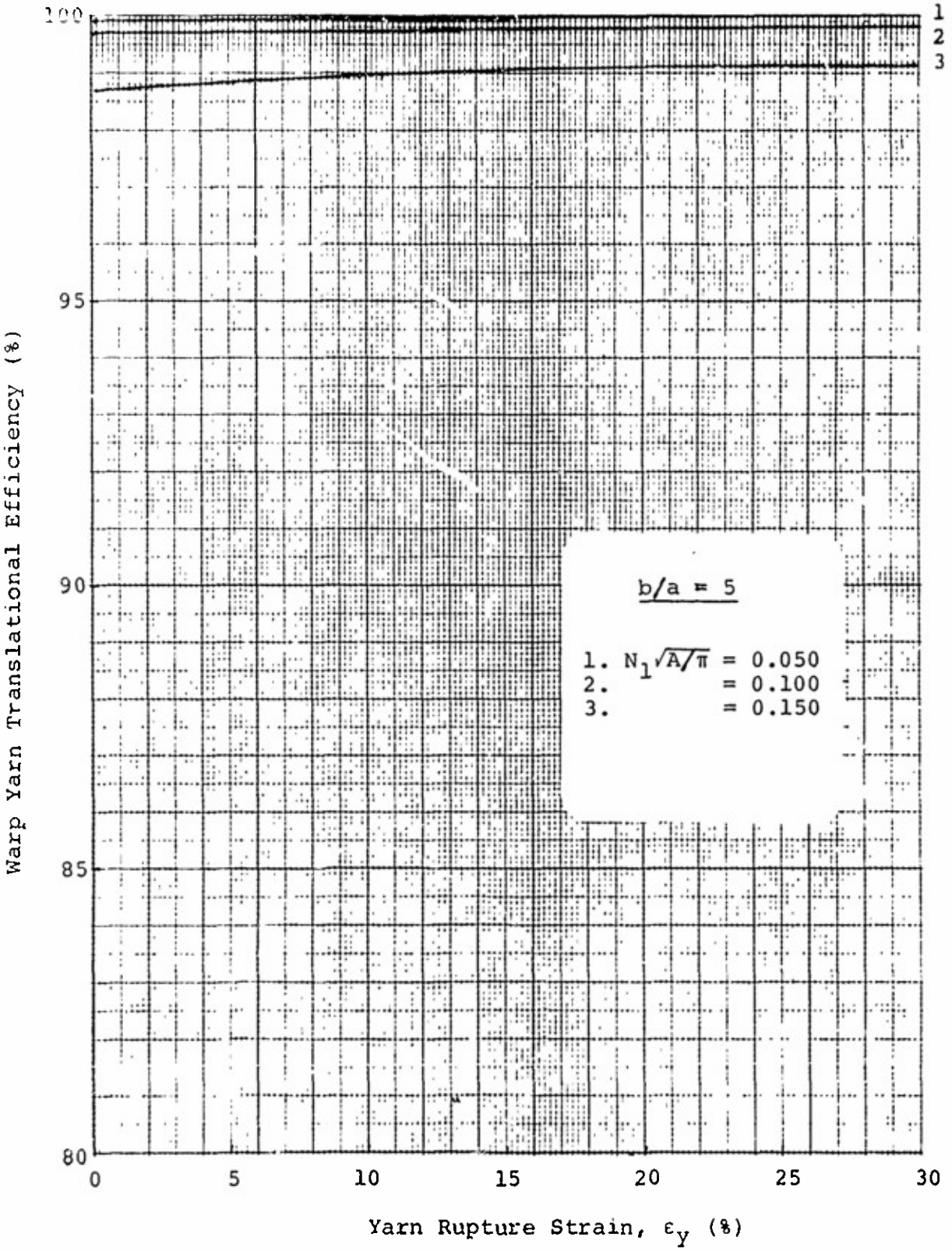

Figure 102. Yarn Translational Efficiency: Linearly Elastic Yarn, Initially Square Fabric, $\sigma_w/\sigma_f = 2$, b/a = 5

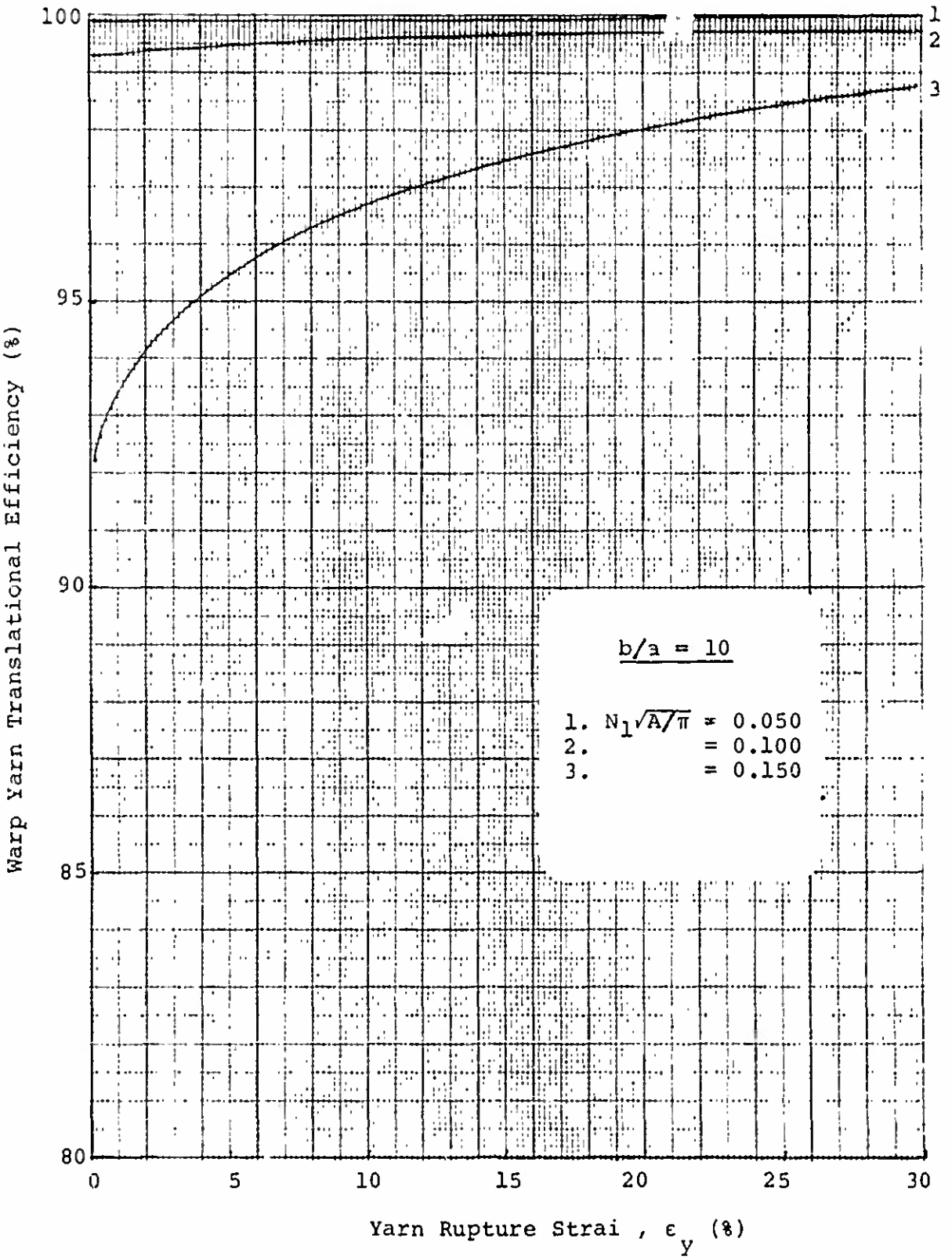

Figure 103. Yarn Translational Efficiency: Linearly Elastic Yarn, Initially Square Fabric, $\sigma_w/\sigma_f = 1$, b/a = 10

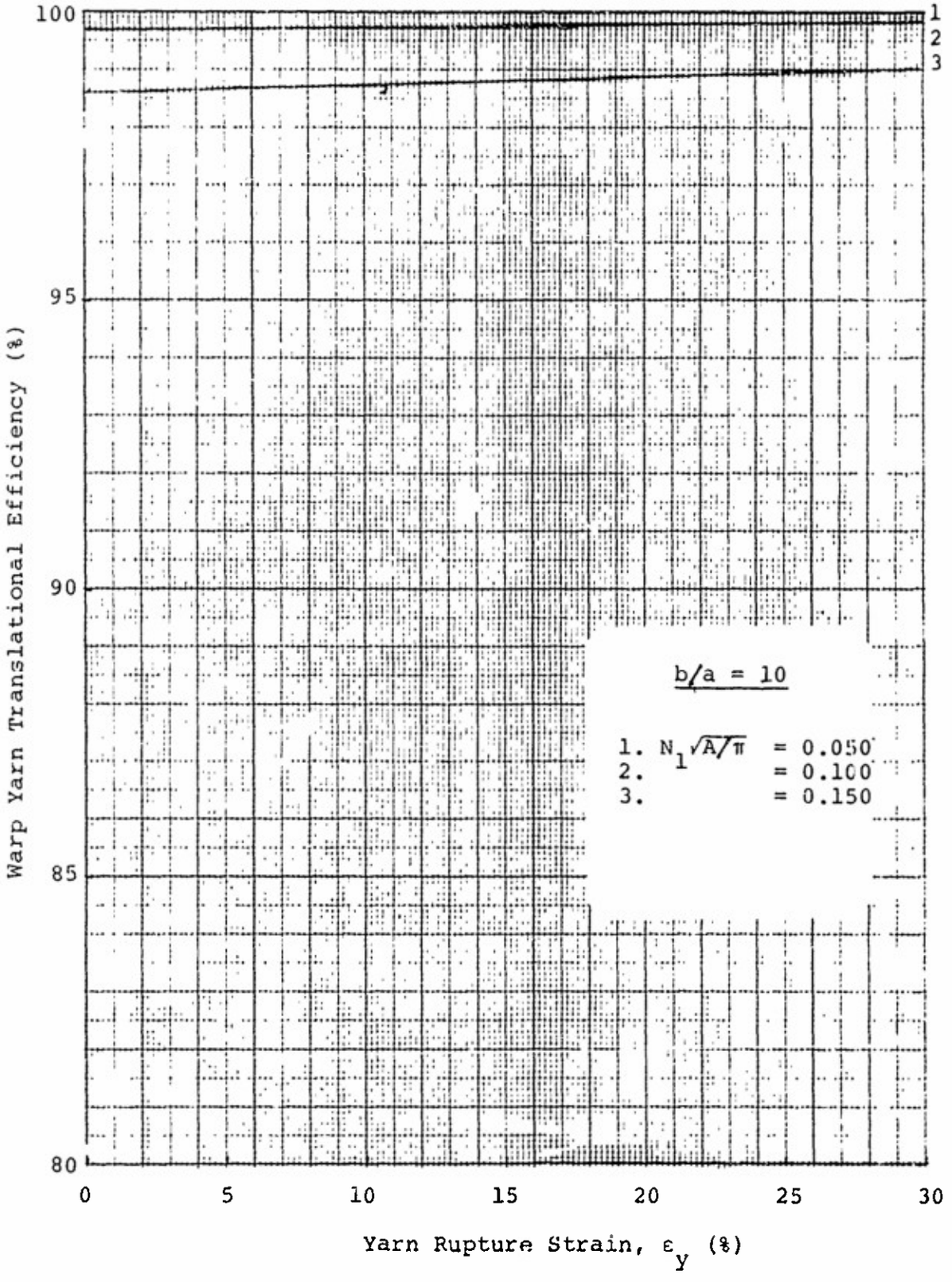

Figure 104. Yarn Translational Efficiency: Linearly Elastic Yarn, Initially Square Fabric, $\sigma_w/\sigma_f = 2$, b/a = 10

CONCLUSIONS

The foregoing investigation shows that the stress-strain response of plain-weave fabric composed of flattened yarn and subjected to biaxial loading can be computed theoretically. Fabrics woven from yarn having a circular cross-section are a special case encompassed by the analysis.

The analysis shows that the maximum number of yarns per unit width that can be woven into a plain-weave construction having an equal number of yarns in the warp and filling is approximately the same for initially square fabric as for fabric with initially straight filling at the larger yarn aspect ratios. However, as the yarns become more nearly circular, the maximum number of yarns that can be accommodated is somewhat larger for the initially square fabric.

For fabric woven from infinitely flexible, inextensible yarn, the amount of warpwise extension and filling contraction - crimp interchange - resulting from the application of a particular ratio of loads in the two directions decreases as the degree of yarn flattening increases. Additionally, the effective fabric Poisson's ratio is approximately the same for all yarn aspect ratios.

A comparison of the results for initially square fabric and fabric with initially straight filling shows that the warpwise extension is considerably greater and the filling contraction somewhat greater when the filling yarns are initially straight. The difference between the extensions decreases as the yarn aspect ratio increases.

For initially square fabric woven from infinitely flexible, linearly elastic yarn, the slope of the fabric warp and filling load-extension diagrams subsequent to the extension that occurs instantaneously upon application of infinitesimal loads ($\sigma_w/\sigma_f > 1$) decreases with increasing yarn aspect ratio.

EXTENSIONS OF THE ANALYSIS

The analysis developed herein can also be used directly to theoretically compute the load-extension response of basket-weave fabrics. Since in this weave two or more yarns are woven as one in a plain-weave pattern, the results for a plain weave describe the response of a basket-weave fabric when an appropriate aspect ratio describing the pair of yarns is used (see Figure 105). The load-extension results for the plain weave are not, however, directly applicable to other common weaves such as twills and sateens. However, the appropriate analytical expressions could be readily derived and solved for such weaves in an analogous manner to the procedure used for the plain weave.

Investigation of the yarn cross-section in fabrics woven from yarns twisted to low-to-moderate levels and that have not been calendered indicates that they are best described by a lenticular shape. The biaxial load-extension response of fabrics comprised of yarns with this geometry is also being studied [7].

As discussed in reference 1, the divergence between the predicted and measured response of some types of real fabrics becomes quite large at low levels of applied load when the loading ratio is greater than one. This is because the load-deformation behavior of fabrics at low-to-moderate loads--in the crimp-interchange region--is strongly dependent upon the yarn bending rigidity, which has not been included in the analyses developed to date. However, attempts at doing so should be made in a continuation of the present work.

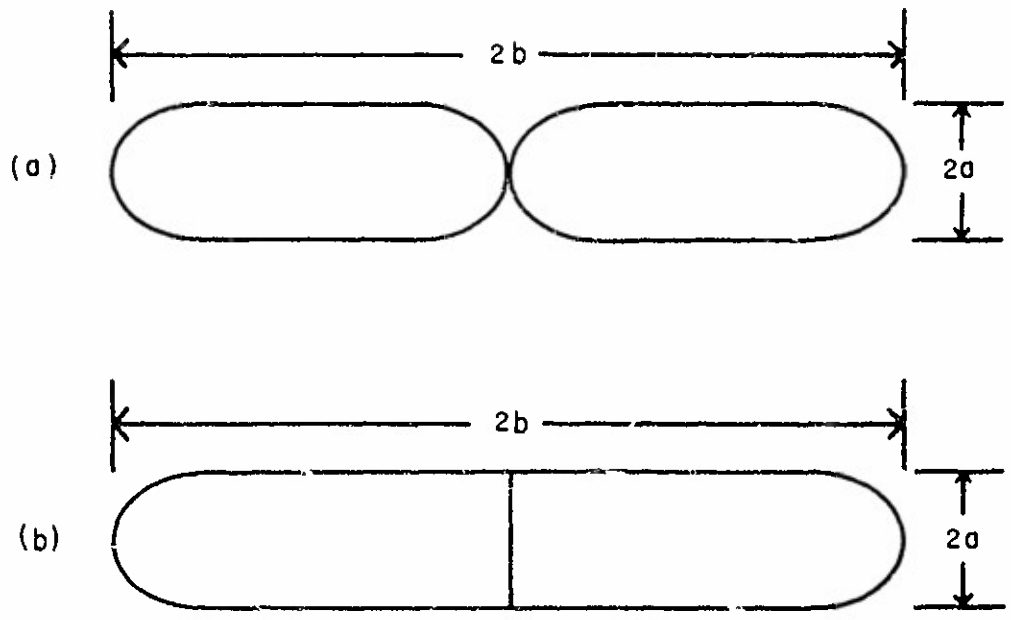

Figure 105. Basket Weave

END

5/1/73